This is to certify that the
thesis entitled

ENHANCEMENT OF CONCRETE-BASED
SANITARY SEWER INFRASTRUCTURE
THROUGH SYNTHETIC FIBER REINFORCEMENT

presented by

SHERVIN JAHANGIRNEJAD

has been accepted towards fulfillment
of the requirements for the

M.S. degree in CIVIL ENGINEERING

Major Professor's Signature

7/26/15

Date

ENHANCEMENT OF CONCRETE-BASED SANITARY SEWER INFRASTRUCTURE THROUGH SYNTHETC FIBER REINFORCEMENT

By

Shervin Jahangirnejad

A THESIS

Submitted to
Michigan State University
in partial fulfillment of the requirements
for the degree of

MASTER OF SCIENCE

Department of Civil and Environmental Engineering

2005

ABSTRACT

ENHANCEMENT OF CONCRETE-BASED SANITARY SEWER INFRASTRUCTURE THROUGH SYNTHETIC FIBER REINFORCEMENT

By

Shervin Jahangirnejad

A comprehensive literature review was conducted on fiber-reinforced concrete, which provided a basis for use of synthetic fibers in concrete-based infrastructure. The focus of this research was to develop structural designs with synthetic fibers, to increase the protective concrete cover over steel, and the service life of concrete pipes in sanitary sewer systems.

An industrial-scale production and test program was implemented to verify the constructability and structural performance of concrete pipes incorporating synthetic fibers. The results indicated that synthetic fibers enable design of pipes with increased protective concrete cover over steel (for improved durability), with adequate strength and ductility. Refined materials and designs were found to be compatible with conventional pipe production practices.

Analytical models were developed for prediction of the load-carrying capacity of fiber-reinforced concrete pipes, with or without steel reinforcement. These models provided a reasonable basis to predict the experimental values of the load-carrying capacity of concrete pipes.

To my wife, and my family

ACKNOWLEDGEMENTS

I would like to express my deepest gratitude to my major professor and research advisor, Dr. Parviz Soroushian, for his instruction and guidance during my Master's study, and his patience, and kindness towards me. Without his help and contribution, I could not perform this research program.

I wish to express my thanks to Dr. Ronald Harichandran and Dr. Rigoberto Burgueño for their advice and comments during my Master's study.

Special thanks to my wife who greatly helped me during the term of this research by her understanding, sacrifice, and support.

TABLE OF CONTENTS

LIST OF TABLES

LIST OF FIGURES

CHAPTER 1

INTRODUCTION

1.1 Concrete Based Sewer Systems

Concrete pipes, manholes, pump stations, wet wells, etc. represent close to half of the investment in the infrastructure for the 20,000 sewer systems of the United States. Concrete has reached its position of prevalence in sewer infrastructure through satisfactory performance over long periods of time. Some concrete aqueducts constructed by Romans about 2000 years ago to transport sewage are still in use. The concrete-based sewer infrastructure complements desirable durability with structural efficiency and initial as well as life-cycle economy. In recent years, however, incidents of severe damage to the concrete-based sanitary sewer infrastructure (Figure 1.1) have increased significantly; "microbial-induced corrosion" has been identified as the primary cause for this growing problem. The significant rise in microbial-induced corrosion of concrete sewer system has been partly attributed to new environmental regulations concerning loads of toxic chemicals discharged into sewers and water bodies. Such regulations have led to a significant rise in microbial activity within wastewater systems. The problem is further aggravated by uncoupling of sewage and surface water, leading to higher concentrations of nutrients and longer residence durations of sewage in pipes.

Microbial-induced corrosion of concrete in sewer system (Figure 1.2) involves sulfuric acid attack on concrete, with a complex microbial ecosystem generating the sulfuric acid in three distinct stages. Anaerobic conditions in sewage support microorganisms that convert sulfur and sulfate within sewage to sulfides (Stage 1). The resulting hydrogen sulfide volatizes to the sewer atmosphere (Stage 2) and dissolves in the condensate on sewer crown; sulfur-oxidizing bacteria then convert hydrogen sulfide to sulfuric acid (Stage 3) which is responsible for attack on concrete. While many sanitary sewer concrete pipes installed in 1800's were found in excellent condition after more than 100 years, today's severe microbial-induced corrosion can reduce the service life of reinforced concrete pipes to less than 10 years, with significant economic implications.

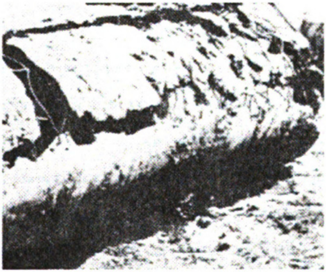

Figure 1.1. An Example of Damage to Reinforced Concrete Caused by Microbial-Induced Corrosion.

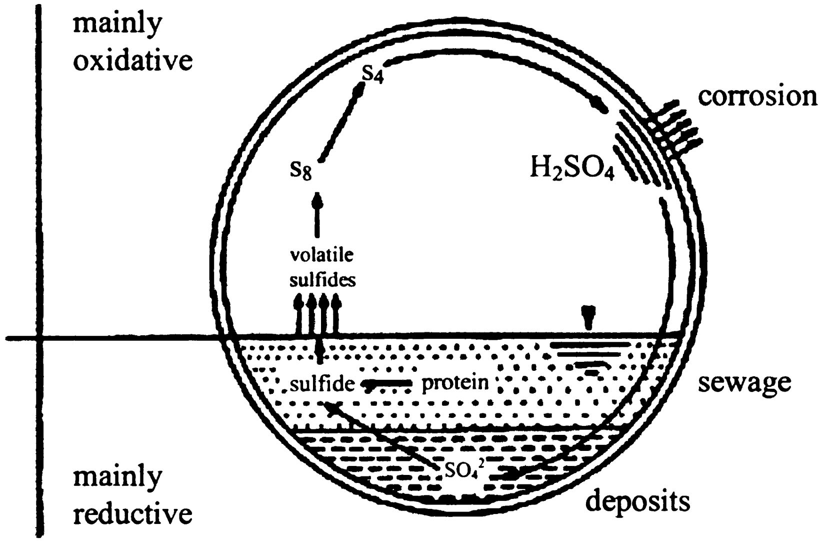

Figure 1.2. Schematic Presentation of the Process

Microbial-induced corrosion of concrete relies on interdependent biological, physical and chemical phenomena to attack the concrete-based sewer infrastructure. All these phenomena should be addressed for effective mitigation of this complex mode of attack on concrete; the following concrete attributes have particularly significant effects on such phenomena: (1) amenability to microbial growth; (2) alkalinity; (3) acid resistance; and (4) absorbency. Refinement of these attributes should define the objectives for efforts towards development of concrete materials which effectively resist microbial-induced corrosion in sanitary sewer environment. The focus of this investigation is, however, on refinement of the structural design of concrete pipes in order to increase the protective cover of concrete over steel. This would increase the time it takes for microbial-induced corrosion to reach the level of steel, soon after which corrosion of steel defines the end of service life. Synthetic fiber reinforcement of concrete is used in this investigation to enable refinement of concrete pipe structural design. The basic strategy involves shifting of steel reinforcement away from the interior surface of concrete pipes, with synthetic fibers compensating for the structural losses associated with this shift. At the same time, one needs to reduce the total volume of steel reinforcement in order to control the rise in initial cost associated with the introduction of fibers.

Recent advances in fiber reinforcement technology have opened new prospects for design of highly efficient reinforced concrete systems. Today's concrete pipe designs, relying strictly on conventional steel reinforcement, have not yet taken advantage of advanced fiber reinforcement systems towards achieving higher levels of structural efficiency and resolving some critical structural performance issues. The weight of structurally inefficient pipes limits their economically viable shipment distances; hence, today's concrete pipe production facilities have limited capacity and cannot benefit from the economy of scale. The structural inefficiency of concrete pipes also has negative durability implications. The excess reliance on conventional steel reinforcement frequently forces use of two steel layers (Figure 1.3.a); this reduces the thickness of concrete cover needed to protect steel against the highly corrosive environment in sanitary sewer system. Microbial-induced corrosion would thus have less concrete thickness to overcome before exposing the reinforcing steel which effectively marks the end of service life. Today's structurally inefficient pipes also rely on an enlarged bell segment in order to control joint shear failure (Figure 1.3.b); the enlarged bell segment complicates transportation and field placement of concrete pipes. Today's steel reinforcement systems cannot be continued into the spigot segment of concrete pipe (which fits into the enlarged bell); this makes the spigot highly susceptible to shear failure caused by differential settlements (Figure 1.3.c) which occur commonly near manholes and other fixed structures to which concrete pipes connect. Fiber reinforcement can effectively overcome all structural issues depicted in Figure 1.3.

The research reported herein was part of a broader project concerned with development of a new generation of concrete-based sewer infrastructure systems which effectively resist microbial-induced corrosion and also offer high levels of structural efficiency and performance attributes. Control of microbial-induced corrosion is accomplished through a multi-faceted approach which mitigates the chemical, physical and microbial deterioration processes through control of concrete absorbency, chemistry and amenability to microbial growth. Recent advances in fiber reinforcement technology are adapted, in the particular component of the broader project which is subject of this research, towards structural design of more efficient pipes with reduced steel reinforcement, increased cover thickness over reinforcement (which greatly benefits durability), reduced weight, streamlined geometry (for ease of handling and installation), and enhanced shear resistance. Integrated analytical/experimental studies were implemented towards design and experimental verification of new pipe materials and structural systems; laboratory-scale investigations were complemented with industrial-scale production and structural evaluation of concrete pipes embodying the new material and structural design principles.

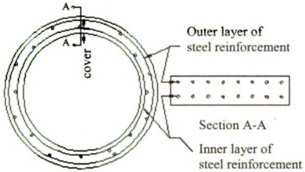

(a) Two-Layer Steel Reinforcement

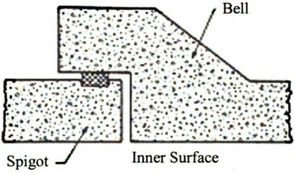

(b) Enlarged Bell Segment of Concrete Pipes

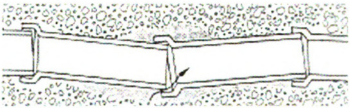

(c) Shear Failure Caused by Differential Settlement

Figure 1.3. Structural Considerations in Reinforced Concrete Pipe Design

1.2. Thesis Organization

In the next chapter (Chapter 2), fundamental concepts, theories, and applications of fiber reinforced concrete are presented. The experimental program for refinement of the concrete pipe structural design with the use of synthetic fibers is described in Chapter 3. The theoretical concepts leading to development of structural design methodologies for the new concrete pipes are introduced in Chapter 4. The conclusions of the investigations and future research needs are presented in Chapter 5.

CHAPTER 2

FIBER REINFORCED CONCRETE: FUNDAMENTAL CONCEPTS, THEORIES AND APPLICATIONS [1,6,13,17,20]

2.1 Introduction

Fiber reinforcement, when used properly, can enhance the cracking resistance, mechanical properties and longevity of concrete in different fields of application. Selection of the fiber type and dosage are keys to successful usage of this growing technology.

Traditional measures of concrete performance, including slump and compressive strength, may not adequately represent performance characteristics of fiber reinforced concrete.

The concrete mix proportions also influence the reinforcement efficiency of fibers. The primary purpose of this chapter is to provide a clear picture of the state of the art and practice in the field of fiber reinforced concrete.

The following topics will be covered in this chapter:

- Basic Concepts and Classes of Fiber Reinforced Concrete
- Fiber Types and Characteristics
- Testing of Fresh and Hardened FRC
- Properties of Synthetic Fiber Reinforced Concrete
- Applications and Advantages
- Mix Design and Construction Practices

2.2 Basic Concepts and Classes of Fiber Reinforced Concrete

This section covers the structure of fiber reinforced concrete, interactions of fibers with concrete, and the mechanics and efficiency of fiber behavior in concrete.

2.2.1 Structure of Fiber Reinforced Concrete

The structure of fiber reinforced concrete comprises the fibers, the bulk matrix and the interface zone between fibers and matrix. Fibers can be oriented or random (in 2D or 3D); they may also be continuous or (more commonly in the case of fiber reinforced concrete) discontinuous (discrete), as shown in Figure 2.1. A microscopic image of fiber reinforced concrete is presented in Figure 2.2. The bulk concrete matrix is not significantly different from that in conventional concrete, except that with finer and more numerous fibers, the matrix may suffer less microcracking under restrained drying and thermal shrinkage movements which are predominant in field placement of concrete. Depending on the application of fiber reinforced concrete, the matrix might be either concrete (with coarse aggregates) or mortar (without coarse aggregates).

Discrete fibers are more dominant in conventional concrete applications; their dispersion in concrete is relatively uniform and the short fibers tend to assume a more random orientation. If the ratio of the fiber length to the thickness of concrete placement is sufficiently large, the fibers will assume a 2-dimensional distribution. A preferred 2-dimensional distribution can also be promoted in thick components due to vibration.

This will give rise to anisotropic behavior. The interface zones between fiber and concrete matrix differ in terms of microstructure and composition from the bulk of concrete matrix.

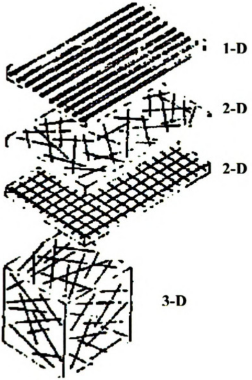

Figure 2.1. Fiber Orientations.

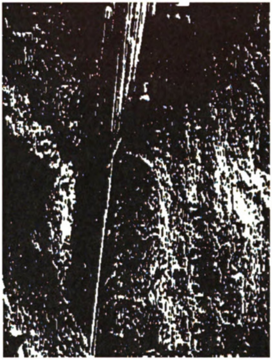

Figure 2.2. Fiber Reinforced Concrete.

The relatively high surface area of fibers introduces a relatively large volume of interface zone, which may strongly influence the behavior of fiber reinforced concrete.

Fiber reinforced concrete is characterized by a transition zone in the vicinity of fibers, in which the microstructure is considerably different from that of the bulk concrete away from interfaces. Fiber type and concrete production technique influence the nature and size of this transition zone and thus fiber-to-concrete bonding characteristics.

The special microstructure of the transition zone in fiber reinforced concrete is closely related to the particulate nature of cement (Figure 2.3). Cement consists of discrete particles ranging in diameter form about 1 to about 100 micrometer (average size of about 10 micrometer). Hydration of these particles yields mainly colloidal CSH particles and larger crystals of CH. The particulate nature of the fresh mix exerts an important influence on the transition zone, since it leads to formation of water-filled spaces around the fibers due to two related effects: (1) inefficient packing of the about 10 micrometer cement grains in the 20-40 micrometer zone around the fiber surface; and (2) bleeding and entrapment of water around the reinforcing fibers. The nature of cement hydration products in the interface zone is thus different from that in the bulk cement paste (Figure 2.4). Finer fibers which offer diameters comparable to those of cement particles provide for better packing of the fresh system, which favors the density and microstructure of interface zone.

As shown in Figure 2.4, the matrix in the vicinity of fibers is generally more porous than the bulk concrete, and this is reflected in the development of the microstructure as hydration advances.

The initially water-filled transition zone does not develop the dense microstructure typical of the bulk concrete, and it contains a considerable volume of CH crystals, which tend to deposit in large cavities.

The formation of a CH rich zone at the fiber interface is probably the result of its precipitation from the solution in the space around the fiber, with the fiber surface being a nucleation site. The CH layer adjacent to the fiber surfaces is not necessarily continuous, and it contains some pockets of very porous material consisting also of CSH and some ettringite.

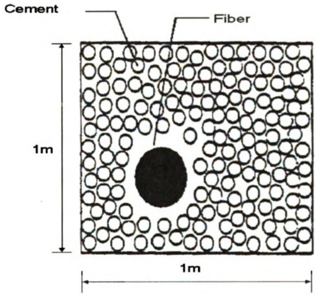

Figure 2.3. Disruption of Packing of Cement Particles by Fibers.

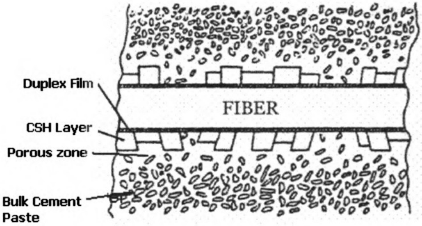

Figure 2.4. Microstructure of Fiber Reinforced Concrete.

The weak link between the fiber and the matrix is not necessarily at the actual fiber-matrix interface; it can also be in the porous layer, which extends to a distance of about 10 to about 40 micrometer from the interface, between the massive CH layer and the dense bulk concrete.

In the case of finer fibers, which provide for improved packing of the fiber-cement system, the interface microstructure after hydration could be rather dense simulating that of bulk concrete.

2.2.2 Spacing of Fibers in Concrete

A key contribution of fibers in concrete involves their interaction with microcracks and cracks; frequent encounters between cracks propagating in concrete and fibers have positive effects on concrete performance under load and environmental effects. Closely spaced fibers are thus expected to provide concrete with more effective reinforcement effects. The average fiber spacing in concrete can be calculated as follows, assuming a uniform fiber distribution, and using basic statistical concepts:

$$S = \frac{K.d_f}{\sqrt{V_f}}$$

where,

S = Fiber spacing

K = Constant

d_f = Equivalent fiber diameter

V_f = Fiber volume fraction

In the expression presented above, K varies in the range of 0.8 to 1.12 depending on the orientation of fibers (1-, 2- or 3-dimensional) and the assumptions made in calculation. The equivalent diameter here provides the same cross-sectional area as that of actual fibers.

Examples of fiber spacing for different fiber diameters at a constant fiber volume fraction of 0.2% are presented in Tables 2.1. At this relatively low fiber volume fraction, the fiber spacing is observed to be relatively small (2.3 mm) in the case of synthetic fibers. Fiber spacing, at the same volume fraction, is proportional to fiber diameter. Fibers of finer diameters would thus be preferred because they yield closed fiber spacing within concrete.

Table 2.1 Typical Values of Fiber Spacing for Fiber Volume Fraction of 0.2%.

Fiber diameter inch (mm)	Fiber Spacing mm (in)
Synthetic: 0.004 (0.1)	2.3 (0.089)
Steel: 0.016 (0.40)	8.9 (0.36)

2.2.3 Fiber Weight Fraction versus Volume Fraction

While practitioners generally express fiber dosage in concrete in terms of fiber weight per unit volume of concrete, researchers generally use fiber volume fraction as the measure of fiber content. Table 2.2 presents examples for fiber weight dosage depending on fiber specific gravity for a constant fiber volume fraction of 0.2%.

Table 2.2. Fiber Weight Fractions for a Constant Fiber Volume Fraction of 0.2%.

Fiber	Specific Gravity	kg/m^3 (lb/yd^3)
Synthetic	0.9	1.8 (3)
Steel	7.8	15.6 (26)

It may also be rationale to work with fiber/cement ratio because fibers reinforce the paste, and more fibers would be needed as the cement paste content of concrete increases.

2.2.4 Fiber Count per Unit Volume of Concrete

Fiber count per unit volume of concrete is a parameter comparable in significance to fiber spacing. Fiber count per unit volume can be expressed as a function of the fiber volume fraction, length and diameter:

$$FC = 1.27 \frac{V_f}{l.d_f^2}$$

where,

FC = Fiber count per unit volume of concrete

l = Fiber length

d_f = Fiber Diameter

Examples of fiber count per unit volume for typical synthetic and steel fibers are presented in Table 2.3. The fact that lower-diameter fibers offer closer fiber spacings is an advantage in terms of microcrack control in concrete.

Table 2.3. Examples of Fiber Count Per Unit Volume At A Constant Fiber Volume Fraction of 0.2%.

Fiber	Count per in^3
Synthetic	160
Steel	10

2.2.5 Fiber Surface Area per Unit Volume of Concrete

Fibers relay their reinforcing effects to concrete through their interfaces with concrete. Larger interface areas thus enhance the reinforcement efficiency of fibers in concrete. The fiber surface area per unit volume of concrete (*SS*) can be calculated as follows:

$$SS = 4\,\frac{V_f}{d_f}$$

Typical synthetic and steel fibers at 0.2% volume fraction provide 0.12 and 0.03 in^2 surface area per in^3 of concrete, respectively.

2.3 Fiber Interactions with Matrix Damage Mechanisms

Fibers at relatively low volume fractions enhance the performance of concrete through control of microcrack and crack propagation at three stages: (i) stress control and damage suppression; (ii) microcrack control and damage stabilization; and (iii) crack control and failure inhibition. These three stages of fiber interaction with damage mechanisms in matrix are described below.

2.3.1 Stress Control and Damage Suppression

Failure of concrete under load and environmental effects generally initiates through propagation and interconnection of pre-existing microcracks. These microcracks grow rather easily in concrete due to the concentration of stresses near microcrack tips and the low fracture toughness of concrete.

Once relatively stiff fibers of high surface area are located near microcrack tips, fibers (assuming that they are stiffer than concrete) resist large deformations (strains) near crack tips and thus reduce matrix stresses (see Figure 2.5). This phenomenon delays (suppresses) the initiation of damage (microcrack propagation). In effect, since in the presence of cracks the matrix tends to extend more than the fibers (due to stress concentrations just ahead of crack tips), fibers oppose this tendency; through interfacial shear bond stresses, they apply 'pinching forces' which effectively reduce the stress intensity factor of the crack (Figure 2.5). As a result, higher levels of applied stress would be required to produce a stress field ahead of the crack tip such that maximum stress exceeds the critical stress intensity factor of concrete.

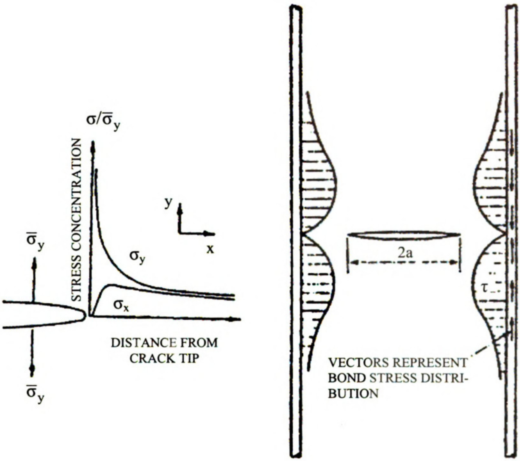

Figure 2.5. Stress Control and Damage Suppression Action of Fibers in Concrete.

Fiber characteristics that yield enhanced stress control and damage suppression effects include:

- High Elastic Modulus (higher than that of concrete)
- Close Fiber Spacing
- High Fiber Surface Area and Bond Strength
- High Fiber Tensile Strength

High elastic modulus of fibers (must be higher than that of concrete matrix) is essential for the control of stresses at microcrack tips, which delay the initiation of damage processes. Also, it is essential that fiber be located near microcrack tips for effective relief of stress concentration there; close spacing of fibers is thus critical. Stress transfer from matrix to fibers is through fiber-matrix interfaces; hence, large interface areas and strong bond strengths are always helpful. Finally, fibers should be capable of resisting transferred stresses, which makes their tensile strength important.

It is important to note that tensile strength is not the only, or in this case even the key, criterion for the judgment of the reinforcement efficiency of fibers in concrete.
As noted above, fiber spacing is one important factor determining the damage suppression effects of fibers which lead to increased cracking strength of concrete. The experimental results shown in Figure 2.6 validate the 'spacing concept' in application to steel fiber reinforced concrete.

The criteria governing effectiveness of fibers in damage suppression can now be used to compare different fiber types (Table 2.4).

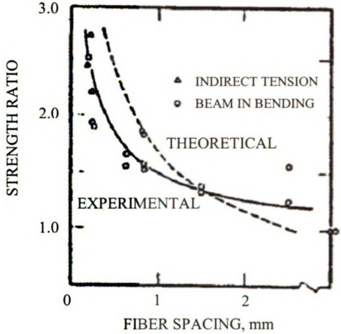

Figure 2.6. Effect of Fiber Spacing on Tensile and Flexural Strength of Concrete.

Table 2.4. Comparison of Fibers Based on Damage Suppression Criteria.

Fiber	Steel	Synthetic
Elastic Modulus	29,000	2,500
Spacing @ 0.2% V_f	0.36	0.089
Surface Area @ 0.2% (in^2/ in^3)	0.03	0.12
Bond Strength (psi)	350	100
Tensile Strength (psi)	100	150

2.3.2 Microcrack Control and Damage Stabilization

The stress field ahead of microcrack tip (Figure 2.7a) consists of the familiar stress concentration profile in the direction of tensile stress (y direction), and a tensile stress field in the perpendicular direction (x direction). The latter field has its maximum not at the crack tip, but slightly ahead of it. As the propagating microcrack approaches the fiber (Figure 2.7b), the perpendicular tensile stress may cause debonding at the fiber-matrix interface, before the crack has reached the interface. This will occur if the interfacial bond strength is low, less than about 1/5 of the tensile strength of the matrix. When the crack finally reaches the interface, its tip will be blunted by the already present debonding crack. The stress concentration will be reduced, and the forward propagation of the crack will be arrested. Thus, the crack path will be diverted, and instead of continuing straight across the fiber it will choose the path of least resistance which involves debonding along the weak interface. In fiber reinforced concrete, the weak interface is not at the fiber surface, but rather in the porous layer of the transition zone, and it is here that crack arrest, debonding and crack branching takes place

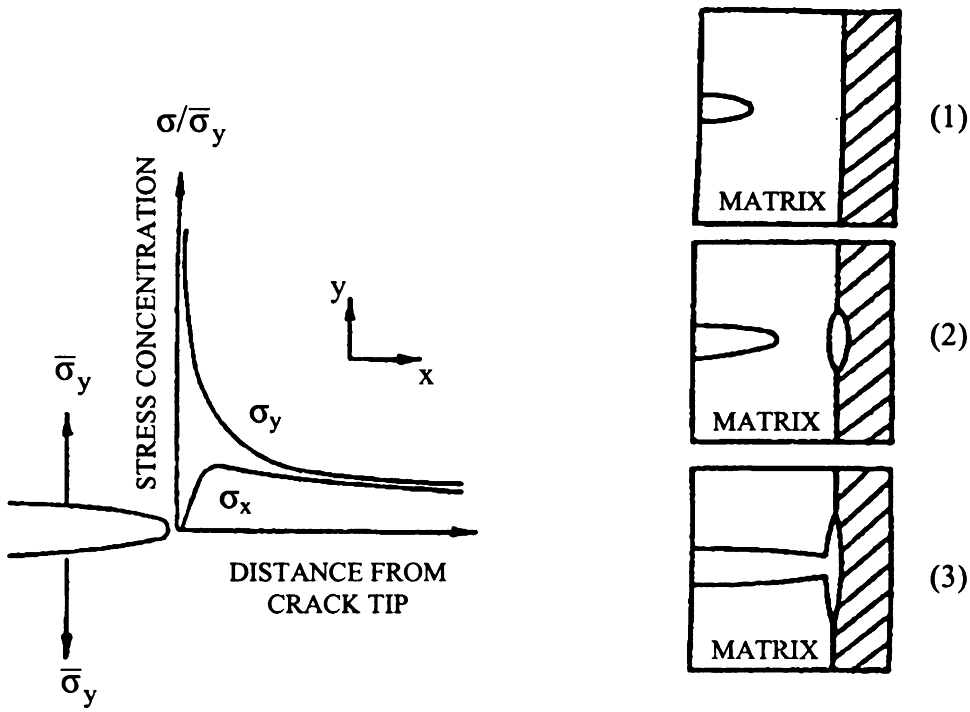

(a) Stress Concentration *(b) Microcrack/Fiber Interaction*

Figure 2.7. Microcrack Control and Damage Stabilization by Fibers.

Once first microcrack propagation has taken place in concrete, the fibers serve to inhibit unstable crack propagation (Figure 2.8). At this stage, the microcrack propagation patterns are complex, possibly with discontinuous microcracks present ahead of the principal microcrack.

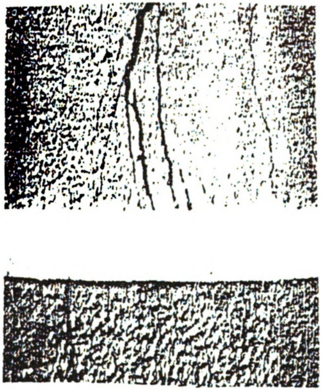

Figure 2.8. Inhibition of Unstable Microcrack Propagation by Fiber.

At the damage stabilization stage, the following parameters govern, based on above illustration, the effectiveness of fibers.

- Close Fiber Spacing
- High Fiber Surface Area
- Bond Strength

Fibers would be more effective in microcrack stabilization if they provide closer spacing and larger surface areas. Bond strength is also important; the nature of microcrack stabilization effects of fibers alters as bond strength increases beyond a limit. Moderate bond strength, not extremely low or high, could actually benefit the microcrack stabilization action of fibers. Table 2.5 presents typical values for above parameters for example cases of steel and synthetic fiber reinforcement. Synthetic fibers with typically smaller diameters have a definite advantage in terms of specific surface area.

Table 2.5. Comparison of Steel and Synthetic Fibers at Damage Stabilization Stage of Behavior.

Fiber	Steel	Synthetic
Spacing @ 0.2% V_f (in)	0.36	0.089
Surface Area @ 0.2% (in^2/ in^3)	0.03	0.12
Bond Strength (psi)	350	100

2.3.3 Crack Control and Failure Inhibition

Eventually, microcracks propagate, concentrate and interconnect to the point that large visible cracks are produced. The pull-out resistance and tensile strength of fibers at this point essentially involves applying a crack-closing pressure which controls crack propagation and delays final failure of the system.

As shown in Figure 2.9, three distinct zones can be identified across the crack: (1) traction free zone; (2) fiber bridging zone, in which stress is transferred by frictional slip of the fibers; and (3) matrix process zone, containing microcracks, but with enough continuity and aggregate interlock to transfer some stress in the matrix itself (the concepts of microcrack suppression and stabilization would apply here).

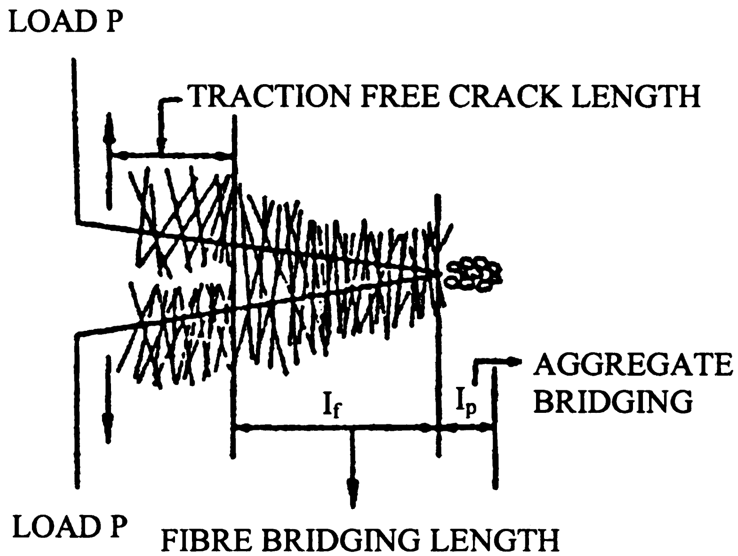

Figure 2.9. Crack Control and Failure Inhibition Action of Fibers.

Fibers bridging across cracks could either rupture or pull-out after debonding. The pull-out process is generally preferred as far as it does not occur prematurely because it dissipates large frictional energy, and increases the deformation capacity of concrete after cracking.

The pull-out process (Figure 2.10) starts with debonding of fibers from matrix, which essentially involves the propagation of a crack along the interface. After full debonding, the pull-out process starts which is resisted by frictional forces. Fibers pull-out on the side of crack where their embedment length is shorter, ranging from 0 to $l_f/2$. The average pull-out length is $l_f/4$.

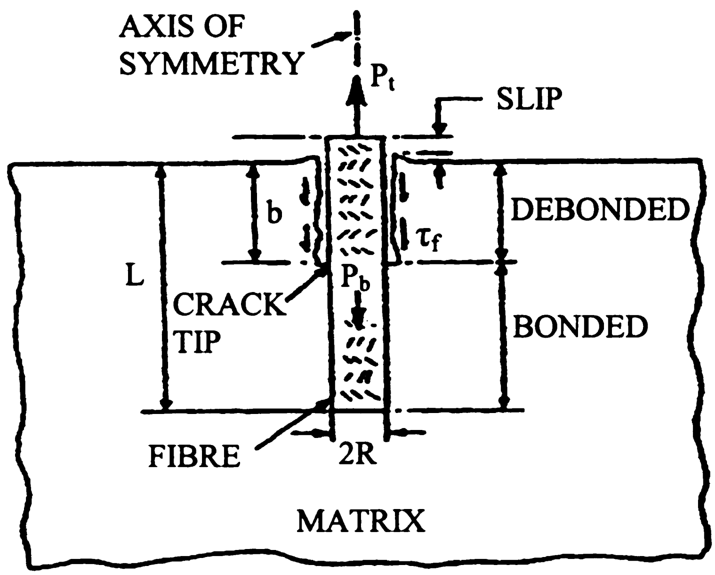

Figure 2.10. Fiber Debonding for Pull-Out.

Based on the above considerations, fiber parameters which govern the crack control and failure inhibition action include:

- High Fiber Area
- High Bond Strength and Balanced Pull-Out & Rupture Strengths Encouraging Pull-Out
- Large Fiber Length

With fiber length and surface area both critical, some use fiber aspect ratio (l/d) as a measure of reinforcement efficiency at this stage of behavior. Also, specific surface area times bond strength could be used as another measure of reinforcement efficiency. Table 2.6 makes a typical comparison of steel and synthetic fibers based on parameters which govern the crack control and failure inhibition action of fibers in concrete.

Table 2.6. Comparison of Steel and Synthetic Fibers at Crack Control and Failure Inhibition Stage of Behavior.

Fiber	Steel	Synthetic
Surface Area @ 0.2% (in^2/ in^3)	0.03	0.12
Bond Strength (psi)	350	100
Bond Strength Spec Surf (lb/in^3)	10.5	12
Pull-Out / Rupture Strength	0.3	0.2
Length (in)	1.5	0.7
Length / Diameter	94	188

2.3.4 Practical Implications of Microcrack and Crack Control

The microcrack suppression and stabilization as well as the crack control actions of fibers in concrete yield improvements in diverse aspects of concrete performance, listed below. The degree of improvement in each property depends on particular fiber properties and volume fractions.

- Restrained shrinkage microcrack and crack control, yielding enhanced impermeability and durability
- Increased tensile / flexural strength, ductility and toughness
- Improved impact resistance
- Improved fatigue life

Depending on the fiber type and volume fraction, various fiber reinforced concretes exhibit diverse types of behavior. For example, fiber reinforced concrete can be designed with high-modulus, high-bond-strength, high-surface-area fibers to provide highly improved levels of tensile strength, but with limited fiber pull-out and post-peak ductility and toughness (Figure 2.11a). Also, fiber reinforced concrete can be designed with moderate bond strengths which encourage fiber pull-out and thus improved post-peak ductility and toughness (Figure 2.11b). At high volume fractions of high-surface-area fibers with reasonable pull-out resistance, one may observed an ascending inelastic (post-cracking) associated with multiple-cracking of concrete (Figure 2.11c).

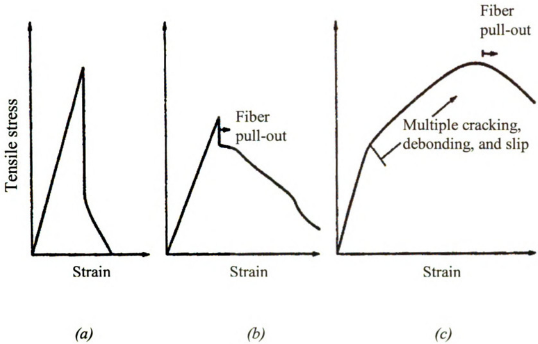

Figure 2.11. Diversity of the Tensile Behavior of Fiber Reinforced Concretes.

2.4 Properties of Synthetic Fibers

Synthetic polymeric fibers have been produced as a result of research and development in the petrochemical and textile industries. Fiber types that have been tried with cement matrices include (see Table 2.7) acrylic, aramid, nylon, polyester, polyethylene and polypropylene. They all have a very high tensile strength, but only few have a relatively high modulus of elasticity.

The quality of polymeric fibers that makes them useful in fiber reinforced concrete is their very high length-to-diameter ratios; their diameters are on the order of micrometer. Table 2.7 presents a summary of physical properties of various polymeric fibers. Examples of the stress-strain curves of different synthetic fibers are presented in Figure 2.12.

Table 2.7. Properties of Synthetic Fibers.

Fiber Type	Eff. dia. $x10^{-3}$ in. ($x10^{-3}$mm)	Specific Gravity	Tensile Strength, ksi (MPa)	Elastic modulus, ksi (GPa)	Ultimate elongation(%)
Acrylic	0.5-4.1 (13-104)	1.17	30-145 (207-1000)	2000-2800 (14.6-19.6)	7.5-50.0
Nylon		1.16	140 (965)	750 (5.17)	20.0
Polyester		1.34-1.39	130-160 (896-1100)	2500 (17.5)	
Polyethylene	1.0-40.0 (25-1020)	0.96	29-35 (200-300)	725 (5.0)	3.0
Polypropylene		0.90-0.91	45-110 (310-760)	500-700 (3.5-4.9)	15.0

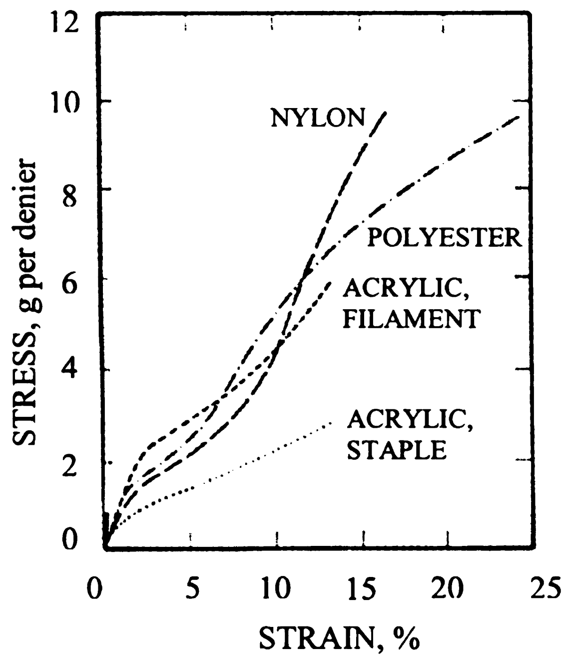

Figure 2.12. Examples of Tensile Stress-Strain Curves of Synthetic Fibers.

2.5 Effects of Fibers in Fresh Concrete Mixtures

Fibers, even when added to concrete at relatively low volume fractions, provide a relatively high surface area that needs to be coated with the paste for effective boding to concrete. The consumption of wet paste for coating of fibers reduces the paste content for lubrication of aggregates, and thus damages workability. However, static tests such as slump overestimate this damage to workability; low-slump fiber reinforced concrete mixtures could still compact favorably when vibration is used for consolidation.

Coarser and longer fibers such as steel experience difficulty in dispersion within concrete at higher aggregate contents and with larger maximum aggregate size (see Figure 2.13). Hence, mixes of smaller maximum aggregate size which are richer in cement and sand content favor uniform dispersion of fibers in concrete. Fiber interlocking (balling) can occur in improperly proportioned or mixed fiber reinforced concrete particularly at higher fiber volume fractions.

Fibers with specific gravities substantially higher and lower than that of concrete may tend to settle and flow, respectively, within high-slump concrete mixtures. Some finer fibers could actually improve the cohesiveness and segregation resistance of fresh concrete mixtures.

When using fibers at relatively low volume fractions of 0.2% or less, hardly any change would be required in a properly proportioned normal concrete mix.

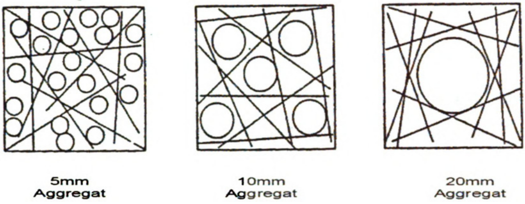

Figure 2.13. Effect of Aggregate Size on Fiber Dispersion.

2.6 Testing of Fresh and Hardened Fiber Reinforced Concrete

Some properties of FRC are matrix-dependent, and can thus be measured by the methods commonly used for conventional concrete, e.g., compressive strength. Other properties, however, differ substantially from those of matrix, and must be evaluated by test methods which are not used for normal concrete. These properties are of the greatest interest because they represent the areas in which the addition of fibers yields the greatest effects on properties, such as crack control and impact resistance. Some, but not all, of these tests have been developed to the level of standard practices.

2.6.1 Workability of Fresh Fiber Reinforced Concrete

Fibers usually tend to stiffen the fresh mix, and make it seem harsh in static condition; in spite of this, the mix can still respond well to vibration. Under vibration, the stiffening effect of the fibers may largely disappear, and a properly designed FRC mix can be handled in much the same way as plain concrete in terms of mobility and ability to flow. Therefore, workability tests based on static conditions, such as the slump test, can yield misleading results since the fresh fiber reinforced concrete is in fact workable when vibrated. Hence, it is generally recommended that workability tests in which dynamic effects are involved should be used to assess the properties of fresh fiber reinforced concrete mixes. At low volume fractions of about 0.1%, one may still use the slump test. Various tests involving dynamic effects have been considered; these include Inverted Slump Cone (ASTM C 995), and Vebe Consistometer (Figure 2.14).

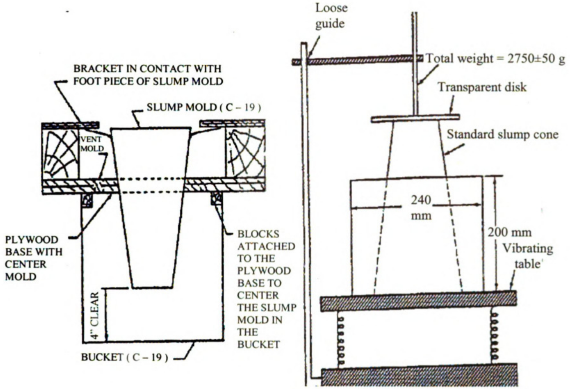

(a) Inverted Slump Cone *(b) Vebe Consistometer*

Figure 2.14. Fresh Mix Workability Test Set-Ups Applicable to Fiber Reinforced Concrete.

Example correlations between different workability test methods are presented in Figure 2.15, indicating that even at a low slump the fresh fiber reinforced concrete could respond well to vibration. It should be noted that all workability tests discussed here, including slump, provide a comparative assessment of different fresh fiber reinforced mixes; they do not measure parameters of physical significance.

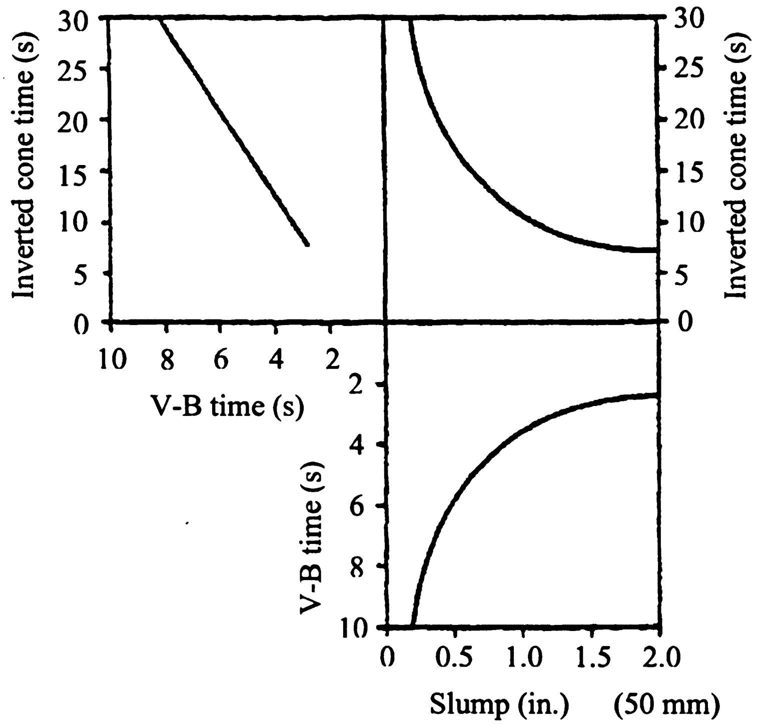

Figure 2.15. Correlations Between Different Fiber Reinforced Concrete Fresh Mix Workability Test Results.

2.6.2 Restrained Plastic Shrinkage Cracking Resistance of Fiber Reinforced Concrete

Many applications of fibers, in particular those involving relatively small dosages (less than 0.3 vol.%) of low-modulus fibers, are intended to increase resistance to plastic shrinkage (and plastic settlement) cracking at early ages (within few hours after concrete placement). It should be noted that measurement of free plastic shrinkage does not give an indication of the effect of fibers on resistance to plastic shrinkage cracking. The cracking tendency can only be judged on the basis of tests in which shrinkage movements are restrained in order to promote tensile stresses in concrete, and by observing the timing and extent of crack development. The physical significance of most tests used for this purpose is limited, and therefore they can be used only for qualitative, comparative assessment of the effects of fibers on the resistance of concrete to plastic shrinkage cracking.

One common plastic shrinkage test (Figure 2.16) passes dry, warm air over a slab. The slab is restrained at its bottom face by two end deformations, with another central deformation raising stress level to promote cracking. The total crack area is typically used as a measure of plastic shrinkage cracking. Other tests are also available, but none has been developed to the level of a recognized standard. These tests exhibit a relatively high level of variability, and any conclusions should be derived based on several replications, of the order of 10 or more.

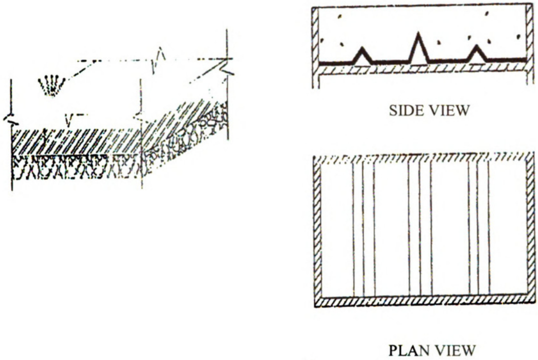

Figure 2.16. Restrained Plastic Shrinkage Test Set-Up.

2.6.3 Restrained Drying Shrinkage Resistance of Fiber Reinforced Concrete

The problem of evaluating the shrinkage and cracking potential in hardened fiber reinforced concrete involves the same concepts discussed earlier for plastic shrinkage cracking of fresh fiber reinforced concrete. Here too, the evaluation of free shrinkage is not relevant. The sensitivity to cracking is a function of both the shrinkage strain and the improvements in tensile resistance and toughness provided by fibers. The test procedure should involve restraint of shrinkage movements. A ring test (Figure 2.17) is commonly used where an internal steel ring restrains shrinkage movements of an external concrete ring. Concrete is cured, and the external ring and base are removed before drying is initiated. The concrete ring is allowed to dry only from its outside perimeter surface (top and bottom surfaces are sealed). As a result of concrete shrinkage, compressive stresses are induced in the steel ring, and tensile stresses develop in the concrete ring. By monitoring the time of cracking and the crack width over time, as the ring is exposed to a controlled relative humidity of, say, 50%, one can assess the resistance of hardened fiber reinforced concrete to restrained drying shrinkage cracking. Normal concrete mixtures may require more than a month of drying before appearance of restrained drying shrinkage cracks; many investigators use mixtures which are rich in cement and high in water-cement ratio in order to promote early cracking and make a quick comparative assessment of different fiber types and volume fractions.

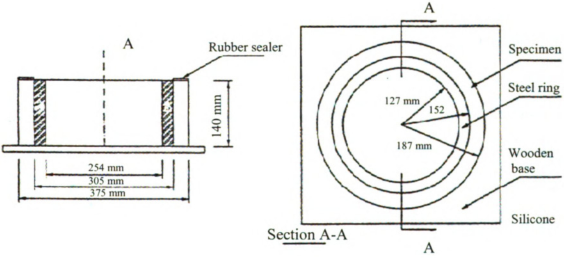

Figure 2.17. Restrained Drying Shrinkage Test Set-Up.

2.6.4 Flexural Toughness (and Strength)

Fibers enhance toughness of concrete by delaying microcrack formation and propagation (occurring mostly in the pre-peak region under tensile/flexural stresses), and by controlling the propagation of cracks (occurring in the post-peak region). Available test methods focus on post-peak toughness associated with crack control, which is significant at higher fiber volume fractions and when fiber pull-out (in lieu of fiber rupture) is prevalent.

ASTM C 1018 is a typical specification concerning calculation of post-peak toughness in flexure tests (4-point loading). The complete load-deflection curve is necessary for the performance of this test. The interpretation of the curves according to ASTM C 1018 in terms of modulus of elasticity, first-crack stress and flexural strength is presented schematically in Figure 1.18, with, loads shown at characteristic points. The first-crack stress may not correspond exactly with the limit of proportionality. However, the values are very close and, as a practical matter, the two terms are used interchangeably by different investigators. Of particular importance in the interpretation of the load-deflection curves is the post-cracking zone. Various attempts have been made to quantify such curves in terms of a parameter which would be useful for comparison between different fibers and fiber contents, and for specifications and quality control. Some attempts use the area under load-deflection curves up to a particular deflection. This area, termed toughness, represents the energy expended in deflecting the specimen to the specified point. If the test is continued until the specimen is completely broken, i.e. the load drops to zero, the area under the load-deflection curve would represent the total energy to fracture. The disadvantage of such parameters is that they are highly dependent on the specimen size and loading geometry, and therefore their physical significance is limited. Also, toughness values of this type are influenced by the matrix quality, and therefore do not provide an indication which is dependent only on the fibers. To overcome at least some of these difficulties, ASTM C 1018 uses a different approach in which toughness is characterized by a unit-less value. This value, termed toughness index, is the area under the flexural load-deflection curve up to a specified deflection, relative to the area up to the point of first cracking (i.e. the total energy expended relative to the elastic energy). The toughness indices at deflections of 3d, 5.5d and 15.5d are termed I-5, I-10 and I-30, respectively (5,10 and 30 would be toughness indices for an ideally elastic-plastic material).

The definition of toughness index per ASTM C 1018 has been subject of much criticism. The dependence of this index on pre-peak measurements makes it quite variable and susceptible to error. This is because conventional flexural deflection measurements are subject to large errors in the pre-peak region, largely due to local penetrations at supports and load points into concrete. It is thus important to measure actual flexural deflections using the 'yoke' apparatus shown in Figure 2.18a.

2.6.5 Residual Flexural Strength (an indirect measure of toughness)

In a more practical approach to assessment of toughness, ASTM C 1399 suggests a two-step flexure test where the beam specimen is first cracked with a supporting steel plate preventing catastrophic failure (Figure 2.19) which is quite possible given the elastic energy buildup within basic hydraulic test machines as the specimen approaches its cracking load. This catastrophic failure occurs commonly at relatively low fiber volume fractions.

The supporting steel plate is then removed, and the beam specimen is tested again, with the new peak load, denoted residual strength, providing an indirect measure of toughness in terms of post-peak flexural resistance.

2.6.6 Impact Resistance

Fiber reinforcement improves the performance of concrete under dynamic loading. In a qualitative test (Figure 2.20), the response to impact is evaluated by determining the number of blows up to first crack and ultimate failure. This type of test has been used mainly for a comparative evaluation of the differences between plain and fiber reinforced concrete. The results are variable, and several replications are needed to derive reliable conclusions. However, given the effectiveness of fibers in improvement of concrete impact resistance, this test provides a strong basis for comparative evaluation of the reinforcement efficiency of different fiber types and volume fractions.

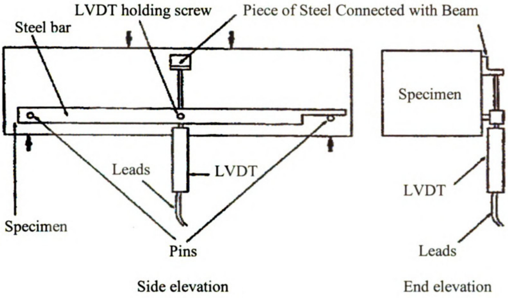

(a) Test Set-Up

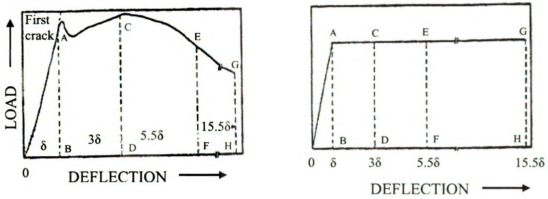

(b) Interpretation of Flexural Load-Deflection Curves

Figure 2.18. ASTM C 1018 Flexure Test Set-Up and Interpretation of Flexural Load-Deflection Curves.

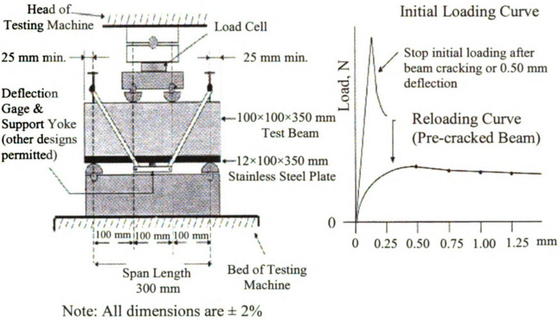

Figure 2.19. ASTM C 1399 Residual Strength Test Set-Up and Results

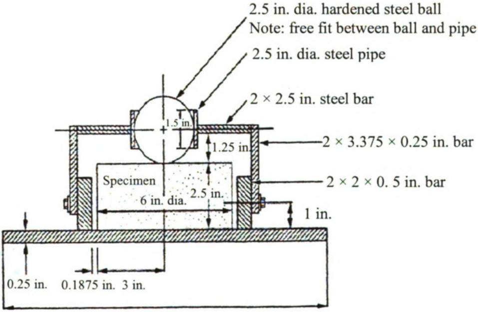

Figure 2.20. Impact Test Set-Up.

2.6.7 Durability Test Principles

Durability evaluation is important for fiber reinforced concrete. The service life of construction materials is expected to be several decades, and considering the fact that the field experience with modern fiber reinforced concrete is relatively limited, there is a need to evaluate the long-term performance of fiber reinforced concrete on the basis of relatively short-term accelerated tests. Since the causes for potential degradation may be different in each category of fiber reinforced concrete, it is impossible to develop a single accelerated procedure that is universally applicable to all fiber reinforced concrete. Accelerated aging tests must be developed in two stages. First, the potential aging mechanisms should be identified in order to choose an appropriate means of accelerating them, such as temperature, radiation or moisture condition. Second, the duration or number of cycles in accelerated aging tests should be translated into time under natural weathering conditions. The correlation between the time in accelerated and natural aging is not unique, since it depends on the climatic conditions in different zones, and even within the same zones there may be differences in micro-climate, for instance, the direction in which the component faces. Establishing correlations of this kind requires at least some limited time data from behavior in exposure sites, which could be compared with the results of accelerated tests. However, even without this information, it is very useful to carry out accelerated aging tests since they can provide an indication of whether there is an aging problem, and how severe it might be. Also, accelerated tests provide data for comparing the durability performance of different commercial products.

There are three classes of aging processes to be considered for accelerated durability tests of fiber reinforced concrete. These cover aging effects associated with: (1) the matrix, (2) the fiber, or (3) changes at the fiber-matrix interface. Matrix problems such as freeze-thaw and sulfate attack are not unique to fiber reinforced concrete, and they can be tested by procedures developed for conventional mortars and concretes. The most common fiber problem is its sensitivity to alkali attack. This is a concern with, say, glass fibers.

The most direct test usually applied is to expose the fibers to cement extract solutions at various temperatures, and testing the strength of the fibers before and after aging. Since there is uncertainty as to how well the extract solution represents the actual pore solution in concrete, various alternatives have been developed in which the fibers are cast in a block of concrete, and the whole assembly is tested, before and after exposure to warm water. Immunity of fibers to alkali attack is not by itself sufficient to ensure an adequate durability. Aging effects which lead to densification of the matrix at the interface and increased bond strength may cause a reduction in toughness (i.e. embitterment), and under certain conditions may also result in reduced tensile (flexural) strength. This can be most efficiently evaluated by testing the properties of the actual composite before and after aging, which is a suitable way to proceed with durability testing, for obtaining the overall effects associated with the combination of changes in the fiber itself and at the fiber-matrix interface. The changes in properties by which the durability performance should be assessed must include strength as well as toughness; properties which greatly benefit from the presence of fibers (e.g., impact resistance and residual flexural strength) provide effective means of evaluating the effects of accelerated aging effects on fiber reinforced concrete performance. The accelerated aging conditions depend on the particular aging phenomena being accelerated, and may involve immersion in warm water, exposure to wetting-drying cycles, exposure to carbon dioxide-rich environments, or different combinations thereof.

2.6.8 ASTM Standards Applicable to Fiber Reinforced Concrete

Table 2.8 lists various ASTM tests which are applicable to fiber reinforced concrete. These tests either measure the properties of concrete matrix and thus suit assessment of the matrix-dependent attributes of fiber reinforced concrete, or are specifically developed to measure the reinforcing effects of fibers in concrete.

Table 2.8. ASTM Test Procedures Applicable to Fiber Reinforced Concrete.

A 820	Specification of Steel Fibers for Fiber Reinforced Concrete
C 31	Practice for Making and Curing Test Specimen in Field
C 39	Compressive Strength
C 42	Obtaining and Testing Drilled Cores and Sewed Beams of Concrete
C 78	Flexural Strength
C 94	Specifications for Ready-Mixed Concrete
C 138	Unit Weight, Yield and Air Content (Gravimetric) of Concrete
C 143	Slump
C 157	Length Change of Hardened Hydraulic Cement Mortar and Concrete
C 172	Procedure for Sampling Freshly Mixed Concrete
C 173	Air Content by Volumetric Method
C 231	Air Content by Pressure Method
C 293	Flexural Strength of Concrete (Center-Point Loading)
C 360	Ball Penetration in Freshly Mixed Concrete
C 418	Abrasion Resistance by Sandblasting
C 469	Static Modulus of Elasticity and Poisson's Ratio of Concrete in Compression
C 496	Splitting Tensile Test
C 512	Creep of Concrete in Compression
C 597	Pulse Velocity through Concrete
C 666	Freeze-Thaw Durability
C 685	Specification for Concrete Made by Volumetric Batching and Continuous Mixing
C 779	Abrasion Resistance of Horizontal Concrete Surfaces
C 827	Early Volume Change of Cementitious Mixtures
C 947	Flexural Properties of Thin-Section Glass-Fiber Reinforced Concrete
C 948	Bulk Density, Water Absorption, and Porosity of Thin-Section Glass FRC
C 995	Time of Flow of Fiber Reinforced Concrete Through Inverted Slump Cone
C 1018	Flexural Toughness and First Crack Strength of Fiber Reinforced Concrete
C 1116	Specification for Fiber Reinforced Concrete and Shotcrete
C 1185	Thin Reinforced Cement Products
C 1228	Preparing Coupons for Flexural and Washout Test on Glass FRC
C 1229	Glass fiber Content in GRFC
C 1230	Tension Tests on Glass Fiber Reinforced Concrete Bonding Pads
C 1399	Obtaining Average Residual-Strength of Fiber Reinforced Concrete
E 84	Surface Burning Characteristics of Building Materials
E 119	Fire Test of Building Construction and Materials
E 136	Behavior of Materials in a Vertical Tube Furnace at 750C

2.7 Properties of Synthetic Fiber Reinforced Concrete

2.7.1 Fresh Mix Workability

Introduction of synthetic fibers into concrete matrix has a considerable influence on the properties of the fresh mix in particular on flow (workability) and plastic shrinkage cracking. An increase in fiber content results in a reduction in the consistency of the concrete; this reduction is greater for fibers of higher aspect ratio and also for higher fiber contents (Figure 2.21)

Typical effects of varying the volume content and length of synthetic fibers on the water/cement ratio of concrete which is required for maintaining a constant slump of 50mm are presented in Figure 2.22. Increasing the fiber content and aspect ratio is observed to increase the water/cement ration required for maintaining constant workability. Figure 2.23 summarizes the results reported in the literature (see Appendix A) on the drop in slump of concrete with introduction of different types of synthetic fibers at relatively low volume fractions.

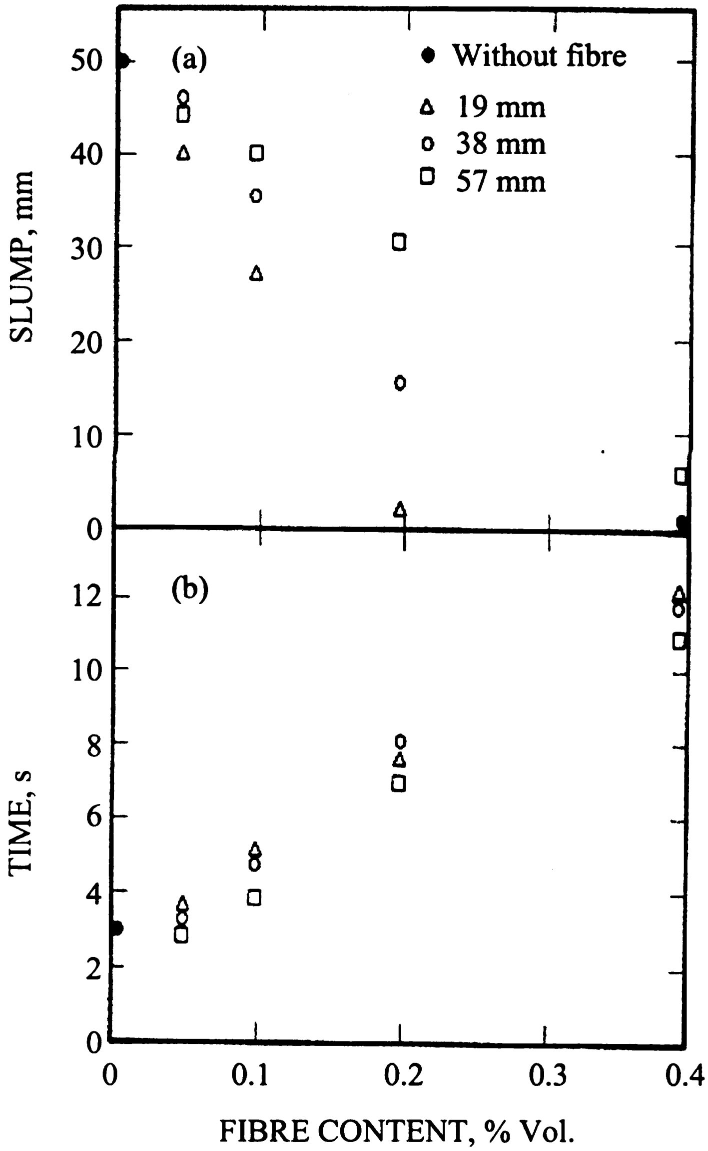

Figure 2.21. Typical Effects of Fiber Length and Content on Fresh Mix Workability: (a) Slump; (b) Vebe Time.

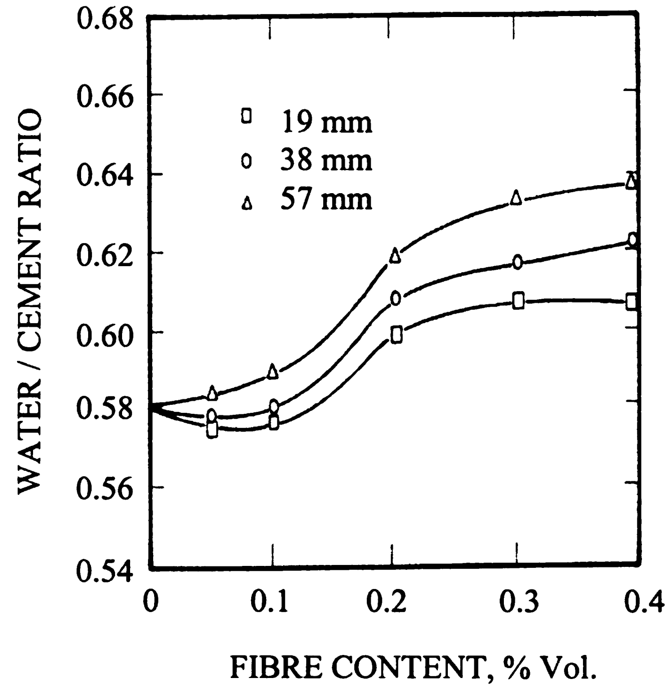

Figure 2.22. The Water/Cement Ratio Needed for Maintaining 50 mm Slump Versus Fiber Content and Length.

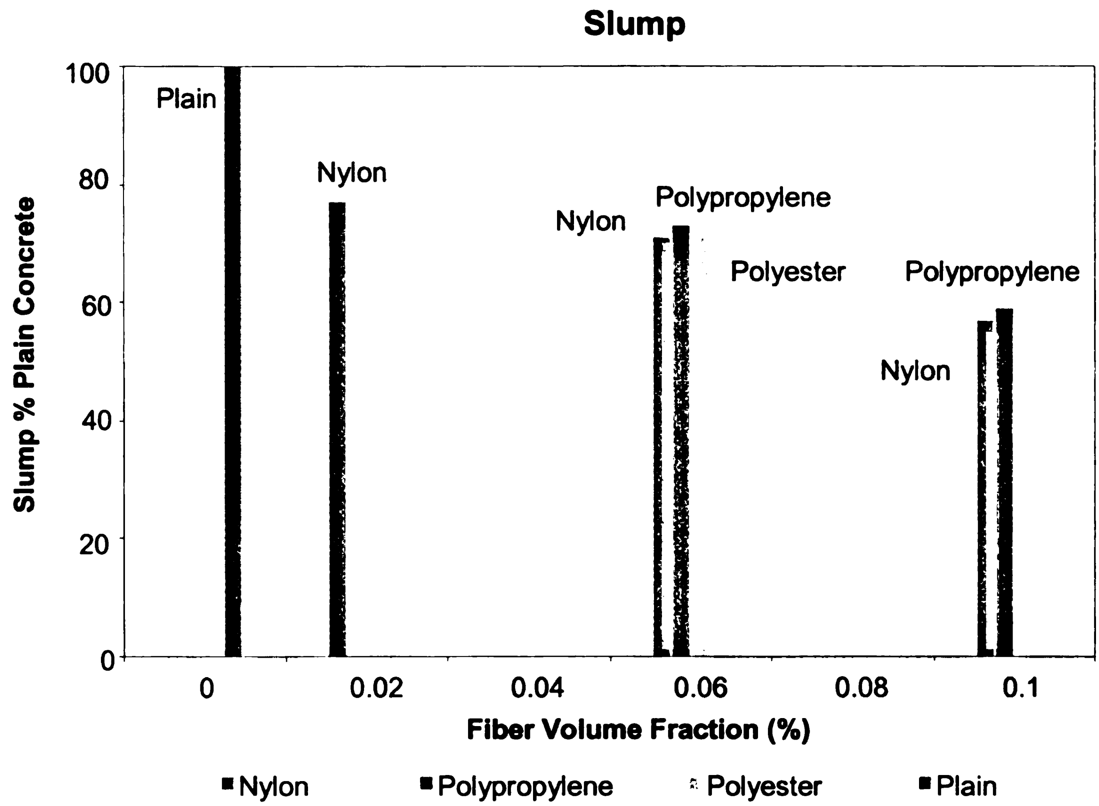

Figure 2.23. Effects of Synthetic Fibers on Slump of Fresh Concrete.

2.7.2 Resistance to Restrained Plastic Shrinkage Cracking

The available test data on restrained plastic shrinkage cracking of synthetic (and steel) fiber reinforced concrete are summarized in Figure 2.24. The synthetic fiber types covered in Figure 2.24 include polyester (Recron 3S), polypropylene, nylon, and polyethylene. It should be noted that the test data presented in Figure 1.24 were generated using different concrete materials and fiber geometric attributes; the test procedures were also somewhat different in various experimental studies reported here. It should be noted that control of restrained plastic shrinkage cracking is the primary reason (based on technically sound criteria) for use of synthetic fibers at low volume fractions (of about 0.1%) in concrete. Given the fact that different materials and test conditions are expected to cause variations in test results, Figure 2.24 provides the general indication that various synthetic fibers at relatively low volume fractions can significantly reduce the plastic shrinkage cracking of concrete. In the case of steel fibers, however, higher fiber volume fractions (exceeding 0.5%) would be needed for effective restrained plastic shrinkage crack control. The experimental procedures and test data based on which Figure 2.24 was developed are presented in Appendix B.

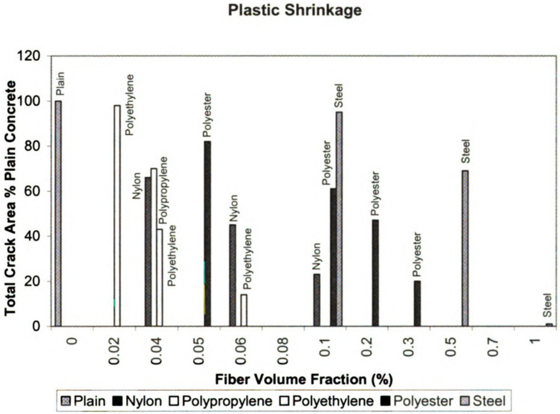

Figure 2.24 Restrained Plastic Shrinkage Cracking Test Results.

2.7.3 Resistance to Restrained Drying Shrinkage Cracking

Drying shrinkage cracking is a major problem in concrete flatwork construction. Control of drying shrinkage cracks with synthetic fibers would enable increased joint spacing, which benefits the construction process and long-term performance of diverse concrete flatwork systems including industrial floors and pavements.

The available test data on restrained drying shrinkage cracking of synthetic (and steel) fiber reinforced concrete are summarized in Figure 2.25. Synthetic fibers are observed to provide for about 70% reduction of drying shrinkage crack potential when added to concrete at volume fractions exceeding about 0.3% (depending on the particular type of synthetic fiber). The available test data cover largely low-modulus fibers; higher-modulus synthetic fibers with greater reinforcement efficiency are expected to offer enhanced drying shrinkage crack control attributes. The experimental procedures and test data based on which Figure 2.25 was developed are presented in Appendix C.

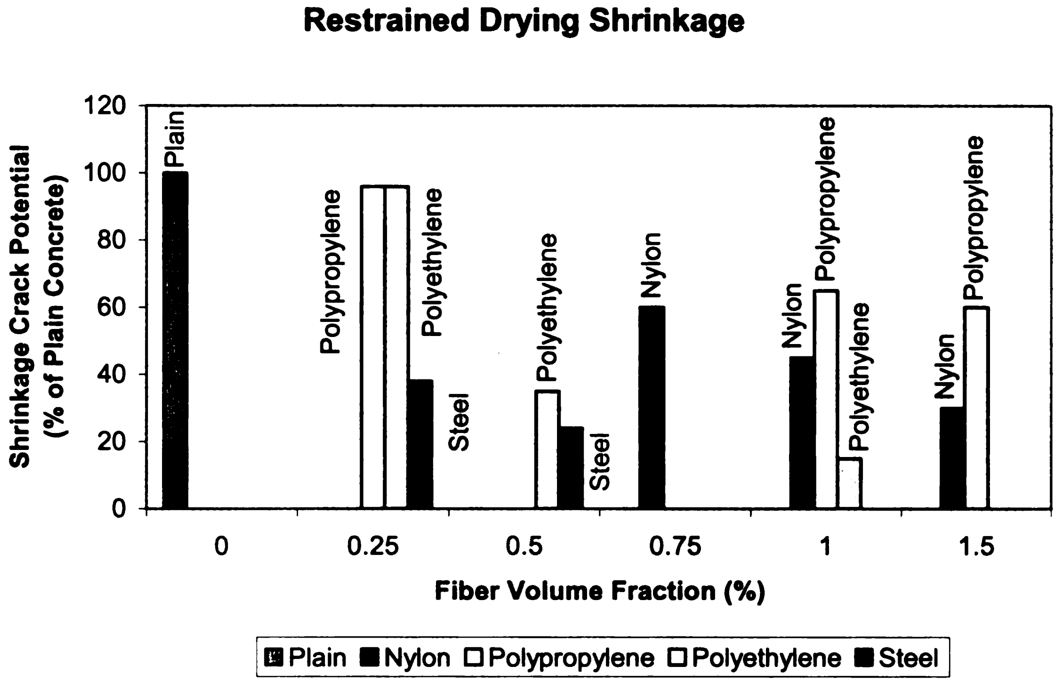

Figure 2.25 Restrained Drying Shrinkage Cracking Test Results.

2.7.4 Compressive Behavior

Typical effects of fiber reinforcement on compressive stress-strain behavior of concrete are depicted in Figure 2.26. The compressive strength of concrete is altered only slightly with the addition of fibers. There are, however, important gains in post-peak ductility of concrete in compression with the addition of increasing volume fractions of fibers.

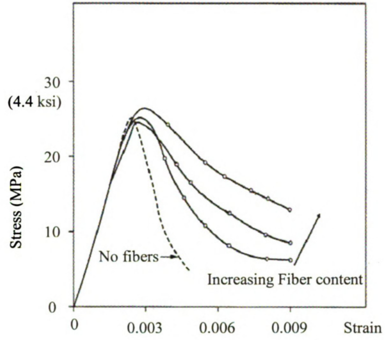

Figure 2.26. Typical Effects of Fiber Reinforcement on Compressive Stress-Strain Behavior of Concrete.

2.7.5 Flexural Behavior

Fibers make important contributions to both the flexural strength and toughness of concrete. Figure 2.27 schematically presents the effects of increasing fiber volume fraction on flexural load-deflection behavior of concrete.

Figure 2.28 summarizes the test data reported in the literature on the gains in flexural strength of concrete with the introduction of different types and volume fractions of fibers.

The results suggest that synthetic fibers at volume fractions of about 0.5% or higher make significant contributions to the flexural strength of concrete. The test data based on which Figure 1.28 was developed are presented in Appendix D.

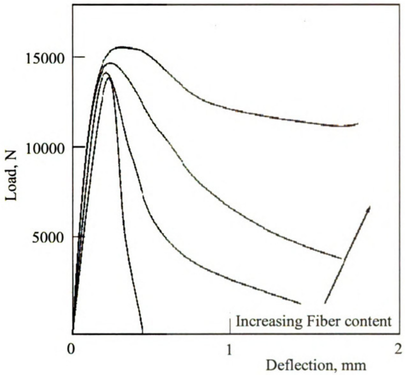

Figure 2.27. Typical Effects of Fiber Reinforcement on Flexural Load-Deflection Behavior of Concrete.

The available test data on flexural toughness of synthetic (and steel) fiber reinforced concrete are summarized in Figure 1.29. The test data reported here are presented as different toughness indices (I5, I10 & I30) of ASTM C 1018. Flexural toughness as defined here benefits from fiber pull-out at relatively high bond stress values which can account for substantial frictional energy absorption.

High bond strengths which, depending on the fiber geometry and tensile strength, favor fiber rupture prior to pull-out could favor flexural strength of fiber concrete but adversely influence flexural toughness.

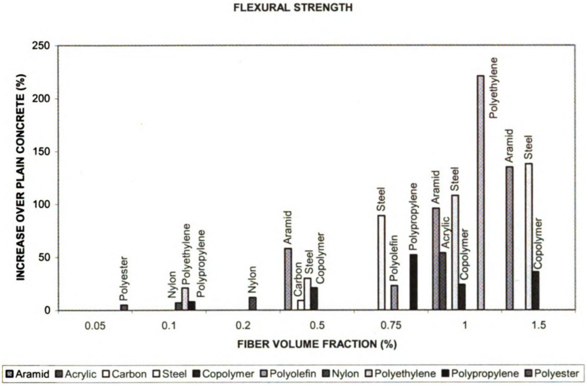

Figure 2.28. Flexural Strength Test Results.

Also, finer fibers (with smaller lengths and diameters) with relatively high surface area and relatively small fiber spacing, which could be highly effective in microcrack control and enhancement of tensile strength, may not yield favorable results in terms of flexural toughness. The results presented in Figure 2.29 should be evaluated with caution because they are produced with fibers of different geometric attributes (and also with concrete materials of different mix proportions). The results, however, provide a global view of the potentials for enhancement of the flexural toughness of concrete through fiber reinforcement. Gains of about 25% in flexural toughness of concrete can result from introduction of synthetic fibers at about 0.5% volume fraction. . The experimental procedures and test data based on which Figure 2.29 was developed are presented in Appendix E.

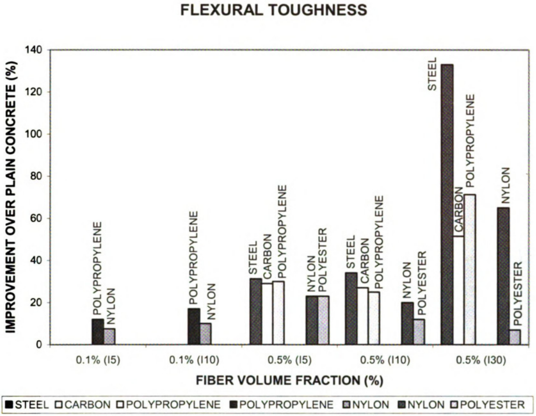

Figure 2.29 Summary Presentation of Flexural Toughness Test Results.

2.7.6 Fatigue Life

The contribution of fibers to fatigue life of concrete is a primary reason for use of fibers in applications involving repeated load application, such as pavements and machine foundations. While steel fibers have been traditionally used in such applications, the summary presentation of fatigue test data is in Figure 2.30. indicates that synthetic fibers can compete reasonably well with steel fibers in terms of contributions to the fatigue life of concrete. Fiber volume fractions of about 0.5% or more would be needed if meaningful contributions to fatigue life are desired. Synthetic fibers offer a more convenient and practical replacement for steel fibers in concrete applications where fatigue life is an important consideration. The available test data presented in Figure 2.30 on the fatigue life of synthetic fiber reinforced concrete cover low-modulus fibers; synthetic fibers of higher modulus could be even more effective in enhancement of the fatigue life of concrete. The test data based on which Figure 2.30 was developed are presented in Appendix F.

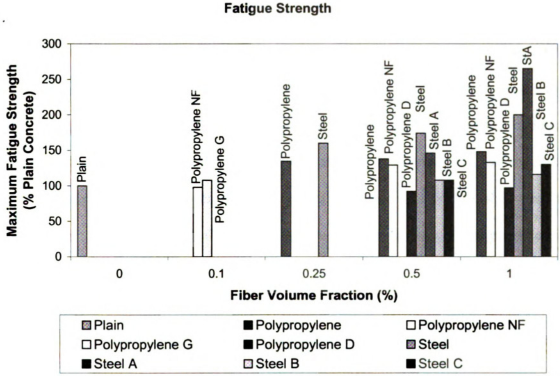

Figure 2.30. Summary Presentation of Fatigue Test Results.

2.7.7 Impact Resistance

Figure 2.31 summarizes the (drop-ball) impact test data on synthetic fiber reinforced concrete reported in the literature. The reported data cover various fiber geometric attributes and concrete mix proportions. The results, however, provide strong indications that the Recron 3S (polyester) fibers are more effective than competing synthetic fibers in enhancement of the impact resistance of concrete. More than 100% gain in impact resistance (over plain concrete) is achieved at a fiber volume fraction of 0.08%. The effectiveness of Recron 3S in enhancement of impact resistance can be attributed to the following favorable aspects of its physical and geometric attributes: (i) high elastic modulus; (ii) fine diameter and high aspect ratio; and (iii) triangular cross-section, which yields higher surface areas per unit volume of fibers when compared with the prevalent circular cross-section. The test data based on which Figure 1.31 was developed are presented in Appendix G.

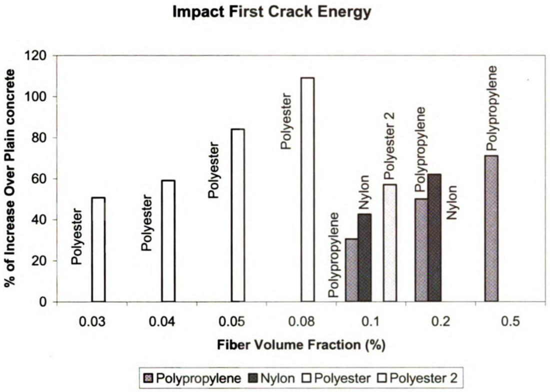

Figure 2.31. Summary Presentation of Impact Resistance (First-Crack) Test Results.

2.7.8 Abrasion Resistance

The available test data on abrasion resistance of synthetic (and steel) fiber reinforced concrete are summarized in Figure 2.32. The abrasion test results are not consistent, and the reported gains in abrasion resistance with synthetic fiber reinforcement vary between 0% to 20% (for fiber volume fractions up to 0.1%); the lack of consistency in abrasion test data also applies to steel fiber concrete where the reported gains in abrasion resistance range from 0% to 60% (for fiber volume fractions of 0.5% to 1%). More comprehensive experimental investigations are needed before reliable conclusions can be derived regarding the contributions of fibers to the abrasion resistance of concrete. The test data based on which Figure 2.32 was developed are presented in Appendix H.

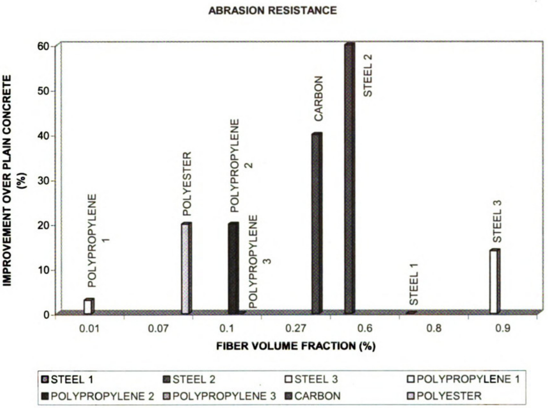

Figure 2.32. Summary Presentation of Abrasion Resistance Test Results.

2.8 Comparative Assessment of Triangular Versus Circular Fiber Cross-Sections

Fiber surface area is a key measure of its reinforcement efficiency in concrete. Fiber volume fraction, on the other hand, is a measure of cost and mixing difficulty. Higher fiber surface area-to-volume ratios are thus indicative of more efficient fiber reinforcement systems for concrete. The analysis presented below compares the surface area-to-volume ratio of fibers with triangular and circular cross-sections.

The geometric attributes of fibers with circular and (equilateral) triangular cross-sections are depicted in Figure 1.33. The surface areas (A) of the circular and triangular fibers can be calculated as follows:

Circular: $$A_{circular} = (\pi.d_f).l_f$$

Triangular: $$A_{triangular} = (3.a).l_f$$

The volumes (V) of the two fibers can be calculated as follows:

Circular: $$V_{circular} = \left(\frac{\pi.d_f^2}{4}\right).l_f$$

Triangular: $$V_{triangular} = \left(\frac{h.a}{2}\right).l_f = \left(\frac{a.\sin 60.a}{2}\right).l_f = (0.433\ a^2).l_f$$

For the circular and triangular fibers to provide the same surface areas, the following relationship should be met:

$$(\pi . d_f).l_f = (3\ a).l_f$$

For the same fiber length, this relationship implies that:

$$a = \frac{\pi . d_f}{3}$$

The triangular fiber volume can be calculated with this value of "a" as follows:

Triangular: $V_{triangular} = (0.433\ a^2).l_f = \left[0.433\left(\frac{\pi . d}{3}\right)^2\right].l_f$

The ratio of triangular-to-circular fiber volume for achieving similar fiber surfaces areas would thus be:

$$\frac{V_{triangular}}{V_{circular}} = \frac{\left[0.433\left(\frac{\pi . d_f}{3}\right)^2\right].l_f}{\left(\frac{\pi . d_f^2}{4}\right).l_f} = 0.6$$

The above calculation indicates that, in order to provide the same fiber surface area (a key measure of fiber reinforcement efficiency), with triangular fibers one needs only 60% the volume needed with circular fibers. For example, in order to provide the same fiber surface area as circular fibers at 0.3% volume fraction, one needs only 0.18% volume fraction of triangular fibers.

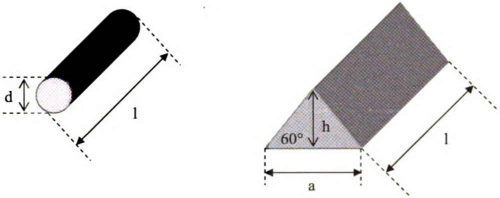

Figure 2.33. Geometric Attributes of Fibers with Circular and Triangular Cross-Sections.

2.9 Flexural and Shear Analysis of Reinforced Concrete Structural Elements with Fiber Reinforcement

2.9.1 Introduction

Structural applications of fiber reinforced concrete require design methodologies which account for the contributions of fibers to structural performance of reinforced concrete systems. In order to facilitate structural applications of fiber concrete, equations were developed which account for the contributions of fibers to flexural and shear strength of reinforced concrete structures.

2.9.2 Design Equations Flexural Strength of Fiber Reinforced Concrete Structural Elements with Conventional Steel Reinforcement

The behavior of fiber reinforced concrete in flexure comprises a linear behavior up to first crack, followed by a post-crack nonlinear behavior (Figure 2.34). The post-cracking flexural behavior for different fiber types and contents can be explained by the flexural (tensile) stress distribution at fiber concrete sections beyond first crack (Figure 2.35), which determines the effectiveness of fibers in enhancement of the flexural strength of reinforced concrete structural elements.

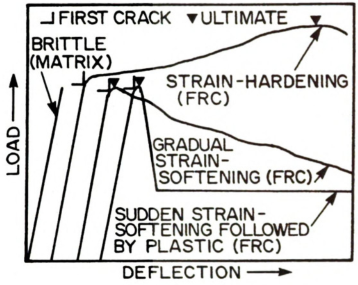

Figure 2.34. Typical Flexural Behavior of Plain Concrete Versus Fiber Reinforced Concretes With Different Fiber Volume Fractions.[17]

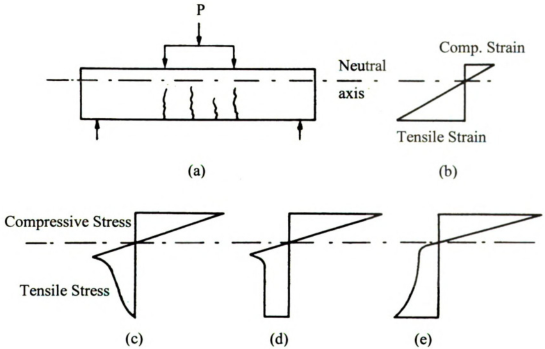

Figure 2.35. Flexural Strain and Stress Distributions in Cracked Fiber Concrete Sections. (a) Flexural Specimen Under Load; (b) Strain Distribution After Cracking; (c) (d) (e) Alternative Stress Distributions Depending on Fiber Type and Content.[13]

A beam reinforced with both fibers and steel bars, the tensile strength computed for the fibrous concrete is added to the tensile contribution of reinforcing bars at flexural failure. The basic design assumptions and nomenclature for formula are shown in figure 2.36. The equation for nominal flexural strength, M_n, of a singly reinforced fibrous concrete beam is:

$$M_n = A_s f_y \left(d - \frac{a}{2} \right) + \sigma_t \, b(h-e)\left(\frac{h}{2} + \frac{e}{2} - \frac{a}{2} \right)$$

where, $e = [\varepsilon_s \text{ (fibers)} + 0.003] \, . \, c/0.003$

The tensile strength in fiber reinforced concrete (σ_t) for use in above equation can be calculated as follows:

σ_t = (number of fibers per unit area).(mean fiber frictional bond resistance)

$$\sigma_t = \left(\frac{0.5 V_f}{\frac{\pi d_f^2}{4}} \right) \left(\tau_f \, \pi \, d_f \frac{l_f}{4} \right), \text{thus}: \quad \sigma_t = 0.5 V_f \, \tau_f \frac{l_f}{d_f}$$

$$= 0.5 (\text{volume fraction of fibers})(\text{frictional bond resistance of fibers}) \left(\frac{\text{length of fibers}}{\text{diameter of fibers}} \right)$$

For synthetic fibers which offer an ultimate bond strength exceeding frictional bond strength, we can assume that "e" is equal to "c", yielding the following equation for nominal flexural strength:

$$M_n = A_s f_y \left(d - \frac{a}{2} \right) + \left[\left(0.5 V_f \, \tau_f \frac{l_f}{d_f} \right) b(h-e) \left(\frac{h}{2} + \frac{e}{2} - \frac{a}{2} \right) \right]$$

In the above equation, "a" can be derived based on equilibrium of axial forces:

$$a = \frac{A_s f_y + \left[0.5 V_f \tau_f \frac{l_f}{d_f} b(h-c) \right]}{0.85 f_c'.b}$$

Since $c = \frac{a}{\beta_1}$, a trial and adjustment approach would be needed to solve the above equation; β_1 can be derived as follows:

$$\beta_1 = 0.85 - \left(0.05 \frac{f_c' - 4000}{1000} \right) \qquad 0.65 \leq \beta_1 \leq 0.85$$

The above expressions assume that fibers pull out of the matrix rather than rupture. For this to be true, the following expression needs to be satisfied:

$\sigma_{fu} \geq \tau_{fu} \,.\, \pi \,.\, d_f \,.\, (0.5\ l_f)$

where, σ_{fu} = ultimate tensile strength of fibers, and τ_{fu} = ultimate fiber-to-matrix bond strength.

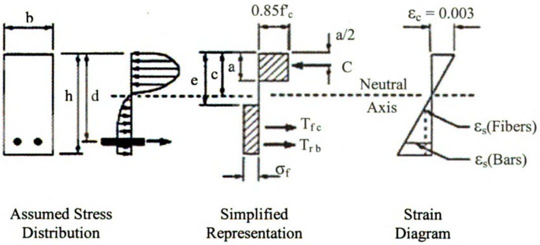

Figure 2.36. Design Assumptions for Flexural Analysis of Singly Reinforced Concrete Beams With Fiber Reinforcement.[1]

2.9.3 Design Equations for Contributions of Fiber Reinforcement to Shear Strength of Reinforced Concrete Structural Elements [20]

The random distribution of fibers in concrete provides for close spacing of fibers in three dimensions that helps with effective bridging of cracks in all directions. This behavior increases the shear capacity as well as the post-peak ductility of shear failure in structural elements. The key factors governing shear behavior of reinforced concrete elements with fiber reinforcement are shear span-to-depth ratio (a/d), fiber type, fiber volume fraction, and the compressive strength of concrete. When using fiber reinforced concrete with conventional shear reinforcement (stirrups), it is possible to increase the spacing of stirrups and reduce congestion of reinforcement through introduction of fibers.

In a fiber reinforced concrete with steel reinforcement, the contribution of reinforcement is assumed to be the same as that without fiber reinforcement; this is because this contribution is governed by yielding of steel reinforcement. The additional contribution of fiber reinforced concrete to shear strength (f_v) can be calculated as follows:

$$f_v = \alpha + \left[\beta \, (f_f \, f_t)^{3/4} \left(\rho \frac{d}{a} \right)^{1/3} (d)^{-1/3} \right] \text{ (for } a/d \geq 2.5\text{)}, \text{ (for concrete } \alpha = 1.25,\ \beta = 4.68\text{)}$$

$$f_v = 9.16 \left[\, (f_f)^{2/3} \, (\rho)^{1/3} \left(\frac{d}{a} \right) \right] \qquad \text{(for } a/d \leq 2.5\text{)}$$

where, f_f and f_t are the flexural and tensile strengths of fiber reinforced concrete, respectively, ρ is the reinforcement ratio, and a/d is the shear span-to-depth ratio.

2.10 Applications and Advantages of Fiber Reinforced Concrete

2.10.1 Historical Background

The use of fibers to improve the physical properties of a brittle matrix dates back to ancient times where straws or animal hair was used to reinforce mud bricks. Randomly oriented short fibers like straw were used in sun-baked bricks and horsehair was used to reinforce masonry mortar and plaster.

In modern times, the use of asbestos fibers in a cement paste matrix began in early 1900s. More recently, steel fibers was used in concrete in early 1960s. The concept of using polymeric fibers in concrete was tried in 1965, and their large-scale use began in late 1970s. Currently, a wide variety of steel, glass, synthetic, and natural fibers are used in different construction applications. Considerable research, development, and applications of Fiber Reinforced Concrete are taking place throughout the world.

2.10.2 A General Review of Fiber Reinforced Concrete Applications [19]

Current applications of fibers in construction can be divided to two categories: (1) non-structural and semi-structural applications; and (2) structural applications.

2.10.2.1 Non-Structural Applications

These applications usually affect the serviceability and aesthetic of the structure. In these cases, fibers are intended principally to augment the integrity of the matrix and subsequently enhance the integrity of the structural system. This can be done by crack control (crack width and area reduction). The use of relatively low fiber volume fractions minimizes the effect of fibers on the batching, mixing, and placing operations. Also, the energy absorption capability of the matrix can be improved by fibers.

Most current applications of fibers are non-structural. Fibers are often used for control of (plastic and drying) shrinkage cracks, a role classically played by steel reinforcing bars or steel wiremesh. Examples include floors and slabs, large concrete containers, and concrete pavements. In general, these structures and products have extensive exposed surface areas as well as movement constraints, resulting in high cracking potential. For such applications, fibers have a number of advantages over conventional steel reinforcement. These include: (a) uniform reinforcement distribution (with respect to location and orientation); (b) corrosion resistance, especially for synthetic fibers; and (c) labor saving by avoiding the need of deforming the reinforcing bars and placing them in form-work, yielding savings in construction time. Elimination of reinforcing bars also relaxes the constraints on concrete element shape. In some applications, the use of fibers enables elimination or reduction of the number of cut-joints in large continuous structures such as containers and pavements. Especially in pavements, joints are locations of weaknesses at which failure frequently occurs. Thus, fibers have been exploited to enhance the durability of concrete elements.

Durability is an important performance-enhancement characteristic in many industrial applications of fiber reinforced concrete. Naturally, durability has different connotations in different application contexts. For example, for containers, durability implies the life-

time prior to unacceptable leakage. For pavements, durability implies the repair time interval in order to maintain drivability. The reasons for loss of durability are also very much dependent on the specific application and field conditions.
Repair of concrete structures appears to be a sizable application of fiber reinforced concrete. This includes restoration of pavements, airfields, bridge decks, and floor slabs.

With the decaying infrastructure coupled with increasing demand on their performance, it is expected that the need for durable repairs will increase over time. A fundamental understanding of durable repairs is lacking at present. However, it is generally agreed that repair failures are often related to mechanical property incompatibility between the repair material and the substrate concrete. Dimensional stability of the repair material and delamination resistance is often cited as some of the controlling factors. Fibers have been used to advantage in this area. The adoption of new materials in the highly cost-sensitive construction, building, and precast products industries generally requires demonstration of cost advantages. The economic value of durability is difficult to quantify, but the demand for durability clearly represents one of the driving forces in use of fibers, especially when shrinkage crack resistance is considered. As mentioned above, labor saving via elimination of joints or steel reinforcement provides extra financial incentives. Another cost advantage associated with the use of fibers in concrete results from element thickness and/or weight reduction, such as in concrete pipes, pavements and building curtain wall panels. In the case of building curtain walls, weight reduction can lead to significant savings in building foundation cost, hoisting machinery, steel reinforcement, and transportation cost. Reduction of construction time is also highly valued (e.g., in fiber reinforced concrete shotcreting of tunnel linings), and translates into major cost savings for the construction industry.

The performance improvements associated with the use of fibers in concrete favor the benefit part of the cost/benefit ratio consideration. Apart from enhancement of crack resistance, fibers are valued for enhancing the energy absorption capability of concrete - often described in terms of impact resistance (e.g. in floors and slabs), and delamination and spall resistance (e.g., in concrete repair). Other performance improvements include corrosion and fatigue resistance. To achieve such performance gains, two essential properties of fiber reinforced concrete are utilized. As replacements for steel reinforcements and joints, fibers contribute to the shrinkage crack resistance of concrete. Impact resistance (and to a certain extent flexural strength) is linked to the fracture toughness of concrete. Fibers are very effective in this respect, much more so than in increasing tensile strength. The shrinkage crack resistance and toughness attributes of fiber reinforced concrete are well recognized and exploited in concrete applications in the construction industry. Because of the improved mechanical properties of fiber reinforced concrete, some industrial applications can be categorized as semi-structural. These applications involve carrying dead loads, handling (or construction) loads, loads related to restraints against dimensional movements, etc. Wall panels and some pavement applications belong to this category. However, in most of these applications, fibers are not expected to contribute to the load-carrying function of elements.

At the present time, structural applications of FRC are relatively small.

Most commercial applications of synthetic fiber reinforced concrete use relatively low volume percentages of fibers. These applications include non-structural and non-primary load bearing systems. Major applications include residential, commercial, and industrial slabs-on-grade, slabs for composite metal deck construction, floor overlays, shotcrete for slope stabilization and pool construction, precast units, slip-formed curbs, and mortar applications involving sprayed and plastered Portland cement stucco.

The fiber content in fiber reinforced concrete is generally limited by cost (the cost of fibers per unit weight is relatively high when compared with Portland cement and aggregates) and processability (measured in terms of workability for concrete mixing and casting). In special product lines, such as thin roofing tiles and other thin-sheet products, as well as in protective shields and other products that can tolerate higher cost for additional performance needs, larger amounts of fibers have been used. Examples include SIFCON (slurry infiltrated fiber concrete, invented in the United States and used in airfield pavements) and CRC (compact reinforced concrete, invented in Denmark and used in safety vaults). These fiber reinforced concretes have fiber content ranging from 5% to 20%; special processing techniques are used for their production. SIFCON requires bedding of fibers into a concrete form followed by infiltration of the fiber bed by high water/cement ratio mortar slurry. CRC requires high frequency vibration applied directly to a dense array of steel reinforcements to reach acceptable material compaction. For thin-sheet products, the slurry-dewatering technique is commonly used with high fiber contents which serve as the main reinforcement in such products.

One of the major drawbacks in many current applications of fiber reinforced concrete is that the detailed effect of fiber addition on performance improvements of concrete are often not quantified. Instead, decisions on the choice of fibers and the fiber content are often reflections of experience on the part of the user. Unfortunately, this often leads to results that fail to meet expectations. A good example is the use of steel fibers in pavements. Many successful uses of fibers in pavements have been reported, in some cases even with the pavement thickness reduced. However, just as many cases have shown disappointing results. There are a variety of reasons for this; for example, loading conditions (environmental or mechanical) can be different, and there is a certain amount of luck factor involved in successful applications. A ramification of this condition is that users become disenchanted over the use of fibers. The lack of systematic design guidelines complemented with mixed experience with fiber reinforced concrete applications can slow the spread of fiber reinforced concrete to even broader industrial applications, despite their many advantages as described above. Efforts to broaden the scope of fiber concrete applications should also account for: (1) the high cost of fibers compared with other constituents of concrete; (2) the cost-sensitive nature of the construction industry; (3) the mixed experience with the use of fiber reinforced concrete in certain applications; and (4) the lack of quantitative data on the contributions of fibers to relevant aspects of concrete performance. Both end-users and fiber suppliers need to be realistic in what performance gains can be achieved with different fiber types and contents. Research is needed to continuously improve the benefits brought about by fibers, while reducing the cost of fiber applications. Users need to be educated that part of the fiber cost can be offset by reduction or elimination of other costs associated with the use of conventional concrete without fibers. The cost pressure will always be present. One way to overcome this pressure is to continuously and systematically enhance the benefit/cost ratio of fiber addition to concrete.

2.10.2.2 Structural Applications

In structural applications, fiber reinforced concrete acts as a primary load-carrying component to provide structural integrity. At present, despite much laboratory research, the use of fiber reinforced concrete in load-carrying structural members is very limited. Use of fibers to carry load across cracks in a hardened concrete in structural design is still a novel practice. This is because of a lack of clear understanding of how fibers contribute to load-carrying capacity, confusion between material and structural strengths, lack of structural design guidelines for fiber reinforced concrete members, uncertain cost/benefit ratio, and insufficient material property specification, characterization, and test standards. These deficiencies not only limit broader use of fibers in structural applications, but also make it difficult for fiber suppliers to optimize fibers for concrete structural applications. Research findings in the last decade clearly establish that ductility of certain structural members can be greatly enhanced with the use of fibers. In addition, fibers generally favor improvements in first-crack and ultimate strengths, impact resistance, and shear resistance. If properly designed, fibers can add to member structural performance even when used together with conventional steel reinforcements. Currently, several construction projects are contemplating the application of fibers in load-carrying concrete members.

Table 2.9 reviews structural applications of fiber reinforced concrete, categorized by failure modes, and presents the performance gains associated with the addition of fibers in each application.

Table 2.9. Failure Modes of Typical Structural Members and Performance Improvements by Fbers.[19]

Structural Member/Load	Example Application	Performance Modification by Fiber
Flexural Members 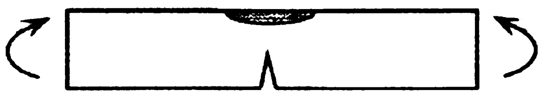	Tunnel Lining Beams Slabs	Bending Strength Pre-peak and Post-peak Ductility
Shear Members 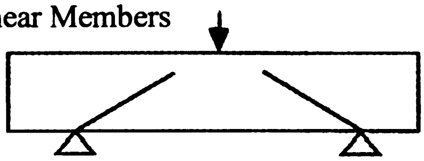	Bridge Decks Corbels Keys in Segmental Construction Steel Anchors in Concrete Members	Shear Capacity Post-cracking Safety
Torsional Members 	Poles Bridge Decks	Torsional Capacity Post-cracking Safety
Uniaxial Tension Members 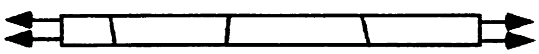	Pavements	Expand Joint Spacing
Beam-Column Connections 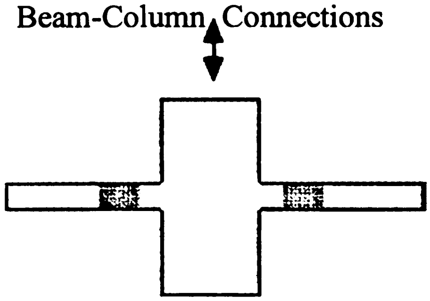	Building Frames	Seismic Resistance Reduce Reinforcement and Congestion
Column 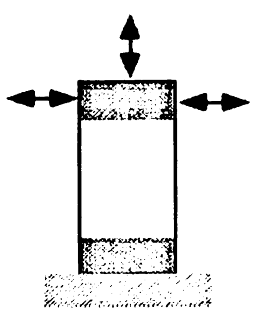	Building Columns Bridge Columns	Seismic Resistance Reduce Spalling and Enhance Steel Confinement

2.10.3 Summary Review of Fiber Reinforced Concrete Applications

Table 2.10 presents the applications of fiber reinforced concrete together with the fiber types, volume fractions, and performance and cost implications associated with these applications.

Table 2.10. Applications of Fiber Reinforced Concrete (S=Structural; SS=Semi-Structural; N=Non-Structural).[19]

Applications	Fiber	V_f (%)	S?	Properties Utilized	Performance Improvements	Cost Reduction
Pavement overlay 95 m long, 10 cm thick	synthetic + steel	0.75+0.75	SS	Shrinkage crack res. Tensile strength cap.	Durability: no failure at joints	Thick. red. to ½ No steel Reinf. No cut joint
Pavement 75-175 mm thick	steel	0.5-1	SS	Shrinkage crack res. Flexural Strength	Drability?	Greater joint spacing
Pavement "full depth" Thin bridgedeck overlay	synthetic monofils	1	SS	MOR, toughness	Impact resistance chemical resistance fatigue resistance	compare with steel fibers
Pavement 200 mm thick, 80 m long	synthetic	0.7	N	Shrinkage crack res.	Drability	No steel No shrinkage control joint
Pavement whitetopping 100 mm	steel	1	N	Wear resistance	Durability Stop rutting of asphalt Noise reduction	Less than complete replacement of flex. pavement
Repair pavement	synthetic	1-1.5	N	toughness Interface bond	Crack res. Delamination res.	Life-cost

Table 2.10. Continued

Applications	Fiber	V_f (%)	S?	Properties Utilized	Performance Improvements	Cost Reduction
Repair Airfield pavement	SIFCON steel	5 0.75	SS	Toughness Interface bond Energy absorption MOR Tensile strain cap.	Crack & spall res. Delamination res. Impact res. (dyn. Load from planes) Fatigue res.	Life-cost Simplicity in slip-form paving Incr. in joint spacing
Repair Airfield runway patch	steel	?	N	Elastic modulus COE	Compatibility with substrate concrete Durability	Life-cost
Repair Bridge substructure	steel synthetic	0.3 0.2	N	Toughness	Fatigue res. Impact res.	Reduced thickness
Repair General	synthetic + steel	1.7-2.5	SS	Toughness Interface bond	Crack res. Delamination res.	Life-cost No shrink. Reinf. Thick red.
Industrial floor restoration	Metglas	1	SS	Adhesion 3 MPa, compress. 80 MPa MOR 12 MPa	Self-leveling, Chem. corr. Res. Shock, abrasion, crack res.	Life-cost
Industrial floor rehabilitation Thin overlay	steel	0.5	SS	Ductility Toughness	Long term bond to existing base Spall res. Damage res. From forklift	Reduce production facility downtime Long term performance
Rendering, floor screeding	synthetic	?	N	Shrinkage crack resist. crack stop	Durability	No need for sand →strength and bond

Table 2.10. Continued

Applica-tions	Fiber	V_f (%)	S?	Properties Utilized	Performance Improvements	Cost Re-duction
Floors & Slabs	synthetic steel Metglass	0.1 0.3-0.5	N	Shrinkage crack re-sist. Toughness Energy absorpt. ,MOR, toughness	Durability Impact res. (dyn. Wheel load from fork lift):Easy processing, High reliabil-ity Spall res. Fatigue res. Chemical res.	Life-cost replaces mesh, re-duce la-bor, incr. joint spac-ing, faster construc-tion, lower maint. cost
Parking ga-rage floor 150 mm thick slabs 16x8 m	synthetic	0.9	N	Shrinkage crack res.	Durability	No steel mesh
Bridge deck slabs	synthetic	0.88	SS	Shrinkage crack res. Shear Re-sistance	Durability	Replace steel re-inf., con-trol corro-sion
Curtain wall panels	carbon	2-4	SS	Low den-sity Strength Shrinkage crack res.	Light-weight Seismic force red. Fire res. Dim. Stability Durability	Build. weight red. Found. cost red. Steel red. Transp. Cost red. Erec. Cost red. Const. time red. Shape flexibility

Table 2.10. Continued

Applications	Fiber	V_f (%)	S?	Properties Utilized	Performance Improvements	Cost Reduction
wall panels	carbon	2	SS	MOR Low density	Avoid corner damage & cracking Durable against sunlight, heat and salt	Increase design flexibility Lightweight
Lightweight cladding panels skin 40,75 mm thick	stainless steel	1.3	SS	MOR Low density	Durability, Res. Wind load	
Thin shells & facades	AR glass	4-5	SS	Shrinkage crack res. Tensile strength Toughness MOR	Durability Shape design flex.	No steel reinf. Low weight per unit area, building deadload, foundation cost
Tunnel lining	steel Metglass	0.5-1 >25 kg/m^3	S	Strength, MOR Toughness Energy absorption Shrinkage crack res.	Safety Durability Better bonding to underlay Maintain contour Water tightness	Replace wire-reinf., No reinf. corrosion Constr. time & labor red. (with shotcreting) Thickness red. Constr. safety
Sewage network linings	Metglass	6	SS	MOR Crack resistance	Corrosion resistance Durability	Replace wire-mesh, labor, Reduce thickness

Table 2.10. Continued

Applications	Fiber	V_f (%)	S?	Properties Utilized	Performance Improvements	Cost Reduction
Sewage network linings	Metglass	6	SS	MOR Crack resistance	Corrosion resistance Durability	Replace wire-mesh, labor, Reduce thickness
Drainage canal in tunnel	CRC steel		S	MOR	Fatigue resistance durability (100 yrs) non-conducting (elec. sys. of train) chem. res. Durability	Thin cover
Wear linings, hydraulic structures	steel		N	Abrasion res.	Durability	Life-cost
Underground railway system	synthetic	"sm. amt."	N	Shrinkage crack res.		Durability
Containers agriculture process sludge purifying	synthetic	2	SS	Shrinkage crack res. Elastic modulus	Durability Water-tightness	Mat'l cost 2x thickness red. No cut joint No steel reinf.
Septic tanks	steel	?	SS	MOR	Bending load res.	Wall thick. red., Labor &mat'l red. Mass & weight red. Cost less than mesh

Table 2.10. Continued

Applications	Fiber	V_f (%)	S?	Properties Utilized	Performance Improvements	Cost Reduction
Pipe	steel	0.3-0.5	SS	MOR Crack res. Ductility	Bending load res. Spall res. Corrosion res.	Economical w/o wire mesh reinf.
Pipe	steel	1.75	SS	MOR	Bending load res.	Wall thick. red. to 3/2 of normal
Anti-blast doors military shelters	Metglass	?	S	Ductility	Lightweight, Dynamic energy absorption	Replace steel, same weight, lower cost
Security products	CRC steel	6	S	Strength Ductility Energy absorp.	Impact res.	High-cost
Vaults and safes	steel	1-3	S	Energy absorp.	Impact res.	Thickness reduction (≈ 2/3)
Tetrapods (dolosse)	steel	?	SS	Energy absorption	Impact res.	
Sea defense work	synthetic	0.9	N	Plastic shrinkage crack res.	Durability against wind/exposure	
Concrete refractories	stainless steel	?	SS	Tensile MOR	Thermal shock resis. Spall resist.	Durability Reliability
Refractories e.g. lip ring for iron ladles, furnace hearths	stainless steel	?	SS		Thermal shock resis.	
Columns (RPC in steel tube)	steel	2-4.5	S	Strength, Toughness	Seismic resistance	Slender columns
Column/Slab cast-in-place joint	CRC steel	?	S	Toughness	Short development length for reinf.	Building system flexibility

Table 2.10. Continued

Applications	Fiber	V_f (%)	S?	Properties Utilized	Performance Improvements	Cost Reduction
Truss system	SIFCON	?	S	Tensile Compress. strength	Truss members	
Roofing tiles Extruded or Hatscheck	cellul. synthetic wollas.	4-5	N	Shrinkage crack res. Tensile strength Toughness MOR	Durability	Life-cost No steel reinf. poss. Light weight
Thin sheet products for cladding	asbestos cellul. synthetic glass synthetic carbon	varies	N	Shrinkage crack res. Tensile strength Toughness MOR	Durability	Life-cost No steel reinf. poss. Light weight
Ferrocement column	Steel- carbon	1 5	N	First crack res. MOR	Corrosion res. Durability Red. in crack width	Life-cost
Packaging and storage nuclear waste	Metglass		N	Micro-crack resist.	Contain radioactivity Durability	300 yr. containers
Stair treads	synthetic	2	SS	Low density Strength Toughness	Rust resistance Light-weight Boltable	Life-cost

2.10.4 Practical and Cost Considerations in Use of Fibers in Concrete [39,41]

Construction is a growing industry, but it does not have a strong track record as far as developments in civil engineering materials are concerned. Part of the reason comes from the lack of cooperation/coordination between the construction industry and the construction material supply industry. Joint research and development between materials suppliers and the construction industry is relatively limited. The negative impact of this stance on construction productivity, durability, and public safety cannot be underestimated.

The economic activities relevant to infrastructure have tremendous worldwide impacts. Put in economic terms, about 10% of gross domestic product derives from infrastructure construction worldwide. In the United States alone, infrastructure construction is a $400 billion industry involving 6 million jobs. There is approximately $17 trillion worth of infrastructure in place. Advanced construction materials must contribute to the growth of infrastructure, and at the same time contribute to maintaining the health of the infrastructure inventory. The implications of advanced civil engineering materials in the world economy are significant. There are a number of unique characteristics of civil engineering materials which set them apart from those used in other industries. These characteristics include:

- Low Cost – for example, concrete costs of the order of $0.1/kg (in contrast to eye contact lens which cost about $100,000/kg).
- Large volume application - e.g., on a worldwide basis, 6 billion tons of concrete and a half billion tons of steel are used in infrastructure construction annually.

- Durability requirement - our infrastructure is generally are designed for much longer life than consumer goods; e.g., most bridges are designed with a 75-year service life, compared with an automobile with a typical design life of 10–20 years.
- Public Safety - it goes without saying that the general public will not tolerate failure of infrastructure systems. The experiences from the recent Northridge earthquake in the United States and the Kobe earthquake in Japan serve important lessons.
- Construction labor - materials have to be processed into infrastructure systems. Construction workers generally do not have the same kind of training as, say, workers in the field of ceramics engineering. This implies that the material, if processed at a construction site, must be tolerant of low-precision processing.

The above unique features need to be accounted for when developing advanced construction materials. They may be regarded as overall constraints. Only materials meeting such constraints will be successfully adopted in the real world. For fiber reinforced concrete, the first two constraints on cost and applications in large-scale structures imply that fibers cannot be overly expensive and must be used in relatively small volume contents. Viewed in a more positive light, some of the above constraints also make materials serve as enabling technologies for infrastructure developments. Proper selection of fiber and matrix materials is critical in producing durable infrastructure systems. Fiber reinforced concrete materials with high ductility, for example, yield safer infrastructure systems. Materials can even lend themselves to bring about improvements in construction productivity.

For example, replacement of wire mesh or steel reinforcement in reinforced concrete structures with fibers has led to reduction in labor cost at construction sites. Finally, because of the large volumes of materials used in construction, their negative impact (through energy consumption and pollution) on environment can be significant. However, we can facilitate sustainable infrastructure development by emphasizing enhanced durability, which can be an important contribution of fibers to concrete.

Worldwide demands for cement and concrete additives (chemical, mineral, polymeric, and fibrous) are expected to expand over eight percent annually. Major technological advances have led to growing use of admixtures in concrete construction, global acceptance of diverse admixture types, higher dosage rates.

The expanding use of value-added products such as fibers represent the fastest growing practice in concrete construction; chemical admixtures will remain the dominant type of additives used in concrete, while fibers grow faster. Higher doses of synthetic fibers in value-added, specialized applications are driving new markets for concrete producers and practitioners. New applications in blast-resistant design and reinforcement for concrete are subject of undergoing research, while proven high-dosage targets like bridge decks and ultra-thin white-topping (concrete overlays) are moving forward.

Up to now, the industry appears to have weathered a period in which a lack of standard specification - and naiveté on the part of contractors and customers - led to inconsistent fiber application and disappointing as-built results. The problematic issue of standard, recipe-style national specifications for fiber-reinforced concrete with which the industry has struggled for years may turn moot as performance specifications become the norm. This would make the actual dosage unimportant as long as the final product performs as warranted. The general consensus is that fiber reinforcement should be used based on the history of performance and test data. Performance specs are getting more popular because they lend themselves to innovation.

While chemical admixtures became a half-billion dollar market in the U.S. by 2002, fibers are the fastest growing segment of the admixture market. Market growth for concrete additives in the United States is fueled by concrete-intensive construction, more widespread admixture use, increasing dosage rates, and expanded use of value-added proprietary products, especially reinforcing fibers.

The use of fibers is escalating at a growth rate of least 10 percent per year. In this context, major synthetic fiber producers are jockeying for market position. The industry has seen marketing of synthetic fibers become even more intense and competitive. Commodity pricing has flourished as new suppliers have initiated activities. Use of increasing dosages of fibers in engineered applications is emerging, in lieu of the standard low (about one pound per cubic yard) dosage. Manufacturers promoting rationale selection of fiber dosage are seeking to separate themselves from the commodity market in the United States and Europe. Current research is aimed at determining optimum fiber dosage for these applications. The commonly practiced usage of synthetic fibers at rates of 0.1 percent by volume does not do much more than effectively control plastic shrinkage cracks.

At higher dosages (more than 0.25% by volume of fibers in concrete) and when optimized for a targeted level of performance gain, fibers can bring about major improvements in concrete mechanical, physical and durability characteristics. Initially, customers and users might view mixes with relatively high fiber dosages as too expensive; they would, however, concede better-performing concrete will be the result. Fibers have been used in volume fractions as high as 10 percent in special military applications. Prospective high-dosage applications are not confined to low-volume markets. The advent of ultra-thin white-topping - placement of a cement-rich concrete pavement over asphalt - represents a growing market for fiber volume fractions exceeding about 0.25%. Fibers added at this rate yield a minimum 100 psi of residual strength, an engineering factor fiber concrete proponents cite in promoting white-topping practices. Concrete pipe is another area getting close attention from the industry. An important opportunity is emerging. Fibers can partially or fully replace corrosion-prone steel reinforcement in concrete for structural purposes and also for control of damage to pipes during shipment and installation. Fibers can also help streamline the geometric attributes of concrete pipes for ease of handling and installation; elimination of steel reinforcement through the use of relatively high fiber volume fractions can also bring about cost savings to concrete pipe manufacturers.

There is growing evidence suggesting that 0.1 percent fiber volume fraction - or 1.5 lbs. per cubic yard – should be viewed as the absolute minimum dosage that should be used when plastic shrinkage cracking is the major concern. Selection of proper fiber dosage for specific applications is a major factor in value-added applications of fibers in concrete at viable cost.

2.10.5 Example Applications and Advantages of Synthetic Fiber Reinforced Concrete [40, 42, 43]

A growing number of construction applications have benefited from use of fiber reinforced concrete. Examples of such applications are listed below.

- Slabs-on-grade, driveways, walkways, pavements subject to heavy traffic and abrasion, curbs, steps, industrial and warehouse floor slabs, tool shed bases, basement and garage floors, airport taxiways and runways.
- Below ground enclosures, appliance and equipment bases, planters and fish ponds, landscape castings, water tanks, barriers, environmental containment.
- Poured walls and footings, tilt-up panels, pre-cast mortar walls, tanks and other specialty precast shapes, burial vaults, pipes, wall panels, elevated decks, aesthetic and small precast concrete products, insulated concrete forms, pools, retaining walls and soil nailing.
- Maintenance, shotcrete, tunnel lining, slope stabilization, repair of airport aprons and taxiways, dry-packaged cement-based products, repair mortars, ultra-thin white-topping, lining large underground cavities, aqueduct rehabilitation, ground support and stabilization, mining, repair and rehabilitation of marine structures, seismic retrofits, composite decks, overlays and toppings.

- Built-in security and seismic safeguards to new structures, security and seismic upgrades of existing structures, protection against fire spalling.
- Thin sections, stucco (Portland cement plaster), poured concrete (e.g., counter-tops), and decorative concrete.
- Seismic designs, blast-resistant structures, hydrodynamic structures, equipment foundation.
- Protection against fire spalling, Retaining walls and soil nailing, Pools.

Some key applications of fiber reinforced concrete can be categorized as:

- Slabs–On–Grade and Shrinkage Crack Control
- Shotcrete
- Precast Concrete and Fiber Cement Products
- Stucco and Decorative Concrete
- Structural Applications

Examples and benefits of fiber reinforced concrete in above classes of applications are presented below.

2.10.5.1 Slabs-On-Grade and Shrinkage Crack Control

Figure 2.37 presents examples for this category of fiber reinforced concrete applications. The key advantages offered by fiber reinforcement in such applications include:

- Shrinkage and settlement crack control
- Fatigue Life
- Impact Resistance
- Load Transfer at Joints
- Abrasion Resistance and Durability
- Speed and Quality of Construction

Industrial concrete floor slab systems are often required to perform under intense loading conditions, including point loads from rack legs and impact stresses at contraction joints from vehicular traffic wheels. If improperly designed and reinforced, concrete slabs can fail, causing significant loss in productivity and increasing maintenance costs. Synthetic fiber reinforcement provides stability and integrity for concrete floor systems.

A properly designed fiber reinforced concrete slab offers an economical and efficient approach to random crack control and load transfer stability at sawed contraction joints. When considering the optimal slab design, emphasis is placed on minimization of random cracks located between joints to reduce long-term maintenance of the floor system. The reality is that the majority of all floor maintenance and repair is at the joints. Rocking, unstable joints with loose or missing filler material are not only costly to repair, but they can also cause damage to vehicles, thereby impeding the productivity of an entire operation.

a. Industrial floors

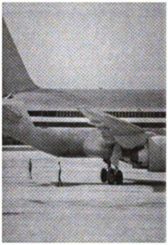

b. Airport Taxiways

c. Thin Whitetopping

d. Commercial Parking Areas

e. Pavements

Figure 2.37. Slab-On-Grade and Shrinkage Crack Control Applications of Fiber Reinforced Concrete.

2.10.5.2 Shotcrete

Examples for shotcrete applications of fiber reinforced concrete are presented in Figure 2.38. The benefits offered by fiber reinforcement in these applications include:

- Cohesion
- Shrinkage and Settlement Crack Control and Impermeability
- Toughness and Residual Strength
- Pull-Out Resistance
- Impact and Abrasion Resistance
- Speed and Quality of Construction
- Early-Age Strength

Concrete reinforcement fibers added directly into the shotcrete mix offer an alternative system to the time and labor of placing traditional reinforcement. From a safety standpoint, using fiber reinforcement prevents workers from having to place welded wire fabric or rebar reinforcement under difficult conditions. Furthermore, fiber reinforced concrete can be applied immediately upon opening the ground (before mucking if required) providing early, critical support. Because fiber reinforcement is in the mix, nozzlemen are not worried about shooting through the reinforcing mesh to ensure encapsulation, nor do they need to be concerned about properly covering the mesh for a durable lining. Rebound and sloughing are reduced because there is no vibrating mesh to knock concrete off of the wall. Using fiber reinforcement allows sprayed concrete to follow the contours of the rock face at a specified thickness. This reduces concrete material and cost because additional concrete is not required to fill the voids behind mesh reinforcement. Fiber reinforcement is in the lining, working to resist flexural and shear loading. Conversely, conventional reinforcement is typically pinned from high spot to high spot, and it varies from sitting at the wall-shotcrete interface to the outside surface of the lining.

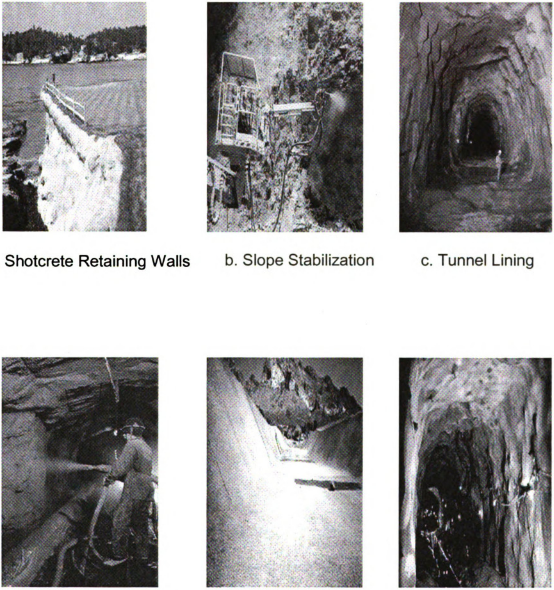

a. Shotcrete Retaining Walls   b. Slope Stabilization   c. Tunnel Lining

d. Structural Rehabilitation   e. Channel Linings   f. Mining

Figure 2.38. Shotcrete Applications of Fiber Reinforced Concrete.

2.10.5.3 Precast Concrete Products

Figure 2.39 presents examples of precast concrete products which have benefited from fiber reinforcement. The advantages of fiber reinforcement in precast concrete applications include:

- Shrinkage Crack Control, Impermeability and Durability
- Early-Age Strength
- Impact Resistance and Toughness
- Load-Carrying Capacity

The early-age stresses that precast concrete products and tilt-up panels are subjected to can be effectively addressed by adding synthetic fibers into the concrete mix. In both of these applications, concrete is subjected to early age stresses than can jeopardize the long-term durability of the product. During early stripping and lifting, concrete is vulnerable to microcracking. These microcracks become "birth defects" that can grow into major flaws during the service life of the product. Fiber reinforcement is the ideal solution to this problem. Synthetic fiber reinforcement inhibits the formation of cracks by providing an internal support system for concrete. Conventional reinforcement, such as rebar or welded wire fabric, does not address or control microcracking. As a result of adding millions of synthetic fibers, concrete is reinforced with an internal reinforcing system that becomes a uniform, integral part of the concrete composite. Fibers at proper volume fractions can be designed to resist structural stresses found in precast/tilt-up applications, either alone or in combination with conventional reinforcement.

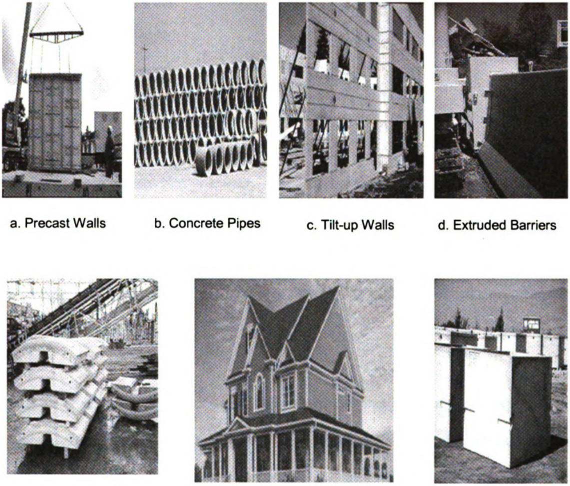

a. Precast Walls b. Concrete Pipes c. Tilt-up Walls d. Extruded Barriers

e. Segmental Tunnel Lining f. Thin Fiber Cement Products g. Tanks and Containers

Figure 2.39. Precast Applications of Fiber Reinforced Concrete.

2.10.5.4 Stucco and Decorative Concrete

Figure 2.40 presents examples of this category of fiber concrete applications. The key benefits offered by fiber reinforcement in such applications include:

- Shrinkage Crack Control
- Impermeability and Durability
- Impact Resistance
- Early-Age Strength
- Abrasion Resistance

Stucco is a thin cement plaster overlay for coating exterior walls and other exterior surfaces of buildings. Stucco relies on an excellent bond to the receiving surface. Synthetic reinforcing fibers are added to the base coat to improve the bond and reduce stucco's cracking potential caused by rapid drying or thermal variations. Modified stucco can be hand or gun-applied.

Decorative (architectural) concrete is a type of concrete that is permanently exposed to view. It requires special care in selection of concrete materials, forming, placing, and finishing to obtain the desired aesthetic appearance. Uniformity and durability are key requirements of decorative concrete. Synthetic fibers modify concrete's macro- and micro-cracking, and distribute internal stresses. Any product from stepping stones to birdbaths and precast picnic tables will profit from use of synthetic fibers.

a. Application of Stucco

b. Residential Stucco Facade

c. Decorative

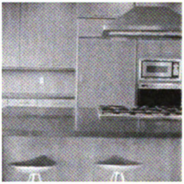

d. Kitchen Countertop

Figure 2.40. Stucco and Decorative Applications of Fiber Reinforced Concrete.

2.10.5.5 Structural Applications

Figure 2.41 presents examples of the structural applications of fiber reinforced concrete. Fiber reinforcement offers the following benefits in structural concrete:

- Toughness and Energy Absorption Capacity (Seismic-Resistant and Secure Structures
- Shear Resistance
- Crack Control, Impermeability and Durability
- Impact Resistance

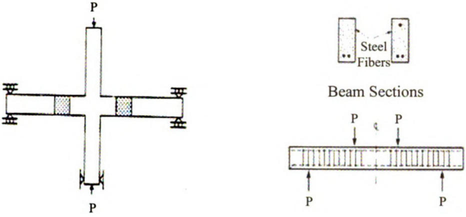

Seismic-Resistant Structures

Secure Structures with High Energy Absorption

a. Seismic- and Blast-Resistant Structures

b. Commercial Decks

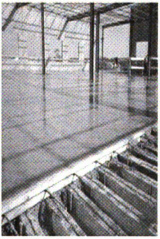

c. Composite Metal

d. Bridge Decks

Figure 2.41. Examples of Structural Applications of Fiber Reinforced Concrete.

2.11 Design of Joint Spacing for Fiber Reinforced Concrete

The equation for the required steel reinforcement in terms of joint spacing, recommended by the American Concrete Institute (ACI Manual of Concrete Practice,1998), has been modified in order to derive a relationship between joint spacing and fiber volume fraction.

The American Concrete Institute expression for the required steel reinforcement area in terms of joint spacing is as follows:

$$A_s = \frac{L.F.w.h}{24 f_s}$$ where,

A_s = the required area of steel reinforcement in sq in. per lineal foot

L = spacing between joints

F = friction factor of subgrade (a value of 1.5 is most commonly used in design)

w = unit weight of concrete (usually 145-150 lb/cu ft.)

h = slab thickness in inches.

f_s = allowable tensile stress in reinforcement in psi.(a value of 2/3 or 3/4 of yield strength is commonly used)

The steel cross-sectional area times the allowable stress in steel yields to the tensile force in the cracked section of slab, which is the force resisting crack opening. We can convert the required area of steel to the required volume fraction of fibers using the criterion that the fiber reinforcement should provide a pull-out force at cracks which is equivalent to that provided by the steel reinforcement.

Considering the random orientation of fibers in concrete, and considering the preferred pull-out (versus rupture) mode of fiber action, one can express the tensile stress (averaged with respect to concrete cross-sectional area) developed by circular fibers at a cracked section of concrete as follows:

$\sigma_t = 0.5\ V_f \,.\, \tau_f \,.\, l_f / d_f$ where,

σ_t = tensile stress in fiber reinforced concrete

τ_f = frictional bond stress of fibers

l_f / d_f = fiber length-to-diameter (aspect) ratio

Since the surface area of fibers governs their reinforcement efficiency in the preferred pull-out mode of fiber action, based on the calculations presented earlier, use of fibers of triangular cross-section in lieu of those with circular sections reduces the required fiber volume fraction for developing the same average tensile stress on concrete cross-section by 40%.The above average tensile stress times the cross-sectional area of slab will yield the tensile force applied by fibers at a cracked section of concrete slab. This force should be equivalent to that provided by the steel reinforcement specified in terms of joint spacing. Equating the force developed by fibers to that developed by steel reinforcement (expressed in terms of joint spacing) yields the relationship between joint spacing, slab thickness and fiber volume fraction (for different fiber aspect ratios) presented in Table 2.11. This relationship assumes a conservative yield strength of 65,000 psi for steel reinforcement (in the form of welded wire fabric typically used in slabs-on-grade), and considered a fiber frictional bond stress of 100 psi. Two fiber aspect ratios of 120 and 240 are considered in this table.

Table 2.11 Joint Spacing of Slab-On-Grade in Terms of Fiber Reinforcement Condition.

SLAB THICKNESS, INCHES						FIBER VOLUME FRACTION			
3.5	4	4.5	5	5.5	6	Aspect Ratio = 240		Aspect Ratio = 120	
JOINT SPACING, FEET						Circular	Triangular	Circular	Triangular
8	10	10	12.5	12.5	15	0%	0%	0%	0%
30	26	23	21	19	17	0.2%	0.12%	0.4%	0.24%
42	37	33	29	27	24	0.3%	0.18%	0.5%	0.3%
60	53	47	43	39	35	0.4%	0.24%	0.8%	0.48%

2.12 Some Practical Considerations in Use of Fiber Reinforced Concrete

A primary concern in development of fiber reinforced concrete is the uniform distribution of fibers throughout the concrete mix. Synthetic fibers are generally marketed in water-disposable bags. Fibers can thus be added to the fresh mix together with their bags. After the addition of fibers and other ingredients, sufficient mixing at proper mixing speed would be needed to thoroughly distribute fibers within the concrete matrix. Synthetic fibers can be added to mix in different sequences, with aggregates or after all other ingredients. Mixers suiting preparation of plain concrete can also be used to prepare fiber reinforced concrete at typical volume fractions below 1%.

Fiber reinforced concretes with typical fiber volume fractions below 1% can be transported, pumped and placed similar to plain concrete. The cohesiveness of fiber reinforced concrete and its segregation resistance actually facilitates pumping operations. Most potential problems related to the placement of fiber reinforced concrete are associated with the reduction in slump associated with the addition of fibers. For example, slope of chute should be increased or high-range water-reducers should be used if concrete with higher fiber dosages does not freely slide down the chute. Also, if concrete buckets are used, steep hopper slopes and large gate openings might be required for steel fiber reinforced concrete; if fibers bridge the opening, a vibrator could be attached to the side of the bucket that is activated when the bucket opens. While some fibers could slightly alter the finishing operations of concrete, concrete with synthetic fibers can be finished to achieve aesthetically pleasing surfaces which are also highly durable.

2.13 Guidelines Towards Standard Development for Use of Synthetic Fibers in Concrete

Fiber reinforced concrete has experienced rapid commercial growth emphasizing relatively low fiber volume fractions with limited effects on hardened material properties. Standard development efforts towards thorough quantification of fiber effects in concrete have been limited. Commercial success of fiber utilization in concrete now requires a technically sound approach to engineering of fiber concrete products to meet specific performance requirements of different applications.

Standards for use of fibers in concrete should emphasize, at a minimum, the following key benefits of fiber reinforcement in concrete:

- Workability (slump and inverted slump cone)
- Restrained drying shrinkage crack control
- Restrained plastic shrinkage crack control
- Residual flexural strength and flexural toughness
- Flexural strength
- Impact resistance
- Durability under extended hot water immersion, wet-dry cycles, and (depending on climatic conditions) freeze-thaw cycles

Depending on specific application requirements, other benefits of fibers in concrete (fatigue life, erosion resistance, etc.) may be subject of standard development efforts. One may also use compressive strength to ensure that the addition of fibers does not compromise basic qualities of concrete.

Standard development efforts should specify minimum gains in key relevant concrete properties (e.g., residual flexural strength, impact resistance, drying shrinkage crack control, flexural strength) which qualify fiber reinforced concrete for specific applications.

2.14 Conclusions

1. Fibers can enhance the cracking resistance, mechanical properties and longevity of concrete in different fields of application.

2. The mechanism of action of fibers in concrete largely involves control of micro-crack and crack propagation.

3. There are several applications for fiber reinforced concrete in non-structural, semi-structural, and structural members; non-structural applications, where shrinkage crack control is a key issue, are currently prevalent.

4. Life-cycle cost analysis generally justifies the initial cost of reinforcing concrete with fibers.

CHAPTER 3

INDUSTRIAL-SCALE PRODUCTION AND EXPERIMENTAL EVALUATION OF CONCRETE PIPES WITH DIFFERENT STRUCTURAL DESIGNS

3.1 Industrial-Scale Production of Concrete Pipes

The trial production runs were conducted in Northern Concrete Pipe Inc. (Charlotte, MI) which uses the dry-cast method of pipe production. The pipes that were produced all incorporated fine pozzolan and polymer emulsion (or hydrophobic admixture) for enhanced resistance to microbial-induced corrosion. The fiber volume fraction and geometry as well as the steel reinforcement ratio were the key variables in this industrial-scale experimental program. Two distinct categories of pipes were produced; one category used structural steel for achieving high load-bearing capabilities. The second category used steel reinforcement to mitigate damage during handling, transportation and installation of pipes. In the first category, synthetic fibers were used to lower the steel ratio and increase the protective cover of concrete over steel. In the second category, synthetic fibers fully replaced steel. Two series of production and testing were conducted: (i) using finer fibers and concrete mix formulations modified with fine pozzolan plus hydrophobic admixture; and (ii) using coarser fibers and concrete mix formulations modified with fine pozzolan plus polymer emulsion.

3.1.1 Production Procedure

The first step in the production process involved addition of the admixtures as well as the synthetic fibers to the empty mixer (Figure 3.1). Subsequently, other mix ingredients (cement, water, aggregates and other additives) were batched normally (Figure 3.2), and mixing followed normal procedures. Introduction of the new additives (for enhanced resistance to microbial-induced corrosion) and fibers did not require any major deviation from normal mixing techniques. The presence of fine pozzolan and fibers could increase the demand for paste and plasticizer, which could be partly compensated for the the addition of polymer emulsion.

The molds for concrete pipes comprise a fixed cylindrical core with a removable tubular casing and two "end-joint molds" in the form of steel rings (bottom ring for the groove and top for the tongue). The steel cage is placed on the bottom ring (Figure 3.3) and tubular casing carries it to the core (Figure 3.4). After placement and adjustment of the steel cage into the mold (Figure 3.5), concrete is poured into the mold (Figure 3.6) and simultaneously vibrated over a period of about 2.5 minutes (which is occasionally increased to about 3.5 minutes at higher fiber volume fractions which yield drier concrete mixtures). The top steel ring (tongue mold) is then placed over the concrete (Figure 3.7), and subsequently, concrete is compacted by placing a heavy metal plate on the top surface of concrete pipe and pressing it down with simultaneous vibration of the mold (Figure 3.8).

After placement and compaction of concrete (generally with steel reinforcement) in pipe molds, the whole assembly, except for the inner core, is moved to the curing area, and the outer case that holds the fresh concrete pipe is then removed (Figure 3.9); this particular practice of immediate demolding is possible because the "dry-cast" method of concrete pipe production uses relatively dry mixtures which provide some resistance against collapse immediately after placement and compaction. Concrete pipes are subject to steam curing at 140°F temperature over a 10-hour period. Concrete specimens were also made (Figure 3.10) with the modified concrete formulations used in production of some pipes, and were cured together with pipes for assessment of the mechanical attributes of concrete materials.

Figure 3.1. Addition of New Admixtures.

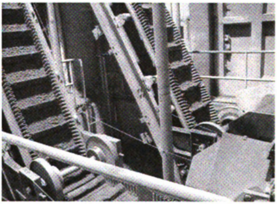

Figure 3.2. Aggregates Being Carried to the Batch

Figure 3.3. Steel Cage on the Bottom Ring

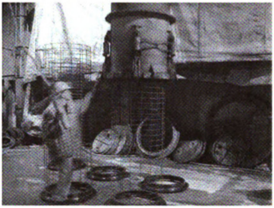

Figure 3.4. Carrying the Cage to the Core

Figure 3.5. Adjustment of Steel Cage into Mold

Figure 3.6. Pouring of Concrete into Mold

Figure3.7 .Placing the Tongue Mold Onto Concrete

Figure 3.8. Compaction Under Pressure & Vibration.

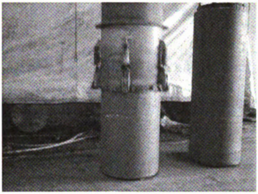

Figure 3.9. Immediate Demolding of Concrete Pipe

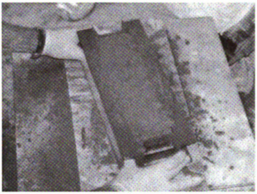

Figure 3.10. Preparation of Concrete Specimens

3.1.2 Materials and Pipe Reinforcement Conditions: First Production Series

The pipes which are subject of the first series of production runs are listed below. The first pipe is a standard class IV C-wall pipe. This pipe provides the reference performance attributes against which pipes 2 through 5 will be evaluated. Pipes 2, 3 and 4 are similar to the first pipe except that the two layers of steel were replaced with one layer of steel reinforcement positioned at the middle of the pipe wall thickness, and the concrete formulation incorporates different synthetic fiber volume fractions. Pipe 5 is distinguished from pipe 4 by the geometric attributes of the synthetic fiber. Pipes 6 through 10 are those which do not need steel reinforcement for load bearing purposes but only for mitigating damage during transportation, handling and installation. Fibers were used at different volume fractions in these pipes to fully replace steel reinforcement. Two types of PVA (Polyvinyl Alcohol) fibers were used in the trial production runs: Type I: RECS 7x6 (Length = 6 mm, Diameter = 0.026 mm); Type II: RECS 100x12 (Length = 12 mm, Diameter = 0.1 mm).

1. ASTM C76 class IV C-wall pipe. (2 layers of reinforcement) with 0% fiber.

2. Same as 1, with 1 layer of reinforcement positioned at the middle of pipe wall. (Reinforcement=0.08 square inches/ft).with 0% fiber.

3. Same as 2, with 1% fiber type I (With reduced fine and coarse aggregates by 10%).

4. Same as 2, with 1.5% fiber type I (With reduced fine and coarse aggregates by 10%).

5. Same as 2, with 1.5% fiber type II (With reduced and coarse aggregates by 10%).

6. Same as 2, with 0% fiber without steel reinforcement.

7. Same as 2, with 0.3% fiber type I without steel reinforcement.

8. Same as 2, with 0.5% fiber type I without steel reinforcement.

9. Same as 2, with 0.5% fiber type II without steel reinforcement.

10. Same as 2, with 1% fiber type I without steel reinforcement. (With reduced fine and coarse aggregates by 10%).

In addition to above pipes, a Control Pipe similar to Pipe 1 above but with conventional (in lieu of refined) concrete mix proportions was also produced and tested.

All pipes had the internal diameter of 27 inches, wall thickness of 4 inches, and length of 8.5 feet. The reinforcing steel cage was 3 x 6 - W 2 x W 2.5 (W 2 circumferential & W 2.5 longitudinal). Relatively fine synthetic fibers (6x0.026 mm; and II: 12x0.1 mm) were used in the first series of pipes produced. All concrete mixtures incorporated fine pozzolan (replacing 7.5% of Type I Portland cement by weight). The concrete mixtures incorporated (cement + fine pozzolan) and fly ash contents of 437.5 and 142.4 lb/yd^3, respectively. The normal mix for concrete pipe production comprised fine-to-coarse aggregate ratio of 1.5, with water content of about 19 gallons/yd^3. In the case of unreinforced concrete pipes, in order to enhance stability of fresh mix for immediate demolding, the coarse-to-find aggregate ratio was adjusted to 1.5 (with 1896 lb/yd^3 coarse aggregate and 1265 lb/yd^3 fine aggregate), and the water content was reduced to 19 gallons/yd^3. In mixtures which incorporated synthetic fibers, the total aggregate content was reduced in order to increase the paste content for enhanced dispersion of (and bonding to) fibers. Also, the plasticizer content was increased at higher fiber volume fractions in order to restore workability (ease of compaction) of fresh concrete mixtures. Concrete formulations were adjusted slightly throughout the first series of production runs in light of the experience gained during the process. It should be noted that "workability" is an application-specific term; an acceptable workability depends strongly on actual production conditions and demands, which cannot be easily reproduced in laboratory. The adjustments in concrete mix listed below were made to meet the workability requirements under industrial-scale production conditions.

1. The first mix was the regular mix for a reinforced concrete pipe.

2. Since the first mix appeared to be somewhat dry, 30% more plasticizer was added to the second mix.

3. Because introduction of fibers makes the mix drier than normal, fine and coarse aggregates were reduced by 5% for this mix.

4. Since this mix had a large fraction of fibers (1.5%), the aggregates were reduced by 7.5%, and also 30% more plasticizer wad added to the mix to enhance its workability.

5. Because of a mistake in the batching process, a regular mix was used in this pipe.

6. This non-reinforced pipe collapsed upon demolding in the first trial effort because it could not support its own weight without the steel cage, and the binding effect of the paste with aggregate interlocking proved to be inadequate to prevent collapse. After changing the mix proportions to the one introduced above for non-reinforced concrete pipes, the demolded pipe did not collapse.

7. This mix is the same as the one used successfully in Pipe No.6, with fibers and 30% extra plasticizer added. This pipe, however, collapsed probably due to the addition of plasticizer which made the fresh mix more mobile, and also possibly because of the interaction of fibers with the moisture content of these dry mixtures, which could lower the binding qualities of cementitious paste in fresh concrete.

8. The same mix as No.7.

9. The same mix as No.7.

10. Because of the high fiber volume fraction (1%), the aggregate content was reduced by 5%, and also 60% extra plasticizer was added. This pipe was difficult to compact, and collapsed upon demolding.

The experience gained with industrial-scale production of refined concrete pipe formulations using relatively high volume fractions of finer fibers highlighted the critical significance of tailoring the aggregate, plasticizer and fiber mix proportions to reduce special workability requirements in concrete pipe production, especially when steel reinforcement is not used and concrete is left alone (in dry-case method of production) to carry its own weight immediately after placement and compaction.

3.1.3 Materials and Pipe Reinforcement Conditions: Second Production Series

The pipes which were subject of the second production series are listed below. The second series of pipes used modified material formulations (with 10% of cement replaced with fine pozzolan and polymer emulsion added at 10% by weight of cementitious materials) for enhanced resistance to microbial-induced corrosion. The first pipe is a standard class IV C-wall pipe. This pipe provides the reference performance attributes against which pipes 2, 3, 3', and 4 were evaluated. Pipes 2, 3, 3', and 4 are similar to the first pipe except that the two layers of steel were replaced with one layer of steel reinforcement positioned at the middle of the pipe wall thickness, and the concrete formulation incorporated different synthetic fiber volume fractions. Pipes 5 and 6 are those which do not need steel reinforcement for load-bearing purposes but only for mitigating damage during transportation, handling and installation. Relatively coarse fibers were used at 2% volume fraction in these pipes to fully replace steel reinforcement. Two types of PVA (Polyvinyl Alcohol) fibers were used in the trial production runs: Type I: (Length = 15 mm, Diameter = 0.3 mm); and Type II: (Length = 12 mm, Diameter = 0.2 mm). Mix formulations were not adjusted to compensate for the effects of fibers in the second series of production runs; as a result, due to compaction problems developed with 2% volume fraction of 12x0.2 fibers, only one fiber type (15x0.3 mm at 2% volume fraction) was finally considered in the successfully produced pipes of the second production series.

0. ASTM C76 class IV C-wall pipe. (2 layers of reinforcement) with 0% fiber (with half the dosage of fine pozzolan and polymer emulsion).

1. ASTM C76 class IV C-wall pipe. (2 layers of reinforcement) with 0% fiber.

2. Same as 1, with 1 layer of reinforcement positioned at the middle of pipe wall. (Reinforcement=0.08 square inches/ft), with 0% fiber.

3. Same as 2, with 2% fiber type I (15x0.3 mm)

3'. Same as 3

4. Same as 2, with 2% fiber type II (12x0.2 mm)

5. Same as 2, with 0% fiber without steel reinforcement.

6. Same as 2, with 2% fiber type I (15x0.3 mm) without steel reinforcement.

All pipes in second series of production had the internal diameter of 27 inches, wall thickness of 4 inches, and length of 8.5 feet. The reinforcing steel cage was 3 x 6 - W 2 x W 2.5 (W 2 circumferential & W 2.5 longitudinal). Relatively coarse fibers (15x0.3 mm or 12x0.2 mm) were used in the second series of production at 2% volume fraction. All concrete mixtures incorporated fine pozzolan and polymer emulsion. The concrete mixtures incorporated (cement + fine pozzolan) fly ash and polymer emulsion contents of 437.5, 142.4 and 58 lb/yd^3, respectively. The normal mix for concrete pipe production comprised fine-to-coarse aggregate ratio of 1.5, with water content of about 19 gallons/yd^3. In the case of unreinforced concrete pipes, in order to enhance stability of fresh mix for immediate demolding, the coarse-to-find aggregate ratio was adjusted to 1.5 (with 1896 lb/yd^3 coarse aggregate and 1265 lb/yd^3 fine aggregate), and the water content was reduced to 16 gallons/yd^3. The exact water content used in different pipe formulations was adjusted throughout the trial production runs in light of the experience gained during the process. It should be noted that "workability" is an application-specific term; an acceptable workability depends strongly on actual production conditions and demands, which cannot be easily reproduced in laboratory. In some cases, some balling of fibers was observed, which could have been reduced with prior wetting of fibers, adjustment of mixing sequences and durations, and also by increasing the paste content of the mix. The adjustments in concrete mix listed below were made to meet the workability requirements under industrial-scale production conditions.

0. The concrete matrix was the normal one used for reinforced concrete pipes, except that the fine pozzolan and polymer emulsion were introduced (at half the desired dosage).

1. The concrete matrix was the normal mix modified with fine pozzolan and polymer emulsion.

2. Same concrete matrix as Pipe 1, but with slightly increased water content.

3. Same concrete matrix as Pipe 1.

3'. Same mix as Pipe 1.

4. Same concrete matrix as pipe 1; this pipe (with 2% volume fraction of 12x0.2 mm fibers) could not be compacted.

5. Aggregate proportions was modified for production of plain pipe, with fine pozzolan and polymer emulsion added at normal dosages.

6. Same concrete matrix as Pipe 5.

The experience gained with industrial-scale production of refined concrete pipe formulations highlighted the critical significance of tailoring the paste and plasticizer contents in the presence of higher volume fractions of finer fibers in order to meet the workability requirements in concrete pipe production.

The concrete pipes produced in the plant were steam-cured at 140 °F for 10 hours, and were prepared for the performance of three-edge bearing tests which will reflect on their load-bearing capacity and also toughness for damage control during transportation and handling.

3.2 Experimental Evaluation of Concrete Pipes

Two sets of tests were performed on concrete pipes.(in Northern Concrete Pipe Inc. facility in Charlotte, MI). The three-edge bearing test) was performed on all pipes for assessment of flexural strength (or external load crushing strength); joint shear capacity tests were performed on some pipes in the first series.

3.2.1 Three-Edge Bearing Test Procedures

In the three-edge-bearing test, the pipe is supported on a lower bearing of two parallel longitudinal strips, and the load is applied uniformly along the pipe length using an upper bearing strip. Both the lower and the upper bearing strips are extended the full length of the pipe. Figure 3.11 through 3.12, and 3.13 show the three-edge bearing test configuration, and Figure 3.14 shows the bearing strips.

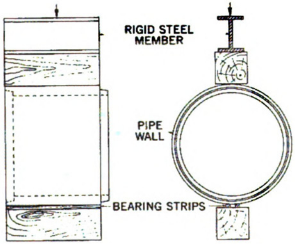

Figure 3.11. Schematics of 3-Edge Bearing Test Set-Up.

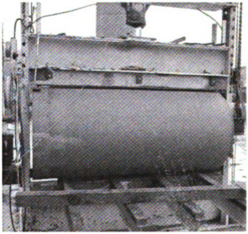

Figure 3.12. 3-Edge Bearing Test Set-Up.

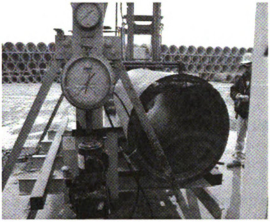

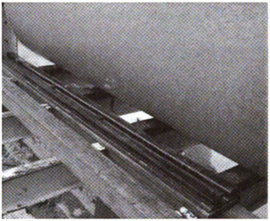

Figure 3.13. Front View of 3-Edge Bearing Test. *Figure 3.14. Loading Strips in 3-Edge Bearing Test*

The objectives in the three-edge test are to determine the load corresponding to 0.01" crack width, and also the peak load-carrying capacity of concrete pipes. With additional instrumentation, we also obtained the load-deflection behavior of pipes during tests, which can be used to assess their ductility and energy absorption capacity. A computer-based data acquisition system was used to collect the outputs of a load cell (Figure 3.15) and a displacement transducer (Figure 3.16) throughout each pipe test.

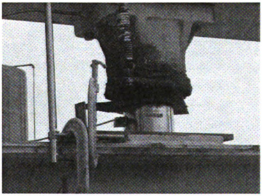

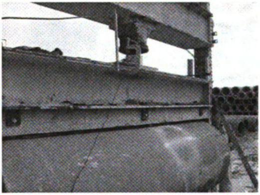

Figure 3.15. Load Cell *Figure 3.16. Displacement Transducer*

Under increasing load levels in 3-edge bearing test, first vertical cracks develop inside the pipe at invert and crown locations as shown in Figure 3.17. Further increase in load generates horizontal side cracks on the outside surface of pipes (Figures 3.18 and 3.19). The load corresponding to 0.01" crack width was determined through monitoring of the width of the first (vertical) crack formed on the pipe (Figure 3.20). Pipes with steel reinforcement exhibit a desirable ductile behavior while those without steel reinforcement (and also without desirable fiber reinforcement condition) fail in a brittle mode (Figures 3.21 and 3.22) in the conventional three-edge bearing test.

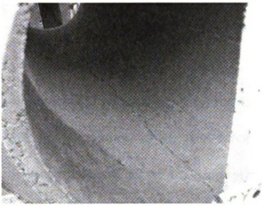

Figure 3.17. First Vertical Crack Inside of the Pipe

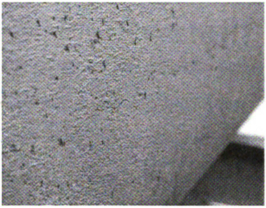

Figure 3.18. Second Horizontal Crack Outside of the Pipe

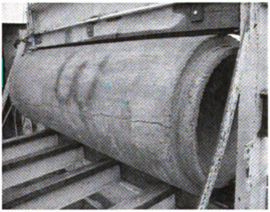

Figure 3.19. Global View of Second Figure Horizontal Crack

3.20. Crack Width Measurement

Figure 3.21. Brittle Failure of Unreinforced Pipe

Figure3.22. Another View of Failed Unreinforced Pipe

3.2.2 Three-Edge Bearing Test Results

The pipes which were produced successfully during the first series of pipe production are introduced in Table 3.1. Figures 3.23 and 3.24 present the load-deflection curves for pipes with and without steel reinforcement, respectively, in three-edge bearing tests. The loads corresponding to the first carck, 0.01" crack width, peak capacity, and post-peak region of concrete pipes are summarized in Table 3.2. Figure 3.25 presents the load at 0.01" crack width and the peak load of different pipes.

Table 3.1. Successfully Produced Series One Pipes.

PIPE	STEEL REINFORCEMENT	FIBER CONTENT	
CONTROL	TWO LAYERS	0%	
# 1	TWO LAYERS	0%	
# 2	ONE LAYER	0%	
# 3	ONE LAYER	1%	TYPE I
# 4	ONE LAYER	1.5%	TYPE I
# 5	ONE LAYER	0.75%	TYPE II
# 6	NO STEEL REINFORCEMENT	0%	
# 8	NO STEEL REINFORCEMENT	0.5%	TYPE I
# 9	NO STEEL REINFORCEMENT	0.5%	TYPE II

TYPE I : L=6 mm, D=0.026 mm , TYPE II : L=12 mm, D=0.1 mm

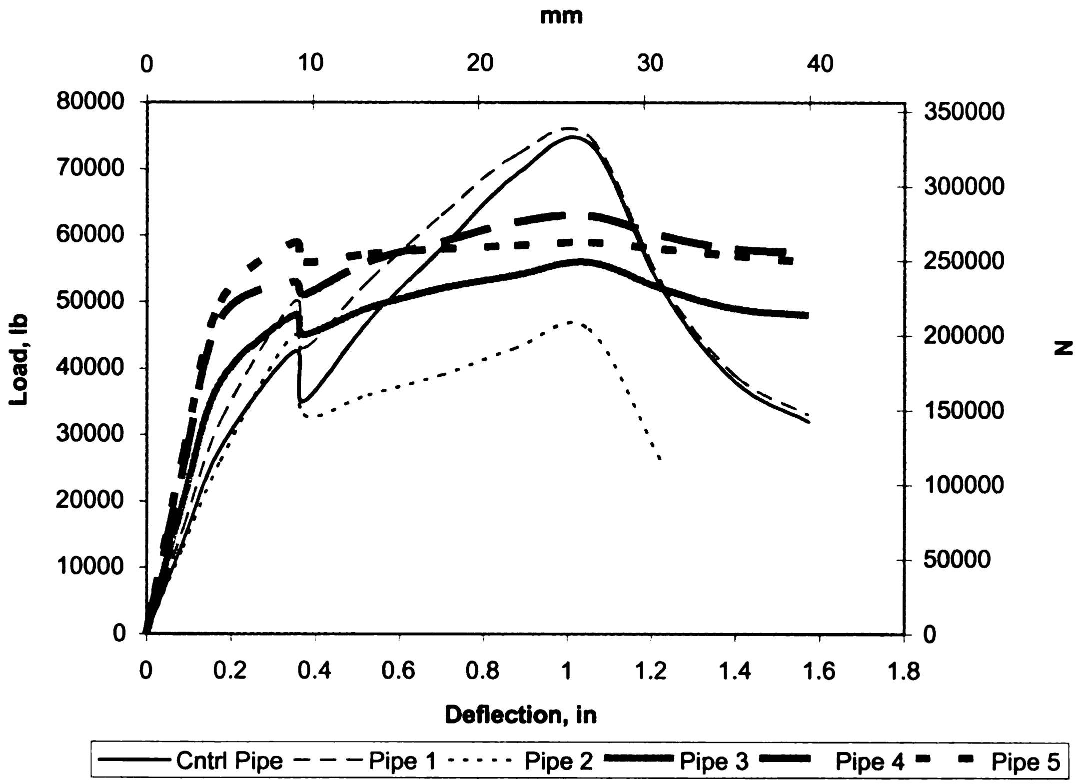

Figure 3.23. Load-Deflection Curves in Three-Edge Bearing Tests on First Series Pipes with Steel Reinforcement.

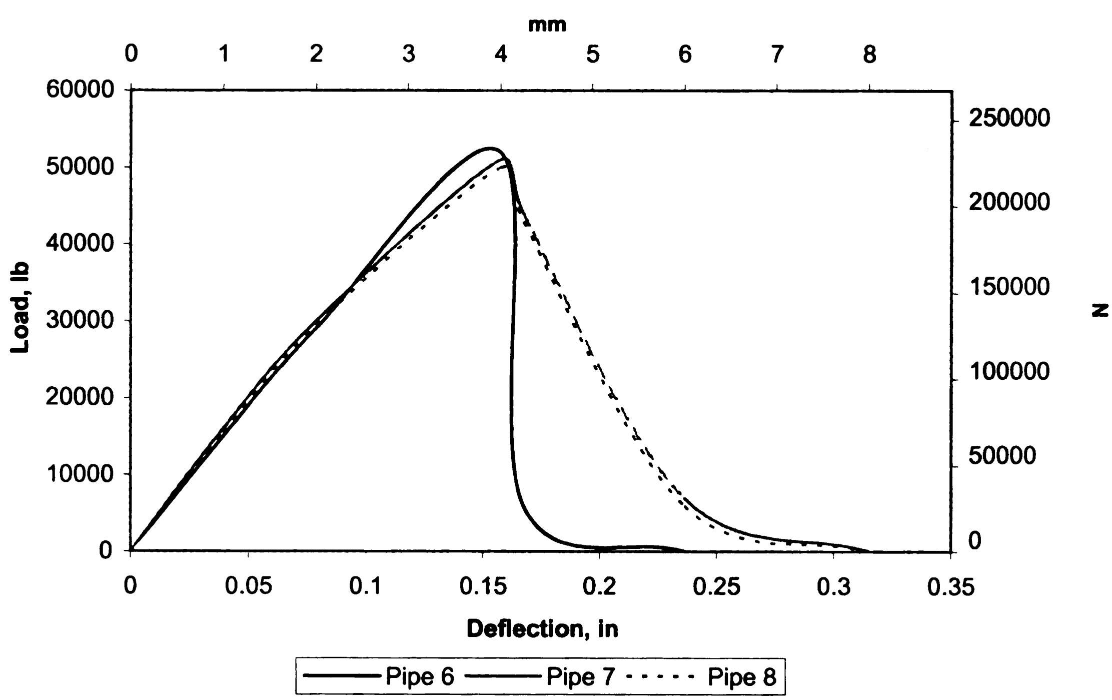

Figure 3.24. Load-Deflection Curves in Three-Edge Bearing Tests on First Series Pipes Without Steel Reinforcement.

Table 3.2. Summary Presentation of Different Load Levels in Three-Edge Bearing Tests on Pipes of First Series.

Pipe	Possible First Crack Load (lb)	Load @ 0.01" Crack (lb)	Peak Load (lb)	Maximum Post-Crack Load (lb)
Control	37500	42500	74000	N/A
# 1	25000	50000	75000	N/A
# 2	26000	45000	46000	N/A
# 3	48000	56000	56000	38000
# 4	53000	63000	63000	47500
# 5	52500	59000	59000	53000
# 6	N/A	47500	47500	N/A
# 8	51000	52000	52000	N/A
# 9	48000	50000	50000	N/A

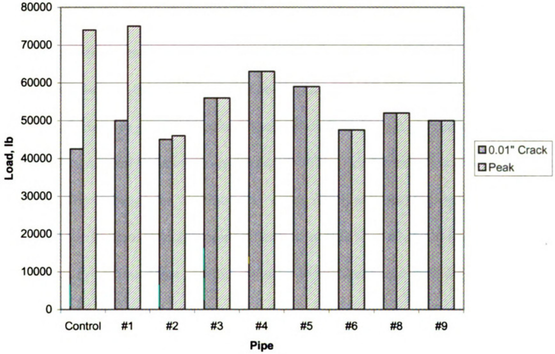

Figure 3.25. Loads Corresponding to 0.01" Crack Width and Peak Capacity of Different Pipes of First Series.

The three-edge bearing test results for the first series of pipes presented above indicates that:

1. Comparison of the Control Pipe Versus Pipe #1 provides a basis to determine the effects of mineral and chemical admixtures (without fibers) on structural performance of concrete pipes. Addition of mineral and chemical admixtures for enhancement of the resistance of concrete to microbial-induced corrosion does not compromise the structural performance of concrete pipes. The control concrete pipe (with conventional concrete mix – without fibers) and Pipe 1 (with refined concrete mix – without fibers) provide similar performance attributes (with the refined mix offering slightly higher load levels).
2. Pipes #2, #3 and #4 were produced and tested in order to determine the effects of fiber reinforcement on concrete pipes with one layer of steel reinforcement. Comparison of these pipes with Pipe #1 also provides a basis to assess the potential of fibers to partially replace steel reinforcement (i.e., to reduce the required number of steel layers from two to one). Fiber reinforcement is observed to substantially enhance the load at 0.01" crack width and also the peak load of pipes with one layer of steel (compare fiber reinforced Pipes #3, #4 & #3 versus Pipe #2 which is without fiber reinforcement). When compared with Pipe #1 with two layers of steel (without fibers), the fiber reinforced pipes with one layer of steel (Pipes #3 & #4) provide increased level of load at 0.01" crack width. Hence, as far as the load at 0.01" crack width is concerned, fiber reinforcement of concrete pipes can reduce the required amount of steel reinforcement from two layers to one. As far as the peak load is concerned, however, fiber reinforced concrete pipes with one layer of steel (Pipes #3, #4 & #5) provide somewhat (about 15%) lower level of peak capacity when compared with the pipe with two layer of steel

and without fiber reinforcement (Pipe #1). In our opinion, the key performance requirements of concrete pipes are the load at 0.01" crack width (which marks the load beyond which pipe is no more functional) and ductility (which reflects on the ability of pipe to resist brittle and catastrophic modes of failure during transportation, installation and service). The peak load requirement could well be an indirect measure of ductility. Pipes with one layer of steel and fibers (Pipes #3, #4 & #5) actually provide a higher level of ductility (post-peak load-carrying capacity) when compared with the pipe with two layers of steel and no fiber reinforcement (Pipe #1). It is thus our conclusion that synthetic fibers can reduce the steel reinforcement requirements (and thus increase the protective concrete cover thickness over steel), which can make major contributions to the longevity of concrete pipes in aggressive sanitary sewer environments.

3. The test results on Pipes #3, #4 and #5 provide a basis to compare the effects of different fiber volume fractions and geometric attributes in concrete pipes with (on layer of) steel reinforcement. The increase in the finer fiber (Type I) volume fraction from 1% (Pipe #2) to 1.5% (Pipe #3) resulted in about 15% gain in load levels at 0.01" crack width, peak, and post-peak region. The 50% increase in finer fiber dosage does not produce a similar percentage increase in load levels because, based on observations of ruptured concrete pipe surfaces, some fiber dispersion problems start to appear at 1% volume of finer fibers; these problems tend to be more pronounced at 1.5% fiber volume fraction. A comparison of the finer (Type I) fiber used in Pipe #3 versus the coarser fiber (Type II) used in Pipe #5 suggests that the coarser fiber is probably more suitable for the high-

performance, dry-mix concrete proportions commonly used for pipe production. Coarser fibers provide reduced fiber dispersion problems; they also exhibit some level of fiber pull-out (compared to finer fibers which almost exclusively rupture at cracked concrete sections). Fiber pull-out, as far as it occurs with sufficient bond strength to mobilize a substantial fraction of fiber rupture strength, is preferred because it provides for a more ductile mode of failure.

4. Pipes #6, #8 & #9 provide a basis to assess the potential of fibers to overcome the brittle mode of failure in plain concrete pipes (without steel reinforcement). Many concrete pipes do not need steel reinforcement for load-carrying capacity. Steel is added to these pipes (with important cost implications) mainly to avoid damage to these brittle pipes during transportation and installation. Synthetic fibers could be a cost-effective replacement for steel as far as they ensure ductility of pipe failure. In the case of plain concrete pipes, with conventional hydraulic loading systems used in three-edge bearing tests, the gains in ductility with 0.5% fiber volume fraction (Pipes #8 & #9) are relatively small (compare with Pipe #6), and the pipe still exhibits a brittle mode of failure. This, however, could be a result of the load-controlled nature of the hydraulic loading systems normally used in three-edge bearing tests. These hydraulic systems (as well as the test frame) act as a spring within which mechanical energy accumulates as the peak load is approached. Although the fiber reinforced concrete pipes (without steel reinforcement) may have some level of post-peak capacity available (and may actually be far more resistant to brittle modes of failure during transportation and installation), the energy accumulated within the hydraulic loading system (and test

frame) is suddenly released beyond peak load, yielding sudden failure of pipe irrespective of some level of post-peak ductility which is probably provided through fiber reinforcement of plain concrete pipes. In other words, brittle mode of failure in fiber reinforced concrete pipes (without steel reinforcement) in three-edge bearing test does not necessarily imply that these pipes are prone to damage during transportation and installation. This hypothesis needs to be tested through implementation of experiments which more closely simulate the damaging effects that concrete pipes experience during transportation and installation.

The second series of pipes, which were produced successfully, are introduced in Table 3.3. The loads corresponding to 0.01" crack width as well as the first-crack and peak loads are presented in Table 3.4. Figures 3.26 and 3.27 show the load-deflection curves in three-edge bearing tests for the second series of steel reinforced and plain concrete pipes, respectively. The loads corresponding to 0.01" crack width as well as the peak loads for the second series of pipes are summarized in Figure 3.28. It should be noted that the plain concrete pipe #6 with 2% volume fraction of coarse (15x0.3 mm) PVA fiber reinforcement, unlike all concrete pipes tested under both first and second series, did not fail in a very brittle (almost explosive) way in three-edge bearing test; reinforcement with 2% volume fraction of the coarse (15x0.3 mm) fiber offers the promise to control damage to plain concrete pipes during handling, transportation and installation. It should be noted that pipes with one layer of steel reinforcement exhibited, after testing in three-edge bearing test, a higher level of integrity and resistance to catastrophic failure when reinforced with 2% volume fraction of coarse (15x0.3 mm) PVA fibers.

Table 3.3. Successfully Produced Series Two Pipes.

PIPE	STEEL REINFORCEMENT	FIBER CONTENT
# 0	TWO LAYERS	0%
# 1	TWO LAYERS	0%
# 2	ONE LAYER	0%
# 3	ONE LAYER	2% TYPE I
# 3'	ONE LAYER	2% TYPE I
# 5	NO STEEL REINFORCEMENT	0%
# 6	NO STEEL REINFORCEMENT	2% TYPE I

TYPE I : L=15 mm, D=0.3 mm

Table 3.4. Summary Presentation of Different Load Levels in Three-Edge Bearing Tests on Pipes of Second Series.

Pipe	Possible First Crack Load (lb)	Load @ 0.01" Crack (lb)	Peak Load (lb)
# 0	47500	52500	85500
# 1	47500	55000	87500
# 2	45000	45000	45500
# 3	60000	60300	60500
# 3'	55000	57500	57700
# 5	46250	46250	46250
# 6	53500	53500	53500

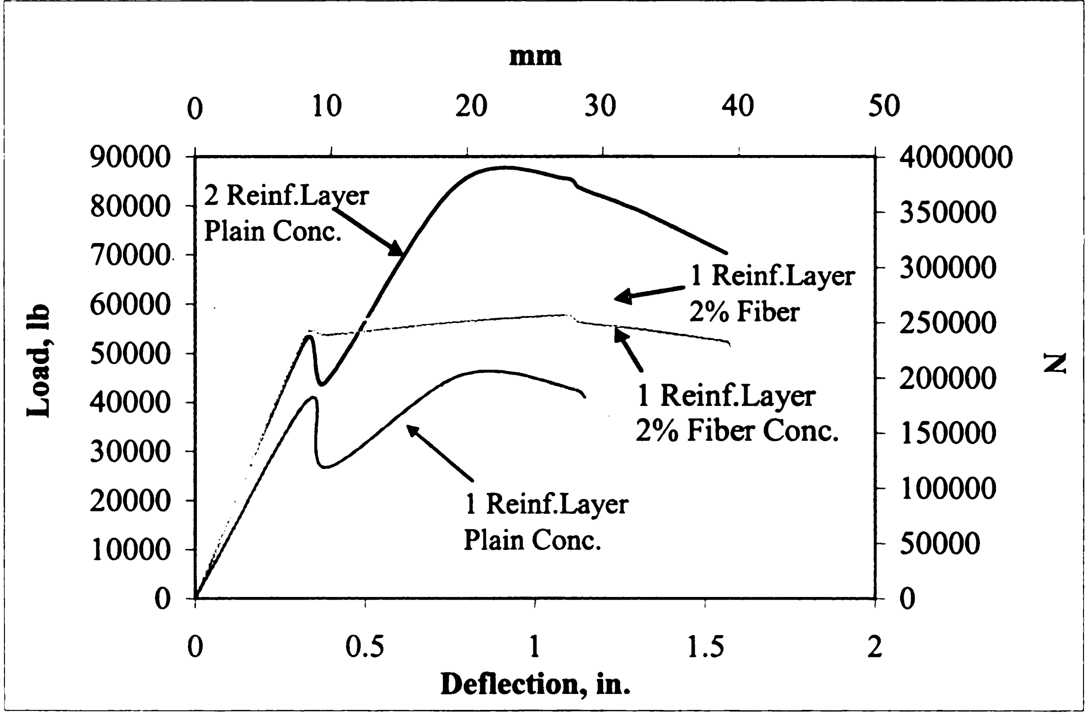

Figure 3.26. Load-Deflection Curves in Three-Edge Bearing Tests on Second-Series Pipes with Steel Reinforcement

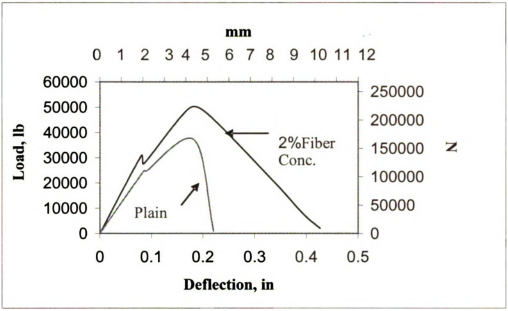

Figure 3.27. Load-Deflection Curves in Three-Edge Bearing Tests on Second-Series Pipes Without Steel Reinforcement.

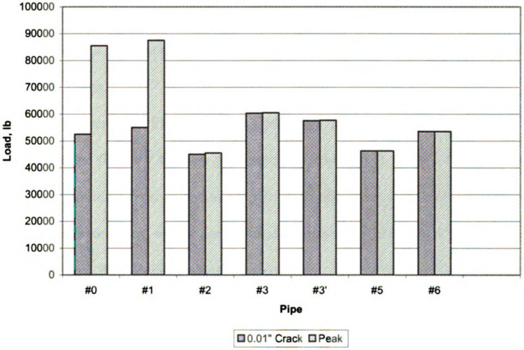

Figure 3.28. Loads Corresponding to 0.01" Crack Width and Peak Capacity of Different Pipes of Second Series.

Test results on second series of pipes (Tables 3.3 and 3.4 and Figures 3.26 through 3.28) yielded the following conclusions:

1. Coarser fibers (15x0.3 mm) can be more conveniently introduced at relatively high volume fractions (2%) into concrete mixtures used in dry-cast method of pipe production. The final selection of additives for enhancement of concrete resistance to microbial-induced corrosion (fine pozzolan and polymer emulsion) is also compatible with conventional method of pipe production. Finer fibers require increased paste and plasticizer contents for uniform dispersion in concrete mixtures which exhibit adequate workability for convenient compaction in concrete pipe production. Figure 3.29.a shows a failure surface of concrete where the uniform dispersion of coarser fibers is apparent; minor balling of fibers during production was observed (Figure 3.29.b), which could be resolved through minor increase in paste content of concrete and also by pre-wetting of the hydrophobic PVA fibers.
2. The coarser PVA fiber exhibited a prevalent tendency towards pull-out at cracks while the finer PVA fibers predominantly ruptured at cracks. The coarser fiber thus provide a more pronounced gain in ductility and energy absorption capacity of concrete pipes, which can be used to prevent brittle failure of plain concrete pipes and thus facilitate production of plain pipes which are resistant to damage during handling, shipment and installation.
3. Coarser fibers were more effective than finer fibers in enhancing the load in three-edge bearing test corresponding to 0.01" crack with of steel reinforced concrete

pipes, and also in increasing the peak load of plain concrete pipes. As far as the load at 0.01" crack width is concerned, coarse (and even fine) fibers could replace one layer of steel in pipes reinforced with two layer of steel (thus allowing an increase in protective cover thickness of concrete over steel). As far as the ultimate strength in three-edge bearing test is concerned, however, one layer of steel (in pipes with two layers of steel reinforcement) could not be replaced with coarse or fine fibers at volume fractions as high as 2%.

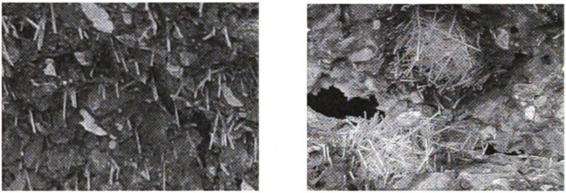

(a) Uniform Dispersion of Fibers *(b) Example of Occasional Fiber Balling*

Figure 3.29. Fiber Dispersion Conditions.

Besides the ultimate load and the load corresponding to 0.01" crack width in the three-edge bearing test, the first-crack load was also recorded during the tests. Figures 3.30.a and 3.30.b present all recorded load levels in the first and second series of tests, respectively. For lighter reinforcement conditions, the first-crack and 0.01" crack loads are relatively close; the difference would increase at higher reinforcement ratios.

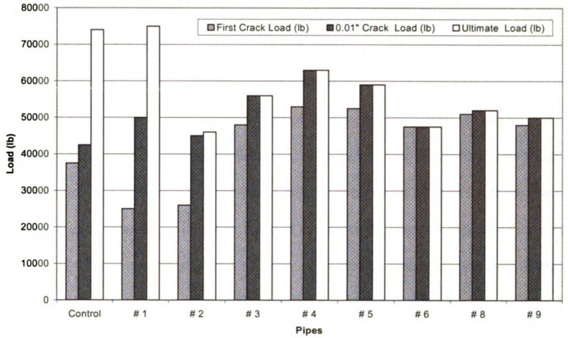

(a) First Series of Pipe Tests

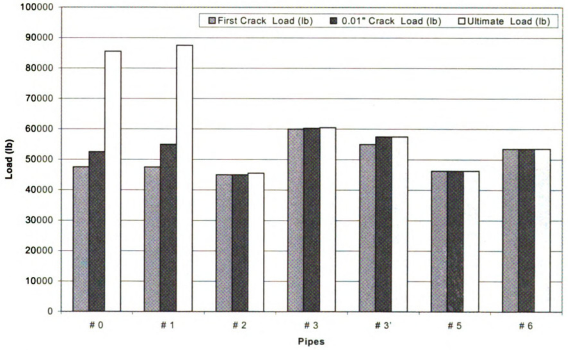

(b) Second Series of Pipe Tests

Figure 3.30. The First-Crack Load in Three-Edge Bearing Tests Versus the 0.01" Crack Width and the Ultimate Loads.

3.2.3 Joint Shear Tests

An initial attempt was made to conduct the joint shear tests using two pipes, with the test pipe providing the interior component of the joint (Figure 3.31). This test would be successful if joint fails as a result of the failure of its interior component (of the test pipe). With fiber reinforced concrete pipe, however, three attempts at the shear test configuration of Figure 3.31 resulted in failure of the exterior component of the joint (a pipe without fiber reinforcement provided this exterior component). The test pipe (interior component of) joint did not fail after few attempts. The test configuration was thus changed to that shown in Figure 3.32, with a concentrated force applied directly at the edge of the pipe end. This is a non-standard test, and the concern is that the concentrated nature of load and the local failure mechanism (Figures 3.32-3.36) lead to large variations in test results. The results of the joint shear test conducted in this investigation should thus be treated cautiously.

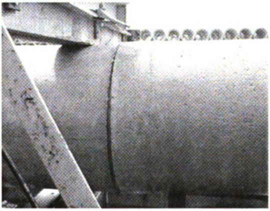

Figure 3.31. Pipe Joint Test Using Two Pipes.

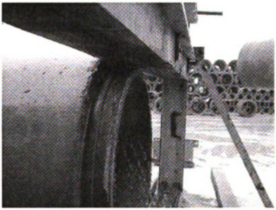

Figure 3.32. Concentrated Load Test on Pipe Edge.

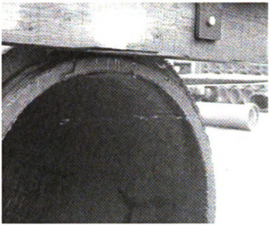

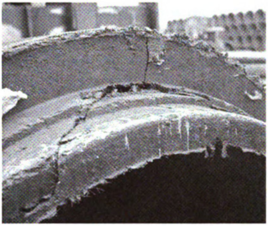

Figure 3.33. Crack Under Concentrated Load. *Figure 3.34. Overall Crack View Under Concentrated Load.*

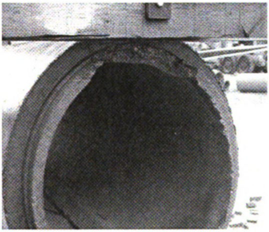

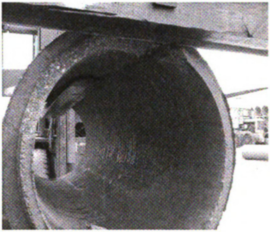

Figure 3.35. Failure Under Concentrated Load. *Figure 3.36. Extended Failure Under Concentrated Load.*

The Steel reinforcement of concrete pipes does not extend into the interior component of joint. Fiber reinforcement, however, would be present in this region. Two pipes without fiber reinforcement (First-Series Pipes # 1 & 3) and two pipes with fiber reinforcement (First-Series Pipes # 4 & 5) were tested in this investigation. Figure 3.37 compares the average peak values of concentrated edge loads at failure for plain and fiber reinforced conditions. On the average, fiber reinforced concrete pipes provide more than 15% increase in capacity when joint shear is assessed approximately using the concentrated edge load configuration of Figure 3.32.

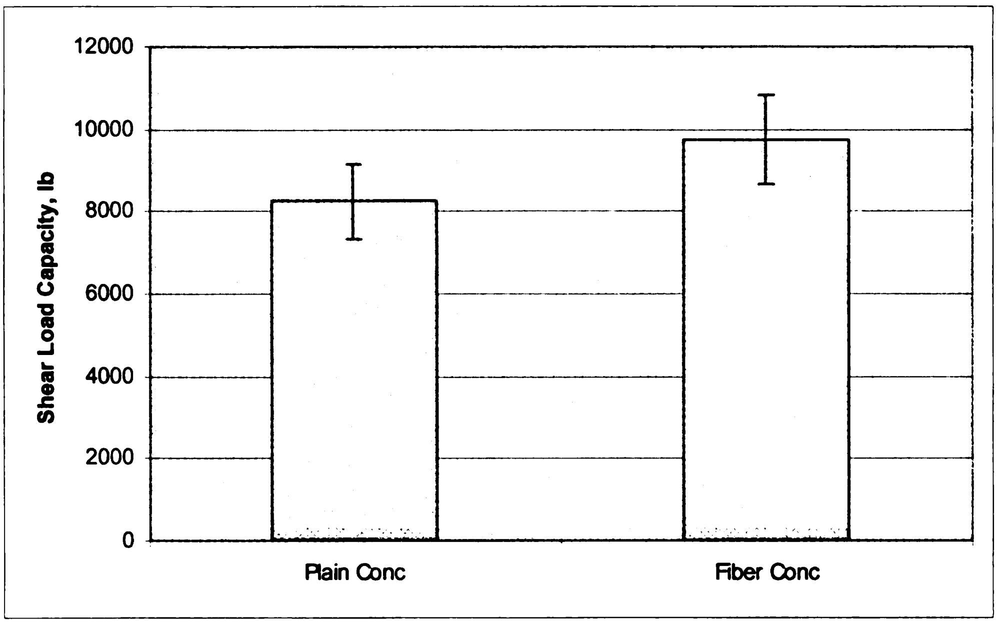

Figure 3.37. Plain Vs. Fiber Reinforced Concrete Joint Shear Capacity under Concentrated Edge Load Configuration (mean values and ranges of test results).

3.3 Design and Life-Cycle Cost Analysis of Concrete Pipes with Synthetic Fiber and Steel Reinforcement for Improved Durability

The analytical models introduced above were used to design concrete pipes with a combination of synthetic fiber and steel reinforcement which provide ultimate strength levels comparable to those of conventional pipes (with steel reinforcement only), but offer a larger thickness of protective concrete cover over steel. Alternative designs with different combinations of cover thickness, steel reinforcement ratio and synthetic fiber volume fractions are introduced in Table 3.5; these pipes were designed with coarser PVA fibers of 0.59 in. (15 mm) in length and 0.012 in. (0.3 mm) diameter which was conveniently dispersed in fresh concrete mix and provided a desirable pull-out behavior in hardened concrete. All pipes introduced in Table 3.5 were designed for an ultimate D-load of 4522 lb/ft/ft (226 N/m/mm).

Table 3.5. Alternative Designs of Concrete Pipes with Different Cover Thickness, and Synthetic Fiber and Steel Reinforcement Combinations

Pipe	Area of Steel Reinforcement, in^2 (cm^2)
No Fiber + 2 Layers Steel	0.16 (1.032)
0.5% Fiber + 1 Layer Steel + 2" (50.8 mm) Cover	0.2794 (1.803)
0.5% Fiber + 1 Layer Steel + 1.5" (38.1 mm) Cover	0.1961 (1.265)
1% Fiber + 1 Layer Steel + 2" (50.8 mm) Cover	0.2516 (1.623)
1% Fiber + 1 Layer Steel + 1.5" (38.1 mm) Cover	0.1598 (1.031)

For the purpose of life-cycle cost analysis, we assumed that: (i) the service life of conventional concrete pipe with 1 in. (25.4 mm) concrete cover thickness in sanitary sewer environment is ten years; and (ii) the service life of concrete pipes in sanitary sewer environment increases proportionally with increasing concrete cover thickness for alternative pipe designs (with a combination of synthetic fiber and steel reinforcement).

The life-cycle cost analyses were performed over a period of sixty years; the conventional design (with 10-year service life) would require an initial installation plus five removals and installations during this sixty-year period. Doubling of the cover thickness to 2 in. (50.8 mm) would increase the service life to 20 years, and would thus require an initial installation plus two removals and installations over the sixty year period. The initial sales price of the conventional concrete pipe (with two layers of steel and no fiber reinforcement) is $170 for an 8.5 ft (2.6 m) standard length of pipes, $45 of which covers the steel reinforcement cost. The sales price considered for synthetic (PVA) fibers was $2.75/lb ($6.05/kg). The inflation and interest rates were considered to be equal for the purpose of life-cycle cost analysis. The installation and removal costs were derived from Reference 29, which suggests installation and removal costs for 8.5 ft (2.6 m) pipes $357 and $86, respectively. The results of life-cycle cost analysis, presented in Table 3.6, suggest that the increase in concrete cover thickness through proper combination of synthetic fiber and steel reinforcement can bring about major life-cycle cost savings with modest rise in the initial cost of pipes. The pipe with 0.5% synthetic fiber reinforcement and 2 in. (50.8 mm) cover, for example, yielded life-cycle cost saving of $1,659 (46%) with a rise of $60 (35%) in initial cost.

Table 3.6. Initial and Life-Cycle Costs Over 60 Years for Different Concrete Pipe Designs

Pipe	Initial Cost ($)	Life Cycle Cost ($)
No Fiber + 2 Layers Steel	170	3592
0.5% Fiber + 1 Layer Steel + 2" (50.8 mm) Cover	230	1933
0.5% Fiber + 1 Layer Steel + 1.5" (38.1 mm) Cover	206	2510
1% Fiber + 1 Layer Steel + 2" (50.8 mm) Cover	248	1987
1% Fiber + 1 Layer Steel + 1.5" (38.1 mm) Cover	222	2574

Another application of synthetic fibers is in concrete pipes with relatively low load-bearing requirements, where fibers replace the relatively low ratio (one layer) of steel reinforcement used for damage control during shipment, handling and installation. Coarser synthetic fibers at 0.5% volume fraction are competitive (in terms of raw material costs) with one layer of steel reinforcement for production of damage-resistant concrete pipes; the use of fibers in this application would stream line the production process because fibers (unlike steel reinforcement) are introduced as an ingredient to concrete mix.

3.4. Conclusions

1. Refined concrete mix formulations incorporating chemical and mineral admixtures as well as fibers are generally compatible with concrete pipe industrial-scale production practices. Introduction of chemical and mineral admixtures for enhancement of concrete pipe resistance to microbial-induced corrosion does not compromise the structural performance of concrete pipes.

2. Synthetic fiber reinforcement substantially enhances the load at 0.01" crack width and also the peak load of pipes with one layer of steel. When compared with pipes with two layers of steel (without fibers), the fiber reinforced pipes with one layer of steel provide increased levels of load at 0.01" crack width. Hence, as far as the load at 0.01" crack width is concerned, fiber reinforcement of concrete pipes can reduce the required amount of steel reinforcement from two layers to one. As far as the peak load is concerned, however, fiber reinforced concrete pipes with one layer of steel provide somewhat (about 15%) lower level of peak capacity when compared with the pipe with two layer of steel and without fiber reinforcement. The key performance requirements of concrete pipes are the load at 0.01" crack width (which marks the load beyond which pipe is no more functional) and ductility (which reflects on the ability of pipe to resist brittle and catastrophic modes of failure during transportation, installation and service). The peak load requirement could well be an indirect measure of ductility. Pipes with one layer of steel and fibers actually provide higher levels of ductility (post-peak load-

carrying capacity) when compared with pipes with two layers of steel and no fiber reinforcement. It is thus our conclusion that synthetic fibers can reduce the steel reinforcement requirements (and thus increase the protective concrete cover thickness over steel), which can make major contributions to the longevity of concrete pipes in aggressive sanitary sewer environments.

3. The increase in the finer fiber volume fraction from 1% to 1.5% resulted in about 15% gain in load levels at 0.01" crack width, peak, and post-peak region. The 50% increase in finer fiber dosage does not produce a similar percentage increase in load levels because, based on observations of ruptured concrete pipe surfaces, some fiber dispersion problems start to appear at 1% volume of finer fibers; these problems tend to be more pronounced at 1.5% fiber volume fraction. A comparison of the finer versus coarser fibers suggests that the coarser fiber is probably more suitable for the high-performance concrete proportions commonly used for pipe production using the popular dry-cast technique. Coarser fibers provide reduced fiber dispersion problems; they also exhibit some level of fiber pull-out (compared to finer fibers which almost exclusively rupture at cracked concrete sections). Fiber pull-out, as far as it occurs with sufficient bond strength to mobilize a substantial fraction of fiber rupture strength, is preferred because it provides for a more ductile mode of failure.

4. Many concrete pipes do not need steel reinforcement for load-carrying capacity. Steel is added to these pipes (with important cost implications) mainly to avoid

damage to these brittle pipes during transportation and installation. Synthetic fibers could be a cost-effective replacement for steel as far as they ensure ductility of pipe failure. In the case of plain concrete pipes, with conventional hydraulic loading systems used in three-edge bearing tests, the gains in ductility with 0.5% volume fraction of finer fibers are relatively small, and the pipe still exhibits a brittle mode of failure. This, however, could be a result of the load-controlled nature of the hydraulic loading systems normally used in three-edge bearing tests. These hydraulic systems (as well as the test frame) act as a spring within which mechanical energy accumulates as the peak load is approached. Although the fiber reinforced concrete pipes (without steel reinforcement) may have some level of post-peak load-carrying capacity available (and may actually be far more resistant to brittle modes of failure during transportation and installation), the energy accumulated within the hydraulic loading system (and test frame) is suddenly released beyond peak load, yielding sudden failure of pipe irrespective of some level of post-peak ductility which is probably provided through fiber reinforcement of plain concrete pipes. In other words, the brittle mode of failure in fiber reinforced concrete pipes (without steel reinforcement) in three-edge bearing test does not necessarily imply that these pipes are prone to damage during transportation and installation. This hypothesis needs to be tested through implementation of experiments which more closely simulate the damaging effects that pipes experience during transportation and installation.

5. Coarser fibers (15 mm length, 0.3 mm diameter) can be more conveniently introduced at relatively high volume fractions (2%) into concrete mixtures used in dry-cast method of pipe production.

6. The coarser PVA fiber exhibited a prevalent tendency towards pull-out at cracks while the finer PVA fibers predominantly ruptured at cracks. The coarser fiber thus provides a more pronounced gain in ductility and energy absorption capacity of concrete pipes, which can be used to prevent brittle failure of plain concrete pipes and thus facilitate production of plain pipes which are resistant to damage during handling, shipment and installation.

7. Coarser fibers were more effective than finer fibers in enhancing the load in three-edge bearing test corresponding to 0.01" crack with of steel reinforced concrete pipes, and also in increasing the peak load of plain concrete pipes.

8. On the average, fiber reinforced concrete pipes provide more than 15% increase in capacity when joint shear is assessed approximately using a concentrated edge load configuration.

9. Synthetic fiber reinforcement (at the relatively high fiber volume fractions considered in this investigation) would be cost-competitive as far as they are used at relatively low volume fractions (less than 1%) to partially (or fully) replace steel reinforcement. Synthetic fibers can enhance the thickness and quality of concrete

cover over reinforcing steel, thereby yielding major life-cycle cost savings. Future investigations should focus on volume fractions below 1% of coarser synthetic fibers.

CHAPTER 4

DEVELOPMENT OF STRUCTURAL DESIGN METHODOLOGIES FOR CONCRETE PIPES WITH STEEL AND SECONDARY SYNTHETIC FIBER REINFORCEMENT

4.1. Introduction

Pipes are subjected to earth and live loads (Figure 4.1.a) which generate transverse bending moment in pipe walls. (Figure 4.1.b). The transverse (circumferential) reinforcement is introduced in concrete pipes to resist bending moment. (Figure 4.1.c). Under loads, pipes first develop vertical cracks (starting on interior surfaces i.e. crown and invert), and then horizontal cracks (starting at mid-height on exterior surfaces i.e. springlines). Figure 4.2 shows the location of crown, invert, and springlines.

Under the effect of bending moments, pipes behave simply as a rectangular reinforced concrete section. (Figure 4.3)

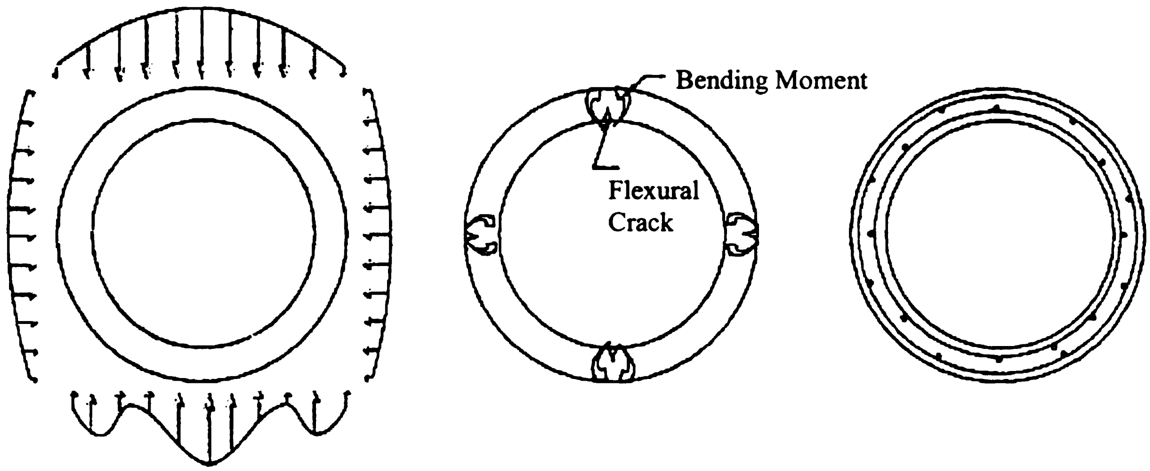

(a) Vertical and horizontal loads *(b) Bending moments and flexural cracks*

(c) Reinforcement system

Figure 4.1. Concrete pipe external loads, internal bending moments and flexural reinforcement system

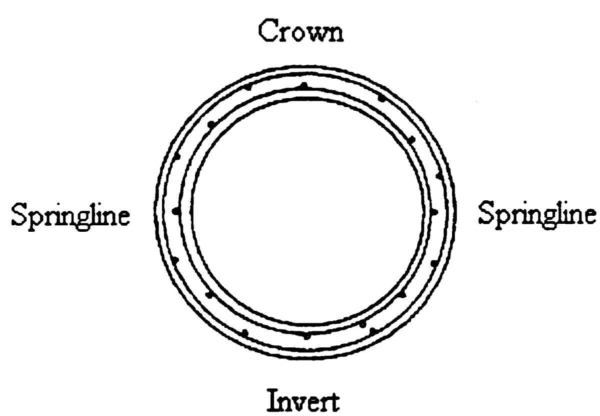

Figure 4.2. Location of crown, invert, and springlines

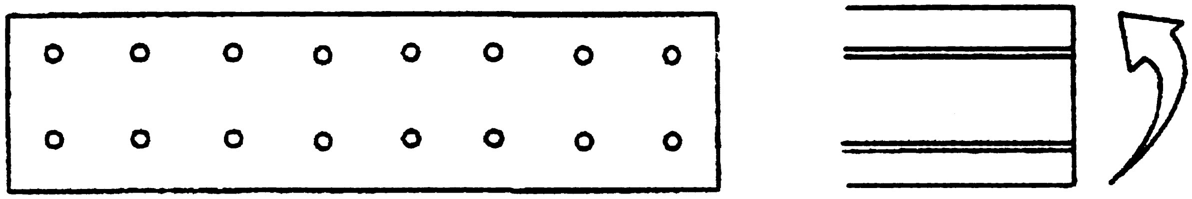

Figure 4.3. Pipe cross-section under bending moment

Figure 4.4 shows two different reinforcement configurations, one with two layers of transverse reinforcement and another with one layer of transverse reinforcement placed in the middle of the pipe wall.

Concrete pipes with limited demand on their load-carrying capacity may be unreinforced. Design of concrete pipes is based preliminary on their flexural performance under external loads. Two load criteria (in three-edge bearing test) are generally used in design of concrete pipes: (i) load at 0.01" crack width; and (ii) ultimate load. The analytical work reported herein seeks to establish the theoretical foundation for prediction of these load levels in plain and steel reinforced concrete pipes with synthetic fiber reinforcement.

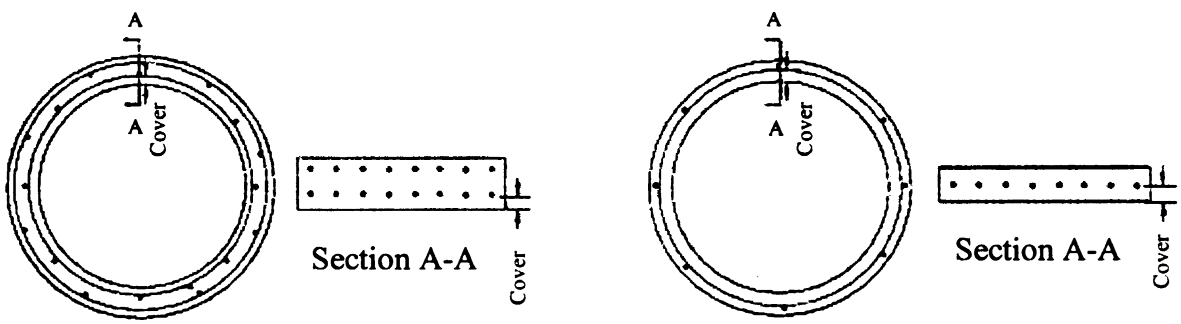

Figure 4.4. Reinforcement configurations

4.2. Design Equations for 3-Edge Bearing Load on Pipes [15]

4.2.1. Ultimate Flexural Strength of Steel Reinforced Concrete Pipes

The produced moments in the pipe are related to the weight of the pipe, W_p, and the total three-edge bearing load, W_t, by following equation:

$$M = (c_{m1} W_p + c_{m2} W_t)\frac{S}{2}$$

Where $S = D_i + h$, D_i is the internal diameter of the pipe (in.), h is the wall thickness (in.), and other terms are introduced below.

For circular pipe, the moments generated in three-edge bearing test vary as shown in Figure 2.1.1. The critical conditions for design for flexure occur at the crown and invert. The invert is used in developing the design equations. Here, the moment caused by the test load is slightly less than at the crown, but the moment caused by weight of the pipe is substantially greater at the invert, thus making the combined moment about the same for the crown and invert.

At the invert one can define the following terms for the above equation for calculation of moment in the elastic range:

$cm1 = 0.75\ cm2$, $cm2 = 0.280$

Hence, the moment equation can be simplified as follows:

$$M = 0.14(0.75W_p + W_t)(D_i + h)$$

With $DL = \frac{W_t}{D_i} \times 12$ and $DL_p = \frac{W_p}{D_i} \times 12$, one can present the moment equation as follows:

$$M = 0.14\left(\frac{9W_p}{D_i} + DL\right)\frac{D_i}{12}(D_i + h)$$

With further simplification one gets:

$$M = 0.0117\left(\frac{9W_p}{D_i} + DL\right)D_i\ (D_i + h)$$

The above moment equation is used to develop the equation for calculating the ultimate D-load strength of concrete pipes in three-edge bearing tests.

Flexural strength of reinforced concrete sections can be expressed as follows:

$$M_U = A_s f_y\left(d - \frac{a}{2}\right)$$

Replacing the above equation for flexural strength in the moment equation yields:

$$A_s f_y\left(d - \frac{a}{2}\right) = 0.0117\left(\frac{9W_p}{D_i} + DL\right)D_i\ (D_i + h)$$

Therefore:

$$\left(DL_U + \frac{9W_p}{D_i}\right) = \frac{85 A_s f_y\left(d - \frac{a}{2}\right)}{D_i(D_i + h)}$$

Before a pipe loaded in 3-edge bearing reaches a collapse state, it develops the full effective tensile strength of the inner reinforcement at the crown and invert and the outer reinforcement at the springlines. In this case, the final moment distribution is shown in Figure 4.5.e. The D-load capacity increases by the factor Cmp over the load which causes first yield in the inner reinforcement. Cmp is equal to 1.10 for circular pipes with two concentric cages, and is equal to 1.25 for one cage. C_m is the coefficient for flexural first yield criterion and is equal to 1.0 for circular cages.

Therefore, the Equation for Utimate Flexural Strength is:

$$\left(DL_U + \frac{9W_p}{D_i}\right) = \frac{85\, C_m\, C_{mp}\, A_s\, f_y \left(d - \frac{a}{2}\right)}{D_i(D_i + h)}$$

Where $a = \dfrac{A_s\, f_y}{0.85 \times 12\, f_c'}$, or $a = \dfrac{A_s\, f_y}{10.2\, f_c'}$

4.2.2. 0.01" Crack Flexural Strength of Steel Reinforced Concrete Pipes

The 0.01" crack width is an arbitrarily chosen test criterion commonly used in design and evaluation of concrete pipes; it is not a criterion for field performance or service limit, is simply a design criterion other than ultimate strength which reflects on the cracking behavior of concrete pipes.

The nominal reinforcement stress at critical section can be calculated as follows:

$$f_s = \frac{M}{A_s \times j \times d}$$

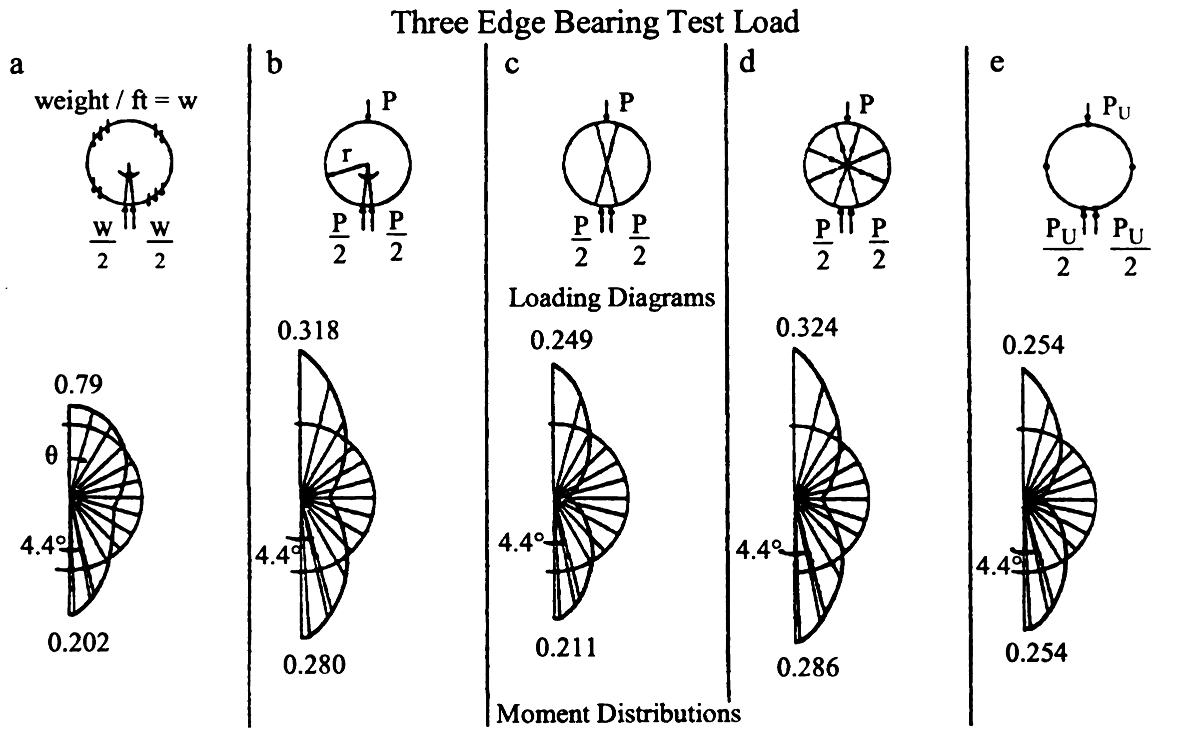

(a)Weight of pipe (b)Uncracked (c)First stage cracking (d)Second stage cracking

(e)Ultimate Flexural Failure

Figure 4.5. Moment distributions in three-edge bearing test loading.

Where j is the coefficient for moment arm at service load stress, and is considered to be 0.9.

In the case of 0.01" crack strength:

$$f_s = \lambda_{.01} \times f_{s.01}$$

Where $\lambda_{.01}$ is a reduction factor for variability in test results and is taken 0.9.

So,

$$M_{.01} = 0.9 f_{s.01} \times 0.9 d$$

From previous discussion,

$$M = 0.0117\left(\frac{9W_p}{D_i} + DL\right) D_i \; (D_i + h)$$

Substituting for M.01 yields:

$$0.9 f_{s.01} = \frac{0.0117\left(\dfrac{9W_p}{D_i} + DL\right) D_i \; (D_i + h)}{0.9 A_s \, d}$$

The D-load at 0.01" crack can thus be derived as follows:

$$\left(DL_{.01} + \frac{9W_p}{D_i}\right) = \frac{70 A_s \, f_{s.01} \, d}{D_i (D_i + h)}$$

Where $f_{s.01}$ is the maximum stress in the reinforcement when the maximum crack width is 0.01 inches, which has been derived, based on many 3-edge bearing test results, as follows:

$$f_{s.01} = \frac{30000}{B_{.01}} + \frac{C_{.01} h^2 \sqrt{f_c'}}{\rho d^2}$$

Where $B_{.01}$ is the crack control coefficient for effect of cover and spacing of reinforcement and is 1.0 for welded smooth wire fabric, with 8 in. maximum spacing of longitudinals.

$C_{.01}$ is the crack control coefficient for type of reinforcement and is 1.5 for welded smooth wire fabric, with 8 in. maximum spacing of longitudinals; and $\rho = \dfrac{A_s}{b d}$

4.2.3. Concrete Pipes without Steel Reinforcement [3]

Flexural design in this case, is always governed by the flexural tension strength limit state. The pipe must have enough strength so that the highest flexural stress around the pipe circumference produced by a combination of moment and thrust will be equal or less than the flexural tensile strength of the concrete (usually taken as the modulus of rupture of concrete, f_{mr}). The governing location for the highest combined flexural tension is at the invert in most installations. To determine the modulus of rupture, two approaches can be followed.

One approach determines the modulus of rupture from results of a three-edge bearing test:

$$f_{mr} = 0.96\phi_{mr} \frac{DL_{ut} \times D_i(D_i + h)}{144h^2}$$

Where DL_{ut} is the test D-load that cracks the pipe (lb/ft/ft), D_i is the internal diameter of the pipe (in.), and h is the wall thickness (in.).

The second approach estimates the modulus of rupture by using the following equation:

$$f_{mr} = k_{mr}\,\phi_{mr}\,\sqrt{f_c'}$$

Where ϕ_{mr} is the strength reduction factor for flexural tension. The maximum value of ϕ_{mr} = 0.85 will provide approximately the same conditions for service loads from three-edge bearing test results. The coefficient k_{mr} varies with wall thickness. A minimum value for any wall thickness is 7.5. Pipe industry experiment, based on many three-edge bearing tests, is that k_{mr} increases with decreasing wall thickness, varying from about 8.5 for 4 in. walls up to 12 or more for 2 in. walls.

4.3 Modification of Design Equations for the Effects of Synthetic Fibers

The ability of fiber reinforced concrete to carry tensile stress increases the flexural load-carrying capacity of fiber reinforced concrete at different stages of behavior. Hence, the equations for flexural strength of pipes have to be modified to account for the structural contributions of fibers.

A semi-empirical approach has been followed here to derive design equations for concrete pipes with fiber reinforcement. They have been developed based on theoretical concepts which are modified to account for experimental results.

4.3.1. Ultimate Flexural Strength of Steel Reinforced Concrete Pipes with Fiber Reinforcement

Fibers in a cementitious matrix show two types of behavior at cracks: pull-out or rupture. The synthetic (PVA) fibers used in this investigation exhibit a stronger tendency towards rupture (especially for finer diameters and higher aspect ratios). The reason is the hydrophobic nature and strong bonding of PVA fibers to the cementitious matrix. The tendency towards fiber pull-out increases with increasing fiber diameter and decreasing fiber aspect ratio. Other methods to promote pullout behavior involve use of an oiling agent and modifying the matrix to reduce the chemical and frictional bond between PVA fibers and the cementitious matrix.

4.3.1.1. Design Equations When Fiber Rupture Dominates

The fiber concrete tensile stress distribution at flexural failure is assumed to be triangular (based on past experience), with tension zone starting at neutral axis and ending at the level of steel reinforcement. It is assumed that at the ultimate stage, the crack width below steel reinforcement is wide enough to have already caused rupture of fibers.

The above assumptions together with equilibrium considerations in Figure 4.7 yield the nominal flexural strength of singly reinforced fiber reinforced concrete section as follows:

$$M_n = \left[A_s f_y \left(d - \frac{a}{2}\right)\right] + \left[\frac{\sigma_t (d-c)}{2} b \left(c - \frac{a}{2} + \frac{2(d-c)}{3}\right)\right]$$

Where σ_t is the tensile stress in fibrous concrete and is calculated as follows:

σ_t = (N = number of fibers per unit area) * (U = ultimate tensile force in a single fiber)

$$\sigma_t = \left(\frac{0.5 V_f}{\frac{\pi d_f^2}{4}}\right)\left(\sigma_{fu} \frac{\pi d_f^2}{4}\right)$$

Therefore:

$$\sigma_t = 0.5\, V_f\, \sigma_{fu}$$

In the above formula, N is the number of randomly distributed fibers in a 3-D matrix. Strain compatibility between fiber reinforced concrete and steel reinforcement is assumed to be maintained in the section.(Figure 4.6)

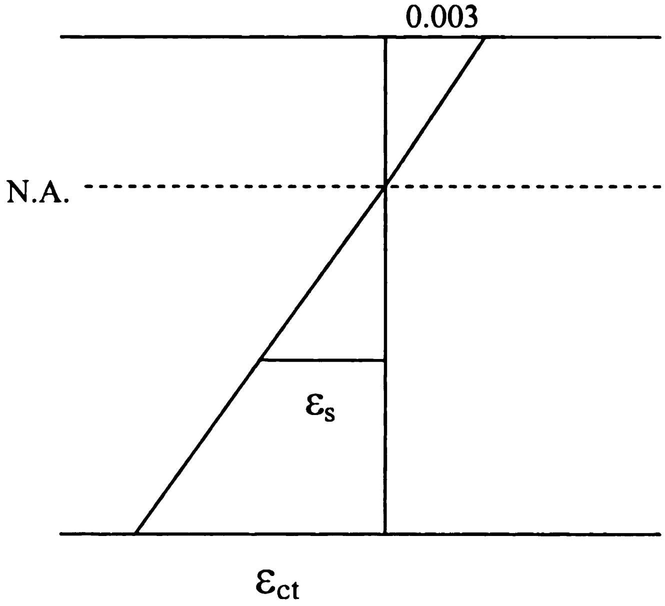

Figure 4.6. Strain Compatibility in the Fiber Reinforced Concrete Section

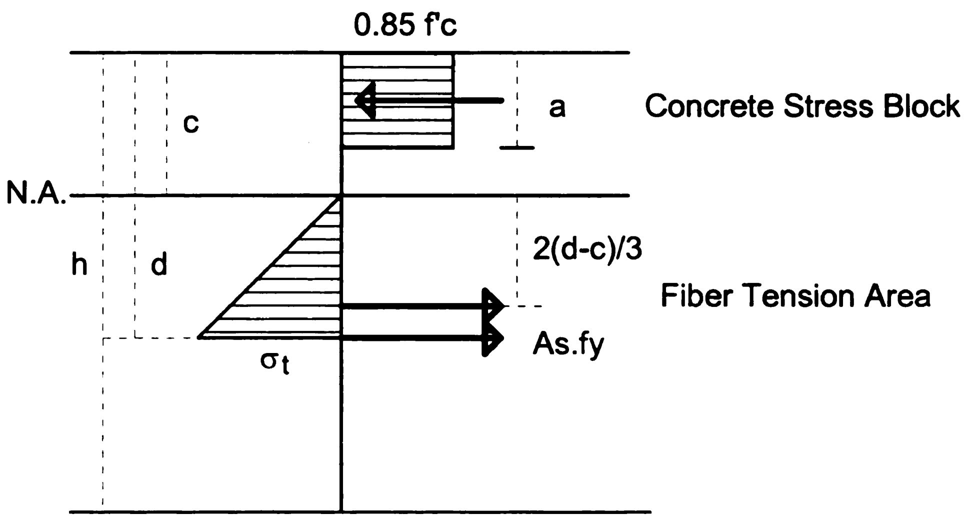

Figure 4.7. Flexural stress distribution at ultimate condition in a singly reinforced fiber concrete section with predominant fiber rupture.

4.3.1.2. Design Equations When Fiber Pull-Out Dominates

When fiber pull-out dominates, the fiber concrete tensile stress distribution is assumed to be uniform. This assumption together with equilibrium consideration in Figure 4.8 yields the following equation for nominal flexural strength of singly reinforced fibrous concrete sections with fiber reinforcement:

By considering these assumptions, the nominal flexural strength of the singly reinforced fibrous concrete is:

$$M_n = \left[A_s f_y \left(d - \frac{a}{2}\right)\right] + \left[(\sigma_t (d-c) b)\left(c - \frac{a}{2} + \frac{(d-c)}{2}\right)\right]$$

The tensile stress in fibrous concrete (σ_t) is equal to:

σ_t = (N = number of fibers per unit area) * (F = mean fiber frictional bond resistance)

For randomly distributed short fibers in a matrix in 3-D state,

$$\mathrm{N} = \left(\frac{0.5 V_f}{\frac{\pi d_f^2}{4}}\right)$$

When fiber pull-out dominates,

$$\mathrm{F} = \left(\tau_f \pi d_f \frac{l_f}{4}\right)$$

(If the composite failure is by fiber pull out, it has been shown that the mean fiber pull out length is $l_f/4$).

Therefore:

$$\sigma_t = \left(\frac{0.5 V_f}{\frac{\pi d_f^2}{4}} \right) \left(\tau_f \pi d_f \frac{l_f}{4} \right)$$

And finally:

$$\sigma_t = 0.5 V_f \tau_f \frac{l_f}{d_f}$$

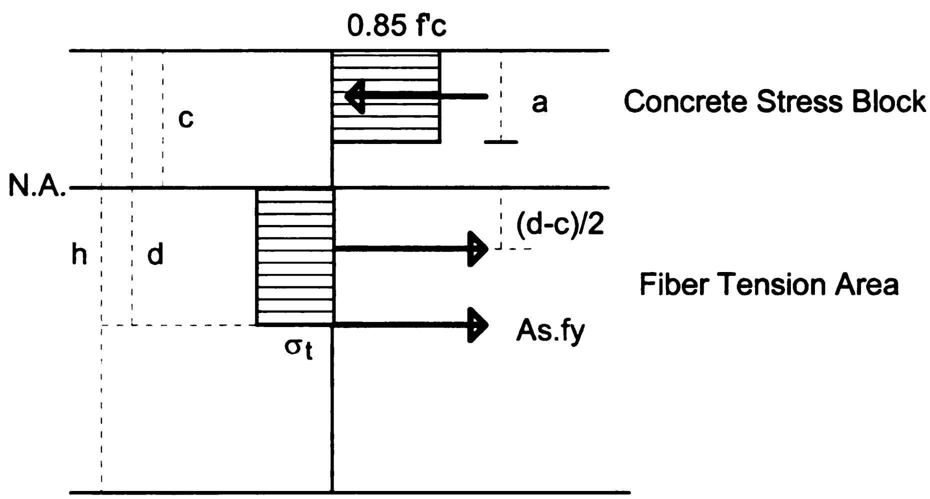

Figure 4.8 Flexural stress distribution at ultimate condition in a singly reinforced fiber concrete section with predominant fiber pull-out.

The same concept of strain compatibility between fiber reinforced concrete and steel reinforcement mentioned above, has been assumed for this section.(Figure 4.6)

4.3.2. Flexural Strength at 0.01" Crack Width for Steel Reinforced Concrete Pipes with Fiber Reinforcement

At 0.01" crack width, considering the contribution of fibers, the stress level in steel reinforcement should be less than that of the non-fibrous concrete. The stress in steel reinforcement can be determined by the aforementioned equation for $fs_{.01}$ and multiplying it by a decreasing index accounting for fiber action. Using geometric relationships for strain distribution, the maximum concrete stress can be determined, and subsequently the moment at section corresponding to 0.01" crack width can be calculated.

For the pipes under consideration (Class IV wall C with D_i = 27"), the steel reinforcement will develop stresses beyond its yield stress, which implies that the 0.01" crack strength will be equal to the ultimate strength. (this prediction was confirmed by test results).

4.3.3. Flexural Strength of Fiber Reinforced Concrete Pipes Without Steel Reinforcement

The stress distribution under ultimate moment in concrete pipes with fiber reinforcement (but no steel reinforcement) is assumed linear (Figure 4.9), with tensile stresses covering the full area below neutral axis; the expressions for σ_t (Figure 4.9) were introduced earlier. Simple equilibrium considerations yield the expression for flexural strength in Figure 4.9.

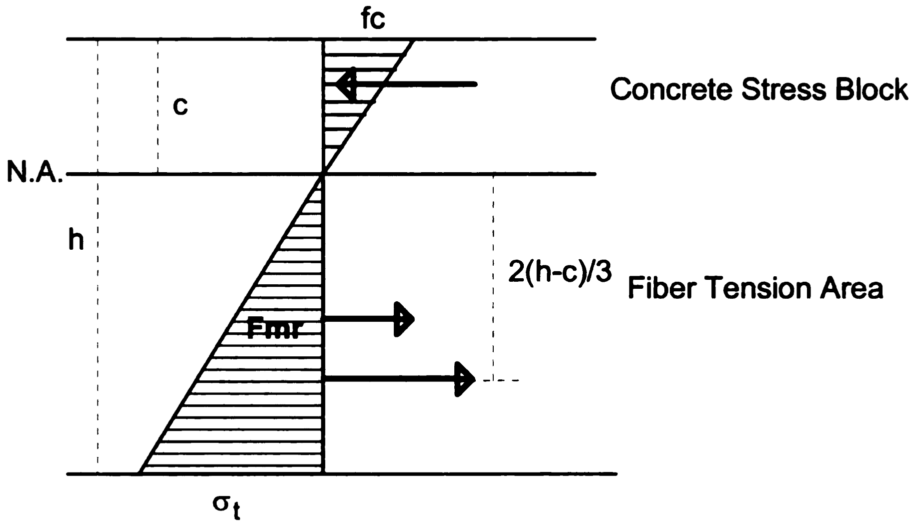

Figure 4.9. Stress distribution in the fiber reinforced concrete section

4.4. Parametric Study and Discussion on Results

The pipes tested in experimental investigations provided the basis for the parametric studies presented below. The following values were used in parametric studies:

$A_s = 0.08$ in^2/ft

$f_y = 0.95 f_{su}$ (f_{su} is the ultimate tensile strength of the welded wire fabric and is 75000 psi for the tested pipes)

$f'_c = 5000$ psi => $\beta = 0.8$, $W_p = 420$ lb/lin.ft.

$f_{mr} \cong 530$ psi $h = 4$ in. $D_i = 27$ in.

The fiber properties are summarized in Table 4.1

Table 4.1. Geometric Attributes of PVA Fibers.

Fiber Type	Length (mm)	Diameter (mm)	Tensile Strength (Mpa)
I	6	0.026	1600
II	12	0.1	1100
III	15	0.3	900

(1 in. ≅ 25.4 mm. , 1 MPa ≅ 145 psi)

Table 4.2 and Figure 4.10 present the experimental and analytical predictions of ultimate loads for different pipes considered in the experimental program; analytical predictions were made based on assumptions on predominance of either fiber rupture or pullout as follows. In Pipes A and B with finer fibers of higher aspect ratio, fiber rupture dominated, and the equations corresponding to fiber rupture yielded desirable results. In the case of Pipes C and G, with fibers of medium aspect ratio, some fiber pullout was observed but fiber rupture was still prevalent. A rectangular tensile stress block was assumed for fiber concrete, with fiber stress assumed to reach the ultimate level. In Pipes D and E, which incorporated coarse fibers of relatively low aspect ratio, a bond strength, τ, of 10 MPa (1,450 psi) yielded a satisfactory analytical prediction of experimental results; Pipe H also contained coarse fibers with pull-out behavior. Fiber rupture was assumed to be prevalent in Pipe F.

Table 4.2. Experimental Results and Analytical Predictions of the Ultimate Flexural Strength of Different Pipes with Various Combinations of Steel and Synthetic Fiber Reinforcement.

Pipe	Corresponding Pipe # *	Steel Cage	Fiber Volume & Type		Test Ultimate D-load (lb/ft/ft)	Theoretical Ultimate D-load (lb/ft/ft)
A	3 (1)	1	1%	TYPE I	2928	3021
B	4 (1)	1	1.5%	TYPE I	3294	3706
C	5 (1)	1	0.75%	TYPE II	3084	2688
D	3 (2)	1	2%	TYPE III	3163	2945
E	3' (2)	1	2%	TYPE III	3007	2945
F	8 (1)	0	0.5%	TYPE I	2718	2740
G	9 (1)	0	0.5%	TYPE II	2614	2161
H	6 (2)	0	2%	TYPE III	2797	2955

* Number in parenthesis corresponds to test series

TYPE I : L=6 mm, D=0.026 mm, TYPE II : L=12 mm, D=0.1 mm, TYPE III : L=15 mm, D=0.3 mm

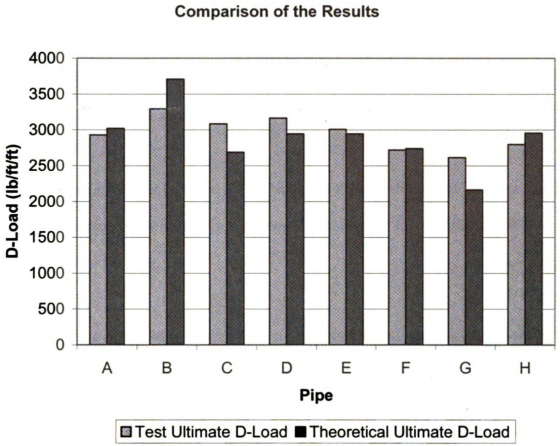

Figure 4.10. Pipe Ultimate Loads: Analytical Predictions and Experimental Results.

4.5. Conclusions

1. Under the effects of earth and live loads, transverse bending moments develop in pipe walls. This yields the rectangular beam type of behavior of the pipe.

2. There are particular formulas for evaluation of flexural strength of the pipes in a 3 edge bearing test, which have to be modified to account for the fiber contribution to flexural strength.

3. Fibers in a cementitious matrix show two types of behavior at cracks: pull-out or rupture. Different sets of formulas were derived for each type of fiber behavior.

4. A semi-empirical approach was adopted for derivation of the formulas for both steel reinforced and non-reinforced fiber reinforced concrete pipes.

5. According to the parametric study conducted for comparison theoretical results predictions versus test results, the models predict the actual performance of concrete pipes with reasonable accuracy.

CHAPTER 5

CONCLUSIONS AND FUTURE RESEARCH NEEDS

5.1. Conclusions

1. Fibers can enhance the cracking resistance, mechanical properties and longevity of concrete. The reinforcing effects of fibers in concrete result largely from control of microcrack and crack propagation.

2. There are several applications for fiber reinforced concrete in non-structural, semi-structural, and structural members. Non-structural applications where shrinkage crack control is a primary issue are currently prevalent. Life-cycle cost analysis justifies the initial cost associated with introduction of fibers.

3. Refined concrete mix formulations incorporating chemical and mineral admixtures as well as fibers are generally compatible with industrial-scale production practices of concrete pipes.

4. Synthetic fiber reinforcement substantially enhances the load at 0.01" crack width and also the peak load of pipes with one layer of steel. Hence, fiber reinforcement of concrete pipes can reduce the required amount of steel reinforcement from two layers to one. Pipes with one layer of steel and fibers actually provide higher levels of ductility (post-peak load-carrying capacity) when compared with pipes with two layers of steel and no fiber reinforcement. It is thus our conclusion that synthetic fibers can reduce the steel reinforcement requirements (and thus increase the protective concrete cover thickness over steel), which can make major contributions to the longevity of concrete pipes in aggressive sanitary sewer environments.

5. Coarser fibers (15x0.3 mm) can be more conveniently introduced at relatively high volume fractions (2%) into concrete mixtures used in dry-cast method of pipe production. The coarser PVA fibers exhibited a prevalent tendency towards pull-out at cracks while the finer PVA fibers predominantly ruptured at cracks. Coarser fibers were more effective than finer fibers in enhancing the load in three-edge bearing test corresponding to 0.01" crack with of steel reinforced concrete pipes, and also in increasing the peak load and post-peak ductility of plain concrete pipes.

6. As far as the cost of pipe production is concerned, fibers would be competitive as partial (or full) replacement for steel reinforcement when used at volume fractions below 1%; significant gains in life-cycle economy of concrete pipes can result

from introduction of fibers to increase the thickness and enhance the quality of protective concrete cover over steel reinforcement.

7. Under the effects of earth and live loads, transverse bending moments develop in pipe walls. This yields a rectangular beam type of behavior in pipes. There are particular formulas for evaluation of flexural strength of the pipes in a 3 edge bearing test, which have to be modified to account for the fiber contribution to flexural performance. Fibers in a cementitious matrix show two types of behavior at cracks: pull-out or rupture. Different sets of formulas were derived for each type of behavior. A semi-empirical approach was adopted for derivation of the formulas for both steel reinforced and non-reinforced fiber concrete pipes. According to the parametric study conducted and based on comparison theoretical predictions versus test results, the models can predict the pipe performance with reasonable accuracy.

5.2. Future Research Needs

- The test results and economic analysis conducted in this investigation indicate that coarser and longer PVA fibers at less than 1% volume fraction can yield particularly desirable balances of performance and initial cost. The validity of this assumption should be verified through integrated experimental and analytical investigations involving full-scale concrete pipes.

- Reduction of the steel reinforcement by as much as 50% (while increasing the protective cover thickness of concrete over steel) is possible by using a proper fiber type, geometry, and volume fraction. Optimization of the fiber and steel reinforcement as well as evaluation of the long-term performance of pipes incorporating the new designs in sanitary sewer systems requires further investigations.

APPENDICES

APPENDIX A

SLUMP EXPERIMENTS[6]

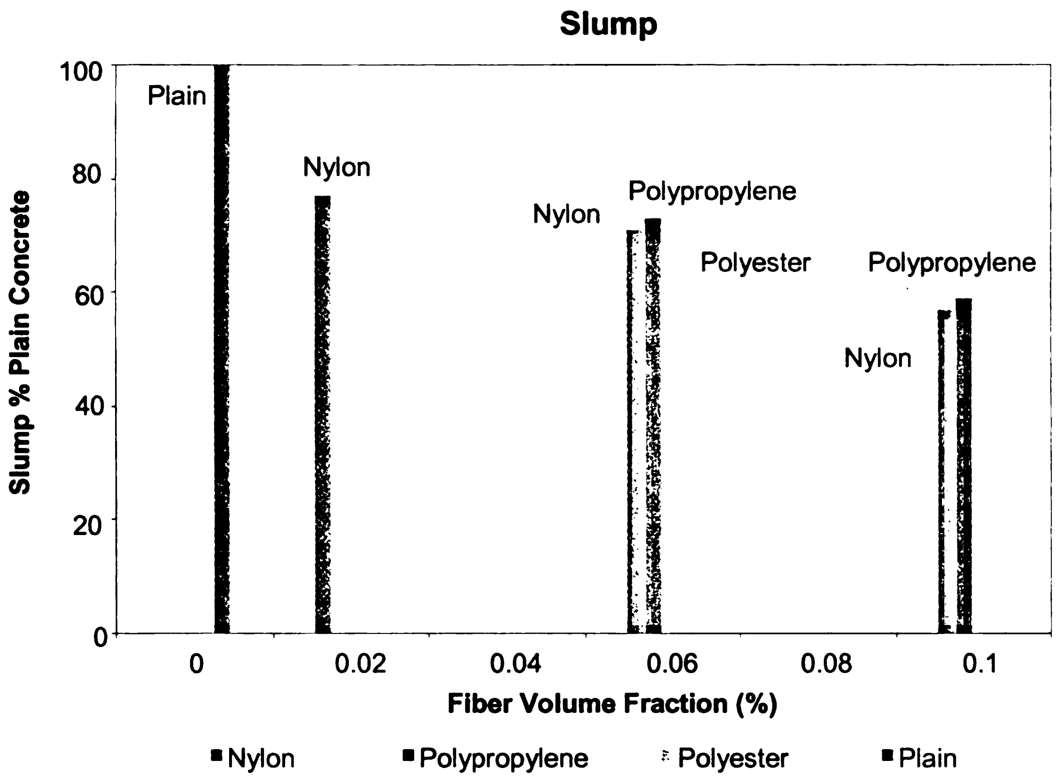

Figure A.1. Summary of the Slump Results for Different Fiber Types

Table A.1. Reference to Different Fiber Results' Tables

Fiber Type	Fiber Geometry L : D (mm)	Fiber Vol. Fraction:	Mix C:S:CA:W	Results
Steel Fiber	see Table A.2	see Table A.2	see Table A.2	Table A.2 Table A.3
Plain	see Table A.4	see Table A.4	see Table A.4	Table A.4 Table A.5
Synthetic Fiber	see Table A.6	see Table A.6 Fig: A.2,A.3	See TableA.6 Fig: A.2,A.3	see Table A.6 Fig: A.2,A.3

Table A.2. Steel Fiber and Mix Properties

Mixture designation	Mixture proportions				
	W/C ratio (by weight)	Cement (lb/yd^3)*	Fibers (lb/yd^3)*	High-range water-reducer (wt %)‡	Air-entraining agent (wt %)‡
F1	0.36	611	55	1.0	0.20
F2,F2R	0.32	564	65	0.8	0.50
F3,F3R	0.32	658	65	0.8	0.20
F4,F4R	0.40	564	65	0.8	0.10
F5,F5R	0.40	658	65	0.8	0.13
F6,F6R	0.32	564	65	1.2	0.20
F7,F7R	0.32	658	65	1.2	0.13
F8,F8R	0.40	564	65	1.2	0.10
F9,F9R	0.40	658	65	1.2	0.10
F10	0.36	611	75	0.6	0.20
F11	0.28	611	75	1.0	0.40
F12	0.36	517	75	1.0	0.20
F13	0.36	705	75	1.0	0.10
F14	0.44	611	75	1.0	0.10
F15	0.36	611	75	1.4	0.20
F16,F16R	0.32	564	85	0.8	0.30
F17,F17R	0.32	658	85	0.8	0.20
F18,F18R	0.40	564	85	0.8	0.13
F19,F19R	0.40	658	85	0.8	0.16
F20,F20R	0.32	564	85	1.2	0.40
F21,F21R	0.32	658	85	1.2	0.20
F22,F22R	0.40	564	85	1.2	0.13
F23,F23R	0.40	658	85	1.2	0.13
F24	0.36	611	95	1.0	0.20
F25	0.36	611	75	1.0	0.30
F26	0.36	611	75	1.0	0.25
F27	0.36	611	75	1.0	0.40
F28	0.36	611	75	1.0	0.25
F29	0.36	611	75	1.0	0.30
F30	0.36	611	75	1.0	0.13
F31	0.36	611	75	1.0	0.20
F32,F32R	0.40	611	75	1.0	0.15
F33,F33R	0.30	799	75	1.2	0.20
F34	0.40	611	75	1.0	0.15
F35	0.30	799	75	1.2	0.20
F36	0.40	611	75	1.0	0.15
F37	0.30	799	75	1.2	0.20
F38	0.40	611	75	1.0	0.15
F39	0.40	611	75	1.0	0.15

Table A.2. Continued

Mixture designation	W/C ratio (by weight)	Cement (lb/yd^3)*	Fibers (lb/yd^3)*	High-range water-reducer (wt %)‡	Air-entraining agent (wt %)‡
	Mixture proportions				
F40	0.40	611	75	1.0	0.15
F41	0.43	690	100	1.3	-†
F42	0.50	690	100	-†	-†
F43	0.43	690	100	0.86	0.101
F44	0.43	690	100	1.09	0.185
F45	0.43	690	100	1.00	0.254
F46,F46R	0.30	799	75	1.2	0.20
F47,F47R	0.40	611	75	1.0	0.15
F48	0.40	611	75	1.0	0.15
F49	0.30	799	75	1.2	0.10
F50	0.30	799	75	1.2	0.20

Note: Replicate mixture proportions (design. by R) are the same as those of the original.
* 1 lb/yd^3 = 0.59 kg/m^3 † Data discarded ‡ Percent by weight of cement

Table A.3. Steel Fiber Slump Results

Mixture Designation	Air Temperature (°F)*	Air Content (vol. %)	Slump (in.)†	V-B time (m)
F1	88	5.7	2.25	8.0
F2	80	4.4	0.0	10.0
F2R	72	3.4	0.0	9.0
F3	80	3.6	0.25	1.5
F3R	76	5.2	0.625	6.0
F4	79	4.2	1.75	8.6
F4R	73	7.2	2.0	8.0
F5	80	6.8	4.5	1.5
F5R	70	9.8	7.625	0.0
F6	80	4.2	0.0	16.0
F6R	74	5.4	1.0	13.5
F7	80	6.8	7.625	0.0
F7R	78	6.0	2.75	5.5
F8	80	8.0	8.0	0.0
F8R	78	8.2	7.875	0.0
F9	84	10.2	7.5	0.0
F9R	70	10.0	9.25	0.0
F10	84	3.5	0.0	27.0
F11	80	3.8	0.0	16.0
F12	84	3.2	0.0	19.5
F13	80	9.2	9.125	0.0
F14	77	7.2	0.0	0.0
F15	85	7.5	5.25	3.0
F16	80	4.8	0.0	19.0
F16R	72	3.0	0.0	15.0
F17	83	3.6	0.0	25.0
F17R	74	5.8	0.0	14.5
F18	79	3.8	0.375	16.0
F18R	75	5.0	0.5	10.8
F19	80	9.6	7.3	0.0
F19R	78	8.0	6.0	3.0
F20	83	5.2	0.0	16.0
F20R	76	7.0	1.375	6.0
F21	86	4.2	0.5	7.8
F21R	74	5.4	1.0	11.0
F22	86	5.0	1.625	11.0
F22R	75	5.8	0.0	8.0
F23	80	8.8	8.5	0.0
F23R	74	11.2	8.25	0.0
F24	88	4.6	0.25	11.7

Table A.3. Continued

Mixture Designation	Air Temperature (°F)*	Air Content (vol. %)	Slump (in.)†	V-B time (s)
F25	81	9.2	4.5	4.4
F26	83	8.6	4.5	4.6
F27	82	7.4	1.5	6.2
F28	83	6.8	2.5	6.0
F29	90	6.0	1.8	6.4
F30	80	4.0	1.75	11.7
F31	81	4.5	1.5	9.4
F32	68	9.6	7.00	0
F32R	72	5.2	3.125	4.0
F33	68	3.3	0.75	11.0
F33R	70	3.8	1.50	6.0
F34	76	8.0	4.25	3.0
F35	76	4.4	2.5	8.0
F36	74	10.8	7.75	0
F37	78	6.6	4.0	3.0
F38	65	4.2	2.25	8.0
F39	66	3.8	2.0	7.5
F40	75	4.2	1.0	9.5
F41	72	2.2	1.0	14.0
F42	68	1.2	6.0	1.5
F43	73	2.6	3.25	3.0
F44	71	3.0	4.0	4.8
F45	71	4.5	4.0	4.2
F46	71	7.4	5.0	5.0
F46R	69	8.4	3.75	8.0
F47	71	8.2	6.375	0
F47R	70	10.8	7.50	0
F48	71	9.10	7.0	0
F49	70	3.6	0	11.0
F50	74	4.8	4.0	3.0

Note: Replicate mixture proportions (design. by R) are the same as those of the original.
* °C = (°F-32) * 5/9
† 1 in. = 25.4 mm

Table A.4. Plain Concrete Mix

Mixture designation	Mixture proportions			
	W/C ratio (by weight)	Cement (lb/yd^3)	Air-entraining agent (wt %)	High-range water-reducer (wt %)
S1	0.38	611	0.1	1.0
S2,S2R	0.33	654	0.095	0.8
S3,S3R	0.33	658	0.095	0.8
S4,S4R	0.43	564	0.70	0.8
S5,S5R	0.43	658	0.095	0.8
S6,S6R	0.33	564	0.130	1.2
S7,S7R	0.33	658	0.120	1.2
S8,S8R	0.43	564	0.095	1.2
S9,S9R	0.43	658	0.085	1.2
S10	0.38	611	0.095	0.6
S11	0.28	611	0.120	1.0
S12	0.38	517	0.200	1.0
S13	0.38	611	0.050	1.0
S14	0.38	705	0.095	1.0
S15	0.48	611	0.050	1.0
S16	0.38	611	0.095	1.4
S17,S17R	0.33	564	0.130	0.8
S18,S18R	0.33	658	0.120	0.8
S19,S19R	0.43	564	0.130	0.8
S20,S20R	0.43	658	0.095	0.8
S21,S21R	0.33	564	0.150	1.2
S22,S22R	0.33	658	0.095	1.2
S23,S23R	0.43	564	0.095	1.2
S24,S24R	0.43	658	0.095	1.2
S25	0.38	611	0.085	1.0
S26	0.28	705	0.095	1.2
S27	0.28	705	0.095	1.6
S28	0.30	705	0.095	1.2
S29	0.30	705	0.120	1.6
S30	0.28	752	0.120	1.2
S31	0.28	752	0.130	1.4
S32	0.28	752	0.130	1.4
S33	0.28	799	0.130	1.2
S34	0.28	799	0.130	1.0
S35	0.28	799	0.160	1.0
S36	0.28	846	0.130	1.0
S37	0.28	846	0.130	1.2
S38	0.28	846	0.130	0.8
S39	0.30	799	0.130	0.8

Table A.4. Continued

Mixture designation	Mixture proportions			
	W/C ratio (by weight)	Cement (lb/yd^3)	Air-entraining agent (wt %)	High-range water-reducer (wt %)
S40	0.30	799	0.130	1.0
S41	0.43	564	0.130	0.8
S42	0.43	564	0.095	0.8
S43	0.33	564	0.095	1.2
S44	0.33	658	0.095	1.2
S45	0.28	611	0.12	1.0
S46	0.38	517	0.12	1.0
S47	0.38	611	0.095	1.0
S48	0.38	611	0.070	1.0

Table A.5. Plain Concrete Slump Results

Mixture designation	Air temperature (°F)	Air content (vol. %)	Slump (in.)	V-B time (s)
S1	76	9.3	7.5	0
S2	68	3.6	0	6.5
S2R	68	3.9	0.5	4.0
S3	69	4.1	1.5	4.0
S3R	70	3.0	0	11.0
S4,	70	7.2	7.625	0
S4R	68	4.6	2.75	2.5
S5	67	8.6	9.0	0
S5R	67	8.0	9.625	0
S6	66	4.9	1.125	5.0
S6R	70	3.2	0	9.0
S7	71	9.2	8.125	0
S7R	71	11.0	8.5	0
S8	76	7.2	7.625	0
S8R	71	9.0	4.0	2.5
S9	67	9.2	10.5	0
S9R	69	6.6	9.750	0
S10	72	7.4	3.625	1.5
S11	76	4.4	0	7.5
S12	73	6.8	1.625	4.5
S13	74	8.0	8.625	0
S14	72	9.0	8.25	0
S15	68	4.0	10.25	0

Table A.5. Continued

Mixture designation	Air temperature (°F)	Air content (vol. %)	Slump (in.)	V-B time (s)
S16	70	10.2	9.5	0
S17	68	6.4	0	7.5
S17R	68	6.6	0	7.5
S18	71	7.0	3.125	
S18R	69	6.8	3.5	2.5
S19	71	8.8	3.25	3.0
S19R	66	11.8	7.375	0
S20	69	9.6	8.125	0
S20R	74	9.2	7.5	0
S21	68	5.6	1.125	5.5
S21R	68	9.2	4.375	2.5
S22	67	7.6	5.5	1.5
S22R	68	5.4	2.0	4.0
S23	68	11.2	9.25	0
S23R	72	9.2	7.0	0
S24	75	9.0	9.5	0
S24R	72	9.8	9.75	0
S25	68	10.4	8.125	0
S26	75	4.8	0	7.5
S27	71	4.3	3.5	6.0
S28	68	4.6	2.25	5.0
S29	68	4.2	7.5	0
S30	70	3.0	0	7.5
S31	65	9.6	9.0	0
S32	68	7.0	9.0	0
S33	70	6.9	4.5	1.5

Table A.6. Synthetic Fiber Mix and Slump Results

Mix designation	Slump (in.)	Inverted slump (s)	Air content (%)	Unit weight (lb/ft^3)
CON*	7.00	-	5.50	145.7
N6 075	5.50	3	6.00	148.2
N6 100	5.25	4	6.00	143.1
N6 150	4.00	4	5.00	147.4
N6M 100	4.00	4	5.25	146.5
MF 100	5.25	4	5.25	148.2
MF 150	6.50	3	6.00	144.8
NU 100	5.25	3	5.75	148.2

* Plain concrete; 1 lb/ft^3 = 16 kg/m^3; 1 in. = 25.4 mm

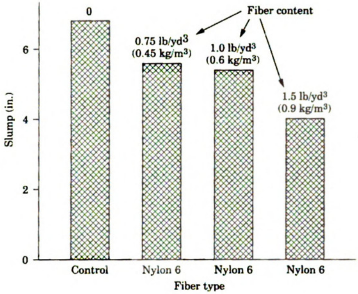

Figure A.2. Synthetic Fiber Slump Results

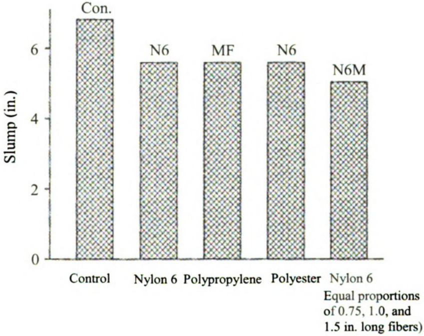

Figure A.3. Synthetic Fiber Slump Results

APPENDIX B

RESTRAINED PLASTIC SHRINKAGE EXPERIMENTS [7,23,30,32,35]

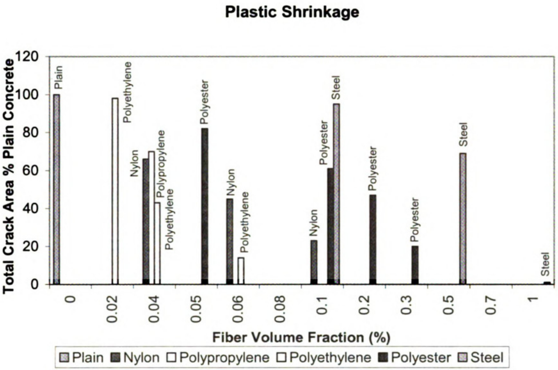

Figure B.1. Summary of the Plastic Shrinkage Results for Different Fiber Types

Table B.1. Test Method I

Fiber Type	Fiber Geometry L : (mm)	Fiber Vol. Fraction	Mix C:S: CA: W	Specimen Dimensions Fig 1	Air/Drying Conditions	Results
Steel Fiber	30 : 0.5 50 : 0.5 60 : 0.5	0.0% 0.1% 0.5% 1.0%	1:1:1 :0.55	H - 40 mm W - 100mm L -1010mm	Air Flow: 340 cfm R.Hum: 5% Temp: 38 °C	Fig. B.3,B.4 table B.3
Polypropylene Fiber	14 mm Rectangular	0.10% 0.20%	see Table B.4	H - 20 mm W - 150mm L - 1200mm	Air Flow : 0.5 ms^{-1} Temp : 40 °C	Fig. B.5
Polypropylene Fiber	14 mm Rectangular	0.10% 0.20%	see Table B.5	H - 15 mm W - 150mm L - 1200mm	Air Flow : 0.5 ms^{-1} Temp : 40 °C	Fig. B.6-B.9 table B.5

TableB.2. Test Method II

Fiber Type	Fiber Vol. Fraction	Mix C:S:CA :W	Specimen Dimensions	Air/Drying Conditions	Results
Polypropylene Fiber	Table B.6,B.7	See Table B.6	See Figure B.10	Air Flow:4 m/s R.Hum: 40% Temp: 20 °C	Fig B.10 – B.16 table B.6.B.7

B.1. Method I

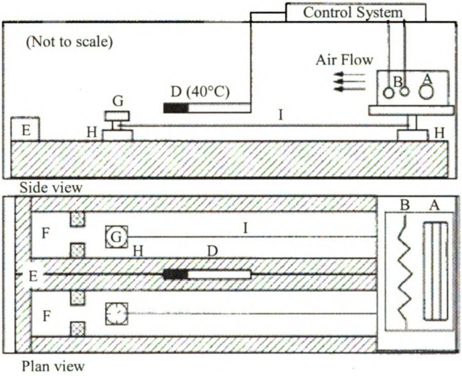

(A) fan, (B) electrical resistance
(B) control system connected to a thermometer (D)
(E) hygrometer
(F) two specimens with dimensions of 20 mm x 150 mm x 1200 mm
The change of length over time is measured with strain Gauges (G) located on steel plates (H) and connected to other steel plates by a steel rod (I).

Figure B.2. Schematic diagram of the plastic shrinkage testing device

B.1.1 Steel Fibers

Table B.3. Results from Shrinkage Test Results (48 h after casting)

	Vf (%)	t_{first} [(1)] (min)	$t_{80\%}$ [(2)] (min)	w_{max} [(3)] (mm)	w_c [(4)] (mm)	L_c [(5)] (mm)	L_c/W_c	A_{crack} [(6)] (mm^2)	n [(7)]
Plain	-	2	40	2.83	4.51	231	51.2	526	2
	0.1	2	65	1.84	4.17	342	82	473	3
SFRC	0.5	17	200	0.69	4.82	821	170.3	368	14
	1.0	50	240	0.38	0.38	72	189.5	27	1

(1) time after demolding at which the first crack appears
(2) time after demolding at which 80% of A_{crack} is achieved
(3) max observed crack width
(4) cumulative crack width
(5) cumulative crack length
(6) total crack area
(7) number of cracks

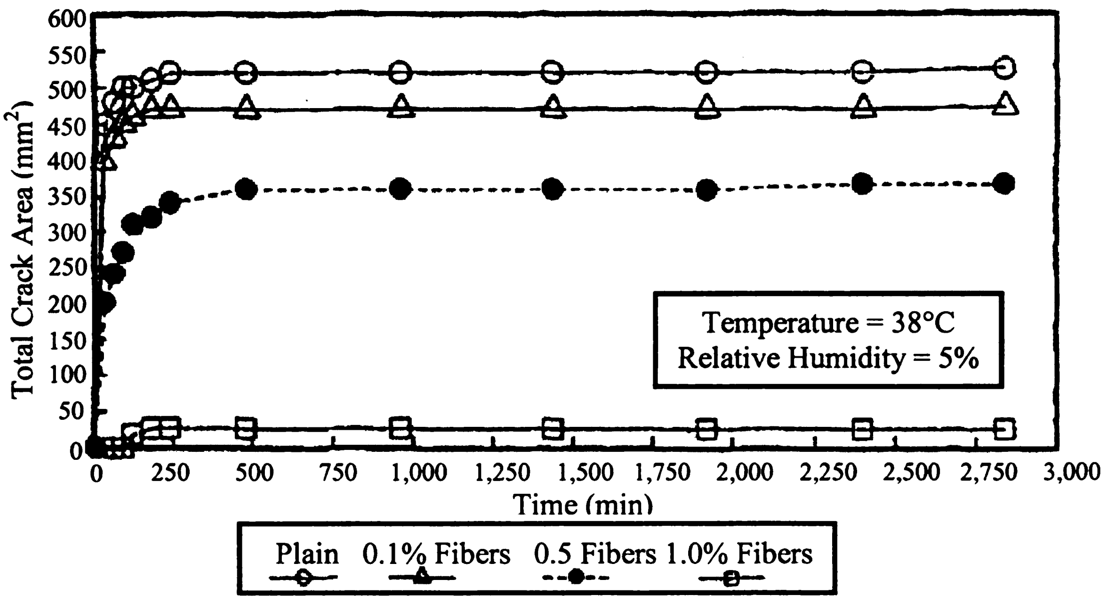

Figure B.3. Evolution in the total crack area in various composites

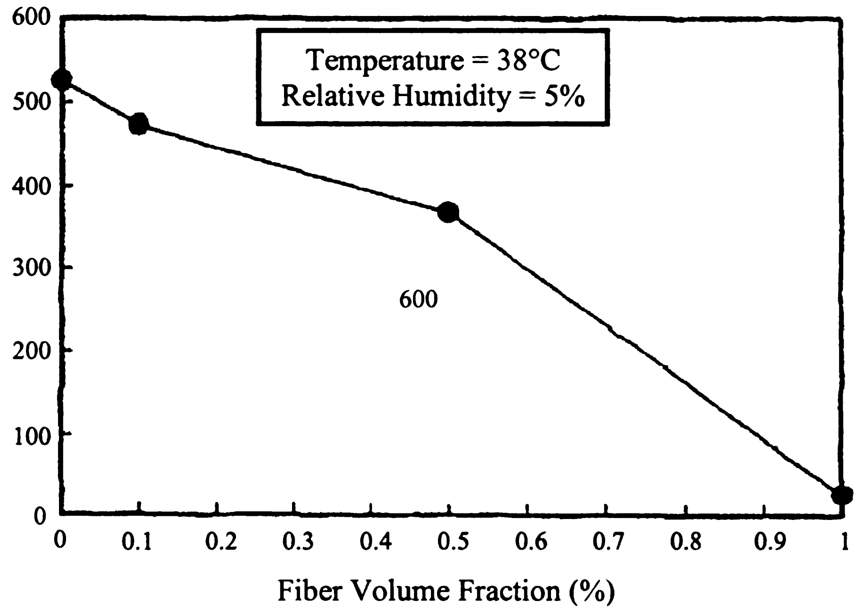

Figure B.4. Total crack area plotted as a function of fiber volume fraction 48h after casting.

B.1.2 Polypropylene Fibers

Table B.4. Time of crack appearance in fresh mortars exposed to restrained shrinkage

Mix proportions	1:2:0.5	1:2:0.5:0.5% Sisal	1:2:0.5:0.5% Polypropylene
Time of cracking (min)	90	180	120

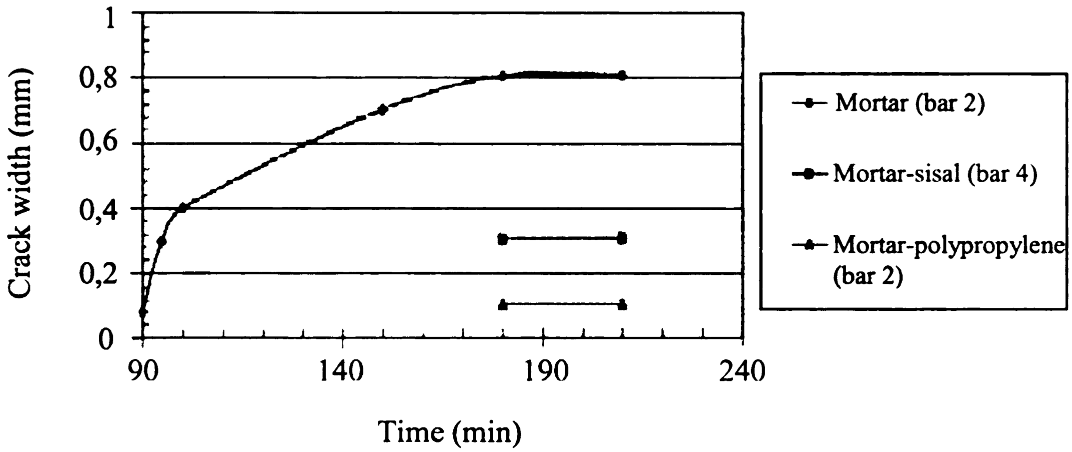

Figure B.5. First crack pattern of mortar, mortar-sisal, and mortar polypropylene at early stage

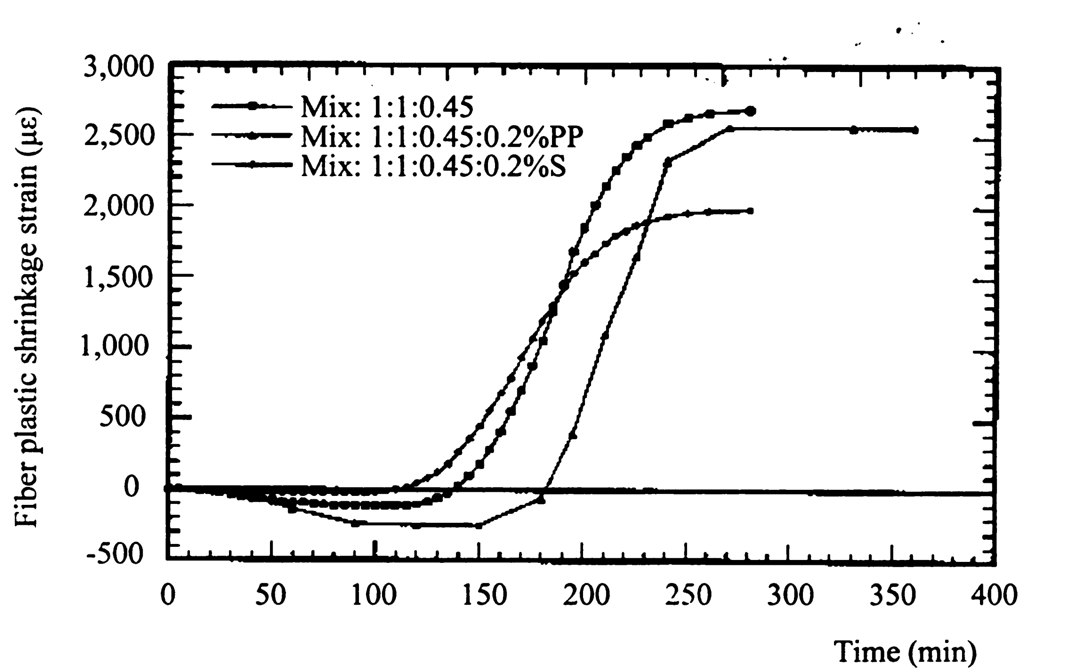

Figure B.6. Plastic shrinkage of mortars reinforced with sisal and polypropylene fiber

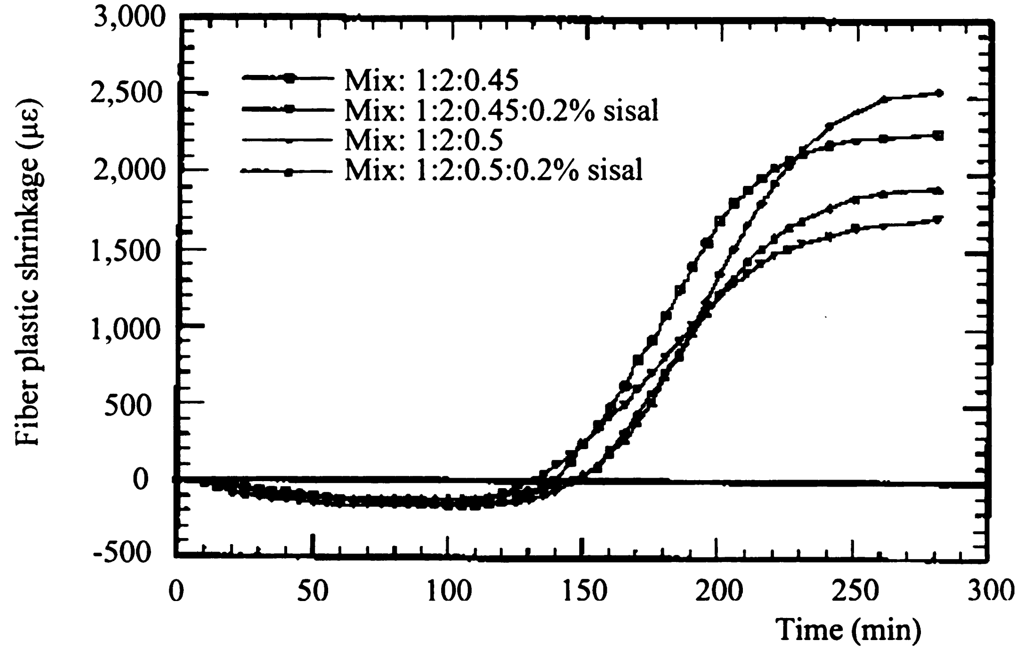

Figure B.7. Shrinkage in Sisal Fiber

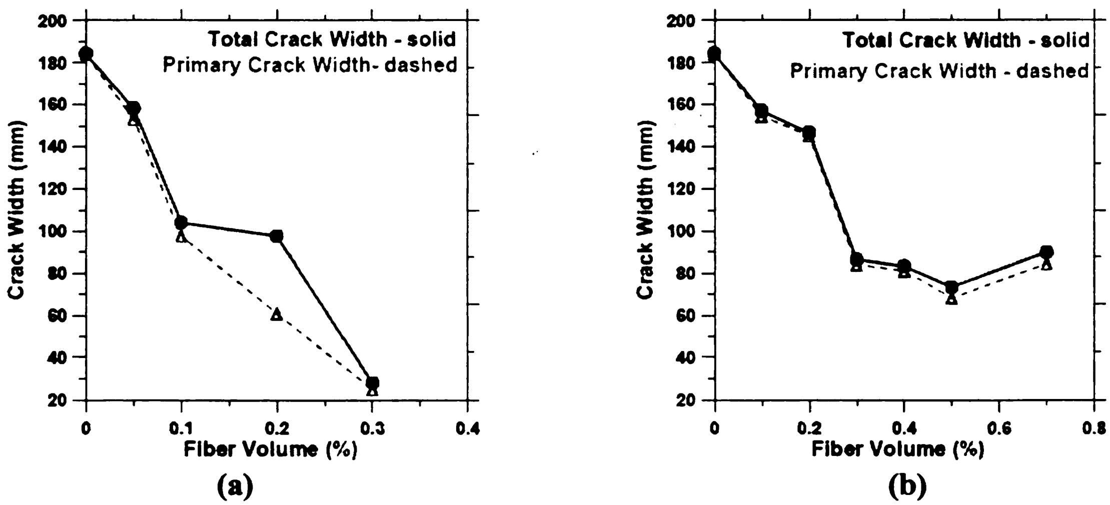

Fig B.8. Comparison of Total and Primary Crack Width: (a) Fibrillated Polypropylene Fiber and (b) Monofilament Polypropylene Fiber

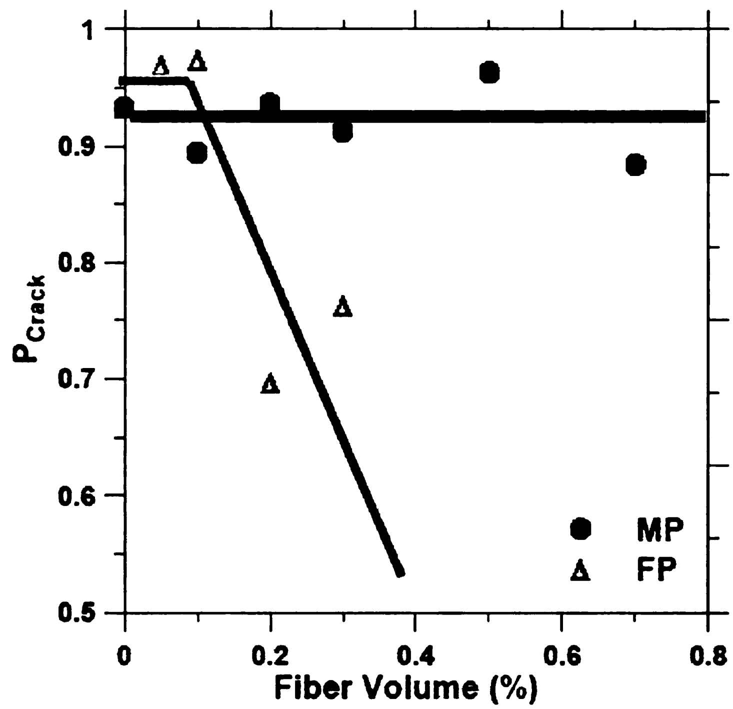

Fig B.9. Measured Value of PCrack as a Function of Fiber Volume

B.1.3 Polypropylene Fibers

Table: B.5 Polypropylene Mix proportions

The mix proportions of the specimens made for studying shrinkage in the plastic state were as follows.
Set 1: A central mix with water/cement ratio, cement/sand ratio and polypropylene content of 0-50, 1/2 and 0/10 vol %, respectively. Eight mixes with water/cement ratios of 0.45 and 0.55, cement/sand ratios of 1/3 and 1/l and polypropylene contents of 0 and 0.20 ~ 01%.
Set 2: Six mixes called 'star' combinations composed as follows: • Four mixes with 0.1 ~ 01% of polypropylene fibers: two of them with cement/ ratio of 1/2 and water/cement ratios of 0.42 and 0.58; and the other two with water/cement ratio of 0.50 and cement/sand ratios of 1/9 and 1/0.8. • Two mixes with a water/cement ratio of 0.50, cement/sand ratio of 1/2 and two polypropylene fiber contents of 0 and 0.27 ~ 01%.

B.2. Method II

B.2.1 Polypropylene Fibers

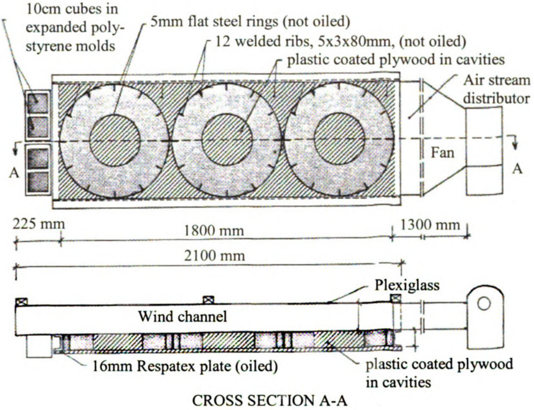

Figure B.10. Schematic diagram of the Test rig for study of cracking tendency due to plastic shrinkage

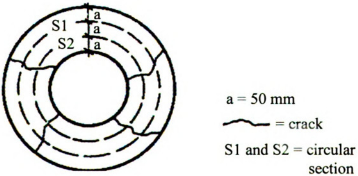

Figure B.11. Location of measuring sections S1 & S2

Table B.6. Concrete Mixes

Test No.	Fibermesh 1 ½ ", kg/m^3	Net reinforcement	Total crack widths, mm (%) Upper side	Lower side
1	0	None	5,9 (100)	2,0 (100)
	1,0		1,8 (31)	0,5 (25)
2	0		2,5 (100)	1,2 (100)
	1,4		0,3 (12)	0,3 (25)
3	-	None	3,1 (100)	1,1 (100)
	-	In the middle	3,3 (106)	1,2 (109)
	-	Towards the bottom	0,9 (29)	1,1 (100)

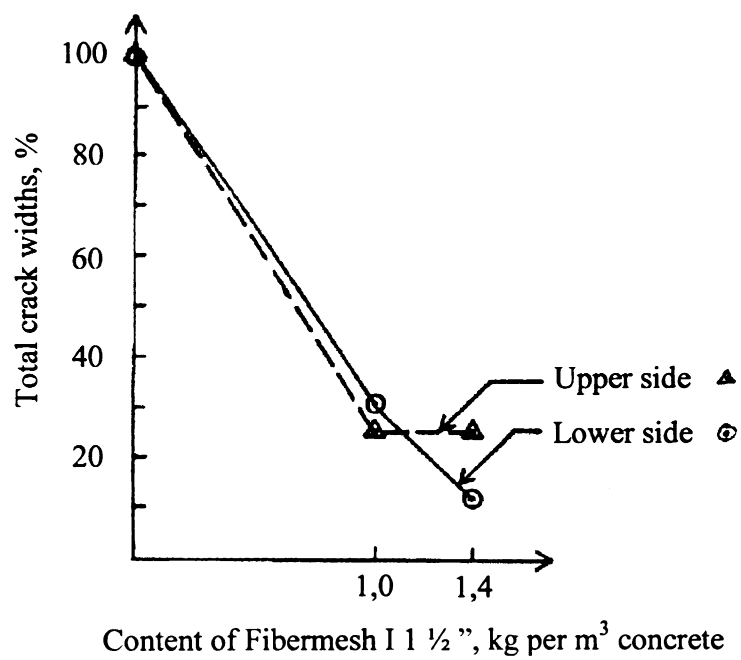

Figure: B.12 Relationship between crack widths and content of fiber mesh I 1.50"in mortar

Table B.7. Mortar Mixes

Test No.	Addition, kg/m^3		Steel net reinforcement	Total crack widths, mm (%)	
	Fibermesh I ¾ ”	Fibermesh II ½ ”		Upper side	Lower side
4	0	-	None	3,5 (100)	3,0 (100)
	1,0	-		1,6 (46)	2,0 (67)
5	0	-		6,1 (100)	3,6 (100)
	1,4	-		0,8 (13)	1,1 (31)
6	0	-		4,3 (100)	2,7 (100)
	14	-		0 (0)	0 (0)
7	-	0		4,5 (100)	2,3 (100)
	-	1,0		1,1 (24)	1,0 (43)
8	-	0		4,7 (100)	2,6 (100)
	-	1,4		1,4 (30)	0,7 (27)
9	-	-	None	4,9 (100)	2,7 (100)
	-	-	In the middle	2,0 (41)	3,1 (115)
	-	-	Towards the bottom	1,9 (39)	2,9 (107)

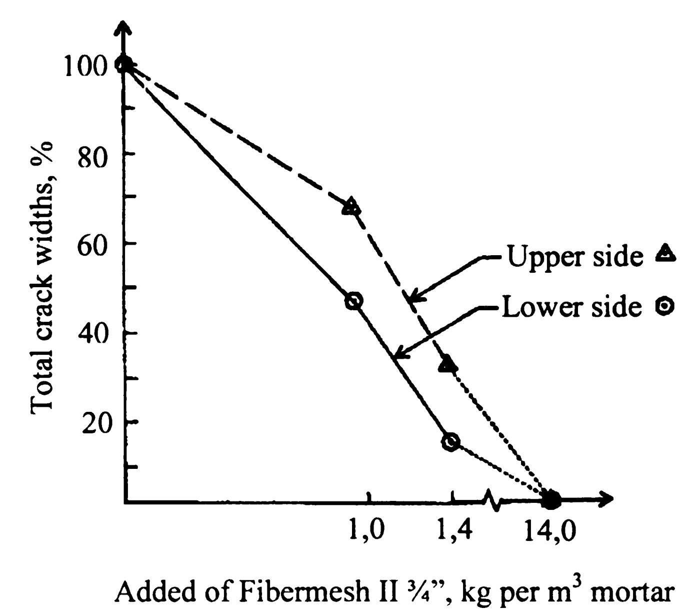

Figure B.13. Relationship between crack widths and content of fiber mesh I 0.75" in mortar

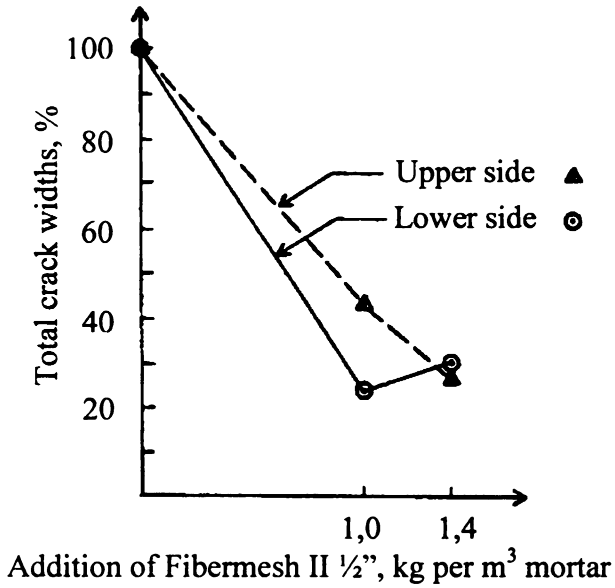

Figure B.14. Relationship between crack widths and content of fiber mesh II .50" in mortar

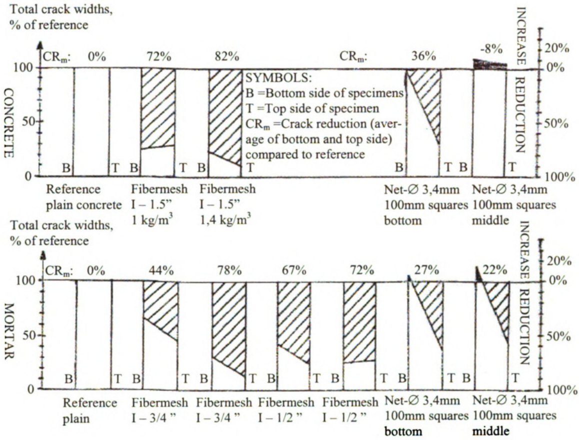

Figure B.15. Crack formation due to plastic shrinkage

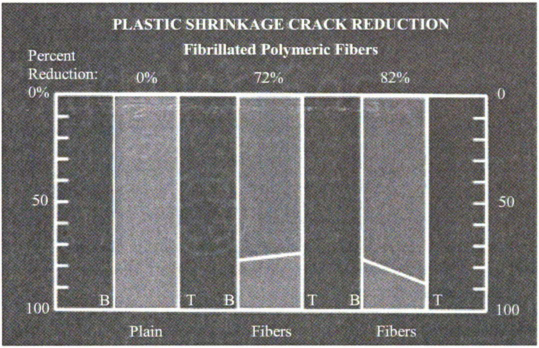

Figure B.16. Plastic shrinkage crack reduction

Plastic Shrinkage Crack Reduction:

The diagram (Fig B.16) shows that over 72 - 82% of plastic shrinkage cracks are prevented from forming when fibers are added to the concrete as compared to the same concrete without fibers. The tests were reported by SINTEF, the Norwegian Research Group. The cracks were measured, top and bottom, in a special ring developed by this group for testing plastic shrinkage cracking of concrete.

It should be noted that the cracks were measured at T (tip) and B (bottom) of each specimen. This shows that most plastic shrinkage cracks extend throughout the slab and are not merely superficial cracks at the surface.

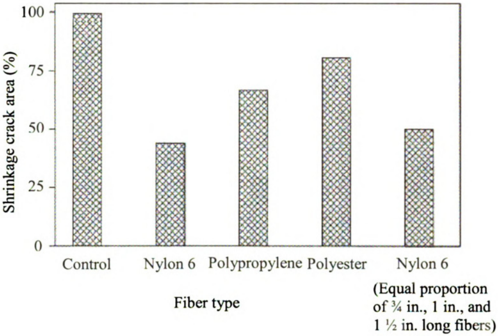

Figure B.17. Shrinkage Crack Area Vs. Fiber Type and size

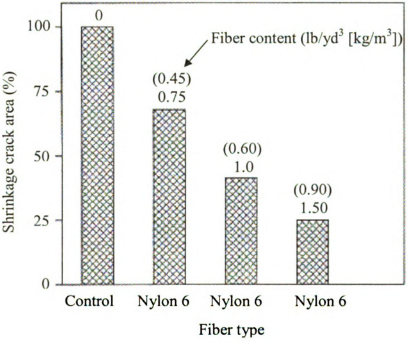

Figure B.18. Shrinkage Crack Area vs. Fiber Type and Content

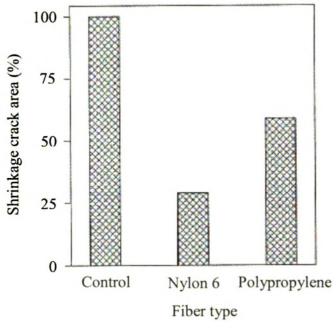

Figure B.19. Shrinkage Crack Area vs. Fiber Type

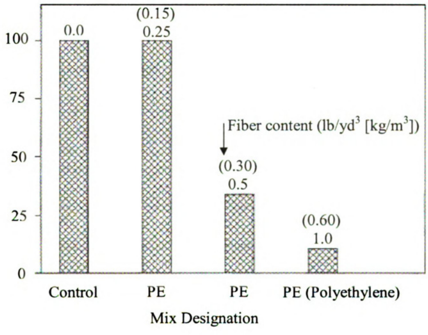

Figure B.20. Shrinkage Crack Area vs. Mix Designation

B.3. Polyester Fibers

Table B.8. Properties of Polyester Fiber

Diameter	0.035 mm
Length	12 mm
Density	0.97 t/m^3
Aspect Ratio	343
Tensile strength	approx. 600 N/mm^2
Melting point	> 250 °C
Acid resistance	Excellent
Alkali resistance	Good

Table B.9. Mix Proportions for Substrate Base

Ingredient	Proportion	kg/m^3
Cement	1	403
Coarse aggregate	1.5	604.50
Sand	3	1209
Water	0.40	161/20

Table B.10. Mix Proportion for Overlay Concrete

Mix type	Proportions			
	Cement	Aggregate	Sand	Water
A	1	1	1	0.50
B	1	1.25	1.25	0.55
C	1	1.5	1.5	0.60

Table B.11. Rate of Free Surface Water Evaporation

Drying environment	A	B	C	D
Temperature (°C)	32	38	45	52
Free surface water evaporation ($kg/m^2/hr$)	0.179	0.285	0.422	0.522

Table B.12. Crack Observations for Mix A

Specimen*	Fibre content (%)	Max. width of crack (mm)	Area of crack (mm^2)	% control	% of crack reduction
AA0	0	0.45	98.31	100	0
AA1	0.05	0.40	88.21	89.73	10.26
AA2	0.10	0.30	28.0	28.48	71.52
AA3	0.20	0.25	22.52	22.91	77.09
AA4	0.30	0.10	10.33	10.50	89.50
AB0	0	0.50	212.34	100	0
AB1	0.05	0.40	192.31	90.56	9.44
AB2	0.10	0.30	112.00	52.72	47.25
AB3	0.20	0.15	67.00	31.55	68.45
AB4	0.30	0.15	21.325	10.04	89.96
AC0	0	0.50	278.00	100	0
AC1	0.05	0.50	216.26	77.79	22.21
AC2	0.10	0.35	146.71	52.77	47.23
AC3	0.20	0.30	108.70	39.10	60.90
AC4	0.30	0.20	62.32	22.42	77.58
AD0	0	0.55	320.00	100	0
AD1	0.05	0.40	280.10	87.53	12.47
AD2	0.10	0.40	203.00	63.44	36.56
AD3	0.20	0.35	161.90	50.59	49.41
AD4	0.30	0.15	65.80	20.56	79.44

* Specimens are designated with one 1st letter for mix type, 2nd letter for environment, 3rd letter for fibre volume fraction.

Table B.13. Crack Observations for Mix B

Specimen*	Fibre content (%)	Max. width of crack (mm)	Area of crack (mm^2)	% control	% of crack reduction
BA0	0	0.45	97.14	100	0
BA1	0.05	0.45e	72.00	74.12	25.88
BA2	0.10	0.30	62.30	64.13	35.87
BA3	0.20	0.15	30.13	31.02	68.98
BA4	0.30	0.10	14.35	14.77	85.23
BB0	0	0.35	103.25	100	0
BB1	0.05	0.35	85.00	82.32	17.68
BB2	0.10	0.35	74.30	71.96	28.04
BB3	0.20	0.25	62.52	60.55	39.45
BB4	0.30	0.15	29.35	28.43	71.57
BC0	0	0.50	240.90	100	0
BC1	0.05	0.40	124.70	51.76	48.24
BC2	0.10	0.35	119.26	49.51	50.49
BC3	0.20	0.30	100.00	41.51	58.49
BC4	0.30	0.20	32.25	12.43	87.57
BD0	0	0.65	206.20	100	0
BD1	0.05	0.60	187.38	90.87	9.13
BD2	0.10	0.50	189.38	77.29	22.71
BD3	0.20	0.40	131.30	63.68	36.32
BD4	0.30	0.25	70.50	34.19	65.81

Table B.14. Crack Observations for Mix C

Specimen*	Fibre content (%)	Max. width of crack (mm)	Area of crack (mm^2)	% control	% of crack reduction
CA0	0	0.35	86.02	100	0
CA1	0.05	0.30	75.62	87.91	12.09
CA2	0.10	0.25	57.48	66.82	33.18
CA3	0.20	0.20	47.00	54.64	45.36
CA4	0.30	0.10	12.00	13.95	86.05
CB0	0	0.40	101.32	100	0
CB1	0.05	0.35	82.35	81.28	18.72
CB2	0.10	0.35	81.30	80.24	19.76
CB3	0.20	0.30	57.35	56.66	43.40
CB4	0.30	0.10	24.35	24.03	75.97
CC0	0	0.40	110.20	100	0
CC1	0.05	0.40	94.14	85.43	14.57
CC2	0.10	0.35	83.00	75.32	24.68
CC3	0.20	0.25	72.00	65.34	34.66
CC4	0.30	0.20	23.20	21.05	78.95
CD0	0	0.50	136.94	100	0
CD1	0.05	0.40	118.20	86.32	13.68
CD2	0.10	0.35	73.133	53.41	46.59
CD3	0.20	0.30	61.00	44.55	55.45
CD4	0.30	0.20	39.90	29.14	70.86

APPENDIX C

RESTRAINED DRYING SHRINKAGE EXPERIMENTS [6,12,14,26]

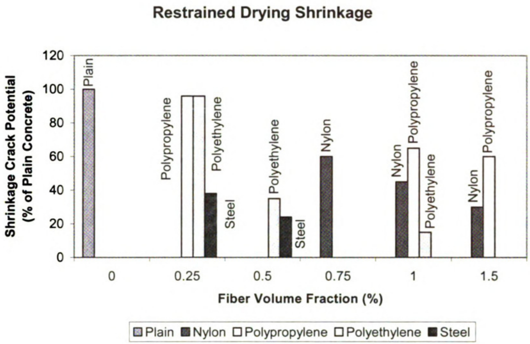

Figure C.1. Summary of the Drying Shrinkage Results for Different Fiber Types

Table C.1. Different Fiber and Mix Properties and Reference to Results' Tables

Fiber Type	Fiber Geometry L : D (mm)	Fiber Vol. Fract:	Mix C:S:CA:W	Specimen Dimensions Fig 1	Curing	Drying Conditions	Results
Steel Fiber	30 : 0.5 50 : 0.5 60 : 0.5	0.0% 0.025% 0.5%	1:1.5:2:0.5	T- 35 mm H - 140 mm D_1- 254 mm D_2- 305 mm	Days – R.Hum - 100% Tem - 20°C.	R.Hum - % Tem - °C	Fig C.3 – C.6
Crimped Steel Fiber	25 38 52	0.0% 0.25% 0.5% 1.0%	1:2:2:0.5	T- 75 mm H - 75 mm D_1- 300 mm D_2- 450 mm	Days – R.Hum - 50% Tem - 23°C.	R.Hum - 50% Tem - 23 °C	Fig C.7 – C.8
Steel Fiber (Brass coated) Straight	see Table 2	see Table 2	see Table 2	T- 35 mm H - 140 mm D_1- 254 mm D_2- 375 mm	Days – 1 R.Hum - 50% Tem - 20°C.	R.Hum - 50% Tem - 20 °C	Table C.2-C.4 Fig C.9-C.20
Poly-propylene Fiber	30 : 0.5 50 : 0.5 60 : 0.5	0.1% 0.25% 0.5% 1.0%	1:2:2:0.5	T- 35 mm H - 140 mm D_1- 254 mm D_2- 305 mm	Days – R.Hum - 100% Tem - 20°C.	R.Hum - % Tem - °C	Fig C.21-C.24
Poly-olefin Fiber	A: 25.4 :0.38 B: 50.8 :0.64 C: 25.4 :0.15	0.1% 0.2% 0.5% 1.0%	1:1.5:2:0.5	T- 38 mm H - 140 mm D_1- 254 mm D_2- 305 mm	Days – R.Hum - 100% Tem - 20°C.	R.Hum - 50% Tem - 20 °C	Fig C.25-C.28

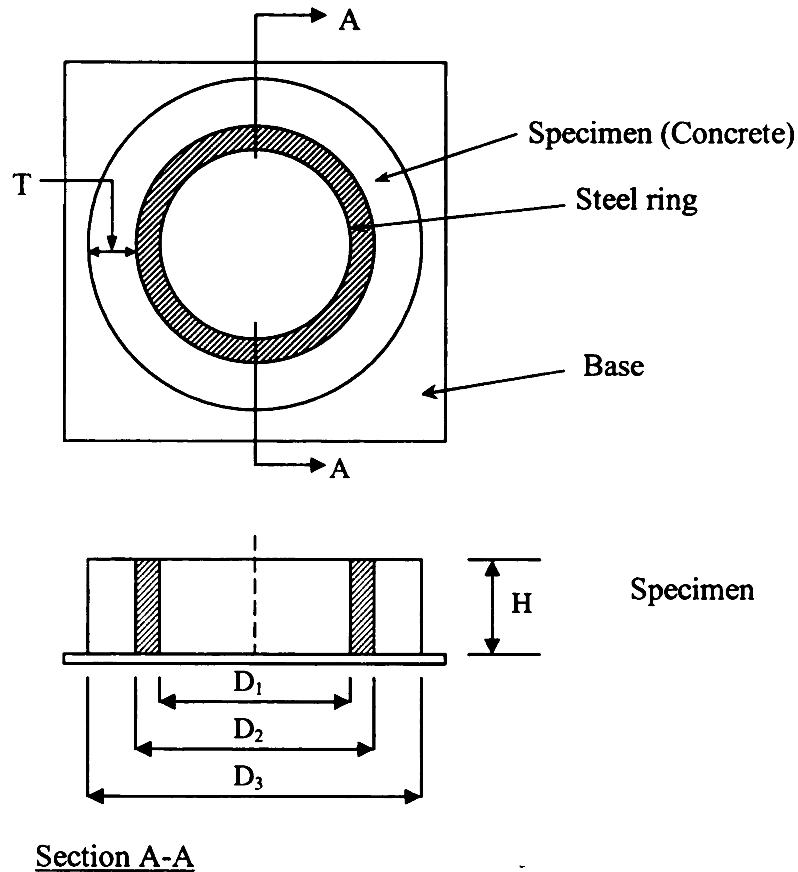

Figure C.2. Dimensions of the Ring Specimen

C.1. Steel Fibers

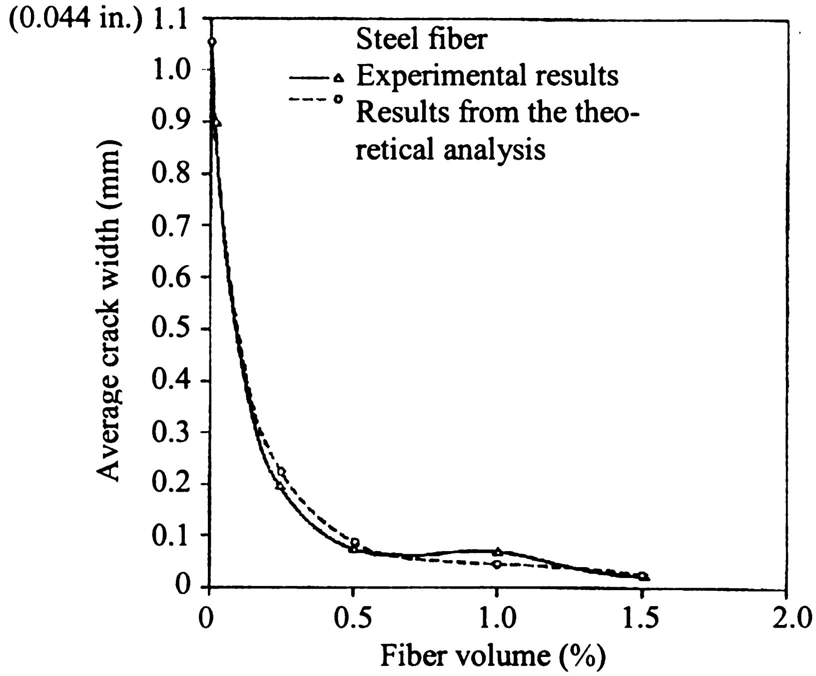

Figure C.3. Average crack width versus steel fiber volume fraction

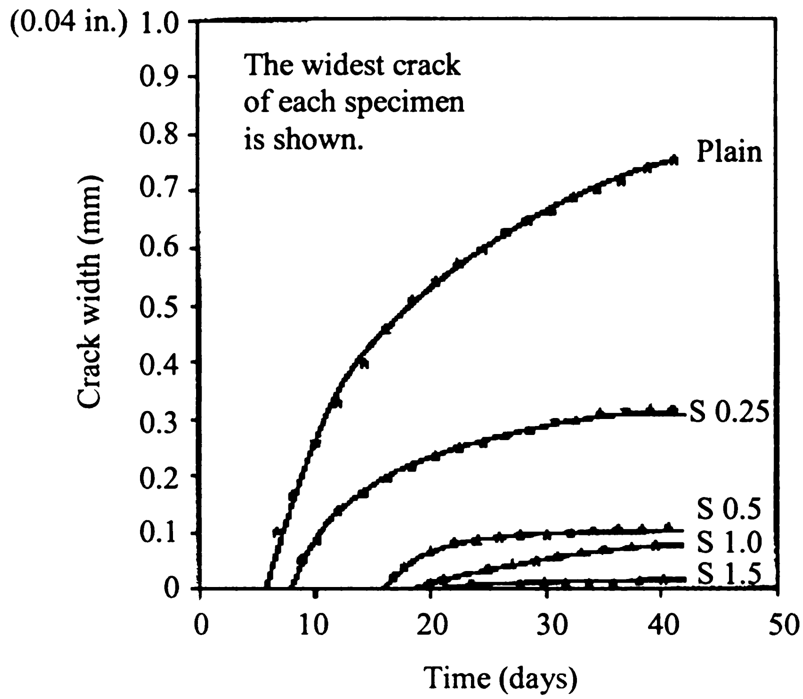

Figure C.4.Crack width versus time for various steel fiber volume fraction

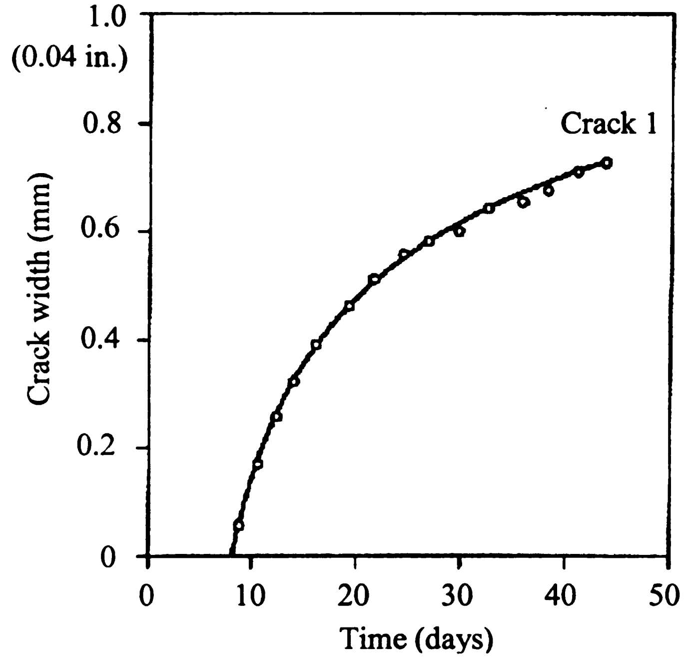

Figure C.5. Crack-width versus time for plain concrete

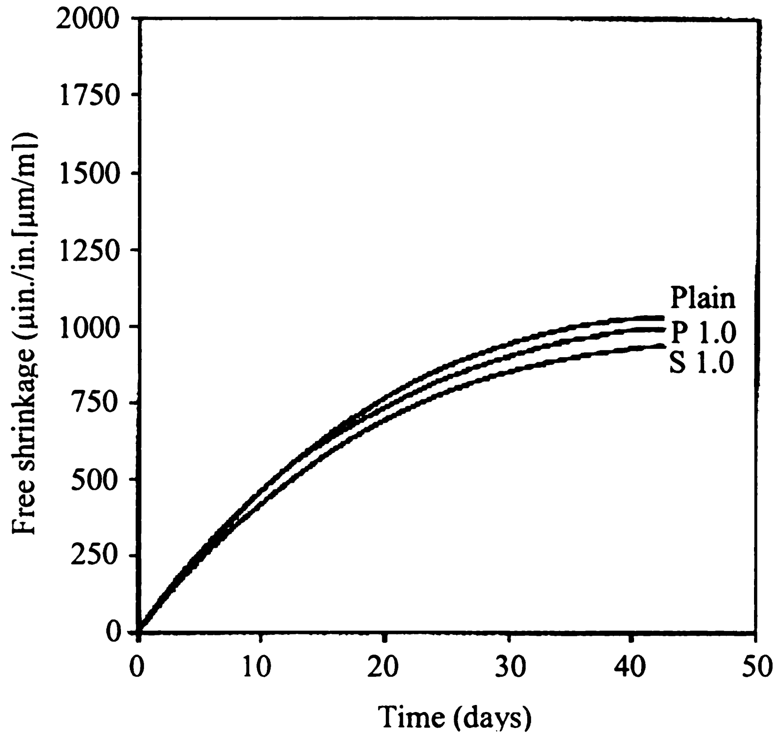

Figure C.6. Free shrinkage versus time for plain, steel fiber, and polypropylene fiber reinforced concrete

C.2. Crimped (Steel) Fibers

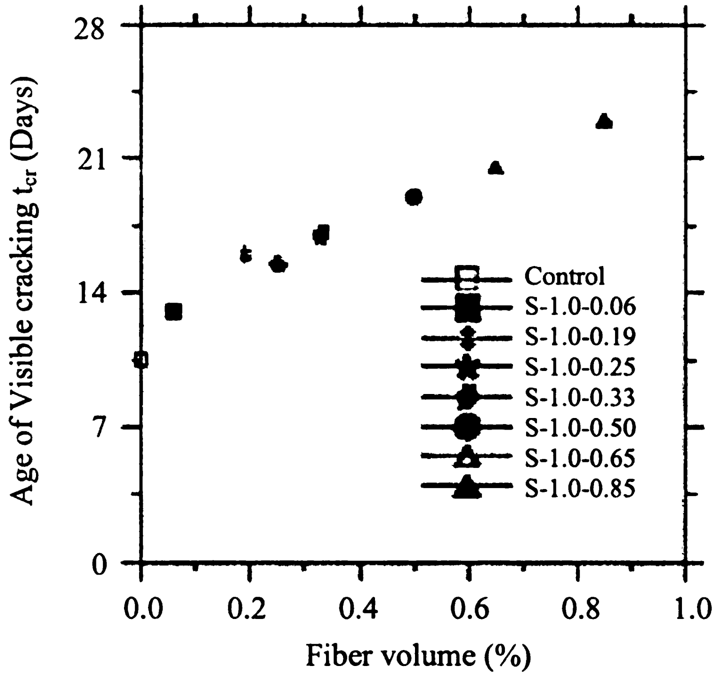

Figure C.7.Age of visible cracking as a function of crimped steel fiber volume fraction

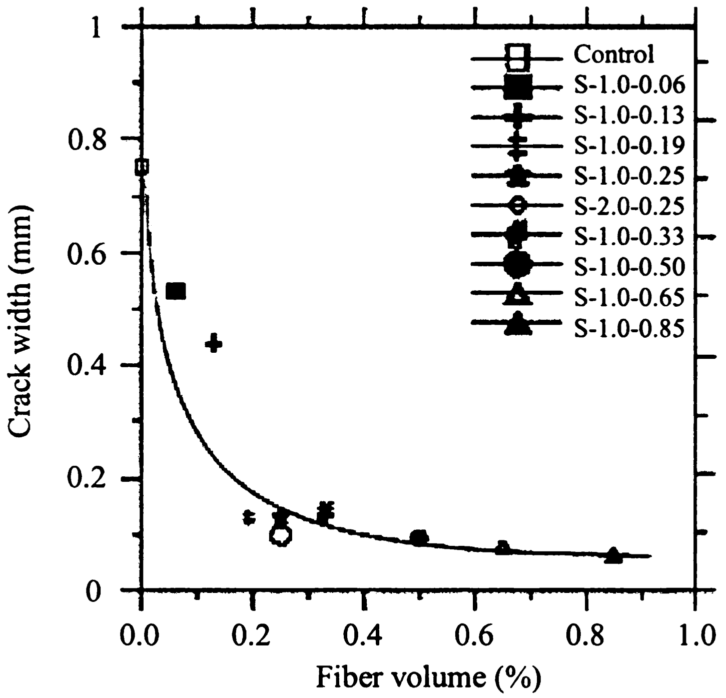

Figure C.8.Crack width versus crimped steel fiber volume fraction

C.3. Steel Fibers – (brass coated straight)

Table C.2. Ring Test Performed

Series	No.	t_0 (h)	L_f (mm)	V_f (%)	m_f (kg/m^3)	f_{cc} (MPa)	Mix
R01	4	24	-	0	0	54	A
R02	3	24	60	0.13	10	54	A
R03	2	24	60	0.26	20	54	A
R04	3	24	60	0.51	40	54	A
R05	3	24	-	0	0	25	B
R06	3	24	35	0.38	30	25	B
R07	3	24	35	0.64	50	25	B
R08	3	24	60	0.38	30	25	B
R09	3	24	60	0.64	50	25	B
R10	3	24	*	*	0.9?	25	B
R11	3	24	-	0	0	123	C
R12	3	24	35	0.38	30	119	C
R13	3	24	35	0.64	50	122	C
R14	3	24	60	0.38	30	119	C
R15	3	24	60	0.64	50	119	C
R16	3	24	-	0	0	58	D
R17	3	24	35	0.38	30	52	D
R18	3	24	35	0.64	50	52	D
R19	3	24	60	0.38	30	50	D
R20	3	24	60	0.64	50	54	D

t_0: (h) curing time between casting and demolding, L_f: fiber length, (mm). V_f: (%), and m_f: (kg/m^3): fiber content. f_{cc}: compressive strength after 28 days of curing, (MPa).

Table C.3. Concrete mixes used for ring test

Mix	w_0/B	d_{max}	Cement type	C	Silica fume	0-8mm	8-18mm	8-12mm	12-16mm	Super plasticizer
		mm		kg/m^3	kg/m^3	kg/m^3	kg/m^3	kg/m^3	kg/m^3	% (of C)
A	0.55	16	Anl	310	0	900	0	550	550	0
B	0.77	18	Std	250	0	268	1162	0	0	0
C	0.308	16		490	48					1
D	0.50	16	Std.	440	0	691	0	441	441	0

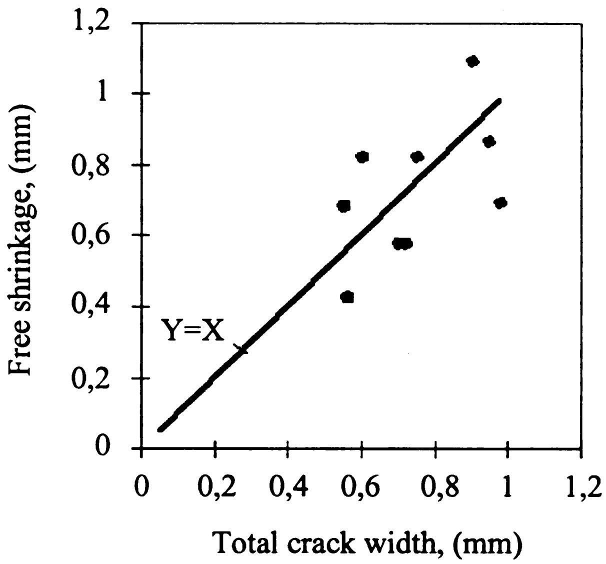

Figure C.9.Correlation between total free shrinkage and total crack width for plain concrete

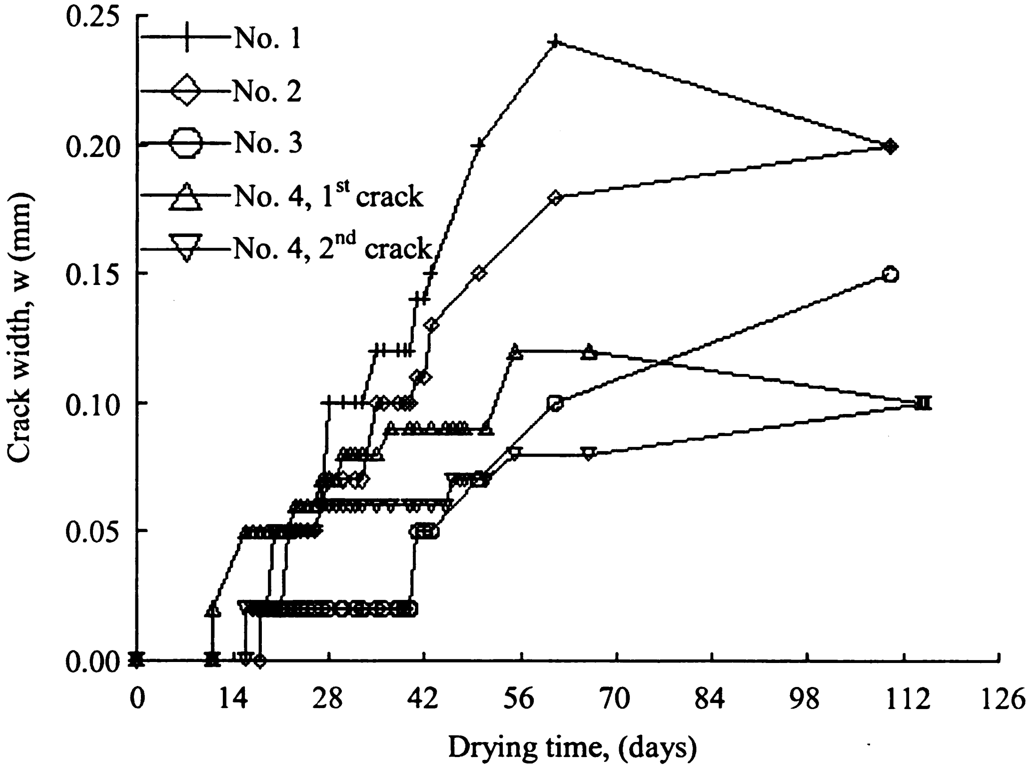

Figure C.10 .Crack development in ring tests for series R01 (plain concrete). The # refer to each of the four rings used

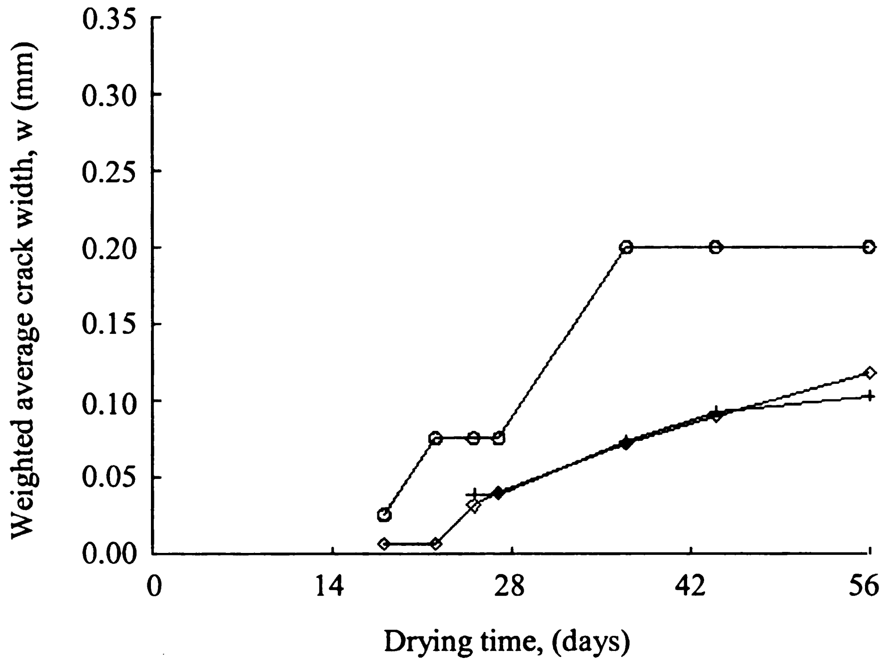

Figure C.11. Crack development in ring tests for series R05 (plain concrete).

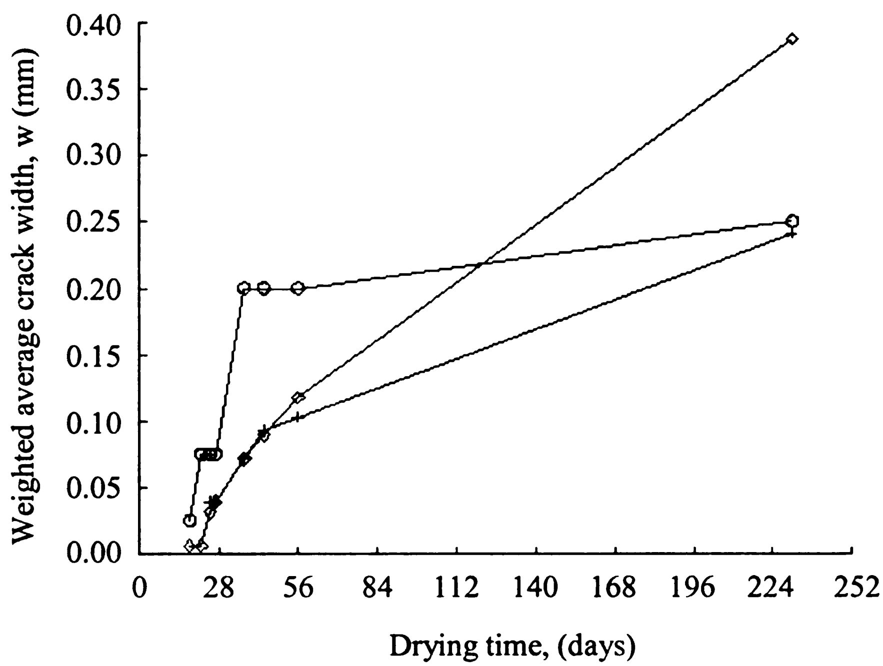

Figure C.12 .Crack development in ring tests for series R05 (plain concrete) Long period

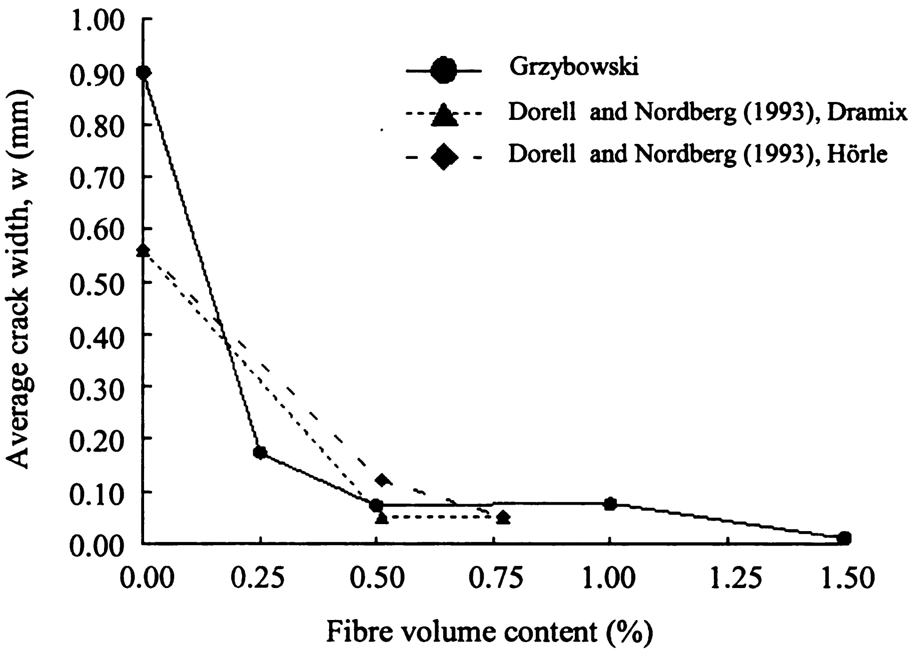

Figure C.13. Average crack widths versus steel fiber volume content

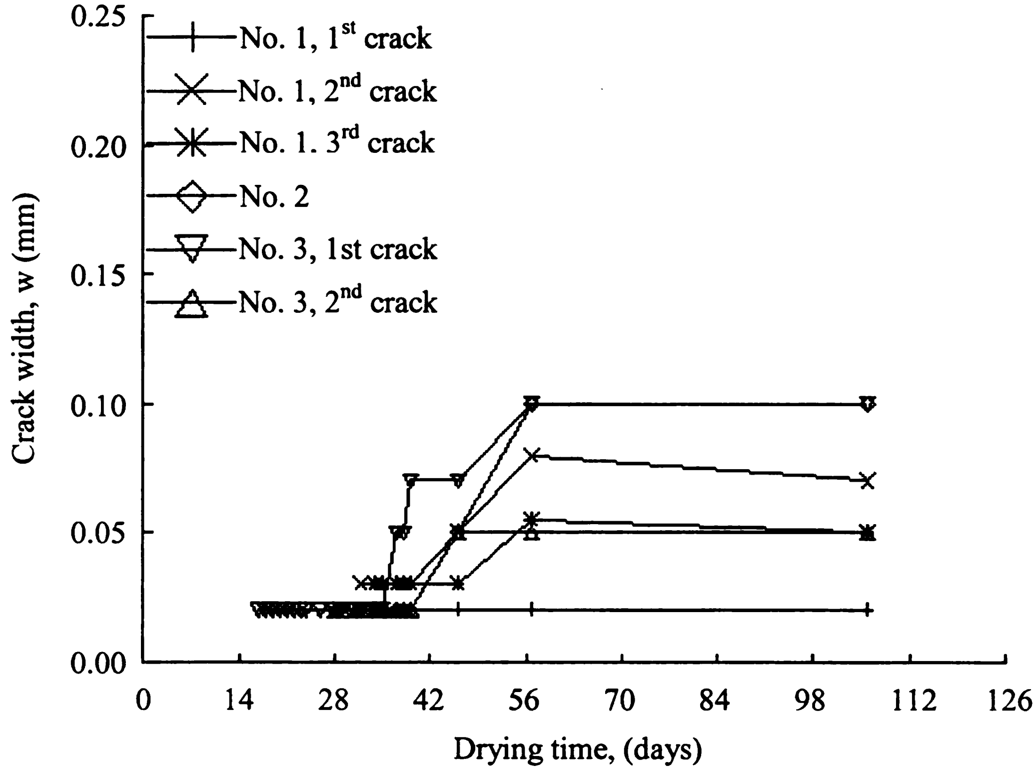

Figure C.14. Crack development in ring tests for series R02 (10 kg/m^3). The numbers refer to each of the three rings used.

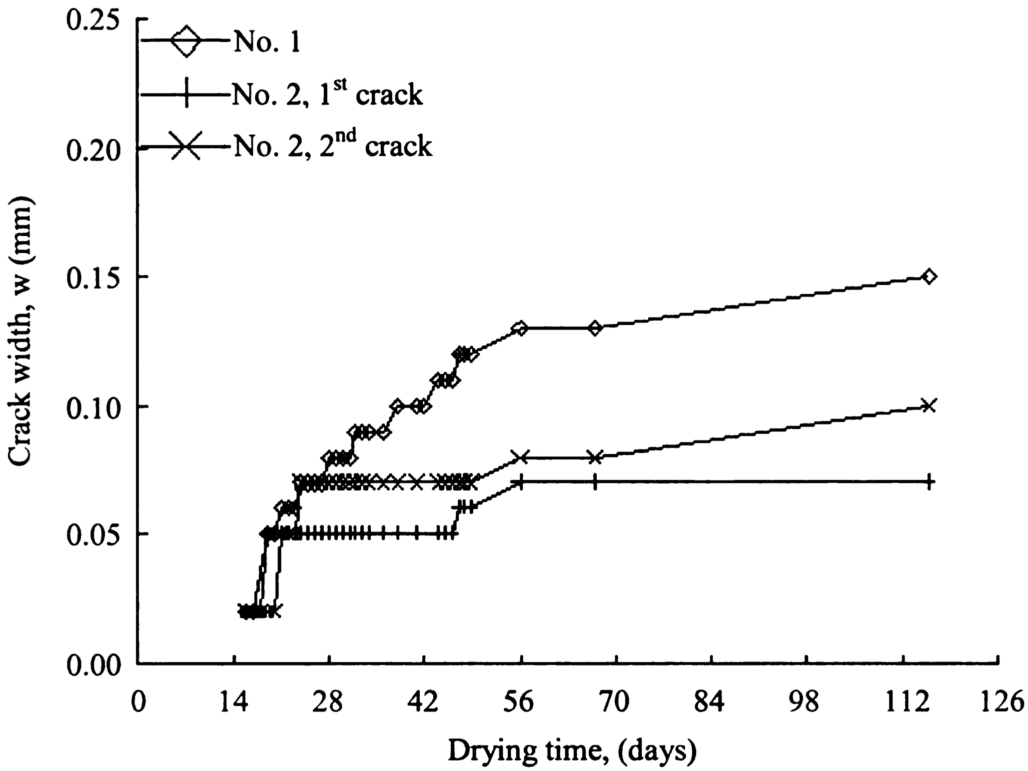

Figure C.15. Crack development in ring tests for series R03 (20 kg/m³). The numbers refer to each of the two rings used.

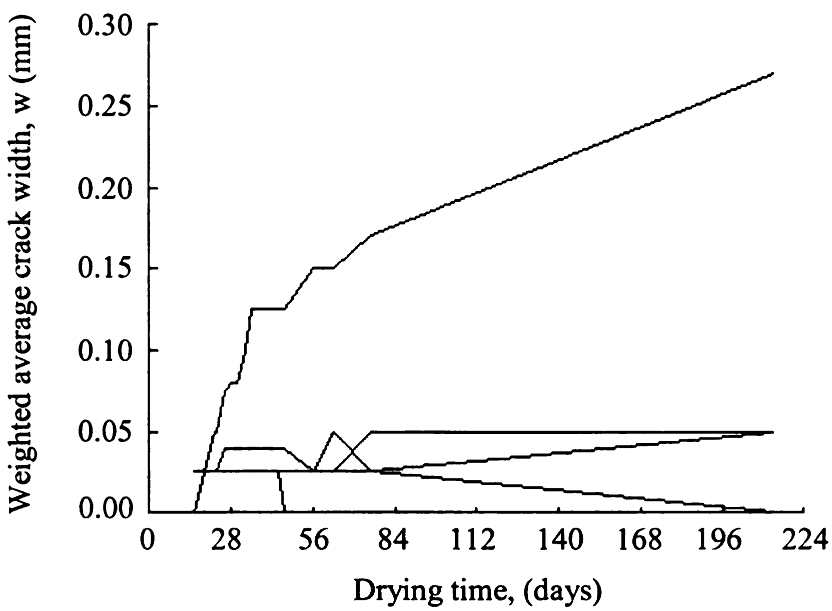

Figure C.16. Crack development of one ring specimen of test series R10 (Synthetic fiber type: Fiber mesh), each curve represents a single crack. The crack width is a weighted average relative the crack length measured at the end of the test period.

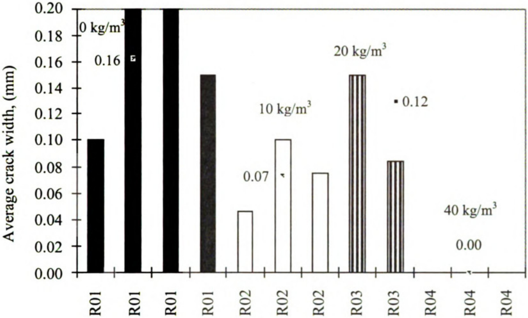

Figure C.17. Results from ring tests for mix A (table 1). The bars represent the average crack width of each ring specimen after 106 to 116 days of curing. The numbers in the diagram are the average crack width, (mm) and fiber content, (kg/m³).

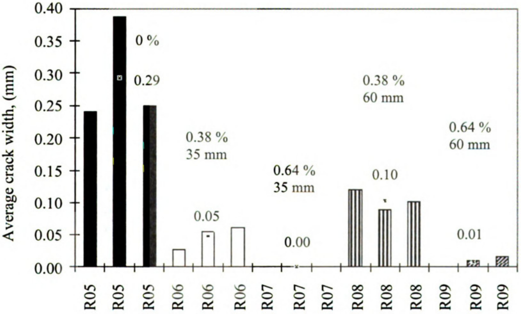

Figure C.18. Results from ring tests for mix B (table 1). The bars represent the average crack width of each ring specimen after 231 days of drying. The numbers in the diagram are the average crack width, (mm) and combinations of fiber volume content, (%) and fiber length (mm).

Table C.4. Results of restrained shrinkage test for test series R11 - R15.

Spec.	No. of cracks 0 - 0.05 mm	Average	Length of longest crack (mm)	Average (mm)
R11-a	33		41	
R11-b	27	26	35	32
R11-c	18		21	
R12-a	13		26	
R12-b	23	15	55	34
R12-c	8		20	
R13-a	15		21	
R13-b	18	17	43	34
R13-c	18		38	
R14-a	12		45	
R14-b	11	14	25	34
R14-c	20		31	
R15-a	23		28	
R15-b	27	30	28	29
R15-c	39		31	

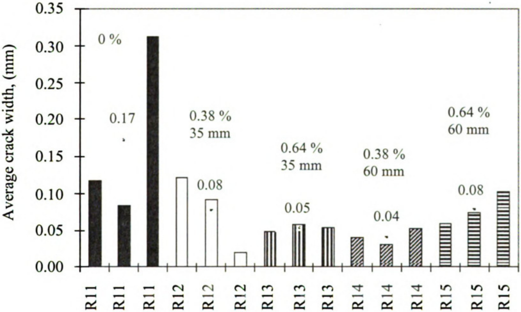

Figure C.19. Results from ring tests for mix C (table 1). The bars represent the average crack width of each ring specimen after 80 days of drying. The numbers in the diagram are the average crack width, (mm) and combinations of fiber volume content, (%) and fiber length (mm).

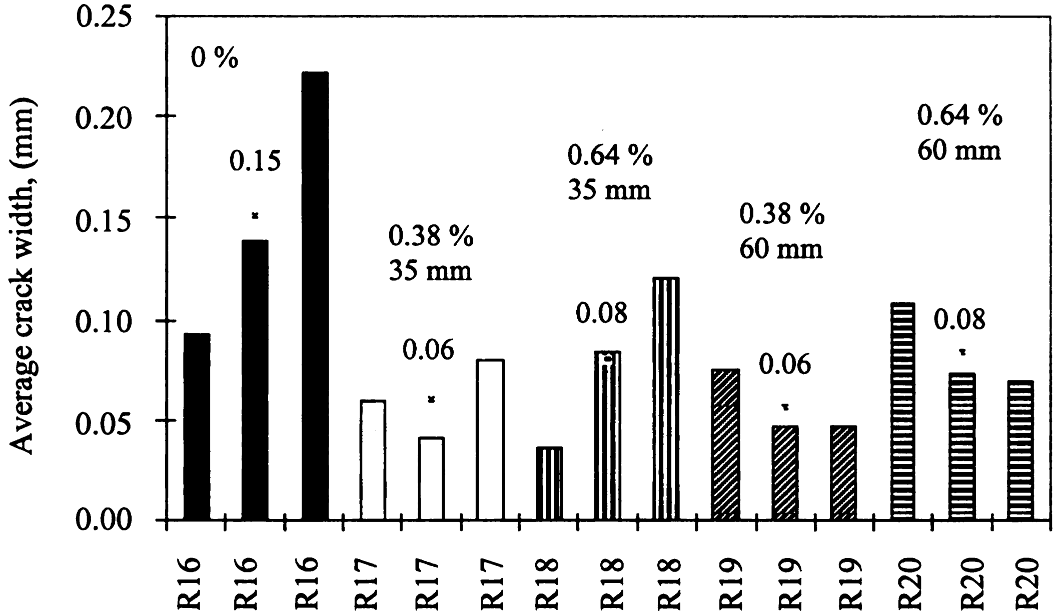

Figure C.20. Results from ring tests for mix D (table 1). The bars represent the average crack width of each ring specimen after 66 days of curing. The numbers in the diagram are the average crack width, (mm) and combinations of fiber volume content, (%) and fiber length (mm).

C.4. Polypropylene Fibers

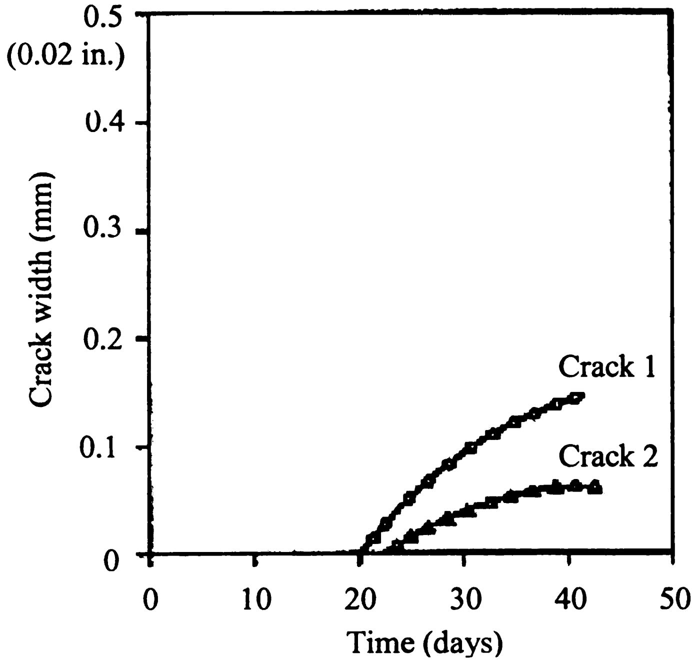

Figure C.21.Crack-width versus time for concrete with 1.0% volume fraction of polypropylene fibers

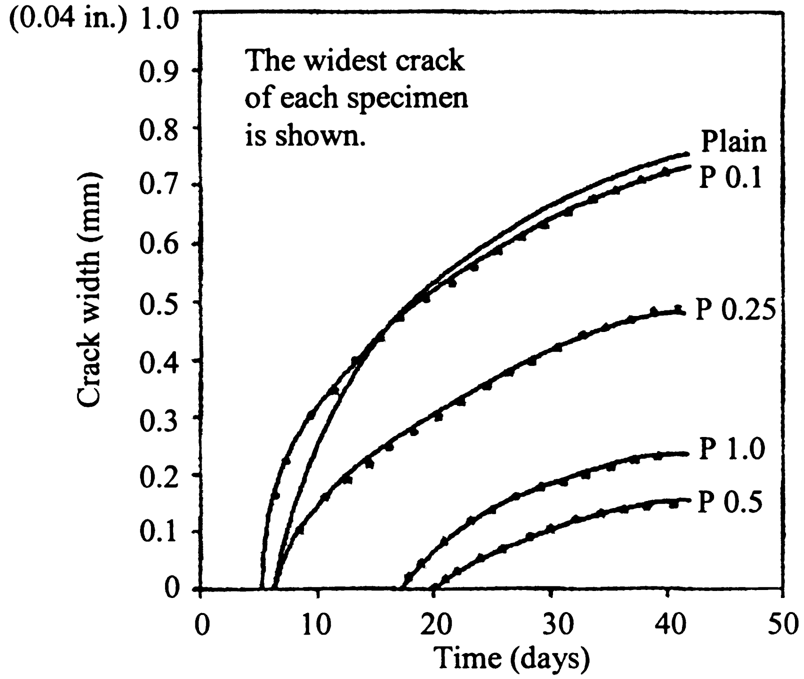

Figure C.22.Crack width versus time for various polypropylene fiber volume fractions

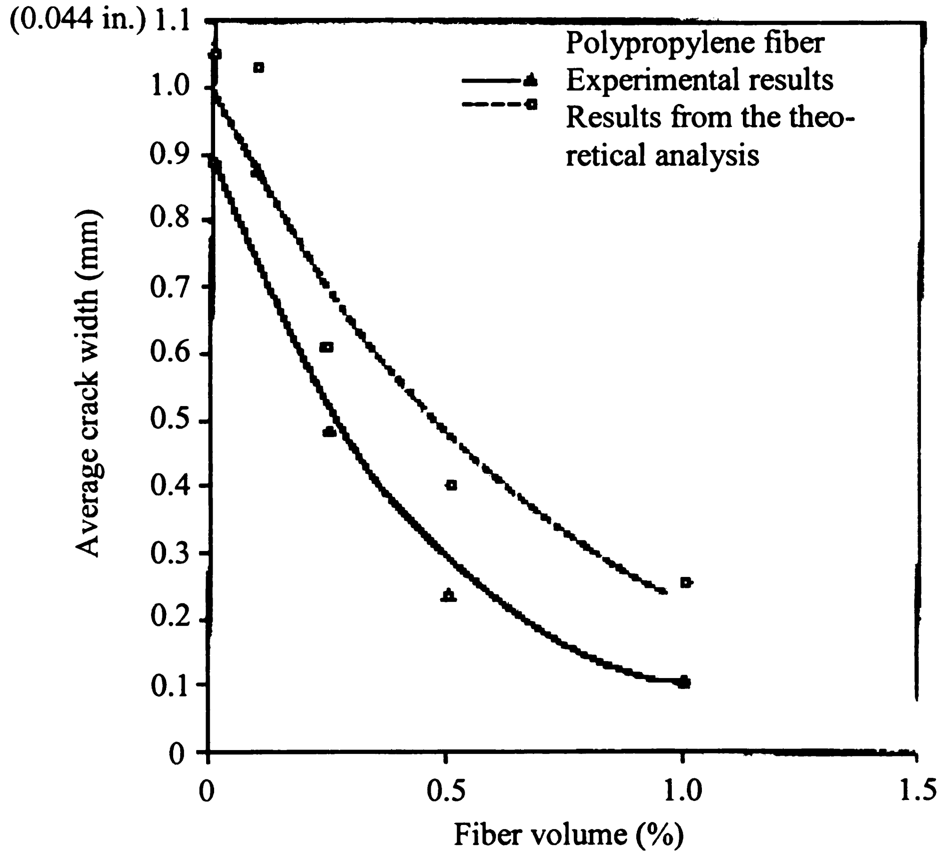

Figure C.23. Average crack-width versus polypropylene fiber volume fraction

C.5. Polyolefin Fibers

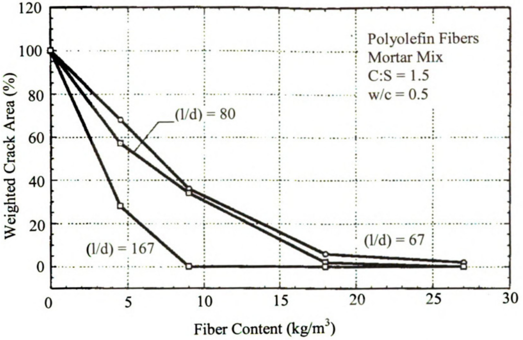

Figure C.24. Effect of fiber content of weighted crack area

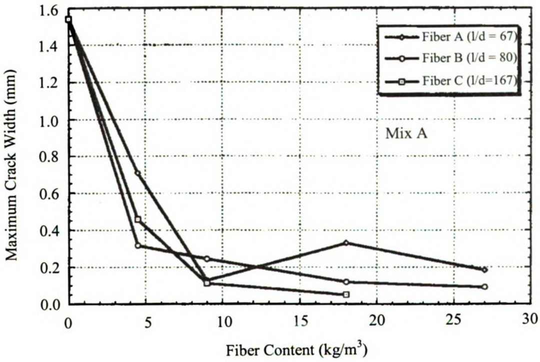

Figure C.25. Crack width versus fiber type (Mixture A)

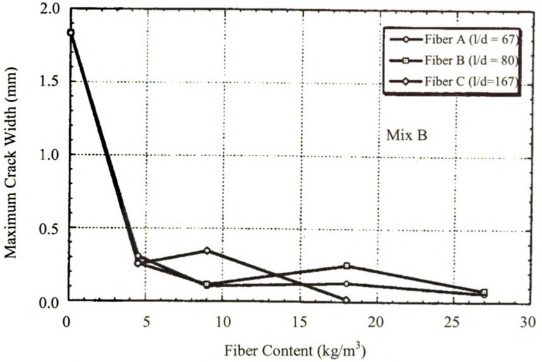

Figure C.26. Crack width versus fiber type (Mixture B)

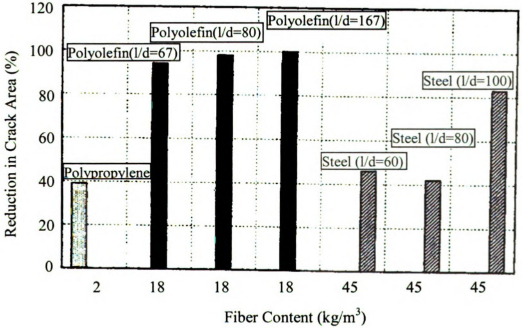

Figure C.27. Crack reduction of PP, Steel, and Polyolefin fibers

APPENDIX D

FLEXURAL STRENGTH EXPERIMENTS [2,4,10,11,33,34,36,37]

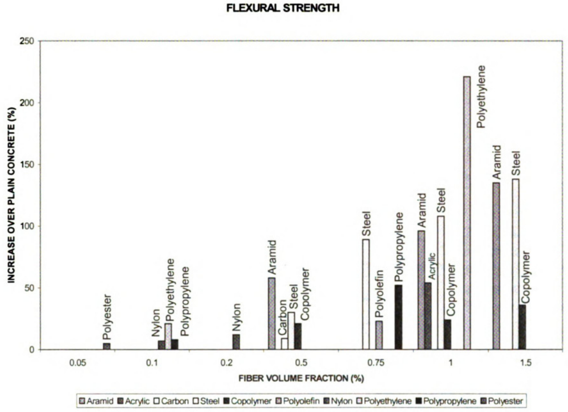

Figure D.1. Summary of the Flexural Strength Results for Different Fiber Types

D.1. Test Methods

D.1.1 ASTM C 78 Standard Test Method for Flexural Strength of Concrete (Using Simple Beam with Third-Point Loading)

D.1.2. ASTM C 1018 Standard Test Method for Flexural Toughness and First-Crack Strength of Fiber- Reinforced Concrete (Using Beam with Third-Point Loading)

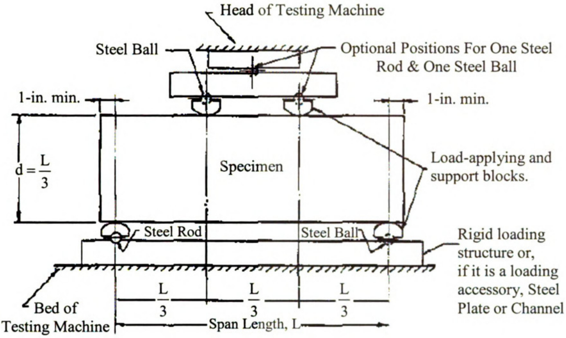

Note 1- This apparatus may be used inverted. If the testing machine applies force through a spherically seated head, the center pivot may be omitted, provided one load-applying block pivots on a rod and the other on a ball.
Note 2- 1 in. = 25.4 mm.

Figure D.2. Diagrammatic View of a Suitable Apparatus for Flexure Test of Concrete by Third-Point Loading Method

D.2. Tests by Ward and Li (Ref. 37)

Table D.1. Fiber Properties

Fiber type	Length, mm	Aspect ratio, l/d_f	Tensile strength, MPa	Modulus, GPa	Density, g/cc	Surface
Steel	25.0	28.5	1000	200	7.9	Crimped
Steel	50.0	57	1000	200	7.9	Crimped
Aramid	6.4	530	2800	130	1.45	Straight
Acrylic	6.4	470	400	6	1.15	Straight
High-modulus Polyethylene	12.7	334	2000	100	0.97	Straight

1 mm = 0.0394 in; 1 g/cc = 0.0361 lb/1n.^{3}; 1 MPa = 145 psi.

Table D.2. Flexural, Splitting Tensile, and Compressive Strengths of Various Fiber Reinforced Mortar

Fiber type	Length, mm	V_f, percent	Flexural strength d = 63.5, MPa	Flexural strength d = 114, MPa	Flexural strength d = 171, MPa	Flexural strength d = 228, MPa	Splitting tensile strength Crack, MPa	Splitting tensile strength Maximum, MPa	Compressive strength, MPa
Plain mortar		0	3.0	2.6	2.3	2.4	2.9	2.9	57.0
Aramid	6.4	0.5	4.9	4.1	4.0	3.9	4.2	4.2	52.1
Aramid	6.4	1.0	5.5	5.1	4.7	5.1	4.4	4.4	50.3
Aramid	6.4	1.5	6.9	6.1	6.0	5.5	4.6	4.6	45.5
Steel	25	0.5	3.6	3.5	3.5	3.5	3.6	5.6	58.9
Steel	25	1.0	5.1	5.4	4.9	4.7	3.9	6.0	62.6
Steel	25	1.5	6.4	6.2	5.7	5.5	4.8	5.9	59.7
Steel	25	2.0	7.0	7.0	6.6	6.6	4.8	5.6	57.0
Steel	50	1.0		7.4		6.2	4.3	6.2	54.1
Steel	50	2.0		8.9		7.8	5.6	7.6	
Acrylic	6.4	1.0		4.0		3.4	4.3	4.3	45.3
Acrylic	6.4	2.0		3.7		3.5	3.6	3.6	33.0
High-modulus polyethylene	12.7	1.0		8.9		7.7	3.2	6.4	45.7

Beam depth in mm: 1 mm = 0.03094 in.; 1 MPa = 145 psi.

D.3. Tests by Sunder, Ramesh, Pitts, AND Ramakrishnan (Ref. 35)

Table D.3. Mixture Proportions

Mix	Water-Cement Ratio	Fibers		Weight			Water kg
		kg	Vol. %	Cement kg	Coarse Agg. kg	Fine Agg. kg	
E1	0.5	0.32	0.5	25.22	64.86	64.86	12.61
E2	0.5	0.64	1.0	25.22	64.86	64.86	12.61
E3	0.55	0.95	1.5	25.22	64.86	64.86	13.88
E4	0.55	1.27	2.0	25.22	64.86	64.86	13.88

Table D.4. Properties of Fresh Concrete

Mix Designation	Room Temp. (°C)	Room Humidity (%)	Concrete Temp. (°C)	Unit Weight (kg/m^3)	Initial Slump	Air Content (%)
E1	18.33	45	18.2	2365	31.75	1.8
E2	29.44	35	20.6	2339	19.05	1.8
E3	26.67	45	21.6	2326	10.16	1.4
E4	29.44	40	22.9	2326	6.35	1.4

Table D.5. First Crack Strength and Maximum Flexural Strength

Mixture Type	Specimen #	First Crack		Maximum Load (kg)	Flexural Strength (MPa)
		Load (kg)	Stress (MPa)		
E1	E1-1	1588	4.3	1633	4.42
	E1-2	1361	3.6	1632	4.36
	E1-3	1361	3.8	1596	4.42
	E1-4	1361	3.5	1762	4.55
	Average		3.8		4.44
E2	E2-1	1389	4.1	1482	4.33
	E2-2	1621	4.2	1742	4.54
	E2-3	1621	4.3	1776	4.75
	E2-4	1621	4.5	1646	4.54
	Average		4.3		4.54
E3	E3-1	1337	3.5	1560	4.06
	E3-2	1604	4.3	1850	4.98
	E3-3	1871	4.7	2008	5.01
	E3-4	2139	5.6	2240	5.81
	Average		4.5		4.96
E4	E4-1	1800	4.7	1907	4.96
	E4-2	1543	4.1	1741	4.62
	E4-3	1800	4.8	2054	5.50
	E4-4	1800	4.9	1895	5.10
	Average		4.6		5.05

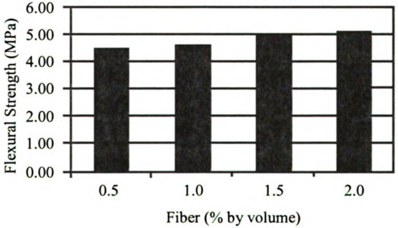

Figure D.3. Modulus of Rupture Versus Fiber Content

D.4. Tests by Balaguru and Khajuria (Ref. 5)

Table D.6. Properties of Fresh Concrete

Mix Designation	Slump (cm)	Air Content (%)	Unit Weight (kg/m^3)
CON	22.0	6.4	2307
N6-060	15.0	7.5	2339
N6-120	11.0	7.75	2387
N6-180	9.5	8.0	2355
N6-240	5.0	8.0	2339

Table D.7. Strength Results

Mix Designation	Compressive Strength* (MPa)	Modulus of Rupture† (MPa) (Flexural Strength)
CON	21.6	-
N6-060	23.6	4.03
N6-120	24.6	4.08
N6-180	22.8	3.90
N6-240	25.3	4.17

* Average of 2 specimens

† Average of specimens

D.5. Tests by Soroushian, Khan, and Hsu (Ref. 34)

Table D.8. Mix Proportions and Fresh Mix Properties

Fiber Type, V_f	*CA/C*	*FA/C*	*SP/C*	*W/C*	Slump, in.	Vebe time, sec
—	1.5	1.5	0	0.39	2.0	15
PP, 1.0 percent	1.5	1.5	0.00293	0.39	2.75	8
PE, 0.025 percent	1.5	1.5	0.000541	0.39	3.0	9
PE, 0.05 percent	1.5	1.5	0.000625	0.39	3.0	10.5
PE, 0.01 percent	1.5	1.5	0.001	0.39	2.8	8.5

Note: CA = Coarse Aggregate; C = Cement; FA = Fine Aggregate; SP = Super Plasticizer; W = Water; PP = Polypropylene; PE = Polyethylene.

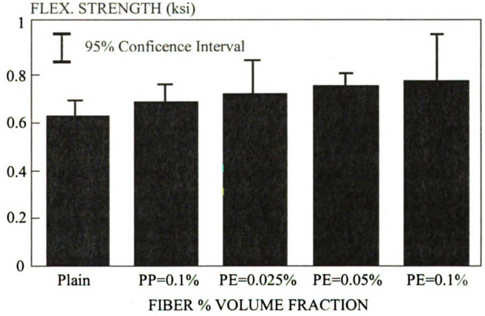

Figure D.4. Flexural Strength Vs. Fiber Volume Fraction

Table D.9. Hardened Material Test Results

Mix Type	Flexural Strength, psi	Compressive Strength, psi	Ultimate Impact, No. of Lows
Plain	630	7410	27
	645	6910	31
	595	6810	29
	705	5910	25
	710	6780	18
	418		20
Mean	617	6764	25
Polyethylene, V_f = 0.1 percent	605	6371	46
	708	6576	42
	768	6526	107
	475	6276	110
	739	6720	54
	718		50
Mean	669	6493	69
Polyethylene, V_f = 0.025 %	753	5430	62
	645	4890	45
	698	5350	46
	685	5540	42
	677	5230	41
	730		46
Mean	698	5290	47
Polyethylene, V_f = 0.05 percent	652	5600	51
	810	5710	39
	732	5730	49
	743	5530	129
	672	5800	79
	780		88
Mean	732	5674	73
Polyethylene, V_f = 0.1 percent	711	5200	160
	783	5130	110
	748	5310	97
	750	5400	183
	770	4900	173
	701		151
Mean	744	5185	146

D.6. Tests by Bindiganavile AND Banthia (Ref. 9)

Table D.10. Properties of Fibers Investigated

Schematic	Fiber	Material	Geometry	Length, mm	Cross section	Tensile strength, MPa	Elastic modulus, GPa
	F1	Polyolefin	Unde-formed	50	Circular	365	2.6
	F2	Polypropyl-ene	Sinusoidal crimping	30	Circular	450	3.5
	F3	Polypropyl-ene	Sinusoidal crimping	50	Circular	450	3.5
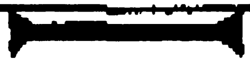	F4	Steel	Flat ended	30	Circular	1198	200

Table D.11. Static and Impact Results for Fiber Reinforced Concrete Beams

Mixture No.	Stress rate σ (for impact)	f'_c, MPa	Flexural strength			JSCE fracture energy*			JSCE SF4 FIF†		
			Static, MPa (standard deviation)	Impact, MPa (standard deviation)	Ratio (impact/static)	Static, J (standard deviation)	Impact, J (standard deviation)	Ratio (impact/static)	Static, J (standard deviation)	Impact, J (standard deviation)	Ratio (impact/static)
MF1	1.33 E4	38	4.50 (0.60)	11.79 (1.45)	2.62	1.74 (0.23)	2.20 (0.27)	1.26	11.62 (0.23)	14.68 (0.23)	1.26
MF2	1.55 E4	40	5.70 (0.70)	13.35 (1.90)	2.34	1.13 (0.12)	2.40 (0.34)	2.12	7.56 (0.12)	16.30 (0.34)	2.12
MF3	1.61 E4	43	5.40 (0.60)	12.60 (1.76)	2.30	2.41 (0.26)	2.54 (0.32)	1.05	16.12 (0.26)	16.96 (0.32)	1.05
MF4	1.29 E4	43	6.90 (0.30)	10.50 (1.66)	1.52	3.93 (0.14)	3.14 (0.28)	0.79	26.25 (0.14)	20.98 (0.28)	0.79

* From area under load-deflection curve computed to deflection of span/150 = 2 mm.
† Flexural toughness factor.

D.7. Tests by Yao, Li, and Wu (Ref. 38)

Table D.12. Mechanical Properties of Fiber Reinforced concrete Mixes

Batch No.	Fiber volume fraction (%)			f'_c (MPa)	f'_{sp} (MPa)	MOR (MPa)	Toughness Index		
	Carbon	Steel	PP				I_5	I_{10}	I_{30}
1	-	-	-	44.3	4.36	5.54	3.16	5.89	9.78
2	0.5	-	-	50.7	5.21	6.02	4.08	7.48	14.82
3	-	0.5	-	47.8	4.80	6.90	4.15	7.90	22.80
4	-	-	0.5	44.5	4.14	5.74	4.04	6.26	16.76
5	0.2	0.3	-	58.2	5.95	7.36	4.23	8.14	29.32
6	0.2	-	0.3	57.8	5.72	7.30	3.89	6.20	15.90
7	-	0.2	0.3	45.3	4.46	5.83	3.40	6.31	18.44

D.8. Tests by Ezeldin, Lowe, AND Balaguru (Ref. 11)

Table D.13. Experimental program

Mix Design.	Compressive Strength, psi	Flexure Strength, psi		First Crack Strength, psi		I_5	I_{10}	I_{10}/I_5
		f_r	$\bar{f}_r$	f_{cr}	$\bar{f}_{cr}$			
RC	2810	436	436	436	436	1.0	1.0	1.0
RF01	3940	640	540	-	-	*	*	*
RF05	4680	647	501	-	-	3.80	5.20	1.37
RF1	4120	617	509	586	484	4.41	6.85	1.55
PC2	4980	670	670	670	670	1.0	1.0	1.0
PF01	4600	731	760	-	-	*	*	*
PF05	4200	598	651	-	-	3.97	4.92	1.24
PF1	4420	698	741	683	725	4.18	5.88	1.41
SC	4500	551	551	551	551	1.0	1.0	1.0
SF01	5380	649	592	-	-	*	*	*
SF05	5320	591	542	-	-	3.3	4.23	1.28
SF1	5810	635	558	602	551	4.17	5.47	1.31
RC	2810	436	436	436	436	1.0	1.0	1.0
RA01	4140	675	556	-	-	*	*	*
RA05	4100	619	512	-	-	3.42	4.80	1.40
RA1	3680	598	522	564	493	4.44	6.2	1.40
PC2	4980	670	670	670	670	1.0	1.0	1.0
PA01	4700	684	704	-	-	*	*	*
PA05	4440	640	678	-	-	3.23	4.85	1.5
PA1	4580	778	812	751	783	3.98	5.15	1.29
SC	4500	551	551	551	551	1.0	1.0	1.0
SA01	5055	539	507	-	-	*	*	*
SA05	5650	586	522	-	-	4.12	5.77	1.4
SA1	4100	577	603	539	563	4.3	6.23	1.45
PC2	4980	670	670	670	670	1.0	1.0	1.0
PG05	5750	860	800	-	-	3.10	4.10	1.32
PG1	4100	652	719	-	-	3.8	4.35	1.14
SC	4500	551	551	551	551	1.0	1.0	1.0
SG05	5630	586	523	-	-	4	5.78	1.45
SG1	5140	567	529	-	-	4.37	6.31	1.44

(-) : not recorded. (*) : no measurable index values.

Table D.14. Results of the Experimental program

Mix Desig.	Fiber Type	Rapid Set Material	Fiber Content % by Volume	Proportions			
				RSM lb	Sand lb	Stone lb	Water lb
RC	F	RH	0	15.6	17.1	25.7	7.3
RF01		RH	0.01	"	"	"	"
RF05		RH	0.05	"	"	"	"
RF1		RH	0.1	"	"	"	"
PC2	F	PY	0	51.5	X	14.5	5
PF01		PY	0.01	"	X	"	"
PF05		PY	0.05	"	X	"	"
PF1		PY	0.1	"	X	"	"
SC	F	SE	0	40.6	X	20.3	3.6
SF01		SE	0.01	"	X	"	"
SF05		SE	0.05	"	X	"	"
SF1		SE	0.1	"	X	"	"
RC	A	RH	0	15.6	17.1	25.7	7.3
RA01		RH	0.01	"	"	"	"
RA05		RH	0.05	"	"	"	"
RA1		RH	0.1	"	"	"	"
PC2	A	PY	0	51.5	X	14.5	5
PA01		PY	0.01	"	X	"	"
PA05		PY	0.05	"	X	"	"
PA1		PY	0.1	"	X	"	"
SC	A	SE	0	40.6	X	20.3	3.6
SA01		SE	0.01	"	X	"	"
SA05		SE	0.05	"	X	"	"
SA1		SE	0.1	"	X	"	"
PC2	G	PY	0	51.5	X	14.5	5
PG05		PY	0.05	"	X	"	"
PG1		PY	0.1	"	X	"	"
SC	G	SE	0	40.6	X	20.3	3.6
SG05		SE	0.05	"	X	"	"
SG1		SE	0.1	"	X	"	"

(X) : Premixed Sand

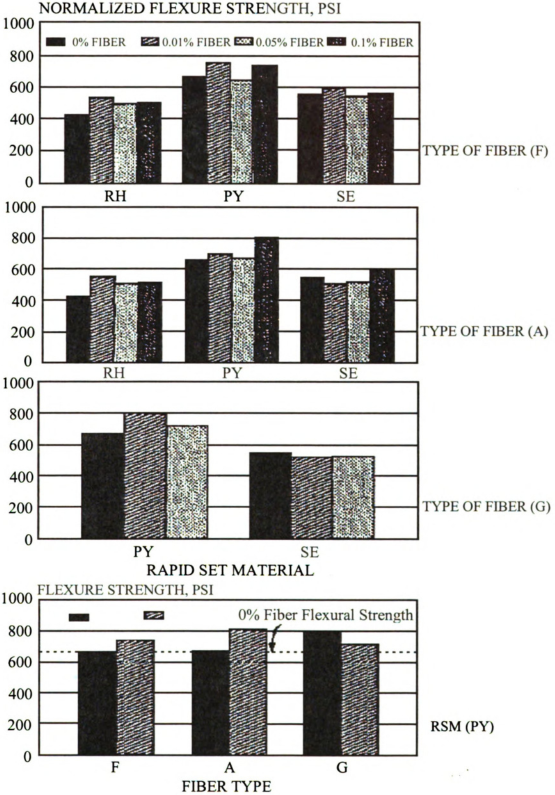

Figure D.5. Flexural Strength

D.9. Tests by Airports Authority of India (Ref. 2)

Table D.15. Flexural Strength

S. NO.	Date of Casting	Date of Testing	Curing Period	Flexural Strength Plain (kg/cm^2)	Flexural Strength Using *Recron 3s* in concrete (kg/cm^2)	%Age Increase	Cement
1	24/7/2003	31/7/2003	7 Days	28.744	29.93	4.13	350 kg
2	24/7/2003	21/8/2003	28 Days	46.821	49.191	5.06	350 kg
3	28/7/2003	4/8/2003	7 Days	29.337	31.115	5.00	340 kg
4	28/7/2003	25/8/2003	28 Days	42.968		5.52	340 kg
5	30/7/2003	6/8/2003	7 Days	29.337		5.05	340 kg
6	30/7/2003	27/8/2003	28 Days	45.043			340 kg
7	5/8/2003	12/8/2003	7 Days	44.45	46.821		350 kg
8	5/8/2003	2/9/2003	28 Days	48.006	50.673	5.56	350 kg
9	5/8/2003	14/8/2003	7 Days	44.746	49.191	9.93	350 kg
10	13/8/2003	10/9/2003	28 Days	48.895	51.562	5.45	350 kg
11	21/8/2003	28/8/2003	7 Days	42.672	45.339	6.25	400 kg with 20 mm MSA
12	21/8/2003	18/9/2003	28 Days	57.785	61.637	6.67	400 kg with 20 mm MSA

APPENDIX E

FLEXURAL TOUGHNESS EXPERIMENTS [4,8,11,18,37]

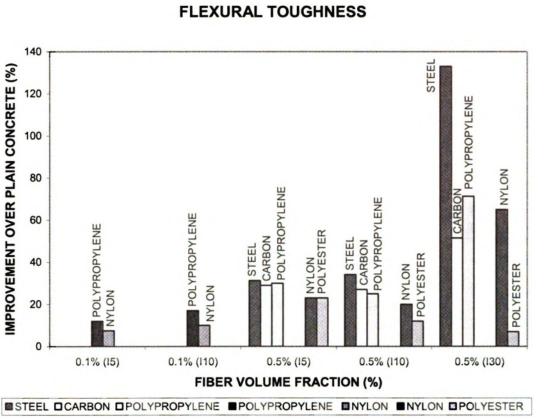

Figure E.1. Summary of the Flexural Toughness Results for Different Fiber Types

E.1. Test Method

E.1.1. ASTM C 1018 – 97

Standard Test Method for Flexural Toughness and First-Crack Strength of Fiber-Reinforced Concrete (Using Beam with Third-Point Loading)

E.2. Tests Done by Ref. 38

Table E.1. Properties of carbon, steel, and PP fibers

	Carbon	Steel	PP
Length (mm)	5	30	15
Diameter (μm)	7	500	100
Density (g/cm^3)	1.6	7.8	0.9
Modulus (GPa)	240	200	8
Elongation at break (%)	1.4	3.2	8.1
Tensile stress (MPa)	2500	1500	800

Table E.2. Concrete mix proportions

Material	Quality
Type I cement (kg/m^3)	490
Sand (kg/m^3)	684
Crushed Limestone (kg/m^3)	1024
Water (kg/m^3)	196
Superplasticizer (kg/m^3)	2.5
Slump (mm)	160

Table E.3. Mechanical properties of fiber-reinforced concretes

Batch No.	Fiber volume fraction (%)			f'_c (MPa)	f'_{sp} (MPa)	MOR (MPa)	Toughness Index		
	Carbon	Steel	PP				I_5	I_{10}	I_{30}
1	-	-	-	44.3	4.36	5.54	3.16	5.89	9.78
2	0.5	-	-	50.7	5.21	6.02	4.08	7.48	14.82
3	-	0.5	-	47.8	4.80	6.90	4.15	7.90	22.80
4	-	-	0.5	44.5	4.14	5.74	4.04	6.26	16.76
5	0.2	0.3	-	58.2	5.95	7.36	4.23	8.14	29.32
6	0.2	-	0.3	57.8	5.72	7.30	3.89	6.20	15.90
7	-	0.2	0.3	45.3	4.46	5.83	3.40	6.31	18.44

E.3. Tests Done by Ref. 11

Table E.4. Material Properties of Mix

Mix Desig.	Fiber Type	Rapid Set Material	Fiber Content % by Volume	Proportions			
				RSM lb	Sand lb	Stone lb	Water lb
RC	F	RH	0	15.6	17.1	25.7	7.3
RF01		RH	0.01	"	"	"	"
RF05		RH	0.05	"	"	"	"
RF1		RH	0.1	"	"	"	"
PC2	F	PY	0	51.5	X	14.5	5
PF01		PY	0.01	"	X	"	"
PF05		PY	0.05	"	X	"	"
PF1		PY	0.1	"	X	"	"
SC	F	SE	0	40.6	X	20.3	3.6
SF01		SE	0.01	"	X	"	"
SF05		SE	0.05	"	X	"	"
SF1		SE	0.1	"	X	"	"
RC	A	RH	0	15.6	17.1	25.7	7.3
RA01		RH	0.01	"	"	"	"
RA05		RH	0.05	"	"	"	"
RA1		RH	0.1	"	"	"	"
PC2	A	PY	0	51.5	X	14.5	5
PA01		PY	0.01	"	X	"	"
PA05		PY	0.05	"	X	"	"
PA1		PY	0.1	"	X	"	"
SC	A	SE	0	40.6	X	20.3	3.6
SA01		SE	0.01	"	X	"	"
SA05		SE	0.05	"	X	"	"
SA1		SE	0.1	"	X	"	"
PC2	G	PY	0	51.5	X	14.5	5
PG05		PY	0.05	"	X	"	"
PG1		PY	0.1	"	X	"	"
SC	G	SE	0	40.6	X	20.3	3.6
SG05		SE	0.05	"	X	"	"
SG1		SE	0.1	"	X	"	"

(X) : Premixed Sand

Table E.5. Flexural Toughness Results

Mix Design.	Compressive Strength, psi	Flexure Strength, psi		First Crack Strength, psi		I_5	I_{10}	I_{10}/I_5
		f_r	$\overline{f_r}$	f_{cr}	$\overline{f_{cr}}$			
RC	2810	436	436	436	436	1.0	1.0	1.0
RF01	3940	640	540	-	-	*	*	*
RF05	4680	647	501	-	-	3.80	5.20	1.37
RF1	4120	617	509	586	484	4.41	6.85	1.55
PC2	4980	670	670	670	670	1.0	1.0	1.0
PF01	4600	731	760	-	-	*	*	*
PF05	4200	598	651	-	-	3.97	4.92	1.24
PF1	4420	698	741	683	725	4.18	5.88	1.41
SC	4500	551	551	551	551	1.0	1.0	1.0
SF01	5380	649	592	-	-	*	*	*
SF05	5320	591	542	-	-	3.3	4.23	1.28
SF1	5810	635	558	602	551	4.17	5.47	1.31
RC	2810	436	436	436	436	1.0	1.0	1.0
RA01	4140	675	556	-	-	*	*	*
RA05	4100	619	512	-	-	3.42	4.80	1.40
RA1	3680	598	522	564	493	4.44	6.2	1.40
PC2	4980	670	670	670	670	1.0	1.0	1.0
PA01	4700	684	704	-	-	*	*	*
PA05	4440	640	678	-	-	3.23	4.85	1.5
PA1	4580	778	812	751	783	3.98	5.15	1.29
SC	4500	551	551	551	551	1.0	1.0	1.0
SA01	5055	539	507	-	-	*	*	*
SA05	5650	586	522	-	-	4.12	5.77	1.4
SA1	4100	577	603	539	563	4.3	6.23	1.45
PC2	4980	670	670	670	670	1.0	1.0	1.0
PG05	5750	860	800	-	-	3.10	4.10	1.32
PG1	4100	652	719	-	-	3.8	4.35	1.14
SC	4500	551	551	551	551	1.0	1.0	1.0
SG05	5630	586	523	-	-	4	5.78	1.45
SG1	5140	567	529	-	-	4.37	6.31	1.44

(-) : not recorded.

(*) : no measurable index values.

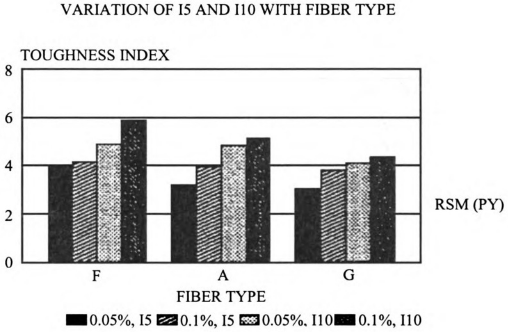

Figure E.2. Variation of Flexural Toughness with Fiber Types

E.4. Tests Done by Ref. 8

Table E.6. Material Properties

Mix No.	Designation	Fiber Volume %	Silica Fume / Binder (%)	Mix Type
1	Standard 1	0.0	0.0	A
2	Series No. 1	0.15	0.0	A
3		0.35	0.0	A
4		0.60	0.0	A
5	Series No. 2	0.00	5	A
6		0.15	5	A
7		0.35	5	A
8		0.60	5	A
9	Series No. 3	0.15	10	A
10		0.35	10	A
11		0.60	10	A
12	Series No. 4	0.15	25	A
13		0.35	25	A
14		0.60	25	A
15	Standard 2	0.00	0.0	B
16	Series No. 5	0.10	0.0	B
17		0.30	0.0	B
18		0.50	0.0	B
19	Series No. 6	0.00	5	B
20		0.10	5	B
21		0.30	5	B
22		0.50	5	B
23	Series No. 7	0.00	10	B
24		0.10	10	B
25		0.30	10	B
26		0.50	10	B

Note : Mix Type A contains more filament polyester fibers while Mix Type B contains fibrillated polypropylene fibers.

Table E.7. Toughness Indices Results

Mix No.	Ultimate Strength (kPa)	Post-Peak Strength (kPa)	Toughness Index	Mix Type
1	4510	-	2.5	A
2	5510	950	3.9	A
3	4650	1800	4.2	A
4	4270	2090	4.9	A
5	4605	-	2.6	A
6	4415	760	4.2	A
7	4750	1710	4.6	A
8	4270	1950	4.6	A
9	5220	1570	5.3	A
10	4130	2280	5.0	A
11	4510	2470	4.6	A
12	4840	1425	5.0	A
13	4370	1805	4.9	A
14	4035	2330	4.9	A
15	5600	-	1.5	B
16	5175	670	3.1	B
17	5220	1500	4.2	B
18	4415	2060	4.3	B
19	5840	-	1.7	B
20	4370	610	3.0	B
21	4795	1350	4.3	B
22	4795	1990	4.8	B
23	5935	-	1.8	B
24	4320	740	3.5	B
25	4415	1490	4.3	B
26	5030	2430	4.4	B

- Not applicable
1 ksi = 6.89 MPa

E.5. Tests Done by Ref. 18

Table E.8. Physical Properties of Fibers

Property	Fiber Type		
	Nylon 6	Polyester	Polypropylene
Tensile Strength, MPa	897	897 – 1104	553 – 759
Young's Modulus, MPa	5175	17250	3450
Water absorption, percent	4.5	-	Nil
Specific gravity	1.16	1.34	0.9
Melting point, °C	242	257	160 – 170
Ultimate elongation, percent	20	-	15

Note: Information provided by manufacturers.

Table E.9. Results of Toughness Indices

Age (weeks)		0	4	8	16	32	52
Toughness index							
I_5	NY	3.9	3.6	5.1	5.0	4.4	4.1
	PP	4.2	4.6	4.8	4.8	4.6	4.9
	PY	3.9	4.3	3.7	4.0	4.3	4.0
I_{10}	NY	6.3	5.8	11.3	9.6	9.0	7.5
	PP	7.3	7.9	10.5	10.2	9.3	10.2
	PY	5.4	6.8	5.1	5.5	6.7	5.7
I_{30}	NY	16.4	15.8	38.9	27.0	27.9	20.8
	PP	20.7	24.6	38.2	36.1	32.6	31.1
	PY	10.1	10.9	7.5	7.8	9.7	7.4
I_{10} / I_5	NY	1.54	1.61	2.12	1.92	2.05	1.85
	PP	1.74	1.72	2.19	2.12	2.02	2.10
	PY	1.38	1.58	1.38	1.38	1.56	1.44
I_{30} / I_{10}	NY	2.73	2.72	3.44	2.81	3.10	2.77
	PP	2.84	3.11	3.64	3.54	3.51	3.04
	PY	1.87	1.60	1.47	1.42	1.45	1.29

NY = nylon 6, PP = polypropylene, PY = polyester

APPENDIX F

FATIGUE EXPERIMENTS [6,25,28]

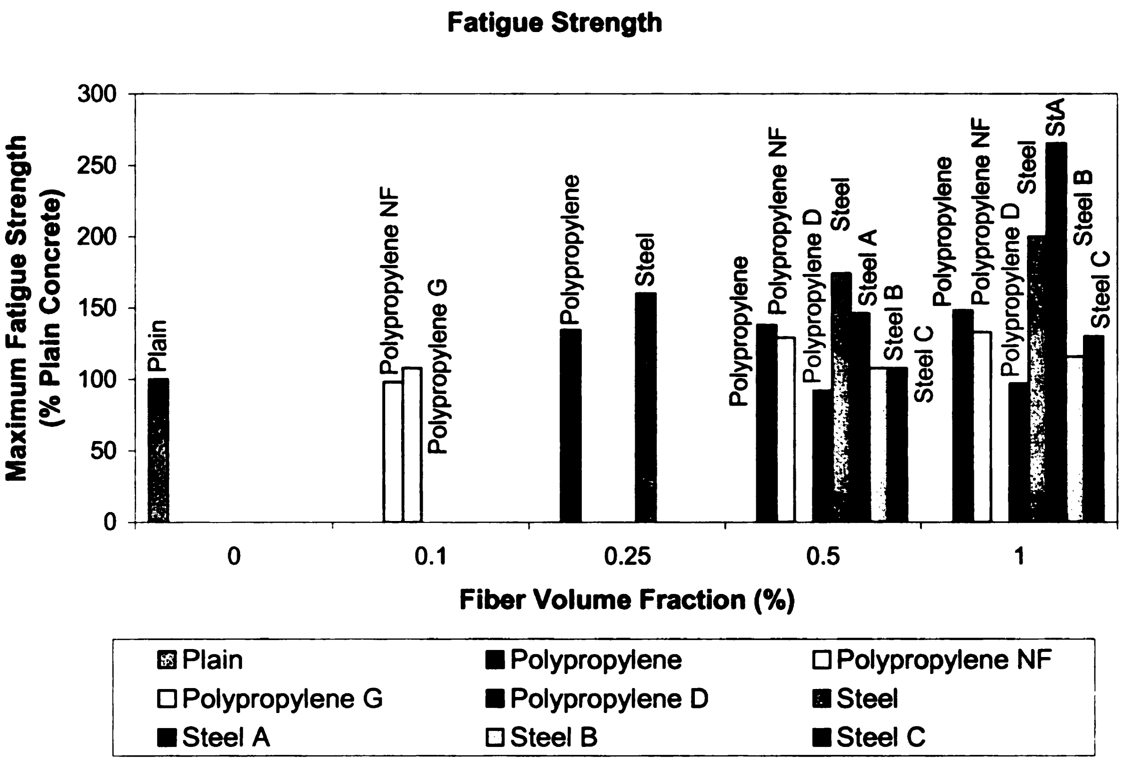

Figure F.1. Summary of the Fatigue Results for Different Fiber Type

Table F.1. Different Fiber and Mix Properties and Reference to Results' Figures

Fiber Type	**Fiber Geometry L : D (mm)**	**Fiber Vol. Fract:**	**Mix C:S:CA:W**	**Curing**	**Drying Conditions**	**Results**
Steel Fiber	50 : 0.5 60 : 0.5	0.0% 0.025% 0.5%	1:1.5:2:0.5	Days – R.Hum - 100% Tem - 20°C.	R.Hum - % Tem - °C	Table F.2
Steel Fiber	50 : 0.5 60 : 0.5	0.0% 0.025% 0.5%	1:1.5:2:0.5	Days – R.Hum - 100% Tem - 20°C.	R.Hum - % Tem - °C	Fig. F.2-F.5
Polypropylene Fiber	30 : 0.5	0.1% 0.2% 0.3%	FR1 FR2	Days – R.Hum - 100% Tem - 20°C.	R.Hum - % Tem - °C	Fig. F.6
Polypropylene Fiber	30 : 0.5	0.1% 0.2% 0.3%	FR3	Days – R.Hum - 100% Tem - 20°C.	R.Hum - % Tem - °C	Fig. F.7,F.8
Steel Fiber	50 : 0.5 18.75:0.5 50:1.25	0.5% 1.0%	C:1 CA:2.37 FA:2.37	R.Hum – 33-58% Tem – 18-27°C.	N/A	Fig F.9, F.10
Polypropylene Fiber	18.75:N/A	0.5% 1.0%	C:1 CA:2.37 FA:2.37	R.Hum – 33-58% Tem – 18-27°C.	N/A	Fig F.9, F.10
Polypropylene Fiber	18.75:N/A	0.1% 0.5% 1.0%	NF & G	24 hours, room temp.	N/A	Fig. F.11 F.12 F.13

F.1. Steel Fiber

Table F.2. Fatigue test results on Steel fiber

Mix design†	Sample number	Flexural fatigue stress (psi)*		Number of cycles to failure	Percent of static flexural strength‡
		Minimum	Maximum		
OB1	1	80	640	2,000,000§	81.5
OB1	2	80	719	2,000,000	91.6
OB1	3	82	779	2,000,000	99.2
OB2	1	85	680	2,000,000	79.5
OB2	2	82	779	2,000,000	91.1
OB2	3	83	790	2,000,000	92.4
OB3	1	83	669	2,000,000	78.7
OB3	2	79	711	2,000,000	83.7
OB3	3	85	850	2,000,000	100.0
OB4	1	94	846	2,000,000	92.0
OB4	2	92	1009	2,000,000	109.7
OB4	3	89	1073	2,000,000	116.6
PL	1	71	356	2,000,000	49.4
PL	2	71	357	2,000,000	49.6
PL	3	71	393	2,000,000	54.6
PL	4	71	393	35,700	55.3
PL	5	74	406	13,400	56.4
PL	6	69	414	55,300	57.5
PL	7	73	679	800	93.6
PL	8	73	655	1,000	90.3
PL	9	73	577	126,400	79.5

* 1 psi = 6.895 kPa
† PL = Plain Concrete
OB1 = 60 mm long fibers at 40 kg/m^3 (66 lb/yd^3)
OB2 = 60 mm long fibers at 60 kg/m^3 (100 lb/yd^3)
OB3 = 50 mm long fibers at 40 kg/m^3 (66 lb/yd^3)
OB4 = 50 mm long fibers at 60 kg/m^3 (100 lb/yd^3)
‡ $\sigma_{max} / f_r * 100$
§ The number 2,000,000 indicates that the specimens did not fail up to 2,000,000 cycles.

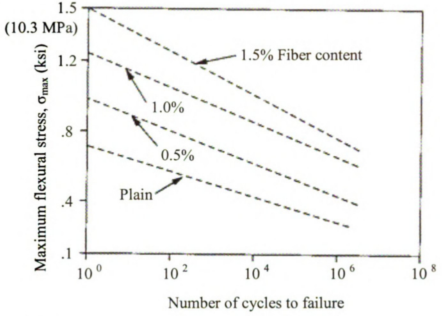

Figure F.2. Maximum fatigue flexural stress No of cycles to failure

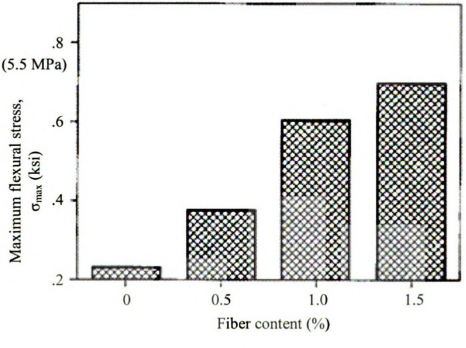

Figure F.3. Comparison of plain concrete and FRC

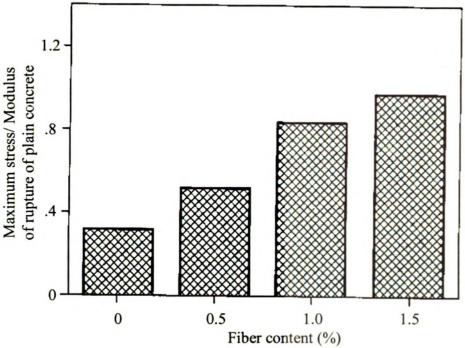

Figure F.4. Maximum fatigue flexural stress vs. fiber content %

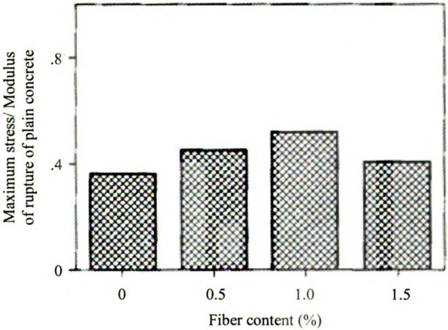

Figure F.5. Comparison of plain concrete and FRC

F.2. Polypropylene Fiber

Table F.3. Fatigue Test Results (Polypropylene)

Mix designation†	Sample beam number	Flexural fatigue stress (psi)*		Number of cycles to failure	% static flexural strength	Com-ments‡
		Minimum	Maximum			
FR1	9	78	313	2,000,000	40.4	a
FR1	9	78	352	2,000,000	45.4	b
FR1	9	78	430	2,000,000	55.5	c
FR1	9	78	469	2,000,000	60.5	d
FR1	9	78	547	2,000,000	70.6	e
FR1	8	76	382	118,600	49.3	
FR1	7	83	454	610,400	58.6	
FR2	8	80	402	2,000,000	52.2	a
FR2	8	80	442	2,000,000	57.4	b
FR2	8	80	483	2,000,000	62.7	c
FR2	8	80	523	2,000,000	67.9	d
FR2	8	80	603	1,562,800	78.3	d
FR2	7	76	417	212,700	54.2	
FR2	9	78	469	192,600	60.9	
FR3	4	73	402	2,000,000	60.9	a
FR3	4	73	438	2,000,000	66.4	b
FR3	4	73	511	17,300	77.4	
FR3	9	71	423	2,000,000	64.1	a
FR3	9	71	458	2,000,000	69.4	b
FR3	9	71	529	27,500	80.2	
FR3	8	72	466	300	70.6	
F1	6	72	578	28,800	80.3	
F1	7	72	493	187,200	68.5	
F1	5	72	431	29,500	60.0	
F2	5	73	453	38,800	62.1	
F2	4	73	395	51,900	54.0	
F2	8	73	385	2,000,000	52.8	
F3	6	72	543	123,000	75.9	
F3	4	74	445	475,007	59.7	
F3	7	75	436	2,000,000	58.5	
PL	4	73	679	800	93.6	
PL	10	73	655	1,000	90.3	
PL	12	73	577	126,400	79.5	
PL	7	71	356	2,000,000	79.4	
PL	12	71	357	2,000,000	49.6	
PL	9	71	393	2,000,000	54.6	
PL	10	71	393	35,700	55.3	
PL	11	74	406	13,400	56.4	
PL	8	69	414	55,300	57.5	

* 1 psi = 6.895 kPa
† PL = Plain Concrete, F1 and FR1 = 0.1% fibers, F2 and FR2 = 0.2% fibers,
F3 and FR3 = 0.3% fibers
‡a – This specimen was tested at higher stress when it did not fail at $2*10^6$ cycles.
b – This specimen was tested for a second time with higher stress.
c – This specimen was tested for a third time with higher stress.
d – This specimen was tested for a fourth time with higher stress.
e – This specimen was tested for a fifth time with higher stress.

Table F.4. Comprehensive and Flexural Strength Results

(a) Compressive strength			
Cylinder	*Fiber volume (%)*	*Sample f'_c (kPa)*	*Average f'_c (kPa)*
A-1	0.0	28550	
A-2	0.0	24900	27800
A-3	0.0	26880	
B-1	0.1	22930	
B-2	0.1	19280	22830
B-3	0.1	26245	
C-1	0.5	17070	
C-2	0.5	20520	19030
C-3	0.5	19520	
(b) Flexural strength			
Beam	*Fiber volume (%)*	*Sample f'_c (kPa)*	*Average f'_c (kPa)*
A-1	0.0	3410	
A-2	0.0	3550	3280
A-3	0.0	2830	
B-1	0.1	2970	
B-2	0.1	2830	3030
B-3	0.1	3340	
C-1	0.5	3070	
C-2	0.5	2660	2720
C-3	0.5	2480	

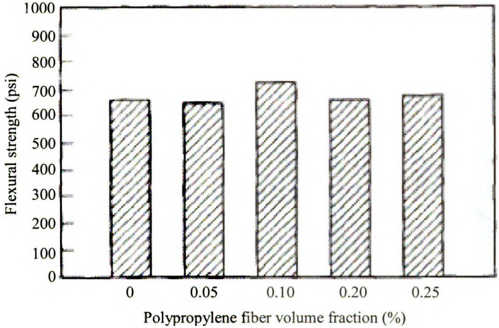

Figure F.6. Flexural Strength Results

F.3. Test Methods

Test Methods for following results is Third Point Loading Test. The test beams had a span of 18 in. and were subjected to a nonreversed fluctuating load.

The frequency of loading was 20 cycles/sec (Hz) for all tests.

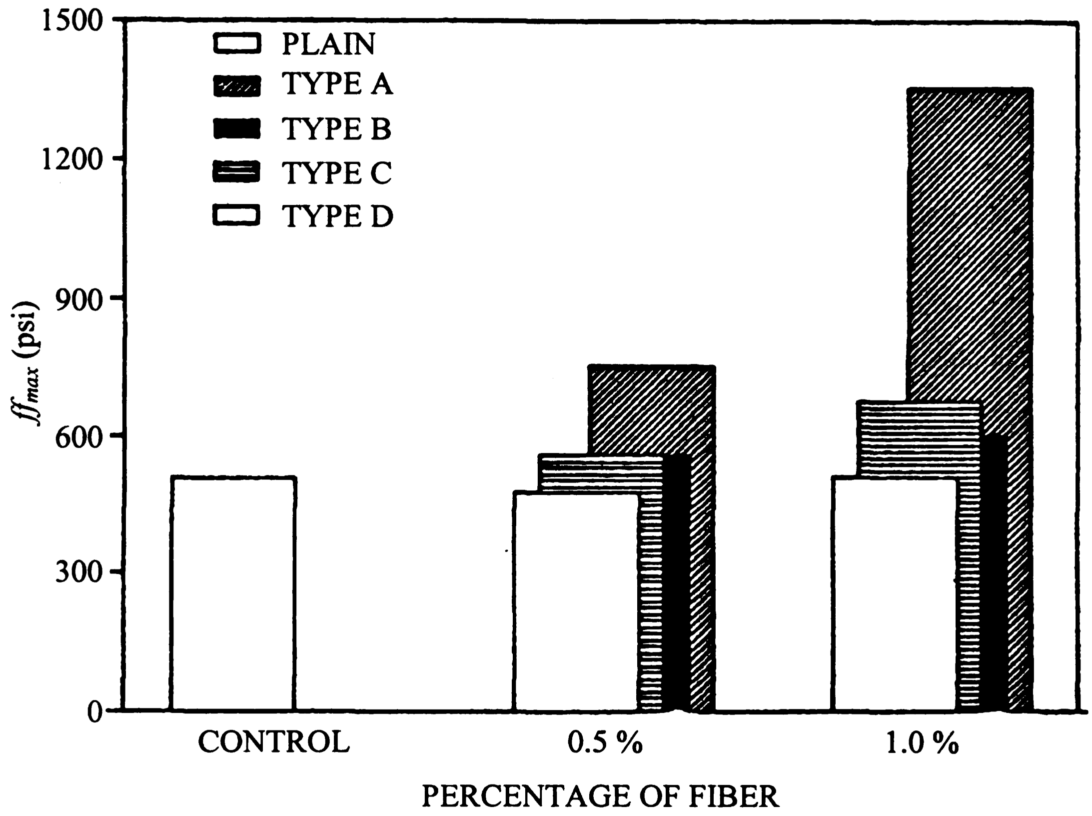

Figure F.7. Fatigue Strength

Table F.5. Mix Quantities and Designations

MIX #	FIBER CONTENT (%)	COARSE AGGREGATE (lbs)	FINE AGGREGATE (lbs)	CEMENT (lbs)	W/C RATIO	SPD (cc)	AEA (cc)
NP4	----	187.8	187.8	79.2	0.40	180	25
NF1	0.1	187.0	187.8	79.2	0.40	240	25
NF7	0.1	187.8	187.8	79.2	0.40	240	25
NF3	0.5	187.8	187.8	79.2	0.40	330	35
NF5	0.5	187.8	187.8	79.2	0.40	330	25
NF2	1.0	187.8	187.8	79.2	0.40	380	25
NF6	1.0	187.8	187.8	79.2	0.40	550	30
G1	----	215.8	169.8	65.0	0.50	78	18
G2	0.1	215.8	169.8	65.0	0.50	78	18
G3B	1.0	181.8	142.5	86.9	0.50	208	23
G4	0.5	181.8	142.5	86.9	0.42	136	22
G5	----	181.8	142.5	86.9	0.42	123	22

SPD = Superplasticizer Dosage
AEA = Air Entraining Agent Dosage

Table F.6. Fiber Quantities and Design

Fiber Type	A		B		C		D		Plain Conc.
Fiber Content (%)	0.5	1.0	0.5	1.0	0.5	1.0	0.5	1.0	
f_{fmax} (in psi)	749	1242	559	594	549	676	478	508	508
EL_1	95	158	71	76	71	86	61	65	65
EL_2	76	85	67	59	70	55	70	65	65

f_{fmax} = flexural strength.
EL_1 = Endurance limit expressed as a percentage of modulus of rupture of plain concrete.
EL_2 = Endurance limit expressed as a percentage of its modulus of rupture.

Table F.7. Fatigue Test results

SP. #	AGE (DAYS)	MAX. STRESS f_{max} (psi)	MIN. STRESS (psi)	STRESS RANGE (psi)	f_{max} / f_r	CYCLES TO FAILURE
NF4-7	36	450	82	368	0.57	5560
NF4-8	34	383	77	306	0.40	2618700+
NF4-9	33	582	83	499	0.74	500
NF4-10	33	483	81	402	0.62	1860
NF4-11	33	477	80	397	0.60	75990
NF4-12	33	409	82	227	0.82	1951330
NF1-4	53	386	64	332	0.58	2190780+
NF1-5	54	521	65	456	0.79	993330
NF1-6	55	467	67	400	0.71	104380
NF1-7	55	483	69	416	0.73	2607340+
NF1-8	56	313	68	445	0.78	3580900+
NF1-9	30	330	66	364	0.60	2000150+
NF1-10	30	409	68	341	0.62	58560
NF1-11	30	481	69	412	0.73	1060
NF1-12	30	521	65	456	0.79	4280
NF7-1	119	749	88	661	0.84	23300
NF7-2	118	758	84	674	0.85	1104600
NF7-3	119	787	87	700	0.86	296000
NF7-4	117	749	88	661	0.84	2032290+
NF7-6	119	730	86	644	0.82	38500
NF7-7	118	659	88	571	0.74	2000000+
NF7-8	118	786	87	699	0.88	633100
NF7-9	119	648	86	562	0.72	2000000+
NF7-10	118	828	87	741	0.93	19200
NF7-11	118	823	87	736	0.92	1700
NF3-4	60	580	83	497	0.69	1050010
NF3-5	59	512	82	450	0.63	3390610+
NF3-6	59	614	88	526	0.73	121900
NF3-7	32	402	84	378	0.55	2810030+
NF3-8	32	405	81	324	0.48	2241100+
NF3-9	33	500	83	417	0.59	16510
NF3-10	32	514	86	428	0.61	8520
NF3-11	31	567	81	486	0.67	9940

Table F.7. Continued

SP. #	AGE	MAX. STRESS f_{max}	MIN. STRESS	STRESS RANGE	f_{max} / f_r	CYCLES TO FAILURE
	(DAYS)	(psi)	(psi)	(psi)		
NF2-4	32	629	76	453	0.70	7830
NF2-5	30	375	75	300	0.50	2308100+
NF2-8	57	521	74	447	0.69	2001710+
NF2-9	58	580	77	503	0.77	372890
NF2-10	58	559	75	484	0.74	2032940+
NF2-11	59	590	74	516	0.70	116360
NF2-12	59	581	74	479	0.73	887210
NF6-5	84	583	65	518	0.83	459260
NF6-6	82	568	70	488	0.80	2382640+
NF6-7	85	540	69	479	0.78	2024730+
NF6-8	84	662	66	596	0.95	46550
NF6-9	84	612	70	542	0.87	11980
NF6-10	87	604	71	533	0.86	2076340+
NF6-11	86	560	66	494	0.80	2006900+
NF6-12	84	550	70	488	0.80	370240
NF6-13	88	572	68	510	0.83	2000000+
G1-2	90	486	81	407	0.60	2029550+
G1-3	89	560	80	480	0.70	1279610
G1-4	88	653	82	571	0.82	316320
G1-5	88	709	79	630	0.89	2020
G1-6	91	545	84	641	0.69	2009760+
G1-10	134	498	77	430	0.66	2013000+
G1-11	136	462	77	394	0.62	2011970+

+ = No failure
f_r = Average modulus of rupture of three to four specimens tested at 28 days.

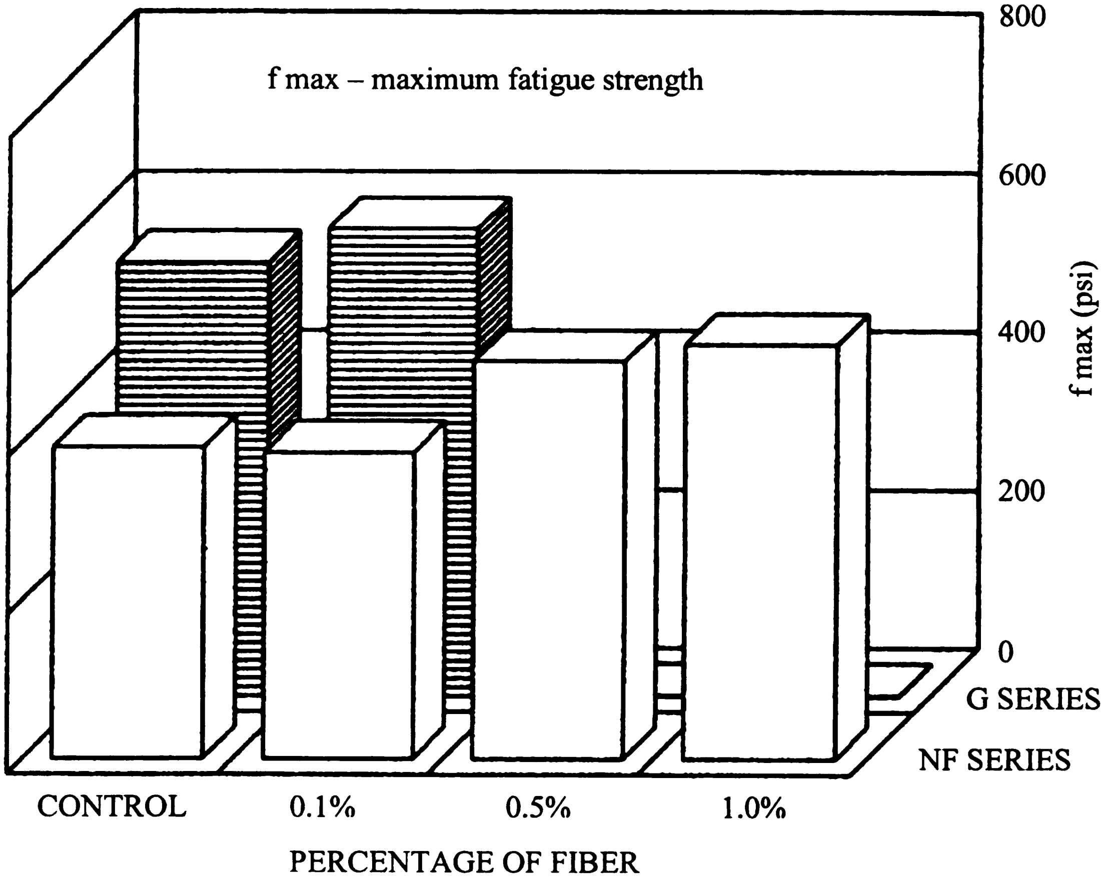

Figure F.8. Fatigue strength Bar Chart

APPENDIX G

IMPACT EXPERIMENTS [6,21,22,24]

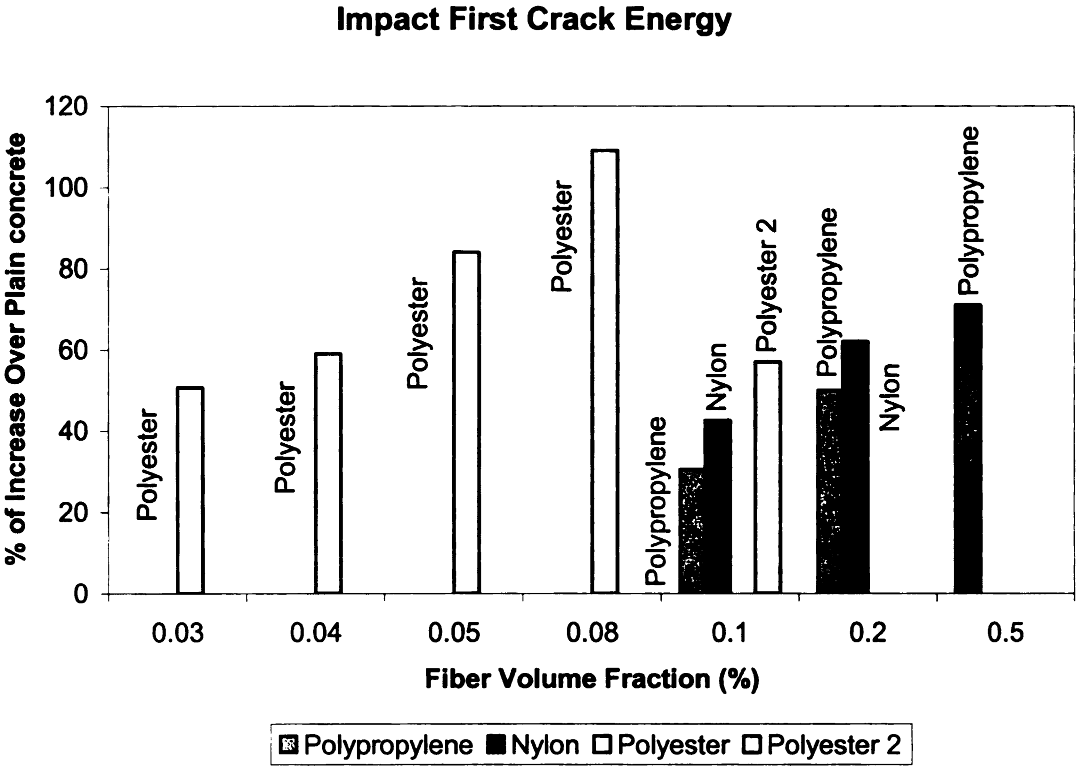

Figure G.1. Summary of the Impact Results for Different Fiber Types

Table G.1. Test Method (I) Drop Weight Test (Figure G.2)

Re f; #	**Fiber Type**	**Fiber Geometry L : D(mm)**	**Fiber Vol. Fraction**	**Mix C:S:CA: W**	**Specimen Dimensions (Fig 1)**	**Results**
1	Steel Fiber	25 : 0.4 50 : 0.4	0.05% 0.1% 0.5% 1.0%	1:2:0:0.50	D - 150mm T - 64mm	Figs G.3,G.4
2	Nylon Fiber	19 : 0.4	0.05% 0.1% 0.5% 1.0%	1:2:0:0.50	D - 150mm T - 64mm	Figs G.5.G.6
3	Polypropylene Fiber	19 : 0.4	0.05% 0.1% 0.5% 1.0%	1:2:0:0.50	D - 150mm T - 64mm	Figs G.7-G.10 Table G.3
4	Polyester Fiber	19 : 0.4	0.05% 0.1% 0.5% 1.0%	1:2:0:0.50	D - 150mm T - 64mm	Figs G.7,G.8

G.1. Test Method I (Drop Weight Test)

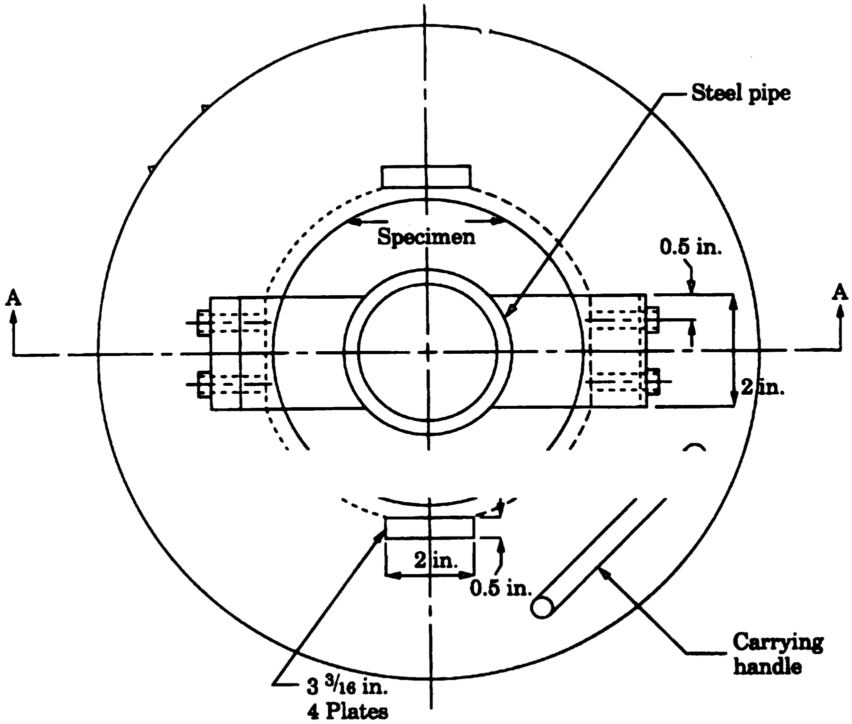

Figure 9-8 Plan view of test equipment for measuring impact strength. Section A-A is shown in 9-9 [9.14] (1 in. = 25.4 mm).

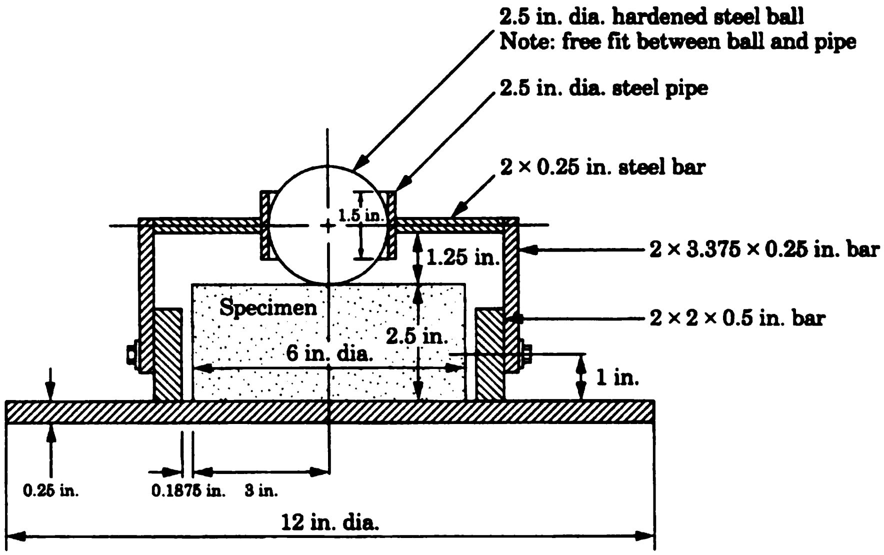

Figure G.2. Instrumented Drop Weight System

G.2. Steel Fibers

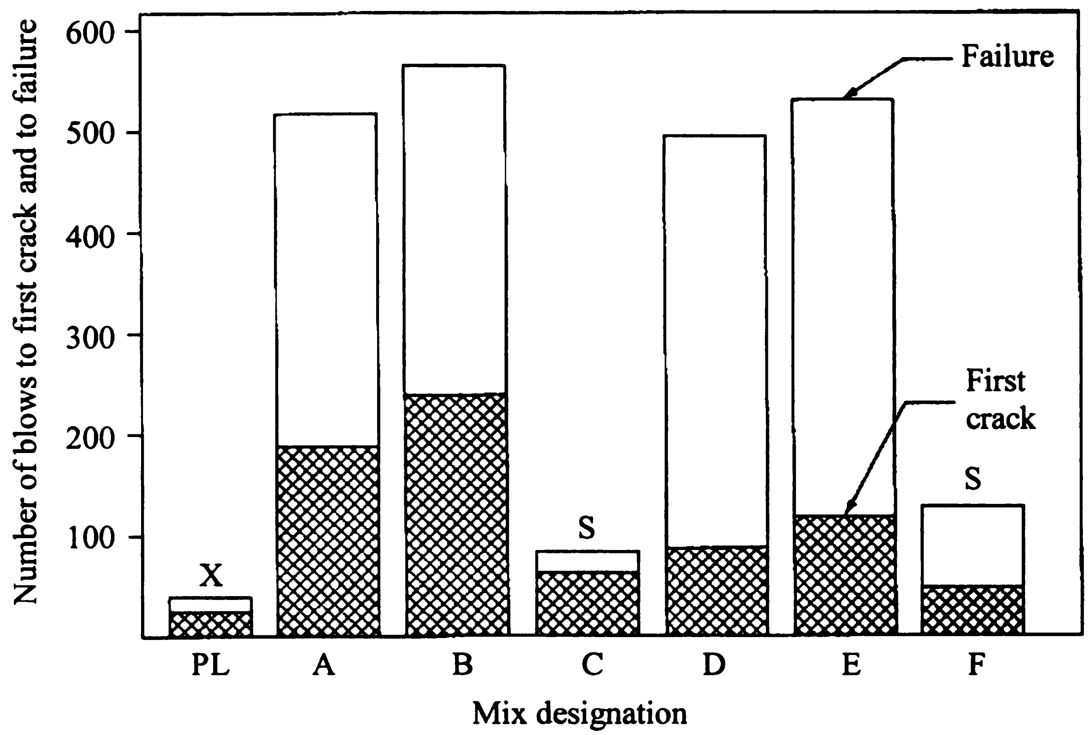

A- 80 lb/yd^3 hooked fibers (48 kg/m^3)
B- 105 lb/yd^3 hooked fibers (63 kg/m^3)
C- 140 lb/yd^3 straight fibers (84 kg/m^3)
D- 80 lb/yd^3 hooked fibers with pozzolan (48 kg/m^3)
E- 105 lb/yd^3 hooked fibers with pozzolan (63 kg/m^3)
F- 140 lb/yd^3 straight fibers with pozzolan (84 kg/m^3)
PL- Plain mix, using basic mix nonpozzolan

Figure G.3. Comparison of impact resistance of plain and steel fiber reinforced concrete

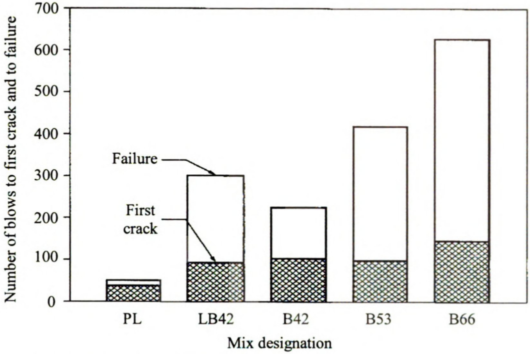

B66- 66 lb/yd^3 hooked fibers (39.2 kg/m^3)
B53- 53 lb/yd^3 hooked fibers (31.4kg/m^3)
B42- 42 lb/yd^3 hooked fibers (24.9 kg/m^3)
LB42- 42 lb/yd^3 hooked fibers with Libby Dam coarse aggregate (24.9 kg/m^3)
PL- Plain mix, using basic mix proportions

Figure G.4. Comparison of impact resistance of plain and steel fiber reinforced concrete Different volume fraction

G.3. Nylon Fibers

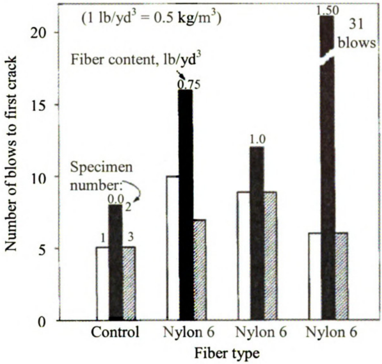

Figure G.5. Comparison of first crack strength for concrete reinforced with three different volume fraction

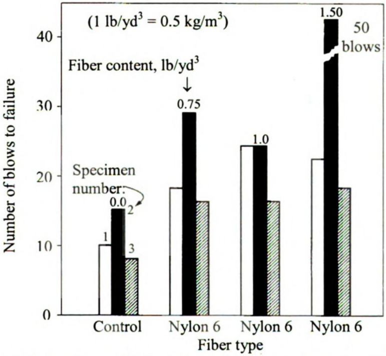

Figure G.6. Comparison of failure strength for concrete reinforced with three different volume fractions

G.4. Synthetic Fibers

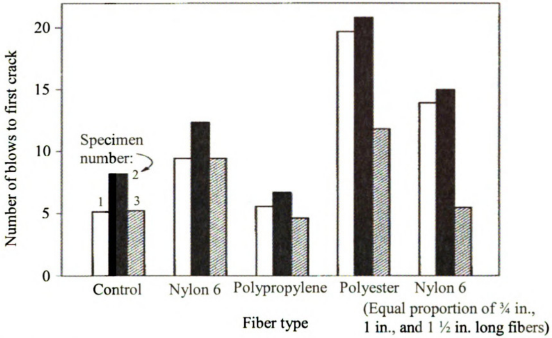

Figure G.7. Comparison of first crack strength for concrete reinforced with by various polymeric fibers volume fraction

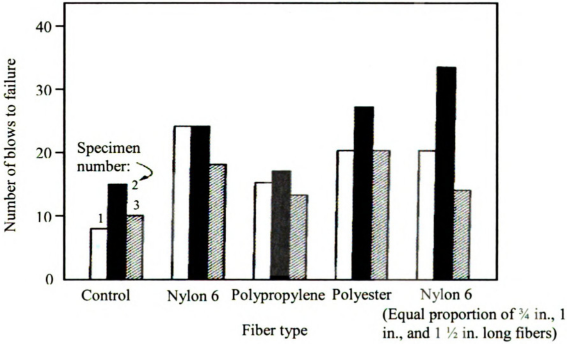

Figure G.8.Comparison of failure strength for concrete reinforced with by various polymeric fibers volume fraction

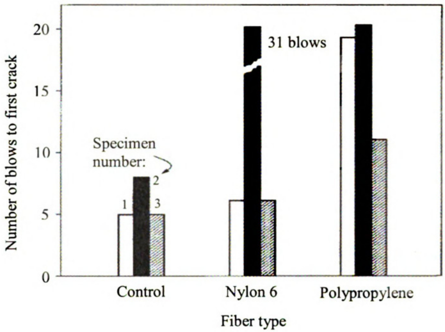

Figure G.9. Comparison of first crack strength for concrete reinforced by Nylon 6 and Polypropylene fibers

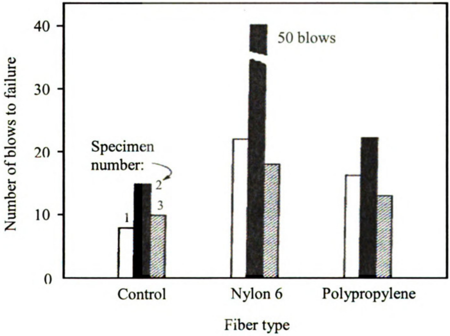

Figure G.10. Comparison of failure strength for concrete reinforced by Nylon 6 and Polypropylene fibers

G.5. Polypropylene Fiber

Table G.2. Impact resistance and relative fracture strength

Boundary condition	*Fiber volume (%)*	*Blows to 1st crack*	*Blows to failure*	*Relative strength*
Elevated	0.0	1	2	1.0
	0.1	1	7	3.5
	0.5	3	12	6.0
On-grade	0.0	1	6	3.0
	0.1	3	6	3.0
	0.5	6	20+	10.0+

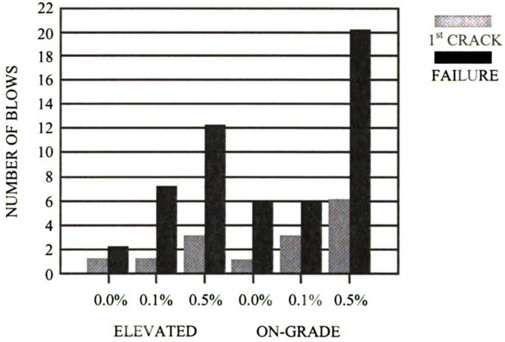

Figure G.11. Impact resistance (Polypropylene fiber)
First crack and Failure

G.6. Polyester Fibers (Recron 3S)

Table G.3. Mix Proportions for Various Mixes arrived Based on the Methodology Adopted

Mix No	Mix Proportions								Remarks	Method of Compaction
	W/c Ratio	Cement	Fine aggregate	Coarse aggregate	Fly Ash	Super Plasticizer	VMA	Fibre		
1	0.51	1.0	1.997	2.785	-	-	-	-	Final trial with a slump of 60 mm	Compaction
2	0.51	1.0	1.997	2.646	0.139	-	-	-	Coarse aggregate reduced by 5% of fly ash	Compaction
3	0.51	1.0	1.997	2.508	0.278	-	-	-	Coarse aggregate reduced by 10% of fly ash	Compaction
4	0.51	1.0	1.997	2.367	0.417	-	-	-	Coarse aggregate reduced by 15% of fly ash	Compaction
5	0.51	1.0	1.997	2.228	0.557	-	-	-	Coarse aggregate reduced by 20% of fly ash	Compaction
1a	0.51	1.0	2.341	3.285	0.172	-	-	-	Mix 1 with cement content reduced to 320 kg/m^3	Compaction
6	0.51	1.0	2.341	2.775	0.489 +0.172	-	-	-	Mix 4 with cement content reduced to 320 kg/m^3	Compaction
15	0.51	1.0	2.341	2.612	0.652 +0.172	0.35	0.10	-	Mix7 with super plasticizer - 0.35, viscosity, M, agent-0.1% weight of powder, (Cohesive & uniform mix).	Pouring
16	0.51	1.0	2.341	2.612	0.652 +0.172	0.35	0.10	0.15	Mix7 with super plasticizer - 0.35, viscosity, M, agent-0.1% weight of powder, fibre-0.15% of cement (Cohesive & uniform mix).	Pouring

Table G.3.Continued

Mix No	Mix Proportions								Remarks	Method of Compaction
	W/c Ratio	Cement	Fine aggregate	Coarse aggregate	Fly Ash	Super Plasticizer	VMA	Fibre		
17	0.51	1.0	2.341	2.612	0.652 +0.172	0.35	0.10	0.20	Mix7 with super plasticizer - 0.35, viscosity, M, agent-0.1% weight of powder, fibre-0.20% of cement (Cohesive & uniform mix).	Pouring
18	0.51	1.0	2.341	2.612	0.652 +0.172	0.35	0.10	0.25	Mix7 with super plasticizer - 0.35, viscosity, M, agent-0.1% weight of powder, fibre-0.25% of cement (Cohesive & uniform mix).	with Recron 3S @ 0.35% Pouring
19	0.51	1.0	2.341	2.612	0.652 +0.172	0.35	0.10	0.40	Mix7 with super plasticizer - 0.35, viscosity, M, agent-0.1% weight of powder, fibre-0.40% of cement (Stiff mix).	Pouring

Table G.4. Impact Resistance

SI No	Mix	7 days						28 days					
		No of blows at first crack	Average No of blows at first crack	Impact energy (Joule)	No of blows at failure	Average No of blows at failure	Impact energy (Joule)	No of blows at first crack	Average No of blows at first crack	Impact energy (Joule)	No of blows at failure	Ave. No. blows at failure	Impact energy (Joule)
1	CONTROL	8			9			43			44		
	CONCRETE(1)	10	10	209	12	11	230	45	46	961	47	47	982
		11			12			48			49		
2	CC+ 15%	33			34			72			73		
	FLYASH(4)	36	33	689	37	34	710	77	74	1545	78	76	1587
		30			31			74			78		
3	CC+ 20%	36			37			79			78		
	FLYASH(5)	36	34	710	38	36	745	80	79	1650	82	80	1671
		30			32			78			79		
4	OPTIMAL	20			21			51			53		
	CEMENT 15%	25	24	501	27	25	529	57	53	1107	58	55	1149
	FLYASH(6)	27			28			52			53		
5	OPTIMAL-	29			31			62			63		
	CEMENT 20%	26	26	550	27	28	578	80	82	1295	62	64	1337
	FLYASH(7)	24			25			65			67		
6	FINAL	15			16			45			51		
	SCC(15)	17	17	382	18	18	383	47	46	988	49	50	1044
		20			21			47			50		
7	FINAL SCC +	28			33			88			78		
	0.15%Fibre	29	27	564	36	34	710	71	69	1448	82	78	1622
	(16)	24			33			69			73		

Table G.4. Continued

SI No	Mix	7 days						28 days					
		No of blows at first crack	Average No of blows at first crack	Impact energy (Joule)	No of blows at failure	Average No of blows at failure	Impact energy (Joule)	No of blows at first crack	Average No of blows at first crack	Impact energy (Joule)	No of blows at failure	Ave. No. blows at failure	Impact energy (Joule)
8	FINAL SCC + 0.20%Fibre (17)	31			40			72			88		
		27	29	606	34	37	780	75	73	1531	90	87	1810
		29			38			73			84		
9	FINAL SCC + 0.25%Fibre (18)	43			50			83			104		R3S at
		39	41	883	52	50	1051	87	85	1768	104	102	2137
		42			49			84			99		0.25%
10	FINAL SCC + 0.40%Fibre (19)	48			57			98			107		
		43	45	940	51	54	1121	95	96	2012	111	110	2304
		44			63			96			113		

APPENDIX H

ABRASION EXPERIMENTS [9,16,27,29,31]

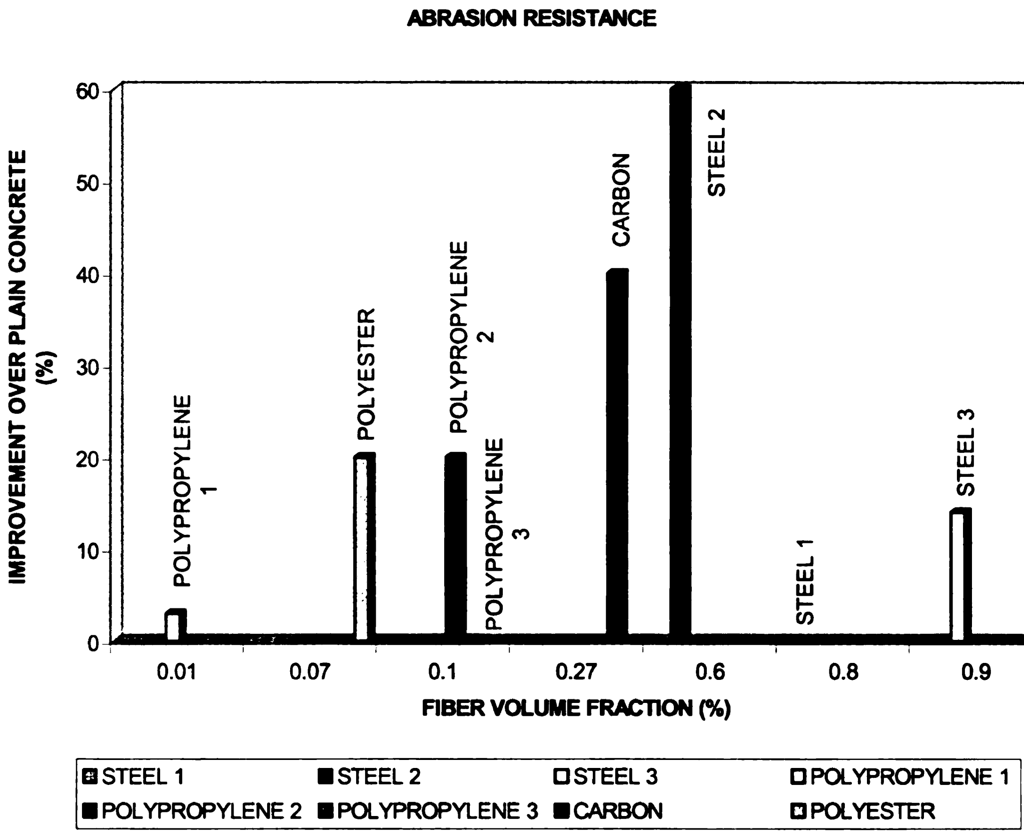

Figure H.1. Summary of the Abrasion Results for Different Fiber Types

H.1. Test Methods

H.1.1. Test Method I

ASTM C 779 – 00 Standard Test Method for Abrasion Resistance of Horizontal Concrete Surfaces (Procedure C)

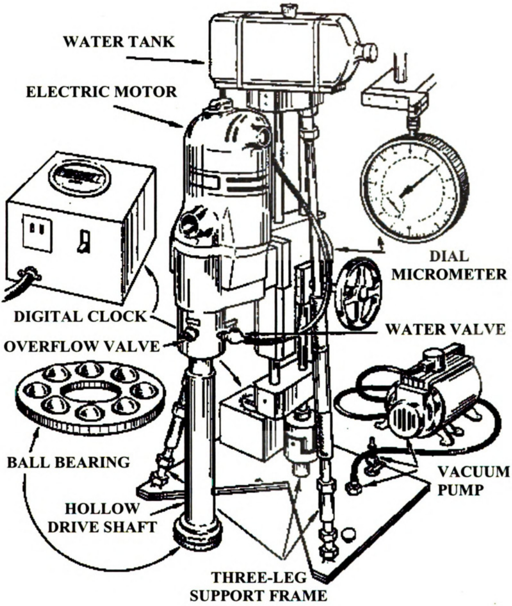

Figure H.2. Ball Bearing Abrasion Test Machine

H.1.2. TEST METHOD II

ASTM C 944 – 99 Standard Test Method for Abrasion Resistance of Concrete or Mortar Surfaces by the Rotating-Cutter Method

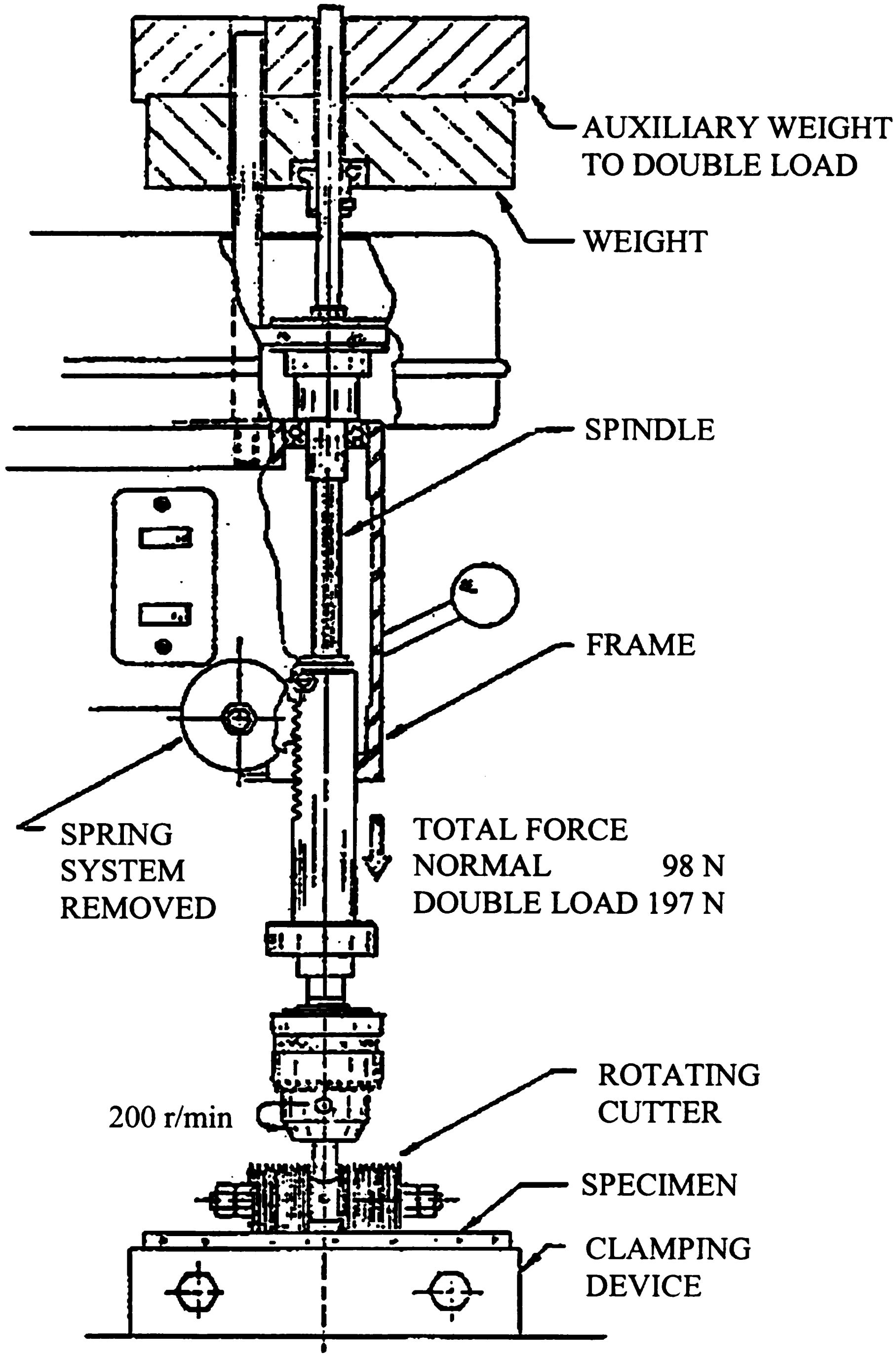

Figure H.3. Test Apparatus

H.1.3. Test Method III

British Standard BS 812

H.2. Experiments Using Test Method I

H.2.1. Antonio Nanni (Ref. 27)

Table H.1. Fiber Characteristics

Code	Type	Length in.	Equivalent diameter, in. * 10^{-3}
HE	Hooked-end drawn wire	1.18	19.6
SS	Straight slit sheet	1.00	16.7
SR	Crimped slit sheet	1.00	16.7
PB	Fibrillated polypropylene bundle	0.75	-----

Table H.2. Effect of Curing regimen on Compressive Strength and Abrasion Resistance

No. of wet-dry cycles	Compressive strength ratio, percent	Abrasion resistance ratio, percent		
		Plain matrix	Steel fiber HE	Synthetic fiber PB
1	74	35	28	23
2	79	45	41	35
3	85	66	43	54
4	86	72	46	58
5	90	62	48	60

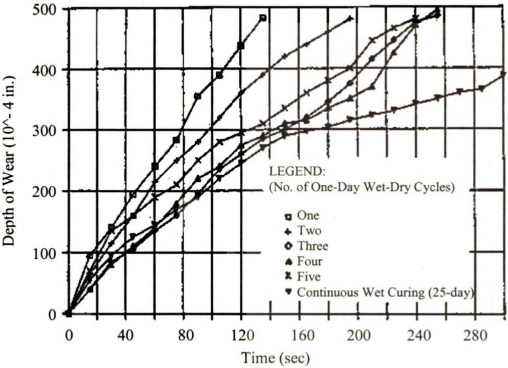

Figure H.4. Abrasion results of laboratory-made beams subjected to different curing regimens - Bottom surface, air-dry condition, plain matrix

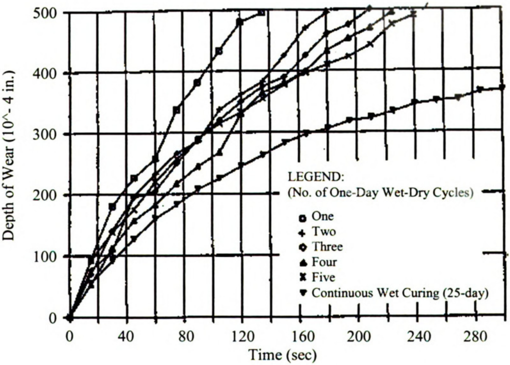

Figure H.5. Abrasion results of laboratory-made beams subjected to different curing regimens - Bottom surface, air-dry condition, 3 percent steel fiber Type HE

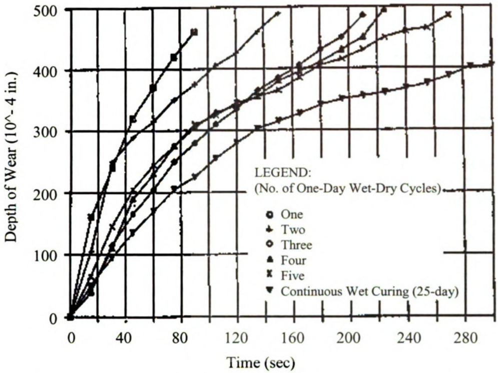

Figure H.6. Abrasion results of laboratory-made beams subjected to different curing regimens - Bottom surface, air-dry condition, 1.5 lb/yd^3 = 0.89 kg/m^3 synthetic fiber Type PB

H.2.2. Canada Center for Mineral and Energy Technology (Ref. 16)

Table H.3. Summary of CANMET Mixture Proportions and Strength Data

Steel Fiber Mixtures :	Mixture Quantities, lb./yd^3(kg/m^3)			
Mixture Designation	S1	S2	S3	S4
Cement, CSA Type 10	845(500)	845(500)	845(500)	845(500)
Fly ash	---	127(75)	---	127(75)
Silica Fume	---	---	51(30)	51(30)
Natural sand	1284(760)	1158(685)	1166(690)	1056(625)
Gravel, 14 mm MSA	1622(960)	1656(980)	1656(980)	1673(990)
Water	230(136)	228(135)	232(137)	232(137)
Steel fibers [a]	85(50)	85(50)	85(50)	85(50)
Water/cementatious ratio	0.27	0.23	0.26	0.23
Air content, %	4.5 ± 1	4.5 ± 1	4.5 ± 1	4.5 ± 1
Avg. Strength, psi (MPa) 28-day Compressive	9630(66.4)	10036(69.2)	11385(78.5)	12356(85.2)
28-day Flexural	1146(7.9)	1494(10.3)	1436(9.9)	1610(11.1)
Abrasion Depth 91-day, in. (mm)	0.016(0.404)	0.006(0.165)	0.008(0.213)	0.003(0.084)

Polypropylene Fiber Mixtures :	Mixture Quantities, lb./yd^3(kg/m^3)			
Mixture Designation	P1	P2	P3	P4
Cement, CSA Type 10	845(500)	845(500)	845(500)	845(500)
Fly ash	---	127(75)	---	127(75)
Silica Fume	---	---	51(30)	51(30)
Natural sand	1183(700)	1048(620)	1124(665)	955(565)
Gravel, 14 mm MSA	1775(1050)	1775(1050)	1766(1045)	1766(1045)
Water	230(136)	230(136)	230(136)	266(134)
Polypropylene fibers [b]	1.7(1)	1.7(1)	1.7(1)	1.7(1)
Water/cementatious ratio	0.27	0.23	0.26	0.22
Air content, %	4.5 ± 1	4.5 ± 1	4.5 ± 1	4.5 ± 1
Avg. Strength, psi (MPa) 28-day Compressive	9224(63.6)	9674(66.7)	10500(72.4)	10544(72.7)
28-day Flexural	1131(7.8)	1247(8.6)	1378(9.5)	1276(8.8)
Abrasion Depth 91-day, in. (mm)	0.008(0.193)	0.024(0.617)	0.019(0.495)	0.015(0.373)

Notes:
a. 0.20 in. (0.5 mm) diameter by 2 in. (50 mm) long steel fiber, sp. gr. = 7.85.
b. 2 in. (50 mm) long polypropylene fiber, sp. gr. = 0.9.

H.3. EXPERIMENTS USING TEST METHOD 2

H.3.1. Shi, Zeng-Qiang and D.D.L. Chung (Ref. 32)

Table H.4. Properties of Carbon Fibers

Filament diameter	10 µm
Tensile strength	690 MPa
Tensile modulus	48 GPa
Elongation at break	1.4%
Electrical resistivity	3.0×10^{-3} Ω.cm
Specific gravity	1.6 g/cm^3
Carbon content	98 wt.%

Table H.5. Depth of Wear (mm, ± 9%)

Plain mortar	1.07
Mortar with latex	0.161
Mortar with latex and fibers	0.096
Mortar with silica fume	0.145

H.3.2. A.M. Brandt, M.A. Glinicki & J. Potrzebowski (Ref. 10)

Table H.6. Components and Mix Proportions

Components	*Mixture proportions [kg/m³]*					
	M-0	*M-1*	*M-2*	*M-3*	*M-4*	*M-5*
Portland cement P35	340	354	350	355	349	354
River sand <= 2 mm	600	590	578	594	584	595
River gravel 2-16 mm	1240	1236	1218	1237	1219	1250
Water	160	194	193	189	185	178
Superplasticizer	7	7.1	7	7.1	7	7.1
Fibers PP1	0.6		0.6			
Fibers PP2				0.91		
Fibers H30/50					30.0	30.5
Fibers H60/80						0.50
w/c	0.47	0.55	0.55	0.53	0.53	

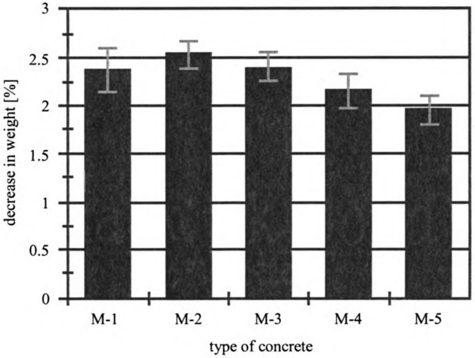

Figure H.7. Results of Abrasion Test

H.4. EXPERIMENTS USING TEST METHOD III

H.4.1. Indian Institute of Technology (Ref. 30)

Table H.7. Mixture Proportions for M20 and M40 Concrete

Ingredient \ Mixture =>	M20	M40
Cement (Birla Rajshree)	330 kg/m^3	390 kg/m^3
Sand (Zone II)	807 kg/m^3	794 kg/m^3
Coarse aggregate (12 mm)	398 kg/m^3	392 kg/m^3
Coarse aggregate (20 mm)	722 kg/m^3	710 kg/m^3
Water	172 kg/m^3	162 kg/m^3
Superplasticizer (Ceraplast 300)	0.75 % by weight of cement	1.0 % by weight of cement

Note: Fibres were used at a dosage of 0.25 % by weight of cement for preparing the fibre-reinforced concrete mixtures

REFERENCES

REFERENCES

1. ACI Committee 544, "Design considerations for steel fiber reinforced concrete" ACI 544.4R-88, ACI manual of concrete practice, Part 5, 1998

2. Airports Authority of India, "Test Results", January 2001

3. American Concrete Pipe Association "Concrete Pipe Technology Handbook" , American Concrete Pipe Association, Texas, 1993

4. ASTM, Annual Book of ASTM Standards, Philadelphia, Standard Vol. 04.02., 2000

5. Balaguru P.; and Khajura Anil, "Properties of Polymeric Fiber-Reinforced Concrete" Transportation Research Record, No. 1532, Sep. 1996

6. Balaguru P. N., Shah S.P. "Fiber-Reinforced Cement Composites", McGrow-Hill, New York 1992, pp. 128-147, 249-277, 179-248

7. Banthia, N., Yan C., Mindess, S.,"Restrained Shrinkage Cracking in Fiber Reinforced Concrete: A Novel Test Technique", Cement and concrete Research, 1996 Vol.26, No. 1, pp. 9-14.

8. Bayasi, Z., Celik, T. "Application of Silica fume in synthetic Fiber-reinforced Concrete", Transportation Research Record,1382 pp. 89-98

9. Bindaganavile, V.; and Banthia, N., "Polymer and Steel Fiber-Reinforced Cementitious Composites under Impact Loading – Part 2: Flexural Toughness", ACI Materials Journal, Vol. 98, No. 1 January – February 2001

10. Brandt, A.M., Glinicki ,M.A. & Potrzebowski, J., "Application of FRC in Construction of the Underground Railway Track", Cement and Concrete Composites, vol.18, 1996 pp.305-312.

11. Ezeldin, A.S., Lowe, S. R., Balaguru, P. N., "Flexural Behavior of Synthetic Fiber Reinforced Rapid Set Materials", Construction Materials Serviceability/Durability pp. 1203-1211

12. Groth, Patrik "Cracking in concrete-Crack prevention with air-cooling and crack distribution with steel fiber reinforcement", Lulea University of technology, Nov 1996. (http://epubl.luth.se/avslutade/0280-8242/96-37/html/paper_D.html.

13. Hannant,D.J. ,"Fibre Cements and Fibre Concretes", John Wiley and Sons,1978.

14. Hardik R. Shah, Akhter B. Hossain, and Jason Weiss,"Using The Restrained Ring Test in Conjunction with Passive acoustic Emission to Quantify the Role of Steel Fiber reinforcement in Shrinkage Cracking Mitigation", Proceedings of conference on Fiber Composites,High-Performance Concretes and smart Materials, ICFRC January 2004, Chennai ,India

15. Heger Frank J., McGrath, Timothy J. "Design Method for Reinforced Concrete Pipe and Box Sections" Simpson Gumpertz & Heger Inc., December 1982

16. Hoff, G. C., "Durability of Fiber Reinforced Concrete in a severe Marine Environment", ACI Special publication SP-100, Vol.100 Issue 4. April 1987.

17. Johnston, C.D. "Fiber-reinforced cements and concretes", Gordon and Breach Science Publishers, 2001

18. Khajuria, A.,Bohra, K.,Balaguru, P. "Long Term Durability of Synthetic Fibers in Concrete", ACI, Special Publication, SP 126-46, pp. 851-868

19. Li, Victor C. "Large Volume, High-Performance Applications of Fibers in Civil Engineering", Journal of Applied Polymer Science, Vol. 83, 660–686 (2002)

20. Li, Victor C. , Robert Ward, and Ali M. Hamza, "Steel and Synthetic Fibers as Shear Reinforcements", ACI Materials Journal, V. 89, No. 5, September-October 1992

21. Magalhaes, A. G., Marques, A. T., Oliveira, F. M. F., Soukatchoff, P.,de Castro, P. T.,"Mechanical Behaviour of Cementitious Matrix Composites", Cement and Concrete composites, 1996 pp. 9-22

22. Manolis, G. D., Gareis, P. J., Tsonos, A. D. & Neal, J. A. ,"Dynamic Properties of Polypropylene Fiber-Reinforced Concrete Slabs" ,Cement and Concrete composites, 1997 pp. 341-349

23. Miguel Angel, Sanjuhn & Amparo Moragues, "Polypropylene Fiber-Reinforced Mortar Mixes: Optimization to Control Plastic Shrinkage."

24. Murthy, Savithri S., "Impact Strength of Synthetic Fibre Reinforced Self Compacting Concrete", Dissertation, Bangalore University, May – 2004

25. Nagabhushanam,M., Ramakrishnan,V., Vondran G., "Fatigue Strength of Fibrillated Polypropylene Fiber Reinforced Concretes", Transportation Research Record 1226 pp.36-47

26. Najm, H. and Balaguru P., "Effect of Large-Diameter Polymeric Fibers on Shrinkage Cracking of Cement Composites", ACI Materials Journal , July-August 2002

27. Nanni, A., "Abrasion Resistance of Roller Compacted Concrete", ACI Materials Journal, November-December 1989 pp. 559-565.

28. Ramakrishnan, V., George Y, Hossali,G., "Flexural Fatigue Strength, Endurance Limit, and Impact Strength of Fiber Reinforced Concretes", Transportation Research Record 1226 pp.17-24

29. RS Means, "2005 Heavy Construction Cost Data," 19th Annual Edition, Reed Construction Data, Inc., Massachusetts, 2004, pp. 36,100.

30. Santhanam, M. "Recron 3S, Test Report of I.I.T. Chennai", Indian institute of Technology, 2003

31. Senthikumar, S. S., Nastean, S. C.,"Effect of Synthetic Fiber Reinforcrmrnt on Early-Age Cracking Behavior of Cement Composites" ICI Journal, April-June 2004.

32. Shi, Zeng-Quang and Chung, D. D. L. "Improving the Abrasion Resistance of Mortar by Adding Latex and Carbon Fibers", Cement and Concrete Research, Vol.27 No.8 1997 pp. 1149-1153.

33. Sintef report,"Plastic Shinkage and Cracking Tendency of Mortar and concrete Containing Fibermesh", 1985.

34. Soroushian Parviz; Khan, Ataullah; Hsu, Jer-Wen, "Mechanical Properties of Concrete Materials Reinforced with Polypropylene or Polyethylene Fibers" ACI Materials Journal, Vol. 89, No. 6 November – December 1992

35. Sunder, Suma S.; Ramesh, K. P.; Pitts, Charles Jr.; and Ramakrishnan, V., "Performance Characteristics of Synergy Fiber-Reinforced Concretes – Strength and Toughness Properties" Transportation Research Record, No. 1775, 2001

36. Toledo, Filho, Sanjuan, M A. "Effect of low modulus sisal and polypropylene fibre on the free and restrained shrinkage of mortars at early age", Cement and concrete Research, 1999 pp. 1597-1604.

37. Ward, Robert J.; Li, Victor C., "Dependence of Flexural Behavior of Fiber Reinforced Mortar on Material Fracture Resistance and Beam Size" ACI Materials Journal, Vol. 86 N0. 6 November – December 1990

38. Yao, W.; Li, J.; Wu, K., "Mechanical Properties of Hybrid Fiber reinforced Concrete at low fiber volume fraction" ,Cement and Concrete research, 33, 2003, pp. 27-30

INTERNET REFERENCES

39. www.Concreteproducts.com

40. www.Fibermesh.com

41. www.Freedonia.com

42. www.Kuraray.co.jp

43. www.Nycon.com